EXPRESSION OF RUNT RELATED TRANSCRIPTION FACTOR 2 AND VASCULAR ENDOTHELIAL GROWTH FACTOR IN THE PULP, PERIODONTAL LIGAMENT AND ALVEOLAR BONE: AN IMMUNOHISTOCHEMICAL STUDY USING A RAT ANKYLOTIC MODEL

A thesis submitted in partial fulfilment of the requirements for the degree of

Doctor of Clinical Dentistry (Orthodontics)

Dr Trudy Ann STEWART (BDS Adelaide, BOccThy UQ)

Orthodontic Unit

School of Dentistry

Faculty of Health Science

The University of Adelaide

South Australia

AUSTRALIA

March 2013

1.2 List of Figures:

1.2.1 Literature Review:

1.2.2 Article 1:

1.2.3 Article 2:

1.2.4 Concluding Remarks:

1.3 List of Tables:

1.3.1 Article 1:

1.3.2 Article 2:

1.4 List of Abbreviations:

ABC	Avidin-biotin complex
AEC	3-Amino-9-EthylCarbazole
ALP	Alkaline phophosphatase
ARF	Activation – resorption – formation cycle
bFGF	basic fibroblast growth factor
BGN	Biglycan
BMP	Bone morphogenetic proteins
Cbfα	Core binding factor subunit alpha
Cbfß	Core binding factor subunuit beta
CNC	Cranial neural crest cells
COL1A2	Collagen, Type 1, Alpha 2
CSF-1	Colony stimulating factor 1
CY3	Cyanine 3
DAPI	4',6-diamidino-2-phenylindole
DFC	Dental follicle cells
DFSC	Dental follicle stem cells
DMP1	Dentine matrix acidic phosphoprotein
DPSC	Dental pulp stem cells
DSC	Dental stem cells
DSPP	Dentine sialophosphoprotein
EDTA	Ethylene diamine tetraacetic acid
ECM	Extracellular matrix
EGF	Epithelial growth factor
FGF	Fibroblast growth factor

FGFR	Fibroblast growth factor receptor
FZD	Frizzled receptor
GEE	Generalised estimating equations
GH	Growth Hormone
HSC	Haematopoietic stem cell
HERS	Hertwig's epithelial root sheath
HSC	Haematopoietic stem cells
IGF	Insulin-like growth factor
Ihh	Indian hedgehog
IL	Interleukin
M-CSF	Macrophage colony stimulating factor
MAPK	Mitogen-activated protein kinase cascade
MSC	Mesenchymal stem cells
MSX1/2	Muscle segment homeobox
OB	Osteoblast
Oc	Osteocyte
OC	Osteoclast
OCN	Osteocalcin
OPG	Osteoprotegerin
OSX	Osterix (SP7)
OTM	Orthodontic tooth movement
Pax	Paired box gene
PBS	Phosphate buffered saline
PDGF	Platelet derived growth factor
PDL	Periodontal ligament

PDLSC	Periodontal ligament stem cells
PFE	Primary failure of eruption
PIGF	Placental growth factor
PTH	Parathyroid hormone
PTH1R	Parathyroid hormone receptor gene 1
PTHrP	Parathyroid hormone related peptide
RANK	Receptor activator of nuclear factor kappa-ß
RANKL	RANK ligand
Runx2	Runt related transcription factor 2
SCAP	Stem cells from apical papilla
SHED	Stem cells from human exfoliated deciduous teeth
Shh	Sonic hedgehog
SP7	C2H2 type zinc finger transcription factor (osterix)
TGF-ß	Transforming growth factor-beta
TNF-α	Tumour necrosis factor-alpha
VEGF	Vascular endothelial growth factor
Wnt	Wingless signalling pathway

Measure of Length

mm	millimetre
µm	micrometre

Measure of Volume

ml	millilitre
µl	microlitre

Measure of Weight

µg	microgram
mg	milligram
g	gram
kg	kilogram
kDa	kiloDalton
mw	molecular weight
N	newton

2. ACKNOWLEDGEMENTS

I wish to express my sincere appreciation to the following people for their support in the completion of this thesis:

Professor W. J. Sampson, P.R. Begg Chair in Orthodontics, The University of Adelaide, for his generosity with his time as well as his expert advice and guidance.

Associate Professor C. W. Dreyer, Senior Lecturer in Orthodontics, The University of Adelaide, for his readily available support as well as the use of research books and materials.

Dr Kencana Dharmapatni, School of Medical Sciences, The University of Adelaide, for her expert advice regarding immunohistochemistry, allowing the use of her laboratory for this project, assistance with developing the staining protocols and generous donation of various tissue blocks. Her dedication and enthusiasm for research is truly an inspiration.

Mr Yen Liu, Division of Population Oral Health, The University of Adelaide, for his expert statistical help.

Mr Jim Manavis, Laboratory Manager, Hanson Institute Centre for Neurological Diseases for teaching me how to use the Nanozoomer Digital Microscope

Last but not least, I must thank my wonderful husband David. Your tolerance, support and proofreading is simply amazing and it has made all the hard work worthwhile.

3. THESIS DECLARATION

This thesis contains no material that has been accepted for the award of any other degree or diploma in any other university or tertiary institution and, to the best of my knowledge and belief, contains no material previously published or written by another person, except where due reference has been made in the text. In addition, I certify that no part of this work will, in the future, be used in a submission for any degree or diploma in any university or other tertiary institution without prior approval of the University of Adelaide.

I give consent for this copy of my thesis, when deposited in the University of Adelaide Library, to be made available for loan and photocopying subject to the provisions of the Copyright Act 1968.

I also give permission for the digital version of my thesis to be made available via the University of Adelaide's digital research repository, the University of Adelaide Library catalogue and also through internet search engines, unless permission has been granted by the University of Adelaide to restrict access for a period of time

_____

Dr Trudy Stewart

13th March 2013.

4. ABSTRACT

The current study investigated the expression Runx2 and VEGF in the pulp, periodontal ligament and alveolar bone following hypothermal insult.

Methods and Materials:

Materials from a previous study performed by Tan (2011) were used for this research. The upper right first molars of fifteen eight-week-old male Sprague-Dawley rats were subjected to a single ten minute application of dry ice. The contralateral molar acted as an internal control. The animals were randomly divided into five groups of three and killed 0, 4, 7, 14 and 28 days post hypothermal insult. A further three Sprague-Dawley rats acted as an external control and were humanely killed on day 0 with no hypothermal insult. The maxilla was dissected out, fixed and embedded in paraffin. Coronal sections were cut to include the control and experimental teeth at 5-micron intervals through the furcation region. Sections were then stained with haematoxylin and eosin (H and E) and Runx2 and VEGF immunostains.

Sections were scanned via a Nanozoomer Slide Scanner 2.0 series and viewed on a personal computer (MacBook Pro with 13 inch screen) using the Nanozoomer Digital Pathology (NDP) software. Semiquantitative counting was performed at a magnification of x20 via the ImageJ software. Data was analysed using SAS 9.3 (SAS Institute Inc., Cary, NC, USA). The level of significance was set at $p<0.05$.

Results:

H and E stained sections indicated that ankylosis had developed on the experimental side at days 7 and 14 and one of the three rats at day 28 post hypothermal insult. No ankylosis was present on any control teeth or experimental teeth at days 0 and 4. Disturbance to the pulpal tissues was also noted.

A number of cells stained positively to the Runx2 and VEGF immunostains. Vascular endothelial cells, bone cells (osteoblasts / osteocytes / bone lining cells), osteoclast-like cells, periodontal ligament cells (fibroblasts, epithelial cell rests of Malassez (ERM)) and bone marrow cells in both experimental and control animals were positive for VEGF. Increased staining intensity for VEGF was noted particularly associated with blood vessels and adjacent to regions of ankylosis. Fibroblast-like cells in the pulp and PDL, osteoclasts in resorption lacunae along the PDL, bone lining cells, osteoblasts/osteocyte like cells, cemental cells, odontoblasts, epithelial cell rests of Malassez (ERM), megakaryocytes and vascular endothelial cells were all found to be positive for Runx2 in both the treated and untreated groups.

Statistically significant differences in the percentage of Runx2 positive cells between treated and untreated molar teeth were found in the pulp and alveolar bone but no statistically significant difference was found in the PDL. Although not statistically significant, trends of changing Runx2 expression with time were noted in the pulp and alveolar bone. Runx2 expression increased at days 4, 7 and decreased at days 14 and 28 in the pulp whilst in the alveolar bone expression increased at day 4, decreased at days 7 and 14 and slightly increased at day 28.

In the pulp, a statistically significant difference was found between VEGF positive cells on the experimental side compared to the internal control side, with more VEGF positive cells on the experimental side at day 7 than at days 14 and 28. In the alveolar bone and PDL, although a statistically significant difference was found between the experimental and control sides, there was no significant interaction with time. However, VEGF positive cells appeared to be fewer in the PDL at days 4, 7 and 14 and greater at day 28. In the alveolar bone, more VEGF positive cells were seen at day 4 than at days 7, 14 and 28.

Conclusions:

1) Runx2 and VEGF was expressed by a number of cells within the rat dentoalveolus.

2) When compared to the control groups, changes in Runx2 expression were found in the experimental pulp and alveolar bone, but not in the PDL. Changes in VEGF expression were found in the experimental pulp, PDL and alveolar bone.

3) Changes in Runx2 and VEGF expression also occurred between the internal and external control groups, suggesting that a localised insult may lead to a systemic impact.

4) Post-hypothermal insult, Runx2 and VEGF may play an important role in the development of bony ankylosis.

The null hypothesis, that the expression of Runx2 and VEGF in the rat dentoalveolus does not differ post-hypothermal insult, is rejected.

5. LITERATURE REVIEW

5.1 The Periodontium

5.1.1 Introduction

The periodontium, which comprises the root cementum, periodontal ligament (PDL), gingiva and alveolar bone, is a dynamic specialized joint that supports and invests each individual tooth in the dentition (Nanci and Bosshardt, 2006; Wilson and Kornman, 1996; Hassell, 1993). Embryologically, the periodontium originates from the dental follicle, a loose connective tissue derived from ectomesenchyme surrounding the enamel organ and dental papilla of the developing tooth germ (Pan et al., 2010). The periodontium has a limited capacity to regenerate, although orthodontic tooth movement studies have demonstrated the PDL, cementum and alveolar bone's ability to repair and remodel following the application of controlled forces (Shi et al., 2005).

Figure 1: Schematic of a coronal section of a mouse molar tooth demonstrating both the mineralized tissued; enamel (blue) dentin (yellow) cementum (green) and alveolar bone (orange), as well as the surrounding soft tissues; pulp chamber, PDL and gingiva. The cementum is divided into the acellular extrinsic fibre cementum (AEFC) and cellular intrinsic fibre cementum (CIFC) (Diagram from Foster, 2012).

5.1.2 Cementum

Cementum is a thin, avascular mineralized tissue that acts to cover the tooth root surface, as well as form the interface between the dentine and PDL (Yamamoto et al., 2010; Nanci and Bosshardt, 2006; Cho et al., 2000). Cementum is produced by cementoblasts, and may be classified by the presence or absence of cells (cementocytes) embedded within the cementum as well as the location of the matrix collagen fibres (Yamamoto et al., 2010; Cho et al., 2000; Nanci and Bosshardt, 2006). Two types of cementum predominate; acellular extrinsic fibre and cellular intrinsic fibre, although both types may also present as mixed stratified layers of both cellular and acellular cementum (Foster, 2012).

Acellular extrinsic fibre cementum (AEFC, primary or acellular cementum) is a thin layer (50 – 200 microns) that develops slowly in the cervical half to two thirds of the tooth root (Foster, 2012; Yamamoto et al., 2010; Nanci and Bosshardt, 2006; Cho et al., 2000). It has a high concentration of periodontal ligament fibres (Sharpey's fibres) and is critical in anchoring the tooth to the alveolar bone (Yamamoto et al., 2010; Nanci and Bosshardt, 2006; Cho et al., 2000).

Cellular intrinsic fibre cementum (CIFC, secondary or cellular cementum) occurs in the apical third to half of the tooth root, as well as in the furcation areas of multirooted teeth (Cho et al., 2000; Nanci and Bosshardt, 2006). Intrinsic collagen fibres, as well as cementocytes, are characteristic features of cellular intrinsic fibre cementum (Nanci and Bosshardt, 2006). This type of cementum is thicker and frequently shows a multilayered appearance (resting lines) on haematoxylin staining, even occasionally presenting with a layer of acellular extrinsic fibre cementum (Yamamoto et al., 2010). This multilayered region may also be termed cellular mixed stratified cementum (Yamamoto et al., 2010; Cho et al., 2000). Cellular mixed stratified cementum is formed depending on the functional requirements of the tooth and is not found in rodent molars (Nanci and Bosshardt, 2006). Acellular

afibrillar cementum occurs at the cemento-enamel junction (Cho et al., 2000). When reshaping or adaptation of the tooth root occurs, cellular intrinsic fibre cementum with few or no extrinsic fibre formation has been reported (Yamamoto et al., 2010).

Biochemically, cementum with its 50% mineralised and 50% unmineralised matrix, closely resembles bone (Nanci and Bosshardt, 2006). Type I collagen forms 90% of the unmineralised matrix, although multiple other collagen groups are present in small amounts (Nanci and Bosshardt, 2006). Almost all non-collagenous matrix proteins identified in cementum are also present in bone; including, bone sialoprotein, dentine matrix protein, dentine sialoprotein, fibronectin, osteocalcin, osteonectin, osteopontin, tenascin, proteoglycans, protolipids and growth factors (Nanci and Bosshardt, 2006). Developmental differences between cementum and bone remain unclear, with cemental cells being proposed to be positional osteoblasts (Foster, 2012). No specific markers have been identified for cellular and acellular cementum, although bone sialoprotein (BSP) and osteopontin (OPN) have been found to strongly localize within the cementum (Foster, 2012).

5.1.3 Periodontal Ligament

The periodontal ligament (PDL) is a dense, fibrous connective tissue 0.15 to 0.38mm in width, which lies between the tooth root cementum and the alveolar bone socket, effectively forming an alveolo-dental ligament (Nanci and Bosshardt, 2006; Beertsen et al., 1997; Hassell, 1993). The PDL forms within the dental follicle; however, timing varies both between species, individual teeth and the deciduous and permanent dentition (Nanci and Bosshardt, 2006).

As with other soft connective tissues, the PDL is composed of an extracellular component; a collagenous and noncollagenous matrix embedded in an amorphous matrix made up of 70% water (ground substance), which contains blood vessels, nerves and a variety of cells including:

osteoblasts, osteoclasts, fibroblasts, epithelial rest cells of Malassez, monocytes, macrophages, undifferentiated mesenchymal stem cells, cementoblasts and odontoclasts (Nanci and Bosshardt, 2006).

Fibroblasts are the principal and arguably the most important cells of the PDL as, under normal circumstances, these cells produce and maintain the connective tissue matrix of the PDL and gingivae (Nanci and Bosshardt, 2006; Lallier et al., 2005; Beertsen et al., 1997; Hassell, 1993). PDL fibroblasts rapidly turn over the structural components of the PDL, including collagen, elastin, glycoproteins and glycoaminoglycans (Nanci and Bosshardt, 2006; Hassell, 1993). Periodontal fibroblasts are also capable of excreting matrix metalloproteinases, which act to degrade the extracellular matrix (Hassell, 1993). From prior experiments, phenotypically distinct and functionally different subpopulations of periodontal fibroblasts have been proven to be present, although all cells appear similar in appearance to light/electron microscopy (Hassell, 1993). In wound healing, cytokine expression is thought to determine the size and behaviour of the fibroblast subpopulation (Lekic et al., 1997). Gingival and PDL fibroblasts have been shown to possess osteogenic potential, with exposure to hydroxyapatite and mechanostimulation shown to express alkaline phosphatase, osteocalcin and bone sialoprotein (Lallier et al., 2005).

Epithelial cells in the PDL are remnants of the Hertwig's Epithelial Root Sheath (HERS) and are also called the epithelial cell rests of Malassez (ERM) (Bastholm Billie et al., 2010; Nanci and Bosshardt, 2006). They present as clusters of cells close to the cementum that, particularly in newly erupted teeth, resemble a perforated sheath (Nanci and Bosshardt, 2006; Hammarström et al., 1996). With time, this sheath degenerates and transforms into an epithelial network (Hammarström et al., 1996). Although ERM are thought to be in the G0 stage of the cell cycle (quiescent) in healthy teeth after completion of the tooth root, post trauma in vitro experiments show ERM can be stimulated to

proliferate (Shinmura et al., 2008). Shinmura et al. theorized that ERM set free from the normal microenvironment of the PDL may have the characteristics of stem cell / progenitor cells. Indeed, ERM have been reported to have the ability to differentiate into cementoblasts as well as ameloblast-like cells in vitro (Shinmura et al., 2008). ERM have also been found to secrete a variety of factors including cytokines, chemokines and growth factors and to express embryonic stem cell markers including octamer binding transcription factor 4 (Oct-4), Nanog and stage specific embryonic antigen 4 (SSEA-4) and, due to this, have been proposed to also function as a source of progenitor cells within the PDL (Xiong et al., 2012).

Undifferentiated mesenchymal cells are present in the coronal, apical and furcation regions of the PDL and ensure a constant supply of new cells for PDL repair (Nanci and Bosshardt, 2006; Machado et al., 2012). As with other dental stem cells, PDL stem cells (PDLSC) are able to differentiate into cells resembling cementoblasts, osteoblasts, adipocytes, chondrocytes and fibroblasts (Sedgley et al., 2012; Machado et al., 2012).

A number of collagen fibres, including collagen type I, III, V and XII, are present within the PDL (Nanci and Bosshardt, 2006; Lallier et al., 2005). These fibres differ from tendon collagen fibres as their diameters are much smaller and they also have a much shorter half-life (Nanci and Bosshardt, 2006). The majority of collagen in the PDL is organized into bundles. The distal portions of these bundles insert into the cementum and alveolar bone and are called Sharpey's fibres. Collagen fibre bundles are also found extending into the gingivae (dentogingival fibres) (Nanci and Bosshardt, 2006). Elastic fibres, namely elastin, oxytalan and elaunin, are also present in the PDL and form the elastic fibre network (Nanci and Bosshardt, 2006). These fibres are differentiated from each other by the relative amounts of microfibrils and elastin fibres present (Strydom et al., 2012). Oxytalan fibres insert into the acellular cementum in the supra-alveolar region and fan out into the interdental

space (Strydom et al., 2012). In the occlusal two-thirds and the apical third, the oxytalan fibres emerge from the cementum and curve apically, crossing the principal collagen fibres and enveloping the vascular system within the PDL (Strydom et al., 2012)

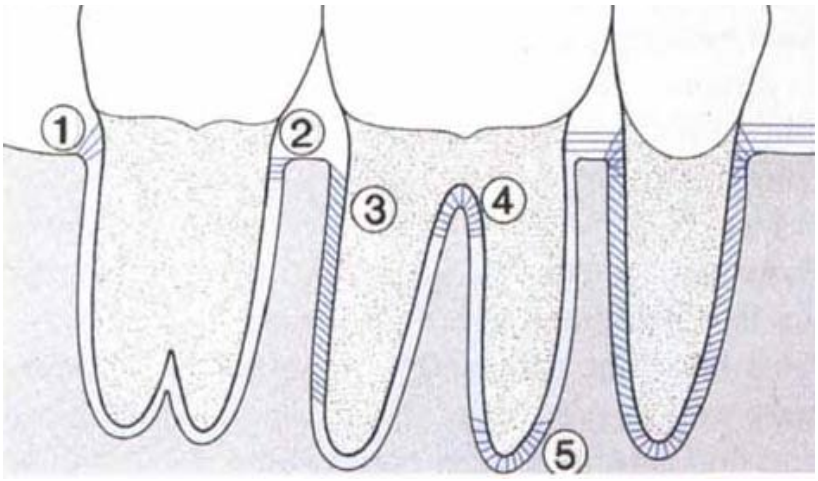

Figure 2: Schematic diagram of the principal fibre network of the PDL (1) alveolar crest fibres (2) horizontal fibres (3) oblique fibres (4) interradicular fibres (5) apical fibres (Diagram from Hassell, 1993).

A number of noncollagenous extracellular matrix proteins are also present in the PDL including fibronectin, osteopontin, fibromodulin, lumican and rheumatoid arthritis antigen (Lallier et al., 2005; Nanci and Bosshardt, 2006).

The PDL performs a number of functions including joining the tooth to its socket, allowing the dentition to withstand masticatory pressure and providing sensory feedback for positioning of the teeth and jaws during mastication (Nanci and Bosshardt, 2006). Due to the ongoing forces of mastication, the PDL constantly is undertaking remodelling and repair (Lallier et al., 2005). The ability of the PDL to support the dentition during function has been explained through three broad theories; tensile, compression, fluid-filled and viscoelastic (Wang et al., 2011). Different roles have

been described for different components of the PDL, with the vascular system and tissue fluid systems proposed to control tooth displacement whilst the fibre network has a very minimal role (Wang et al., 2011). However, the PDL fibre network has varying orientation and depth, thus rather than being a homogenous tissue the PDL is a heterogeneous tissue that is difficult to model using the current approaches (Fill et al., 2012).

5.1.4 Alveolar Bone:

The bony skeleton, which makes up approximately 20% of human body weight, has a number of essential functions, including: mechanical support and mobility, protection of internal organs, calcium and phosphate metabolism and storage, as well as haematopoiesis (Chau et al., 2009). Bone is made up of osteoblasts, osteocytes and osteoclasts (Nakahama, 2010). Osteoblasts, or bone lining cells, communicate with both osteocytes and osteoclasts and drive bone remodelling by expressing differentiation factors to induce the migration of osteoclasts as well as osteoclastogenesis (Nakahama, 2010). Osteoblasts are derived from MSC and are regulated by bone matrix-derived TGFß, bone morphogenetic proteins (BMPs) and their inhibitors, IGF-1, PTH / PTHrP, $1,25(OH)_2D_3$, leptin, glucocorticoids and the Wingless (Wnt)-ß-catenin as well as the Notch signal pathways (Boyce et al., 2013). Osteoclasts are multinucleated cells formed by the fusion of precursor cells from the mononuclear myeloid lineage progenitor cells (Boyce et al., 2013). Osteocytes are the mature differentiated stage of the osteoblast lineage (Kähn and Bonewald, 2012). They are embedded in bone and possess a number of cellular processes which link to other osteocytes as well as osteoblasts via gap junctions (Nakahama, 2010). Osteocytes are thought to have many functions, including regulation of calcium and phosphate homeostasis, detection of load and regulation of bone formation and resorption (Kähn and Bonewald, 2012).

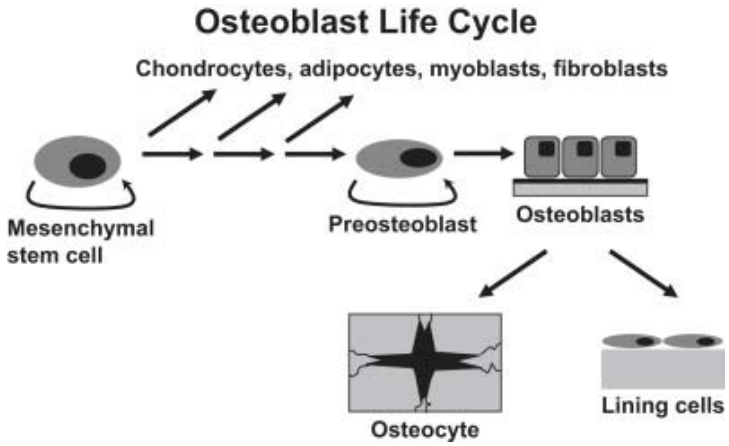

Figure 3: Mesenchymal stem cell precursors develop into osteoblasts and become either embedded in bone as osteocytes or form part of the osteoblasts lining the bone (Diagram from Martin et al., 2011).

Osteogenesis is the process of bone formation, and occurs when osteoblasts increase the expression of several enzymes, including alkaline phosphatase, as well as several proteins including osteoblast cysteine rich protein, osteoblast specific factor and osteoblast stimulatory factor (Lallier et al., 2005). Bone formation and resorption occurs through balanced interactions between osteoblasts and osteoclasts, with mismatch in the number and or activities of bone cells resulting in disruption to skeletal homeostasis and, potentially, local and systemic bone diseases (Street and Lenehan, 2009). This balance between bone cells is controlled by hormones, growth factors, mechanical loading, nutrition and other unidentified factors (Chau et al., 2009).

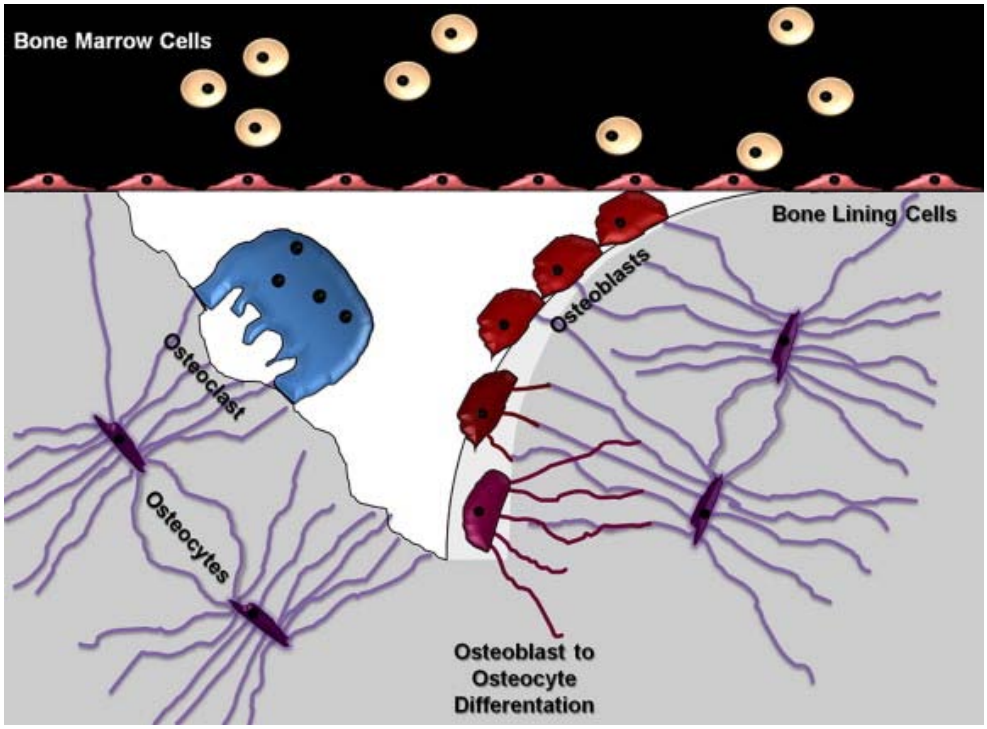

Figure 4: The bone-remodelling unit: Osteoclasts release protons and enzymes into the sealed zone to degrade and digest the mineralized bone matrix. Cuboidal-shaped osteoblasts sit behind the osteoclasts and secrete osteoid. Several differentiation stages of the osteoblast phenotype are illustrated. The spindle-shaped bone lining cells cover all inactive bone surfaces plus the bone-remodelling unit and create an environment where, theoretically, communication between osteoclasts and osteoblasts occurs. Transition stages from the osteoblast to the osteocyte are shown including the early osteoid osteocyte to the mature embedded osteocyte. The role of the osteocyte to create a communication network is demonstrated by the extensive cell processes connecting osteocytes, osteoblasts, bone lining cells and osteoclasts (Diagram from Jähn and Bonewald, 2012).

Two types of bone are present in the mature human skeleton; cortical and trabecular (Hadjidakis and Androulakis, 2006). Cortical bone, which makes up approximately 80% of the skeleton, is dense and compact with a slow turnover whilst trabecular bone is less dense and more elastic with a much

higher turnover (Hadjidakis and Androulakis, 2006). The alveolar process is the maxillary and mandibular bone that contains the tooth sockets (Nanci and Bosshardt, 2006). It consists of buccal and lingual/palatal outer cortical bony plates composed of cortical bone, an inner trabecular structure and bone lining the alveolus (Nanci and Bosshardt, 2006). The bone lining the socket is called alveolar or bundle bone as its walls have a cribriform structure where the Sharpey's fibres of the PDL attach (Cheng et al., 2009; Nanci and Bosshardt, 2006). The alveolar bone and the outer cortical plates meet at the alveolar crest (Nanci and Bosshardt, 2006). The structure of alveolar bone varies between individuals and generally it becomes denser with age (Pham and Kiliaridis, 2011; Cheng et al., 2009).

As throughout the body, the cortical bone contains osteons and Haversian systems and new bone is formed in a lamellar fashion by osteoblasts and the incorporation of osteocytes (Cheng et al., 2009; Nanci and Bosshardt, 2006). The inner spongiosa also contains Haversian systems, although these systems are in large trabeculae filled with predominately yellow marrow (Nanci and Bosshardt, 2006). Trabecular bone is often absent in the anterior region of the anterior teeth, and in these areas cortical bone is directly fused with the alveolar bone (Nanci and Bosshardt, 2006).

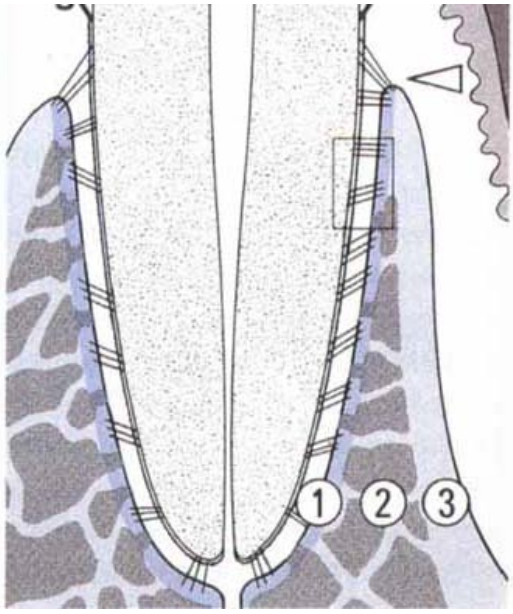

Figure 5: Schematic diagram of the osseous support structure in the mandible. The alveolar process is formed by the alveolar bone proper or bundle bone (1) trabecular bone (2) and compact bone (3) (Diagram from Hassell, 1993).

Alveolar bone continually undergoes remodelling to fulfil physical and physiological requirements (Fleischmannova et al., 2010). Alveolar bone homeostasis differs from that of endochondral bone, as it has a high metabolic turnover, specific extracellular matrix composition, and complex interconnection with the PDL (Fleischmannova et al., 2010). Indeed, resorption of the alveolar process is asynchronous to ensure that the attachment of the PDL is not lost (Nanci and Bosshardt, 2006).

5.1.5 Mesenchymal stem cells and the Periodontium

Stem cells are undifferentiated cells that are able to self-regenerate and differentiate to produce mature progeny cells (Kim et al., 2009). Stem cells may be divided into embryonic or postnatal (adult) (Kim et al., 2009). Cohnhiem, a German Pathologist, first reported the presence of non-haematopoietic adult stem cells in bone marrow approximately 130 years ago (Chamberlain et al., 2007). Throughout the 1980's, Friedenstein demonstrated that adult stem cells isolated in the bone marrow could differentiate into osteoblasts, chondrocytes, adipocytes or myoblasts (Chamberlain et al., 2007). Due to this ability, these cells were called mesenchymal stem cells (MSC) (Chamberlain et al., 2007). Approximately 1 cell in every 10,000 bone marrow cells are MSCs (Chamberlain et al., 2007).

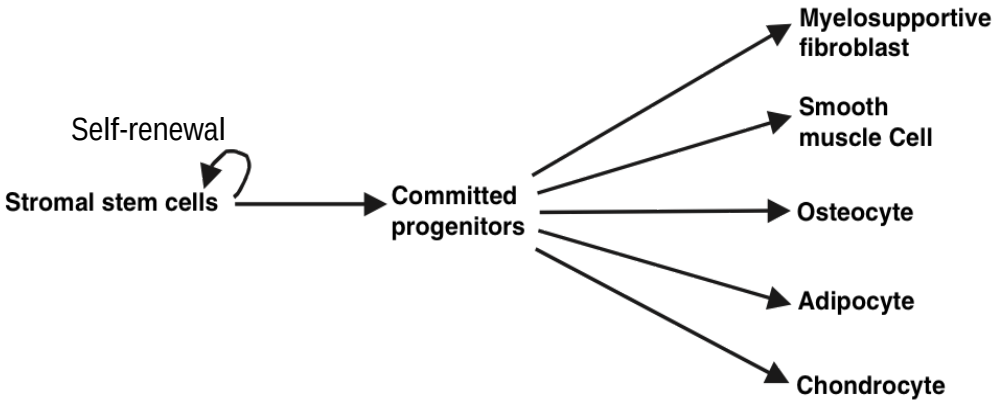

Figure 6: The bone marrow stromal system (Diagram from Shi et al., 2005).

The existence of MSC in dental follicle cells (DFC) has been confirmed through the identification of a number of stem cell markers (Pan et al., 2010). Indeed, five human dental stem / progenitor cells have now been characterized; dental pulp stem cells (DPSCs), stem cells from human exfoliated deciduous teeth (SHED), periodontal ligament stem cells (PDLSC), stem cells from apical papilla (SCAP) and dental follicle stem cells (DFSC) (Pan et al., 2010; Park et al., 2010; Shi et al., 2005). As with other MSC, dental stem cells (DSC) display regenerating capacity for neighbouring and non-neighbouring tissues and are able to differentiate into osteo/odontogenic, adipogenic and neurogenic

cells (Shi et al., 2005; Park et al., 2010). The PDL has multiple cell types and contains progenitor cells for the regeneration and repair of these cells (Park et al., 2010; Shi et al., 2005). Staining of the PDL for MSC markers has shown PDLSC are located predominately in the perivascular region, with small clusters in the extravascular region (Shi et al., 2005).

Shi et al., (2005) noted that previous studies that analysed dental pulp, PDL, cementum and bone marrow derived stem cell populations, found a common expression of antigens associated with endothelium, bone/dentine/cementum and fibroblasts (Shi et al., 2005). From this common antigen expression, Shi et al. (2005) stated that a common molecular regulatory pathway involving transcription factors such as Runx2, Msx1/2 and Pax6/9 and growth factors (BMP, FGF, TGF and WNT) was probably present (Shi et al., 2005). Pan et al. (2010) also reported that Runx2 was important in the differentiation of DFC towards cementoblasts and osteoblasts.

Sununliganon and Singhatanadgit (2011) identified a population of PDLSC clones with high osteogenic potential. These cells were found to express ICAM1 and TGB1 surface markers (Sununliganon and Singhatanadgit, 2011). As with Shi et al. (2005), Sununliganon and Singhatanadgit (2011) found that the expression of key osteoblast marker related genes alkaline phosphatase (ALP), osteocalcin (OCN), biglycan (BGN), collagen type 1, alpha 2 (COL1A2) and Runx2 corresponded to the cells' ability to form mineralised matrix. Sununliganon and Singhatanadgit (2011) suggested that these genes would be a good specific marker of osteoblast differentiation and mineralization of PDLSCs.

5.1.5.1 MSC and Osteoblast proliferation, differentiation and function

The transition of MSC into osteoblasts able to differentiate and form bone is the major event that triggers osteogenesis (Huang et al., 2007). Osetoblast differentiation from MSC precursors is a well-orchestrated process of gene expression that leads to osteoblastic commitment, proliferation and terminal differentiation, and is the primary determinant in bone formation, with cells producing a characteristic extracellular matrix that subsequently mineralizes through the deposition of hydroxyapatite crystals (Jensen et al., 2010; Huang et al., 2007).

The key molecules involved in osteogenesis include extracellular messengers (IL-1, IL-6, TNFalpha, BMP2, 4 and 7, Noggin, FGFbeta, IGF-1 and IGF–II, VEGF, PIGF, PDGF, Wnts, DKK1, Ihh, PTHrP, OPG, RANKL, M-CSF), intracellular messengers (MAPKs, PKA/CREB, ß-Catenin, Runx2, Osterix, Dlx5, Msx2) and cells (MSC, osteoblasts, and adipose tissue derived multipotential cells) (Deschaseaux et al., 2009)

Runx2 is an essential mediator of bone formation by osteoblasts and participates in many signalling pathways regulating osteoblast differentiation (Lin and Hankenson, 2011). Forced expressions of Runx2 in non-osteoblastic fibroblasts has been shown to induce expression of osteoblastic markers such as type I collagen, bone sialoprotein, osteocalcin (OCN) and osteopontin, whilst intramembranous and endochondral ossification is inhibited in Runx2 knockout mice (Lin and Hankenson, 2011; Komori, 2011). BMP, Wnt and Notch signalling pathways all directly regulate Runx2 transcriptional activity and hence affect osteoblast differentiation (Lin and Hankenson, 2011). Indian hedgehog (Ihh) has also been implicated in the activation of Runx2 (Tang et al., 2011). Blood vessel invasion is a critical early step for bone formation, as without it, bone marrow spaces cannot form (Boyce et al., 2013). Runx2 also regulates the VEGF gene in chondrocytes, promoting blood vessel invasion prior to osteogenesis (Boyce et al., 2013). In Runx2 knockout mice (-/-), altered

endothelial cell development and reduced number of blood vessels means that vascular invasion into the cartilage anlagen does not occur (Boyce et al., 2013).

Osterix (Osx) is an osteoblast-specific transcription factor involved in osteoblast differentiation that works downstream to Runx2 and leads to the expression of osteoblast specific markers including type I collagen, OCN, bone sialoprotein and osteonectin (Zhang et al., 2011). Osx may also affect osteoblast proliferation through its action on the Wnt signalling pathway and has been associated with the expression of VEGF in osteoblasts (Zhang et al., 2011; Tang et al., 2011).

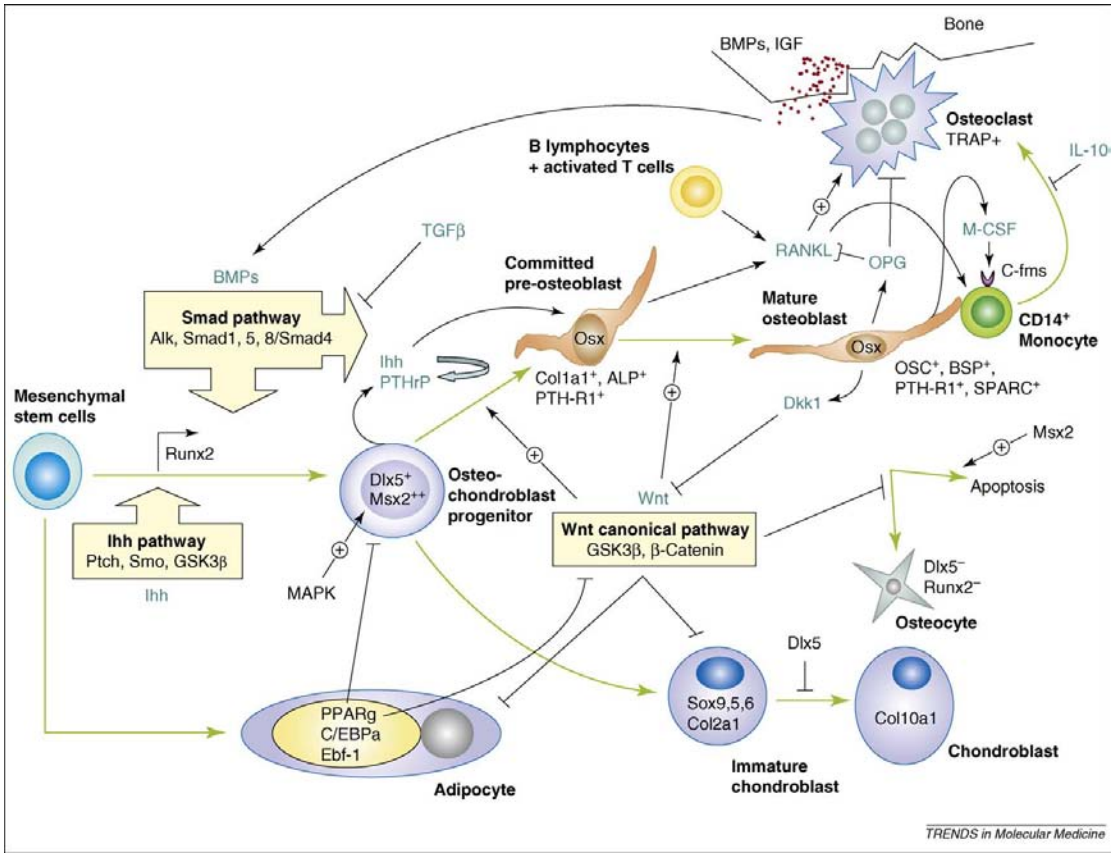

Figure 7: Bone remodelling after fracture showing integration of signalling pathways. MSCs are induced to form new bone following both endochondral and intramembranous pathways. During bone formation, Ihh acts at the initial stages to induce the expression of Runx2. MAPK phosphorylates and activates Runx2. BMPs drive both osteoblastic commitment and maturation through Runx2. Osteochondroblastic progenitors can express Ihh, which induces the secretion of PTHrP and increases the maturation of pre-osteoblastic cells. Wnt induces the proliferation of osteochondroblastic progenitors and pre-osteoblasts. When osteoblasts mature, they can express Wnt inhibitors. Osteoclasts are generated through RANKL and M-CSF cytokines secreted by activated T- and B-lymphocytes and pre-osteoblasts and act to degrade mineralized bone. IL-10 and osteoprotegerin (OPG) regulate the osteoclastic activities. Bone matrix degradation releases several cytokines and growth factors, such as BMPs and insulin-like growth factor (IGF), which in turn activates immature cells (Diagram from Deschaseaux et al., 2009).

5.1.5.2 Synergistic action of MSCs and Haematopoietic Stem Cells (HSC)

All tissue regeneration is limited by angiogenesis (Moioli et al., 2008). Regenerating tissue thicker than 100 – 200 μm exceeds the capacity for diffusion to supply nutrients and remove waste products (Moioli et al., 2008). Both MSC and HSC are found in bone marrow (Moioli et al., 2008). During endochondral bone development, hypertrophic chondrocytes express several critical transcription factors, including VEGF, which promotes angiogenesis (Moioli et al., 2008). Angiogenesis in turn promotes skeletogenesis (Moioli et al., 2008). During fracture healing, a proportion of the mobilized repair cells are derived from vascular tissues (Moioli et al., 2008). HSC and MSC have been found to directly interact, with HSC promoting MSC to differentiate into osteoblasts (Moioli et al., 2008). OBs also promote HSC to mobilize (Moioli et al., 2008).

5.1.6 Features of the Periodontium Unique to Rodents:

The dental patterns of vertebrates vary widely, ranging from anodontia to multiple dentitions replaced throughout life occurring in the oral and pharyngeal cavities (Richman and Handrigan, 2011). Embryological tooth development occurs via a series of interactions between the odontogenic epithelium and neural crest-derived ectomesenchyme (Cobourne and Mitsiadis, 2006). Tight genetic control of this process ensures that both tooth shape and position are highly conserved amongst species and significant variation is rare (Cobourne and Sharpe, 2010). In the human dentition, the deciduous incisor, canine and molar teeth undergo successional replacement by the permanent incisor, canine and premolar teeth whilst the permanent molar teeth erupt as the posterior jaw dimension increases with growth (Moorrees et al., 1969). The rodent dentition is reduced in number compared to the human dentition, with one incisor tooth separated from three molar teeth by a large diastema (Cobourne and Sharpe, 2010). Unlike the human dentition, tooth replacement does not occur and rodents develop only a single dentition. Hence, the rodent molar is

homologous to the human molar, which is also not a successional tooth (Cobourne and Sharpe, 2010).

Rat molars differ from human molars as they undergo physiological distal drift (Milne et al., 2009). Associated with this distal drift is continual resorption of the distal alveolar wall (Milne et al., 2009). In human molars, physiologic mesial drift occurs. The rat molar interradicular bone is composed of the woven or cancellous type bone with osseous trabeculae enclosing a network of vascular channels, some of which are continuous with the PDL (Milne et al., 2009). Rat molars also do not exhibit a distinct lamina dura (Milne et al., 2009). Because of the small size of the rat jaws, secondary osteons are absent and marrow spaces are usually limited to the bone at the level of the apical third of the tooth roots (Milne et al., 2009). Alveolar bone turnover in a rat is also rapid; the duration of each remodelling cycle in the alveolar bone of the mandible in adult rats being estimated at approximately 6 days (Vignery and Baron, 1980).

Rat and human cementum are very similar and can be represented as a woven fabric-like material that provides tissue permeability (Ho et al., 2009). In both species, primary cementum predominately consists of radial collagen fibres whilst secondary cementum presents with wide radial and narrower circumferential collagen fibres (Ho et al., 2009). The cementum and cementodentinal junction from a 9 to 12 month-old rat, however, was noted to be more greatly mineralized, with a noticeably decreased collagen fibre hydration in the cementum and the cementum–dentine interface than a middle aged human adult (Ho et al., 2009).

5.2 Tooth Eruption and Ankylosis

5.2.1 Introduction:

Tooth eruption can be divided into pre-emergent eruption; the intra-osseous phase of eruption, and post emergent eruption; eruption which occurs within the oral cavity. Intra-osseously, eruption occurs when root development begins and the developing tooth moves from its position within its crypt along an eruption pathway, towards the oral cavity (Must et al., 2012; Wise et al., 2011; Proffit and Frazier-Bowers 2007). The dental follicle is essential in the formation of the eruption pathway as it modulates osteoclastogenesis (Wise et al., 2011). Osteogenesis and its resultant alveolar bone growth at the base of the dental follicle has also been proposed to be an important mechanism for eruption (Wise et al., 2011). Many demographic factors such as race and gender, have been associated with altered tooth eruption; however, the underlying molecular mechanisms have yet to be described (Must et al., 2012). Clinically, disruption to the eruption process presents as either delayed, partial or complete failure of eruption secondary to either a mechanical obstruction or biological dysfunction and may be syndromic, isolated or familial in nature (Frazier-Bowers et al., 2010). Non-syndromic eruption disturbances include dentoalveolar ankylosis and primary failure of eruption (Frazier-Bowers et al., 2010). Limited literature is available regarding the aetiology of these disorders, although recently, mutations in the parathyroid hormone receptor gene 1 (PTH1R) have been linked to primary failure of eruption (Frazier-Bowers et al., 2010).

5.2.2 Mechanisms underlying Eruption:

Normal dentofacial growth and occlusal development depend upon normal tooth eruption (Lee and Proffit, 1995). The process of tooth eruption involves a complex array of interactions between osteoblasts, osteoclasts, and the dental follicle, as well as a host of signalling molecules, receptors, transcription factors, and cell adhesion molecules (Ahmad et al., 2006). Experiments by Marks and Cahill in the 1980's demonstrated the importance of the dental follicle in eruption through its

regulation of local osteoclastogenesis and osteoblastogenesis. (Marks and Cahill 1980; Marks and Cahill, 1984; Marks and Cahill, 1987). The stellate reticulum cells found in the dental follicle have been found to secrete parathyroid hormone related peptide, which increases the expression of colony stimulating factor 1 (CSF1) and receptor activator of nuclear factor kappa ß ligand (RANKL), which induce osteoclastogenesis, as well as bone morphogenic protein 2 (Bmp2), which promotes osteoblastogenesis (Wise et al., 2007; Yao et al., 2007). Via scanning electro-microscopy, Marks and Cahill (1986) demonstrated that the alveolar bone architecture surrounding the crypt reflects the physiologic state of the bone, with the coronal region displaying a scalloped edge indicative of osteoclast activity, the sides showing a smooth surface and thus no bony resorption or formation and the apical region indicative of bone formation with trabecular bone present.

5.2.3 Systemic and Local Factors:

Both systemic and local factors ultimately lead to disturbances in either the biologic propulsive mechanism of the eruption process or a mechanical obstruction (Proffit and Frazier-Bowers, 2007). A number of syndromes are associated with eruption failure including cleidocranial dysplasia, ectodermal dysplasia, Gardner syndrome, Down syndrome and Apert's syndrome (Stellzig-Eisenhauer et al., 2010). In these cases, multiple teeth are usually involved. In contrast, local eruption disturbances affect small numbers of teeth (Stellzig-Eisenhauer et al., 2010). Generally, local factors are associated with mechanical obstructions, such as supernumerary teeth, cysts and jaw fractures, ectopic tooth germ position, tooth germ deformity, lack of space, root dilacerations, or bone deficit, for example in patients with cleft lip and palate (Stellzig-Eisenhauer et al., 2010). Influences on the biologic propulsion mechanism are more difficult to define, given that the mechanism itself is also difficult to define. Factors that influence osteogenesis or osteoclastogenesis are often implicated. Osteoclasts resorb bone whilst osteoblasts form new bone in a tightly regulated sequence (Henriksen et al., 2009). A number of regulators are required for this process,

including: parathyroid hormone (PTH), calcitrol, growth hormone (GH), glucocorticoids, thyroid hormone and sex hormones, insulin like growth factor, prostaglandins, tumour growth factor-beta (TGF-ß), bone morphogenetic proteins (Bmp), Indian hedgehog, Wnt signalling family (Wnt), fibroblast growth factors (FGF), and platelet-derived growth factors (PDGF) (Mackie et al., 2008; Hadjidakis and Androulakis, 2006; Henriksen et al., 2009). Events that influence these regulators also influence tooth eruption. For example, during the pre-emergent and eruption stages, the circadian rhythm influences dental eruption (Lee and Proffit, 1995). The influence of this rhythm has been proposed to be secondary to either hormonal / metabolic rhythms, whereby human growth hormone released in relation to the sleep cycle, impacts upon eruptive mechanisms, and/or a rhythmic pattern of forces that oppose eruption, such as resting pressures of the lips and tongue (Lee and Proffit, 1995). Medications may also affect dental eruption. Bisphosphonates are synthetic analogues of pyrophosphate that reduce osteoclast mediated bone resorption (Hiraga et al., 2010). In children with osteogenesis imperfecta, bisphosphonates are utilised to decrease bone fragility (Kamoun-Goldrat et al., 2008). Kamoun-Goldrat et al. (2008) found that tooth eruption was delayed in this group of children in accordance with previous reports from rat studies. Although delayed dental eruption may be a minor side effect when considering the benefits of decreased bone fragility, it may increase the rate of impaction and surgical response required in a group already burdened with a number of dental abnormalities (Kamoun-Goldrat et al., 2008).

5.2.4 Dentoalveolar Ankylosis

Dentoalveolar ankylosis occurs when non-neoplastic bone obliterates the periodontal ligament and fusion occurs between the alveolar bone and cementum or dentine (Raghoebar et al., 1989; Kurol and Magnusson, 1984; Lee et al., 2009; Loriato et al., 2009; Arakeri et al., 2010; Andersson et al., 1984). Dentoalveolar ankylosis has been recorded in two dental conditions: infraocclusion and external root replacement resorption.

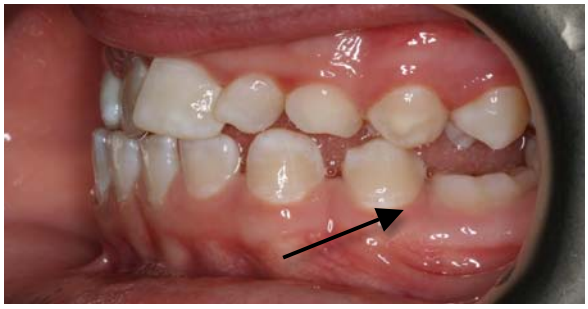

Figure 8: Infraocclusion of tooth 75 (Author's own picture)

5.2.4.1 Aetiology

Infraocclusion (also called secondary retention, submergence, reimpaction or ankylosis) is the cessation of post-emergent tooth eruption when no evidence of a physical barrier or abnormal tooth position is present (Raghoebar et al., 1989; Kurol and Magnusson, 1984; Kurol and Olson, 1991; Ekim and Hatibovi-Kofman, 2001; Ponduri et al., 2009). The prevalence of infraocclusion in the community has been reported to range between 1.3% and 8.9%, with siblings displaying a significantly higher incidence (Ekim and Hatibovi-Kofman, 2001; Kjaer et al., 2008). No difference in occurrence has been identified between males and females (Kjaer et al., 2008). Kurol and Magnusson (1984) reported that the frequency of infraocclusion decreased with age, and that teeth with permanent successors present may erupt normally as local factors involved in deciduous tooth exfoliation may overcome the ankylosis. Generally, deciduous mandibular molars are most frequently affected, followed by the permanent mandibular second molars and permanent maxillary

second molars (Ekim and Hatibovi-Kofman, 2001; Kjaer et al., 2008; Loriato et al., 2009; Shalish et al., 2010).

Although the mechanism leading to the development of dentoalveolar ankylosis remains unknown, various aetiologies have been reported through the literature: including, local trauma causing damage to Hertwig's epithelial root sheath; disturbance to local post-emergent eruptive metabolism; local infection; genetic factors; deficient eruptive force; chemical or thermal irritation; deficient vertical alveolar bone growth; hypercementosis; traumatic masticatory forces and pulpo-periodontal canals (Raghoebar et al., 1989; Kurol and Magnusson, 1984; Kjaer et al., 2008; Ekim and Hatibovi-Kofman, 2001). Once ankylosis occurs, a number of interarch and intraarch consequences may ensue: including, reduced eruption of the affected tooth with concurrent reduced development of adjacent alveolar bone; delayed exfoliation of the deciduous tooth; increased difficulty in performing extraction; abnormal position and development of the permanent successor; tipping of adjacent teeth; over eruption of opposing teeth; as well as dental midline shift. (Ponduri et al., 2009; Loriato et al., 2009; Rosner et al., 2010). Affected teeth are also unresponsive to conventional orthodontic treatment (Rosner et al., 2010). Infraocclusion has been linked with various other dental abnormalities: tooth agenesis; microdont maxillary incisor teeth; delayed tooth development; palatally displaced canine teeth and mandibular second premolar distal angulation (Shalish et al., 2010). It is due to this linkage that a genetic predisposition to infraocclusion has been proposed (Shalish et al 2010).

The development of ankylosis and external root replacement resorption may also occur secondary to trauma to the periodontal ligament (Andersson et al., 1984). The majority of dental injuries involve the anterior teeth and in addition to damage to the dental hard tissues and gingivae, the periodontal ligament and alveolar bone may be impacted upon (Hevoca et al., 2010). Healing depends upon a

range of factors: stage of root development, type and extent of injury and root anatomy as well as the presence of bacterial contamination and repeated injury (Hecova et al., 2010; Andreason et al., 2006). Complications may occur weeks, months or even years post trauma (Hecova et al., 2010). External root resorption is a serious complication post-trauma which may be divided into surface resorption, replacement resorption / ankylosis and inflammatory resorption. A higher incidence of inflammatory and replacement resorption have been reported in dental intrusive luxation and avulsion injuries (Hecova et al., 2010). Root resorption is predominately found on the apical part of the root (58%) although the coronal (23%) and central (19%) root surfaces may also be affected (Crona Larsson et al., 1991). There is no effective treatment for replacement resorption, with root resorption leading to eventual tooth loss (Wigen et al., 2008). Infraocclusion of the affected tooth, impaction and altered mesial drift of adjacent teeth, reduced development of the alveolar process and altered dental midline may occur (Andreason et al., 2006).

5.2.4.2 Diagnosis

In clinical practice, a diagnosis of ankylosis is made through clinical examination, as well as radiographic examination (Andersson et al., 1984; Ekim 2001). A high pitched sound on percussion occurs when greater than 20% of the tooth root surface is ankylosed, whilst decreased mobility may be found when greater than 10% of the tooth root is involved (Andersson et al., 1984; Ekim, 2001). The tooth may also be depressed below the occlusal plane, adjacent teeth may be tipped and opposing teeth may super-erupt (Ekim, 2001). A lateral open bite may also be present secondary to a retardation of the alveolar process (Ekim, 2001). The ability to diagnose ankylosis radiographically is dependent on: the location of the lesion, with labial and lingual ankylotic areas being the least likely to be diagnosed; quality of the radiographs; no overlapping of teeth or bony trabeculae; as well as skill of the operator (Andersson et al., 1984). Clinical examination has been proposed to be more sensitive than radiographic examination (Andersson et al., 1984).

5.5.4.3 Histological Appearance

Histologically, dentoalveolar ankylosis appears as an area of hard tissue resembling bone in direct contact with cementum / dentine, with obliteration of the interceding periodontal ligament (Kurol and Magnusson, 1984). Kurol and Magnusson (1984) found dentoalveolar ankylosis (in infraocclusion) was present on the inner surfaces of the tooth roots; in young children, this ankylosis was located in the apical part of the root whilst in older children it was seen more coronally. Raghoebar et al. (1991) meanwhile, found that dentoalveolar ankylosis was present at the bifurcation and interradicular region of the tooth roots as well as the outer surface. Kurol and Magnusson (1984) suggested that, as the ankylosis was noted to move with age, ankylosis is not a static condition rather it is part of an ongoing remodelling process and, as such, is a developmental change between the tooth and its surrounding alveolar bone. Andersson et al. (1984) identified 2 types of ankylosis microscopically. In the majority of teeth, ankylosis was preceded by resorption of cementum and dentine and no cementum was present at the sites of ankylosis (Andersson et al., 1984). In a few teeth, however, Andersson et al. (1984) observed apposition of bone directly on to the cementum surface without preceding cemental resorption. This ankylosis between cementum and bone was found particularly in the apical regions of the tooth roots. Andersson et al. (1984) also noted two different bony connections; either thin bony trabeculae or wide bony areas. Both types of bony attachment were present in the majority of teeth (Andersson et al., 1984).

5.2.5 Development of Ankylosis in the Laboratory

Ankylosis may also be induced experimentally through mechanical, chemical and thermal means (Dreyer et al., 2000). Dreyer et al., (2000) investigated a cold thermal insult applied to the occlusal surface of a rat molar and the resultant development of aseptic resorption. Application of a cold stimulus was noted to lead to periodontal cell death, with shrinkage and lysis of odontoblasts and other pulpal cells and clastic attack of the root surface with initiation of resorption 2 to 7 days post insult (Dreyer et al., 2000). Dreyer et al. (2000) also reported repair following resorption, and that this reparative ability appeared proportionate to the degree of thermal insult.

Mechanical means of inducing dentoalveolar ankylosis include removal and reimplantation of rat molar teeth with devitalisation of the PDL in Dakin's solution for 5 minutes (Hellsing et al., 1993). Seventeen of the 37 reimplanted teeth showed clinical immobility 14 days post the experiment; however, the remaining 20 rat molars remained mobile and exfoliated during the experiment (Hellsing et al., 1993). Histologically, the ankylosed teeth showed either replacement of the PDL by bone in combination with advanced resorption of the supracrestal root or replacement of part of the peripheral root by bone, although 1 tooth did demonstrate cartilage formation adjacent to the cementum (Hellsing et al., 1993). Teeth that were mobile throughout the experiment showed extensive root resorption and inflammation of their associated soft tissue (Hellsing et al., 1993).

Differences in the response of the teeth may be secondary to the post experiment occlusal forces present (Mine et al., 2005). When no occlusal stimuli were allowed post experimental trauma, dentoalveolar ankylosis was noted in all replanted / transplanted rat molars within a 14 day period, whilst extensive root/bone resorption, an increased PDL width and no dentoalveolar ankylosis was noted if occlusal stimuli were allowed immediately post molar removal and reimplantation (Mine et al., 2005).

5.3 Runx2

5.3.1 Introduction:

Runx2 (also called Cbfa-1, OSF2 and AML3) belongs to the Runx family of transcription factors (Komori, 2011). Isolated in 1994, this family of transcription factors act as master regulators of cell differentiation with Runx1 being essential for haematopoietic stem cell differentiation, Runx2 for osteoblast, chondrocyte and odontoblast differentiation as well as vascular invasion into cartilage and Runx3 for gastric epithelial cell regulation and neurogenesis (Komori, 2011; Ziros et al., 2008; Li et al., 2011). During bone development, Runx2 interacts with a number of major signalling pathways, including FGF, Wnt, Ihh and Osx (Osterix also called Sp7) (Komori, 2011). Runx2 is not essential, however, to maintain osteocytes and is hence time-dependent being seen only in preosteoblasts and osteoblasts (Komori, 2010). Runx2 expression has also been reported during tooth development / eruption and has been reported in all tissues of the periodontium (Lossdorfer et al., 2010). It has also been found in alveolar bone placed under mechanical stress during orthodontic tooth movement (Pavlidis et al., 2009).

5.3.2 Structure and expression

The Runx2 gene has been located to the human chromosome 6p21, contains eight exons and is approximately 220kb in length (Bufalino et al., 2012; Ziros et al., 2008; Camilleri and McDonald, 2006). As with other members of the Runx family, Runx2 has a runt domain; an s type immunoglobulin which acts as a highly conserved binding domain mediating binding between DNA core sequences 5'-PuACCPuCA-3' and 5"-TGPyGGTPy-3' (Ziros et al., 2008). Runx2 interacts with core binding factor ß (CBFß) a small protein which, although itself not binding to DNA, enhances the ability of Runx2 to bind as well as stabilizing Runx2 against proteolytic degradation (Ziros et al., 2008; Camilleri and McDonald, 2006). Transcriptional activity then occurs through Runx2's three

activation domains (AD1-3). AC3, the principal activation domain, is located near the C-terminal end of Runx2, whilst AD1 is located at the N-terminal 19 amino acids and AD2 in a region adjacent to the N-terminal (Ziros et al., 2008). As well as activation, Runx2 is also able to repress transcription via its VWRPY, the last five C-terminal amino acids (Ziros et al., 2008). As a nuclear transcription factor, Runx2 possesses a 9-amino acid sequence between the runt and AD3 regions and nuclear matrix targeting signals (NMTS) direct and supports Runx2's association with the nuclear matrix (Ziros et al., 2008).

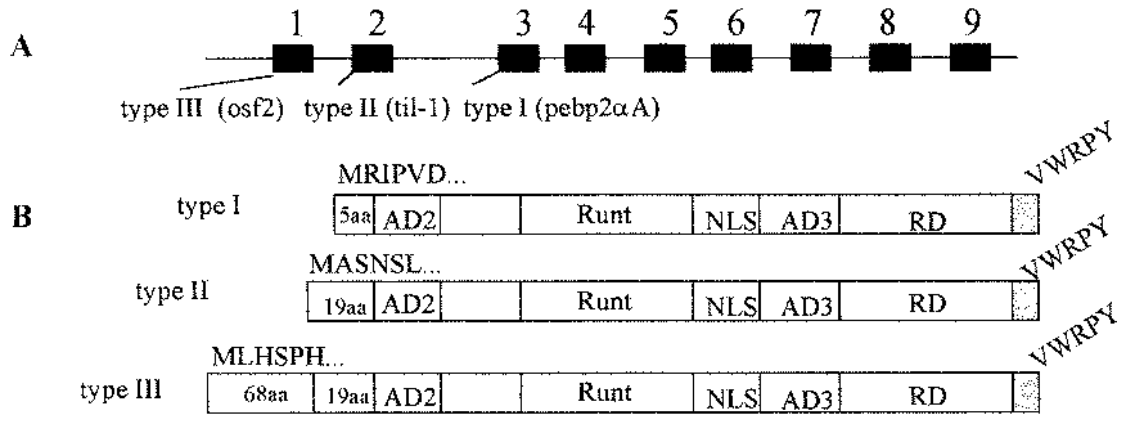

Figure 9: Schematic structure of the three Runx 2 isoforms with N-terminal sequence.

(A) Runx2 gene consists of nine exons and eight introns. (B) Type I contains 513 amino acids starting with the N-terminal sequence MRIPVD. Type II has 19 additional amino acids at the N-terminal and begins with the amino acid sequence MASNSL. Type III contains 87 amino acids at the N-terminal domain and begins with MLHSPH. The runt DNA binding, AD2, AD3, and RD domains are conserved among all three isoforms. Abbreviations: AD, activation domain; RD, repression domain; and NLS, nuclear localization signal (Diagram from Chen et al., 2002).

5.3.3 Biological Functions

5.3.3.1 Skeletal

Osteoblasts form and regulate hydroxyapatite crystals, as well as the extracellular matrix proteins (type I collagen, osteocalcin, osteonectin, osteopontin, bone sialoprotein and proteoglycans) that form bone (Camilleri and McDonald, 2006). While Runx2 plays a crucial role in osteoblast differentiation and function, during embryogenesis, it can be detected on day 9.5 in the notochord and on day 10.5 in all present skeletal elements (Ziros et al., 2008). At this stage, Runx2 directs multipotent MSCs to differentiate towards an osteoblast lineage and upregulates osteoblast specific gene expression; including osteocalcin, alkaline phosphatase, collagenase-3, bone sialoprotein and collagen type I (Ziros et al., 2008). Runx2 expression needs to be carefully regulated, however, as Runx2 knockout mice (-/-) show a total absence of osteoblasts and bone, heterozygous mice display characteristics of the skeletal disorder cleidocranial dysplasia and mice with overexpression display osteopenia, decreased mineral bone density and suffer subsequent fractures (Ziros et al., 2008)

Two forms of Runx2 have been isolated; Isoform type 1 (starting with the sequence MRIPV) involved in intramembranous ossification and 2 (starting with the sequence MASNS) involved in endochondral ossification (Ziros et al., 2008; Komori, 2010). During intramembranous ossification, isotype 1 is widely expressed in osteoprogenitor cells and osteoblasts as opposed to isotype 2 that is located in bone lining cells (Ziros et al., 2008).

5.3.3.2: Non-Skeletal:

Runx2 has been found to be expressed in several non-skeletal tissues, including the testis, ovary, specific compartments of the brain, as well as during the process of spermatogenesis (Jeong et al., 2008). Runx2 is now thought to be involved in many cellular functions beyond the activation of tissue-specific target genes, such as osteocalcin and other bone proteins expressed in the mature

osteoblasts (Jeong et al., 2008). Runx2 has also been found to play a role in cell fate determination, regulate ribosomal genes and control protein synthesis machinery, as well as modulate the expression of a variety of growth factors including VEGF and matrix metalloproteinases (Jeong et al., 2008). Further investigation is required into Runx2 functional activities in non-skeletal tissues.

5.3.3.3: Dental:

Runx2 is also essential in dental development and has been located in rodent tooth germs at E12 (mesenchymal condensates of forming bones and teeth in the maxillae and mandible) and in the dental papilla and follicle at E14 (cap stage of dental development) (Li et al., 2011; Chen et al., 2009). Embryologically, Runx2 is expressed by both CNC derived dental mesenchyme tissues; the dental papilla and dental follicle (Camilleri and MacDonald, 2006). Differentiation of odontoblasts and ameloblasts from the dental papilla is directed by reciprocal interactions between inner enamel epithelium (IEE) and the mesenchymal cells directly facing the inner enamel epithelium and is mediated by molecules including Wnt, Runx2 and TGF beta (transforming growth factor) families (Fleischmannova et al., 2010). Osteoblasts and odontoblasts, whilst sharing many similar genes, also share similar proteins with dentine sialophosphoprotein (DSPP), the main non-collagenous protein in dentine also found to a lesser degree in osteoblasts and ameloblasts (Camilleri and McDonald, 2006; Chen et al., 2002). Multiple Runx2 binding sites have been discovered in the DSPP promoter and Runx2 has been found to upregulate expression of DSPP in immature odontoblasts, whilst repressing its expression in mature odontoblasts (Li et al., 2011). In knockout mice (-/-) molar tooth germ formation does not proceed beyond the cap stage and odontoblasts in the incisor region are absent / deformed and enamel formation does not occur (Li et al., 2011; Camilleri and McDonald, 2006). Enamel knot marker genes including cyclin dependent kinase 1A (p21), FGF4, ectodysplasin A receptor (Edar) and BMP4 are all downregulated and sonic hedgehog (Shh) absent in mandibular molars only, whilst maxillary molars display essentially normal enamel

knot marker genes and weak Shh signals at the tips of the tooth buds (Camilleri and McDonald, 2006). Therefore, whilst Runx2 seems essential for tooth development of the enamel knot and thus up to the bell stage of development, it seems to have different down stream targets within the jaws (Camilleri and McDonald, 2006). In mice exhibiting overexpression of Runx2, odontoblasts differentiate into osteoblasts and osteogenesis replaces normal dentinogenesis (Li et al., 2011; Camilleri and McDonald, 2006). DSPP expression is also severely downregulated in Runx2 overexpression, as is nestin (NES), an intermediate filament protein present in odontoblasts but not osteoblasts (Komori et al., 2010).

Differences between the isotypes have also been noted in dental development, with isotype 1 expression higher than type 2 in odontoblasts, ameloblasts and the dental pulp (Chen et al., 2002). This differs to bone in which type 1 isotype is more weakly expressed than type 2 isotype (Chen et al., 2002). Type 2 isotype was also more strongly expressed in the dental papilla prior to crown development, but then down regulated at the bell stage (Camilleri and McDonald, 2006). Low levels of expression of Runx2 type 2 isotype continue throughout all stages of tooth and root development within cementoblasts, cementocytes, periosteal tissue, osteoblasts and osteocytes of the periodontium (Camilleri and McDonald, 2006).

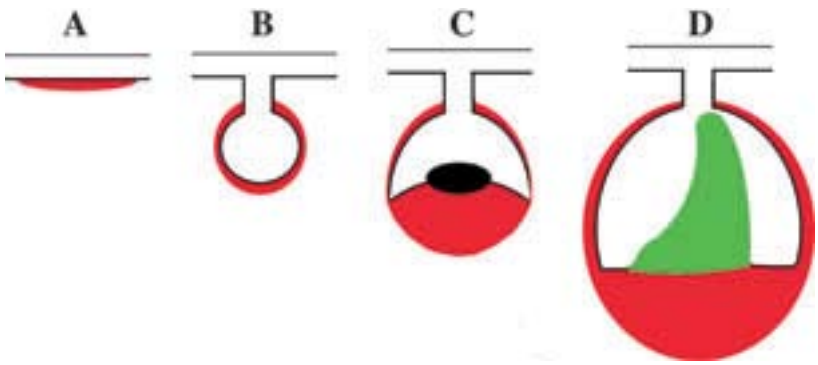

Figure 10: Patterns of Runx2 expression during dental development.

A: Initiation stage. Runx2 expression in the mesenchyme is induced by the odontogenic epithelium.

B: Bud stage. Runx2 expression occurs around the ingrowing dental epithelium.

C: Cap stage. Runx2 expression is maintained in both the mesenchyme and dental follicle. Runx2 is required for formation of the enamel knot as well as Sonic Hedgehog (Shh) expression.

D: Bell stage. Runx2 expression is downregulated in the dental papilla but maintained in the dental follicle and surrounding mesenchyme (Diagram from Camilleri and McDonald, 2006).

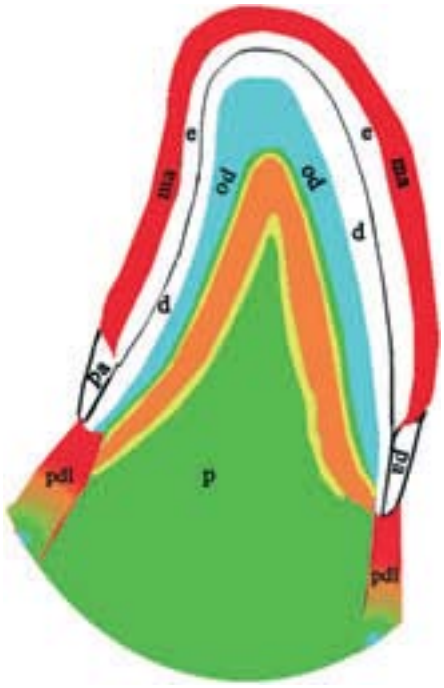

Figure 11: Runx2 mRNA expression in the secretory stage of dental development, with different colours representing different levels of expression.

pa: pre-ameloblasts show no Runx2 expression

ma: maturational phase ameloblasts strongly express Runx2.

p: dental papilla displays diffuse expression.

od: Runx2 up-regulation is seen in pre-odontoblasts although no expression is seen in differentiated odontoblasts.

pdl: periodontal ligament shows strong Runx2 expression as does cementoblasts and cementocytes.

(Diagram from Camilleri and McDonald, 2006).

Fibroblasts within the periodontal ligament (PDL), express isotype 2 Runx2, although in order to maintain the width of the PDL, Runx2 expression is suppressed (Camilleri and McDonald, 2006). Deformation of the PDL secondary to mechanical stress results in differentiation of MSC and increases expression of Runx2, as well as its binding ability via the extracellular signal related kinase

(ERK) MAPK pathway (Camilleri and McDonald, 2006). In mice deficient in Runx2, alveolar bone may be absent or deformed (Fleischmannova et al., 2010). A single functioning Runx2 gene is sufficient to produce an adequate bone remodelling response (Camilleri and McDonald, 2006).

Runx2 may be involved in the formation of bone-like tissues in reparative dentine (Miyazaki et al., 2008). Continuous expression of Runx2 in odontoblasts disturbs odontoblast differentiation and results in the formation of a bone-like structure (Miyazaki et al., 2008). Runx2 down regulates odontoblast specific proteins, nestin and DSPP, and induces osteopontin and DMP1, indicating that Runx2 induces odontoblasts to differentiate into osteoblasts (Miyazaki et al., 2008). Runx2 needs to be down regulated during odontoblast differentiation to acquire odontoblast differentiation for dentinogenesis (Miyazaki et al., 2008).

5.3.4 Signalling Pathways:

A number of chemical and physical stimuli modify the phosphorylation / activation of Runx2, as well as its interaction with other proteins (Ziros et al., 2008). Runx2 is also involved with a number of signalling pathways; FGF, Wnt, Ihh, Osx (Komori, 2011). Osx, a zinc finger containing protein, is also essential in osteoblast differentiation (Komori, 2011). MSC that are Runx2+/ Osx- are able to differentiate into osteoblasts or chondrocytes (Komori, 2011). BMP and IGF mediate Osx expression via MAPK and protein kinase D pathways and Runx2 (Komori, 2011). Osx (also called SP7) can also be mediated by BMP independent of Runx2 through MSX2 (Komori, 2011). As with Runx2, osteoblast precursors under the control of Osx are found intimately associated with invading blood vessels; thus Komori (2011) proposed that Osx might also be involved in blood vessel invasion into developing bone.

Runx2 is also associated with fibroblast growth factor (FGF) signalling. Four FGF receptor genes (FGFR) have been located in mammals and FGFR1, FGFR2 and FGFR3 all regulate osteoblast and chondrocyte proliferation and differentiation (Komori, 2011). Each FGFR has specific and redundant roles during osteoblast differentiation; FGFR1 signalling induces and activates Runx2, FGFR2 enhances Runx2 mRNA expression and activates Runx2 whilst FGFR3 limits the proliferation of chondrocytes and promotes the proliferation of osteoblasts (Komori, 2011; Lian et al., 2011). Several FGF ligands are essential for limb bud growth and are expressed in both endochondral and intramembranous ossification (Lian et al., 2011).

The Wnt pathway has many roles including directing cell fate during development and regulating bone mass post natally (Lian et al., 2011). Currently, the functions of canonical Wnt signalling in Runx2 expression are controversial (Komori, 2011). Wnt signalling has been proposed to enhance Runx2 expression through the promotion of protein-to-protein interactions at the Runx2 promoter region (Komori, 2011). This activation leads to Runx2 up regulating Tcf7 expression in osteoblasts and chondrocytes (Komori, 2011).

Figure 12: Effects of WNT signalling on osteoblastic differentiation. Stages of differentiation are indicated by the expression of specific promoters Prx1, Runx2, Osx and OCN at high and low levels (Diagram from Galli et al., 2010).

Indian hedgehog (Ihh) expression induces Runx2 expression in osteoblast precursors during endochondral bone formation. Ihh also inhibits Runx2 expression by inducing parathyroid hormone related peptide (Komori, 2011).

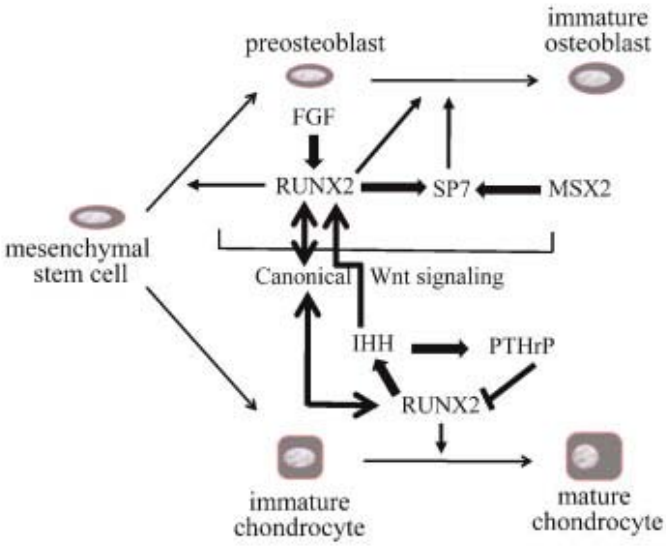

Figure 13: Runx2, SP7 (also called Osterix), and canonical Wnt signalling are essential for osteoblast differentiation and chondrocyte maturation.

Runx2 induces Sp7 expression in preosteoblasts and Ihh (Indian hedgehog) expression in chondrocytes. FGF (fibroblast growth factor) induces Runx2 expression and activates Runx2 in the osteoblast lineage. Wnt induces Runx2 expression and activates Runx2. Ihh induces Runx2 expression in osteoprogenitors (Diagram from Komori, 2011)

Runx2 activity is directly regulated by the mitogen activated protein kinase (MAPK) pathway, which acts to phosphorylate proteins secondary to a variety of stimuli (Wang et al., 2011). MAPK phosphorylate and activate Runx2 by binding type I collagen to alpha2beta1 integrins on the osteoblast surface (Marie, 2008). Runx2 itself is able to act on kinases such as p85 PI3K, thus influencing osteoblast differentiation and survival, as well as on the cell cycle via its interaction with nuclear regulatory proteins, acting to negatively control osteoblast proliferation (Marie, 2008). Thus, Runx2 acts through multiple pathways to control osteoblastogenesis (Marie, 2008).

5.3.5 Runx2 and Tooth Eruption:

In tooth eruption, Hertwig's epithelial root sheath (HERS) stimulates dental papilla cells to differentiate into root odontoblasts under the control of sonic hedgehog (Shh) and enamel matrix protein signalling (Fleischmannova et al., 2010). Cementoblasts differentiate from dental follicle cells migrating through the increasing space between the HERS cells during HERS fenestration (Fleischmannova et al., 2010). Cementoblasts / cementocytes have also been found to express Runx2, although findings are inconsistent and variations in species have been found (Camilleri and McDonald, 2006). In mice studies, data have proved inconsistent in regards to effects on eruption times and no difference has been found in dental development of mice with Runx2 +/- (Camilleri and McDonald, 2006).

5.3.6 Runx2 and Orthodontic Tooth Movement:

Orthodontic tooth movement (OTM) occurs when an orthodontic appliance places a mechanical force on the tooth and its surrounding periodontal tissues leading to bone remodelling and tooth movement. Initially, displacement occurs within the PDL resulting in regions of tension and compression as well as changes in oxygen levels, cellular activity, the influx of inflammatory cytokines and formation of hyalinised tissues (Brooks et al., 2009). Remodelling of the hyalinised tissue results in tooth movement (Brook et al., 2009). Inconsistencies are present in the literature regarding Runx2 expression during OTM, as not all animals display expression (Brooks, et al., 2009). Inconsistencies are also present regarding the timing of Runx2 expression, with studies finding Runx2 present at or prior to 24 hours post onset of force application (Kawarizadeh et al., 2005; Watanabe et al., 2007) as well as post 24 hours (Brooks et al., 2009).

5.3.7 Runx2 and Dentoalveolar Ankylosis:

Currently, no literature is available in regards to Runx2 and its role in dentoalveolar ankylosis. Runx2 is essential for bone formation, acting as a master regulator for MSC cell differentiation to osteoblasts, as well as interacting with a number of signalling pathways and promoting vascularisation through its action on haematopoietic stem cells and VEGF genes (Komori, 2011; Ziros et al., 2008; Li et al., 2011; Boyce et al., 2013). Therefore, Runx2 expression by bone cells, as well as PDL cells, is potentially important for the development of bony ankylosis following hypothermal trauma.

5.3.8 Runx2 and Disease:

Mutations of the Runx gene have been linked to a number of cancers including leukaemia (Runx1), gastric cancer (Runx3) and osteosarcoma (Runx2) (Pratap et al., 2011). Runx2 has also been linked to the promotion of tumour growth and metastasis in breast and prostate cancer by protecting cancer cells against apoptotic mechanisms and regulating proteins such involved in motility and invasion of cancer cells (Pratap et al., 2011).

Cleidocranial dysplasia (CCD) is a rare autosomal dominant disorder secondary to haploinsufficiency of the Runx2 gene (Bufalino et al., 2012). Individuals with CCD present with short stature, delayed closure of the cranial fontanels and sutures, wormian bones, frontal bossing, maxillary hypoplasia, rudimentary or absent clavicles and a wide pubic symphysis (Bufalino et al., 2012). Dentally, individuals may present with absence of cellular cementum, multiple supernumerary teeth, retention of the primary dentition, delayed eruption with consequent impaction of the permanent teeth (Bufalino et al., 2012; Pan et al., 2009). Early and or ectopic Runx2 expression is also thought to be causative in the development of craniosynostosis, ectopic bone formation and limb defects (Maeno et al., 2011).

5.4 VEGF

5.4.1 Introduction

Vascular endothelial growth factor (VEGF) belongs to the superfamily of Platelet Derived Growth Factors (PDGF) (Bates, 2010). Isolated in the 1980's as a tumour secreted factor, it was initially called Vascular Permeability Factor before been identified as a pro-angiogenic factor in 1989 (Bates, 2010). Currently, the VEGF family is made up of VEGF-A (also called VEGF), PlGF (Placental growth factor), VEGF-B (particularly abundant in heart and skeletal muscle), VEGF-C and VEGF-D (involved in lymphatic development), VEGF-E (homologue of VEGF identified in the genome of the parapoxvirus Orf Virus with VEGF-A like activities) and VEGF-F (snake venom VEGF) (Takahashi and Shibuya, 2005; Bates, 2010). All 5 members of the VEGF family have various isoforms with multiple functions in blood and lymph vessel formation and homeostasis and are able to bind to specific receptor tyrosine kinases (RTK) (Bates, 2010; Stuttfeld and Ballmer, 2009; Eichmann and Simons, 2012).

VEGF is a major regulator of physiologic and pathologic angiogenesis and is secreted by tumour and normal cells, as well as in tissues undergoing growth or remodelling (Klagsbrun and D'Amore, 1996; Canavese et al; 2010). VEGF is also important for osteoblast differentiation and osteoclast recruitment (Dai and Rabie, 2007; Maharaj et al., 2006; Wang et al., 2011). A number of factors, including hypoxia, growth factors, p53 mutation, oestrogen, thyroid stimulating hormone, tumour promoters and nitric oxide act to regulate VEGF gene expression (Takahasi and Shibuya, 2005). Expression of VEGF by the inner enamel epithelium has been reported during tooth development in both rats and humans (Ide et al., 2011). It has also been located in the PDL during orthodontic tooth movement and local administration of recombinant VEGF has been shown to enhance tooth movement (Chae et al., 2011; Miyagawa et al., 2009).

5.4.2 Structure and expression

The human VEGFA gene consists of eight exons separated by seven introns and is located on chromosome 6p21.3 (Takahasi and Shibuya, 2005). Secondary to exon splicing, VEGF exists as at least nine different isoforms as designated by the number of amino acids after the signal sequence cleavage (Ferrara et al., 2003). These isoforms include $VEGF_{165}$, $VEGF_{121}$, $VEGF_{145}$, $VEGF_{189,}VEGF_{165}$, $VEGF_{183}$, $VEGF_{189}$ and $VEGF_{206}$, of which $VEGF_{165}$ is the most abundant and best characterized (Ferrara et al., 2003; Supice et al., 2009; Takahasi and Shibuya, 2005). Most parenchymal cells produce VEGF ligands. These ligands act in a paracrine manner on adjacent endothelial cells to influence their VEGF receptor signalling and biology and may be important for the survival of these cells (Koch et al., 2011). Through their common N-terminal portion, all the VEGF protein isoforms can interact with both VEGFR1 and 2, although their affinity with VEGFR1 is much higher (Giacca and Zacchigna, 2012)

In the oral mucosa, VEGF has been located in the epithelium of normal mucosa, particularly in the suprabasal regions (Carille et al., 2001). Positive staining was also noted in blood vessels and in small numbers of fibroblasts, inflammatory cells, salivary glands and muscle (Carille et al., 2001). VEGF expression has also been documented in inflamed epithelium and Malassez's epithelial rest cells in the PDL (Yamawaki et al., 2010). Indeed, the presence of VEGF in saliva has been postulated as one of the reasons for an increased healing rate in the mouth (Carille et al., 2001).

5.4.3 Biological functions

The vascular system is a dynamic structure with diverse functions including the regulation of nutrient, water and waste products, the modulation of vascular tone as well as playing a role in systemic endocrine balance (Eggington, 2011). Rather than being a static system, the vascular network has the ability to alter capillary density according to the needs of the individual through the process of

capillary growth, also known as angiogenesis (Eggington, 2011). Angiogenesis is important component of many physiologic processes including cyclic renewal of the endometrium, corpus luteum formation, placenta formation, tissue growth and differentiation, as well as reparative processes for example fracture healing, wound healing and liver regeneration (Kajdaniuk et al., 2011). A number of cytokines have been identified in the regulation of blood vessel formation, with VEGF seen as the predominant regulator (Street and Lenehan, 2009; Eichmann and Simon, 2012). Indeed, VEGF is one of the most influential genes, regulating a variety of biological functions (Eichmann and Simons, 2012).

Before its role in angiogenesis was realized, VEGF was associated with vascular barrier integrity. Vascular endothelial cell-to-cell contact forms a barrier that is regulated by adherens junction (AJ) protein complexes including VE-cadherin, ß-catenin, p120-catenin and alpha catenin (Chen et al., 2012). VEGF upregulation activates Src-family protein tyrosine kinase (PTK) which promotes AJ phosphorylation and facilitates barrier breakdown and vascular permeability (Chen et al., 2012). VEGF also influences pericytes, branched cells lying within the basement membrane of capillaries, that act to reinforce vascular structure and regulate microvascular blood flow via their contractile mechanism (Riabatti et al., 2011). In hypoxic conditions, VEGF directly induces proliferation and migration of pericytes (Ribatti et al., 2011).

VEGF is also important in bone ossification, modelling and remodelling. VEGF is a potent regulator of osteoblast lifespan in-vitro, as well as also directly effecting osteoblastic cells as it regulates gene expression of ALP (alkaline phosphatase), OCN (osteocalcin) and OPG (osteoprotegerin) through the VEGFR2 signalling pathway (Street and Lenehan, 2009; Tan et al., 2011). Osteoblasts themselves, are able to influence the production of VEGF through their modulation of hypoxia inducible factor (HIF) in response to hypoxia. During endochondral ossification, VEGF expression

was modulated by Runx2 (Zelzer et al., 2001). In Runx2 deficient mice, VEGF was not upregulated in hypertrophic chondrycytes nor the perichondrium (Zelzer et al., 2001). In contrast, mice with overexpression of Runx2 in fibroblasts displayed increased VEGF expression (Zelzer et al., 2001).

5.4.4 Signalling pathways

VEGF binds to three high affinity RTKs; VEGFR1, which acts to trap VEGF and inhibit VEGF signalling, VEGFR2 which appears to mediate most of the pro-angiogenic effects of VEGF including stimulation of endothelial cells differentiation, proliferation, migration and morphogenesis, and VEGFR3, which regulates lymphatic and blood vessel formation (Suplice et al., 2009; Eichmann and Simon, 2012). Structurally, VEGFRs present with an extracellular, ligand-binding domain composed of immunoglobulin-like loops, a transmembrane domain, a juxtamembrane domain, a split tyrosine kinase domain and a C-terminal tail (Koch et al., 2011). Generally, VEGFR1 expression has been reported with monocytes and macrophages, VEGFR2 in vascular endothelial cells and VEGFR3 in lymphatic endothelial cells (Koch et al., 2011) .

At least two important pathways are essential for bony vascularisation during development; hypoxia-inducible factor 1α (HIF-1α), promoted by the hypoxic environment of the early mesenchymal condensations destined to form bone, and Runx2, the master transcriptional activator of bone formation (Kwon et al., 2011) HIF-1 consists of alpha and beta units, with the alpha unit impacted upon by the local oxygen levels (Kim et al., 2002). Lowered tissue oxygenation, for example in wound healing, stabilizes HIF-1α (hypoxia inducible factor 1α) and upregulates genes involved in angiogenesis, cell survival, the glycolytic pathway and apoptosis (Lee et al., 2012; Koch et al., 2011; Kwon et al., 2011). Runx2 is able to both bind and stabilize HIF-1α, inducing and maintaining microvessels during endochondral bone formation (Lee et al., 2012). Indeed a lack of HIF-1α has been found to lead to narrow and poorly vascularised bone whist Runx2 knockout mice have been

found to show no VEGF expression at all (Zhang et al., 2011). Other factors also play a role however, as, in Osx null mice, vascularisation is also lacking and no cortical or trabecular bone is also formed (Zhang et al., 2011). Osteoblasts are able to produce VEGF in normal and pathological conditions in order to stimulate new vessel growth during osteogenesis (Kim et al., 2002; Corrado et al., 2011). This expression of VEGF is upregulated by a number of cytokines and growth factors including prostaglandin E_1 and E_2, transforming growth factor ß1, insulin like growth factor I and 1,25 dihydroxyvitamin D_3 (Kim et al., 2002; Corrado et al., 2011). VEGF, however, is also able to act on osteoblasts, and has been found to increase the differentiation, migration and alkaline phosphatase activity of osteoblasts (Kim et al., 2002). During osteoblast differentiation in periosteal derived cells, VEGF has even been found to increase the transcriptional activity of Runx2 via the MEK/ERK MAPK signalling pathway (Hah et al., 2009).

5.4.5 VEGF and tooth eruption

VEGF has been proposed to work in concert with colony stimulating factor-1 (CSF-1) to upregulate osteoclastogenesis during tooth eruption (Yao et al., 2006). In order for tooth eruption to progress, osteoclasts are required to form an eruption pathway (Yao et al., 2006). Two bursts of osteoclast numbers have been noted during tooth eruption in the rat mandibular region, the first at day 3 post-natally and then again at day 10 post natally (Yao et al., 2006). The dental follicle has been identified as the major regulator of tooth eruption, and this control is exerted by the release of CSF-1 at day 3, which up-regulates RANK (receptor activator of nuclear factor kappa-ß) in osteoclast precursors (Yao et al., 2006). By day 10, however, CSF-1 levels are low (Yao et al., 2006). VEGF was found to increase in expression at day 10 and work in concert with CSF-1 to upregulate RANK and promote osteoclastogenesis as well as osteoclast proliferation (Yao et al., 2006).

5.4.6 VEGF and orthodontic tooth movement

An adequate blood supply is critical to orthodontic tooth movement as the blood vessels within the PDL are actively involved in the regulation of tissue remodelling (Krishnan and Davidovitch, 2009; Ren et al., 2008). OTM is facilitated by bony remodelling with resorption of the alveolar bone in the direction of displacement (compression side) and deposition on the tension side (Dandajena et al., 2011). Differences in the blood vessel behaviour has been noted in these compression and tension regions (Ren et al., 2008).

Rygh et al. (1986) investigated the behaviour and role of blood vessels and blood-borne cells in the PDL of rats following placement of fixed orthodontic appliance with an active spring to cause mesialisation of the first molar. Change in vascularity was measured by blood vessel lumen size, presence of oxytalan and elastic-like fibres within blood vessel walls. Rygh et al (1986) found that vessels on the pressure side of the PDL were occluded, with a subsequent increase in blood vessels adjacent to the hyalinzed zone followed by invasion of blood vessels into this zone. An increase in vasculature was also noted in regions of osteoclastic activity and in areas of tension (Rygh et al., 1986).

Miyagawa et al. (2009) also found that compression of the PDL during orthodontic tooth movement lead to activation of the vascular system. VEGF was localized on the compressive side of rat periodontal tissue during experimental tooth movement and PDL cells were strongly positive for VEGF at day 7 following orthodontic tooth movement (Miyagawa et al., 2009). VEGF was also noted in osteoclasts in resorption lacunae and in multinucleated giant cells appearing along hyalinized tissues on day 7, at which point bone resorption was also present (Miyagawa et al., 2009). On the tension side of orthodontic tooth movement, VEGF was present to a lesser extent in PDL cells and osteoblasts (Miyagawa et al., 2009). From these studies, VEGF is thought to have a role in both

periodontal ligament and bone remodelling (Di Domenico et al., 2012).

Figure 14: Mechanical forces during OTM are transduced to the cells, triggering a biologic response. A number of cytokines are expressed including VEGF (Diagram from Di Domencio et al., 2012)

Dandajena et al (2011) investigated upregulation of osteoclast growth factors from osteoblasts in-vitro and the subsequent conversion of peripheral blood mononuclear cells into OC under hypoxic stress. RANKL levels were found to directly correlate to HIF-1alpha and VEGF levels and functionally active OC were only observed when hypoxia was present (Dandajena et al., 2011). Dandajena et al. (2011) theorized that during orthodontic tooth movement, osteoclasts were formed from peripheral blood mononuclear cells secondary to release of osteoclast growth factors (RANKL) as well as VEGF by osteoblasts subjected to hypoxic conditions.

5.4.7 VEGF and dentoalveolar ankylosis

Currently there is no literature on VEGF and the development of dentoalveolar ankylosis.

5.4.8 VEGF and disease

In chronic wounds, cancer and other pathological conditions characterized by inflammation, tissue remodelling and growth, expression of VEGF is upregulated by both hypoxic cells and infiltrating leukocytes, resulting in sustained and aberrant vascularisation (De Palma, 2012). VEGF is produced by many tumours and, as such, is a key target for many anti-angiogenic therapies. VEGF actively promotes cancerisation through its pro-angiogenic properties, as well as by its ability to increase vessel permeability and upregulation of endothelial adhesion molecules, thus providing an inflammatory tumour environment (Linde et al., 2012). Vascular permeability and pro-angiogenic factors are also thought to be important in the pathogenesis of allergic asthma, with VEGF being released by alveolar macrophages, epithelial cells, smooth muscle cells and CD4+ T cells in the lungs (Song et al., 2012).

5.5 References

1. Adams SL, Cohen AJ, Lassova L. “Integration of signaling pathways regulating chondrocyte differentiation during endochondral bone formation.” Journal of Cellular Physiology 213 (2007): 635 - 641.
2. Ahmad S, Bister D, Cobourne MT. (2006) The clinical features and aetiological basis of primary eruption failure. Eur J Orthod. 28(6): 535-40
3. Al-Awadhi EA, Garvey MT and Smith CP. (2012) An atypical presentation of mechanical failure of eruption of a mandibular permanent molar: diagnosis and treatment case report. European Archives of Paediatric Dentistry 13(3): 152 - 6
4. Andreasen JO, Bakland LK, Andreasen FM. (2006) Traumatic intrusion of permanent teeth. Part 2. A clinical study of the effect of preinjury and injury factors, such as sex, age, stage of root development, tooth location and extent of injury including number of intruded teeth on 140 intruded permanent teeth. Dental Traumatology 22; 90 - 8
5. Andersson L, Blomlöf L, Lindskog S, Feiglin B, Hammarström L. (1984) Tooth ankylosis. Clinical, radiographic and histological assessments. Int. J. Oral Surg. 13; 423 - 31
6. Arakeri G, Kusanale A, Zaki GA, Brennan PA. (2010) Pathogenesis of posttraumatic ankylosis of the temporomandibular joint: a critical review. British Journal o Oral and Maxillofacial Surgery, doi:10.1016/j.bjoms.2010.09.012
7. Bastholm Billie M-L, Thomsen B and Kjaer I. (2011) Apoptosis in the human periodontal membrane evaluated in primary and permanent teeth. Acta Odontologica Scandinavica; Early Online, 1-4
8. Bates DO (2010) Vascular endothelial growth factors and vascular permeability. Cardiovascular Research Advance Access published April 16, 2010.

9. Beertsen W, McCulloch CAG, Sodek J. (1997) The periodontal ligament: a unique, multifunctional connective tissue. Periodontology 2000 13; 20 - 40

10. Boyce B, Zuscik MJ, Xiang L. (2013) Genetics of Bone Biology and Skeletal Disease. Pages 3 – 24 Copyright © 2013 Elsevier Inc. All rights reserved ISBN: 978-0-12-387829-8

11. Breir G, Risau W. (1996) The role of vascular endothelial growth factor in blood vessel formation. Trends in Cell Biology

12. Brooks PJ, Nilforoushan D, Manolson MF, Simmons CA, Gong S-G (2009) Molecular markers of early orthodontic tooth movement. Angle Orthod 79; 1108 - 1113

13. Bufalino A, Paraniba LMR, Gouvea AF, Gueiros LA, MArtelli-Junior HH, Junior JJ, Lopes MA, Graner E, de Almeida OP, Vargas PA, Coletta RD. (2012) Cleidocranial dysplasia: oral features and genetic analysis of 11 patients. Oral Diseases 18; 184 - 190

14. Cahill DR, Marks SC Jr. Tooth eruption: evidence for the central role of the dental follicle. J Oral Pathol 1980; 9:189–200.

15. Canavese M, Altruda F, Ruzicka T, Schauber J. (2010) Vascular endothelial growth factor (VEGF) in the pathogenesis of psoriasis – A possible target for novel therapies. Journal of Dermatological Science, doi 10.1016/j.jdermsci2010.03.023

16. Camilleri S, McDonald F. (2006) Runx2 and Dental Development. European Journal of Oral Sciences 114; 361 – 373

17. Carbonare LD, Valenti MT, Zanatta M, Donatelli L and Lo Cascio V. (2010) Circulating mesenchymal stem cells with abnormal osteogenic differentiation in patients with osteoporosis. Arthritis and Rheumatism 60; 3356 – 65

18. Carille J, Harada K, Macluskey M, Chisholm DM, Ogden GR, Schor SL, Schor AM. (2001) Vascular endothelial growth factor (VEGF) expression in oral tissues; possible relevance to angiogenesis, tumour progression and field cancerisation. J Oral Pathol Med 30; 449 - 457

19. Chadipiralla Y, Yochim JM, Bahuluyan B, Huang CY, Garcia-Godoy F, Murray PE and Steinicki EJ. (2010) Osteogenic differentiation of stem cells derived from human periodontal ligaments and pulp of human exfoliated deciduous teeth. Cell Tissue Res; 340(2):323 - 33
20. Chae HS, Park H-J, Hwang HR, Kwon A, Lim W-H, Yi WJ, Han D-H, Kim YH, Baek J-H. (2011) The effects of antioxidants on the production of pro-inflammatory cytokines and orthodontic tooth movement. Mol Cells 32; 189 – 196
21. Chau JFL, Leong WF and Li B. (2009) Signalling pathways governing osteoblast proliferation, differentiation and function. Histology and Histopathology 24(12); 1593 - 606
22. Chamberlain G, Fox, J, Ashton, B and Middleton J. (2007) Concise Review: Mesenchymal Stem Cells: Their Phenotype, Differentiation Capacity, Immunological Features, and Potential for Homing. Stem Cells; 25: 2739 – 49
23. Chen XL, Nam JO, Jean C, Lawson C, Walsh CT, Goka E, Limt ST, Tomar A, Tancioni I, Uryu S, Guan JL, Acevedo LM, Weis SM, Cheresh DA, Schiaepfer DD (2012) VEGF induced vascular permeability is mediated by FAK. Dev Cell 22; 146 - 157
24. Cheng A, Daly CG, Logan RM and Goss AN. (2009) Alveolar bone and the bisphosphonates. Australian Dental Journal 54(1 suppl1): s51 – 61
25. Cho MI, Garant PR. Development and general structure of the periodontium. Periodontol 2000; 24: 9-27.
26. Chung U-I, Kawaguchi H, Takato T and Nakamura K. (2004) Distinct osteogenic mechanisms of bones of distinct origins. Journal of Orthopaedic Science 9; 410 - 414
27. Cobourne MT and Sharpe PT (2010) Making up the numbers: The molecular control of mammalian dental formula. Seminars in Cell and Developmental Biology. 21(3); 314 - 324
28. Corrado A, Neve A, Cantatore FP. (2011) Expression of vascular endothelial growth factor in normal, osteoarthritic and osteoporotic osteoblasts. Clin Exp Med Nov 29. Epub ahead

of print (Published 2013 13(1); 81 – 4).

29. Crockett JC, Mellis DJ, Scott DI, Helfrich MH. (2011) New knowledge on critical osteoclast formation and activation pathways from study of rare genetic diseases of osteoclasts: focus on RANK/RANKL axis. Osteoporos Int 22; 1 – 20
30. Crona-Larsson G, Bjarnason S, Norén JG (1991) Effect of luxation injuries on permanent teeth. Endod Dent Traumatol 7; 199 - 206
31. Dai J and Rabie ABM. (2007) VEGF: an essential mediator of both angiogenesis and endochondral ossification. Journal of Dental Research 86; 937 - 50
32. Dandajena TC, Ihnat MA, Disch B, Thorpe J, Currier GF (2011) Hypoxia triggers a HIF mediated differentiation of peripheral blood mononuclear cells into osteoclasts. Orthodontics and Craniofacial Research 15(1); 1-9 doi: 10.1111/j.1601-6343.2011.01530.x.
33. De Palma M. (2012) Partners in Crime: VEGF and IL-4 conscript tumour-promoting macrophages. The Journal of Pathology doi: 10.1002/path.4008
34. Deschaseaux F, Sensébé L and Heymann D. (2009) Mechanisms of bone repair and regeneration. Trends in Molecular Medicine 15(9); 417 – 29
35. De Souza Nunes LS, De Oliverira RV, Holgado LH, Fiho HN, Ribeiro DA and Matsumoto MA. (2010) Immunoexpression of CBFA-1/Runx2 and VEGF in sinus lift procedures using bone substitutes in rabbits. Clinical Oral Implants and Research January 22 Epub ahead of print
36. Di Iulio D (2007) Relationship of epithelial cells and nerve fibres to experimentally induces dentoalveolar ankylosis in the rat. Doctor of Clinical Dentistry thesis. The University of Adelaide, South Australia
37. Dreyer CW, Pierce AM and Lindskog S. (2000) Hypothermic insult to the periodontium: a model for the study of aseptic tooth resorption. Endodontics and Dental Traumatology 16; 9 – 15

38. Eichmann A, Simons M. (2012) VEGF signaling inside vascular endothelial cells and beyond. Current opinion in cell biology. Feb 24. [Epub ahead of print]

39. Eggington S (2011) Physiological factors influencing capillary growth. Acta Physiologica 202; 225 - 239

40. Ekim SL and Hatibovic-Kofman S. (2001) A treatment decision-making model for infraoccluded primary molars. International Journal of Paediatric Dentistry 11; 340 – 6

41. Ferrara N, Gerber H-P, LeCouter J. (2003) The biology of VEGF and its receptors. Nature Medicine 9 (6); 669 – 676

42. Fill TS, Toogood RW, Major PW, Carey JP (2012) Analytically determined mechanical properties of, and models for the periodontal ligament: Critical review of the literature. Journal of Biomechanics 45; 9 – 16

43. Fleischmannova J, Matalova E, Sharpe PT, Misek I, Radlanski RJ. (2010) Formation of the tooth –bone interface. Journal of Dental Research 89; 108 – 115

44. Foster BL. (2012) Methods for studying tooth root cementum by light microscopy. International Journal of Oral Science 4; 119 – 128

45. Frankel B, Hong A, Baniwai SK, Coetzee, GA, Ohlsson C, Khalid O and Gabet Y. (2010) Regulation of adult bone turnover by sex steroids. Journal of Cellular Physiology April 16 (Epub ahead of print)

46. Frazier-Bowers SA, Simmons D, Wright JT, Proffit WR, Ackerman JL. (2007) Primary failure of eruption and PTH1R: The importance of a genetic diagnosis for orthodontic treatment planning. American Journal of Orthod Dentofacial Orthop 137; 160e1 – 160e7

47. Frazier-Bowers SA, Puranik CP, Mahaney MC. (2010) The etiology of eruption disorders - further evidence of a 'genetic paradigm. Seminars in Orthodontics 16; 180 - 185

48. Giacca M, Zacchigna S. (2012) VEGF gene therapy: therapeutic angiogenesis in the clinic and beyond. Gene Therapy doi:10.1038/gt.2012.17

49. Gundberg CM. (2003) Matrix proteins. Osteoporos Int 14 (suppl 5); s37 - 42

50. Hadjidakis DJ, and Androulakis II (2006) Bone remodeling. Ann N Y Acad Sci 1092; 385 - 396

51. Hah YS, Jun JS, Lee SG, Park BW, Kim DR, Kim UK, Kim JR, Byun JH. (2009) Vascular endothelial growth factor stimulates osteoblastic differentiation of cultured human periosteal derived cells expression vascular endothelial growth factor receptors. Mil Biol Rep 38; 1443 - 1450

52. Hammarström L, Alatli I and Fong CD. (1996) Origins of cementum. Oral Diseases 2; 63 - 69

53. Hartmann C. (2009) Transcriptional networks controlling skeletal development. Current Opinion in Genetics and Development 19; 437 - 443

54. Hassell TM. (1993) Tissues and cells of the periodontium. Periodontology 2000 3; 9 - 38

55. Hecova H, Tzigkounakis V, Merglova V, Netolicky J. (2010) A retrospective study of 889 injured permanent teeth. Dental Traumatology 26; 466 – 75

56. Hellsing E, Alatli-Kut I, Hammarstrôm L (1993) Experimentally induced dentoalveolar ankylosis in rats. International Endodontic Journal 26; 93 – 98

57. Henriksen K, Neutzsky-Wulff AV, Bonewald LF and Karsdal MA. (2009) Local Communication on and within bone controls bone remodelling. Bone 44; 1026 – 33

58. Ho SP, Yu B, Yun W, Marshall GW, Ryder MI, Marshall SJ. (2009) Structure, chemical composition and mechanical properties of human and rat cementum and its interface with root dentin. Acta Biomateriala 5(2); 707 – 718.

59. Hojo H, Ohba S, Yano F and Ching U-I. (2010) Co-ordination of chondrogenesis and osteogenesis by hypertrophic chondrocytes in endochondral bone development. Journal of Bone and Mineral Metabolism 28(5); 489 - 502

60. Huang GT, Gronthos S and Shi S. (2009) Mesenchymal stem cells derived from dental tissues vs. those from other sources: their biology and role in regenerative medicine. J Dent Res; 88(9): 792 - 806

61. Huang W, Yang S, Shao J and Li YP. (2007) Signaling and transcriptional regulation in osteoblast commitment and differentiation. Frontiers in Bioscience 12; 2068 - 92

62. Ide S, Tokuyama R, Davaadorj P, Shimozuma M, Kumasaka S, Tatehara S, Satomura K. (2011) Leptin and vascular endothelial growth factor regulates angiogenesis in tooth germs. Histochem Cell Biol 135; 281 - 292

63. Jähn K, Bonewald LF (2012) Chapter 1 – Bone Cell Biology: Osteoclasts, Osteoblasts, Osteocytes in Pediatric Bone (Second Edition) Biology & Diseases Pages 1–8 doi: 10.1016/B978-0-12-382040-2.10001-2

64. Jensen ED, Gopalakrishnan R and Westendorf JJ. (2010) Regulation of gene expression in osteoblasts. International Union of Biochemistry and Molecular Biology 36(1); 25 - 32

65. Jeong JH, Jin JS, Kim HN, Liu JC, Otto F, Mundios S, Stein JL, van Wijnen AJ, Lian JB, Stein GS, Choi JY. (2008) Expression of Runx2 transcription factor in nonskeletal tissues, sperm and brain. J Cell Physiol 21; 511- 517

66. Jones GN, Pringle DR, Yin Z, Carlton MM, Powell KA, Weinstein MB, Toribio RE, La Perle KMD and Kirschner LS. (2010) Neural crest specific loss of Prkar1a causes perinatal lethality resulting from defects in intramembranous ossification. Molecular Endocrinology 24; 1559 - 1568

67. Kadar K, Kiraly M, Porcsalmy B, Molnar B, Racz GZ, Blazsek J, Kallo K, Gera I, Gerber G and Varga G. (2009) Differentiation potential of stem cells from human dental origin – promise for tissue engineering. Journal of Physiology and Pharmacology 60 suppl 7; 167 – 75

68. Kajdaniuk D, Marek B, Borgiel-Marek H, Kos-Kudla B. (2011) Vascular endothelial growth factor (VEGF) part 1: in physiology and pathophysiology. Polish Journal of Endocrinology 62; 444 – 455

69. Kaku M, Kohno S, Kawata T, Fujita T, Tokimasa C, Tsutsui K, Tanne K. (2001) Effect of vascular endothelial growth factor on osteoclast induction during tooth movement in mice. Journal of Dental Research 80; 1880 – 1883

70. Kamoun-Goldrat A, Ginisty D, Le Merrer M. (2008) Effect of bisphosphonates on tooth eruption in children with osteogenesis imperfecta. Eur J Oral Sci 116(3); 195 - 198

71. Kawarizadeh A, Bourauel C, Götz W, Jäger A. (2005) Early responses of periodontal ligament cells to mechanical stimulus in vivo. J Dent Res. 84:902–906.

72. Kjaer I, Fink-Jensen M and Andreasen JO. (2008) Classification and sequelae of arrested eruption of primary molars. International Journal of Paediatric Dentistry 18; 11 - 7

73. Koch S, Tugues S, Li X, Gualandi L, Claesson-Welsh, L (2011) Signal transduction by vascular endothelial growth factor receptors Biochem J, 437 (2011), pp. 169–183

74. Kim HH (2002) Stabilization of hypoxia inducible factor 1 alpha in the hypoxic stimuli induced expression of vascular endothelial growth factor in osteoblastic cells. Cytokine 17(1); 14 - 27

75. Klagsbrun M, D'Amore PA. (1996) Vascular endothelial growth factor and its receptors. Cytokine and Growth Factor Reviews 7(3) 259 – 270

76. Kolar P, Gaber T, Perka C, Duda GN, Buttgereit F. (2011) Human early fracture hematoma is characterized by inflammation and hypoxia. Clin Orthop Relat Res 46(9); 3118 – 3126

77. Komori T. (2010) Regulation of bone development and extracellular matrix protein genes by Runx2. Cell Tissue Res 339; 189 – 95

78. Komori T (2011) Signalling Networks in Runx2-Dependent Bone Development. Journal of Cellular Biochemistry 112: 750 – 755

79. Kraan MC, Haringman JJ, Ahern MJ, Breedveld FC, Smith MD, Tak PP (2000) Quantification of the cell infiltrate in synovial tissue by digital image analysis. Rheumatology 39; 43 – 49

80. Kurol J and Magnusson BC. (1984) Infraocclusion of primary molars: a histologic study. European Journal of Oral Sciences 92; 564 – 76

81. Kurol J and Olson L. (1991) Ankylosis of primary molars – a future periodontal threat to the first permanent molars? European Journal of Orthodontics 13; 404 – 9

82. Kwon T-G, Zhao X, Yang Q, Li Y, Ge C, Zhao G and Franceshi RT (2011) Physical and functional interactions between Runx2 and HIF-1α induce vascular and endothelial growth factor gene expression. Journal of Cellular Biochemistry 112(2); 2582 - 2593

83. Kwun IS, Cho Yem Lomeda RAR, Shin HI, Choi JY, Kang YH and Beattie JH. (2010) Zinc deficiency suppresses matrix mineralisation and retards osteogenesis transiently with catch-up possibly through Runx2 modulation. Bone 46; 732 – 41

84. Lallier TE, Spencer A, Folwler, MM (2005) Transcript profiling of periodontal fibroblasts and osteoblasts. Journal of Periodontology 76, 7; 1044 – 1055

85. Lee CF, Proffit WR. (1995) The daily rhythm of tooth eruption. Am J Orthod Dentofacial Orthop. 107(1); 38-47.

86. Lee KJ, Joo E, Yu HS and Park YC. (2009) Restoration of an alveolar bone defect caused by an ankylosed mandibular molar by root movement of the adjacent tooth with miniscrew implants. American Journal of Orthodontics and Dentofacial Orthopedics 136; 440 - 9

87. Lee SH, Che X, Jeong JH, Choi JY, Lee YJ, Lee YH, Bae SC, Lee YM (2012) Runx2 stabilizes hypoxia-inducible factor-1α through competition with pVHL and stimulates angiogenesis in growth plate hypertrophic chondrocytes. J Biol Chem. 2012 Feb 20. [Epub ahead of print]

88. Lekic PC, Pender N, McCulloch CA. (1997) Is fibroblast heterogeneity relevant to the

health, diseases and treatments of periodontal tissues? Crit Rev Oral Biol Med 8(3); 253 – 268

89. Li S, Kong H, Yao N, Yu Q, Wang P, Lin Y Kuang R, Zhao X, Xu J, Zhu Q, Ni L. (2011) The role of runt related transcription factor 2 (Runx2) in the late stage of odontoblast differentiation and dentin formation. Biochemical and Biophysical Research Communications 410; 698 – 704
90. Lian JB, Stein GS, Montecino M, Stein JL, van Wilnin AJ (2011) Genetic and epigenetic control of regulatory machinery for skeletal development and bone formation: contributions of Vitamin D3 Chapter 16 in Principles of Bone Biology, 3rd edition pp. 301 – 319. Academic Press Inc.
91. Lin GL and Hankenson KD (2011) Integration of BMP, Wnt, and Notch signalling pathways in osteoblast differentiation. J. Cell. Biochem DOI 10.1002/jcb.23287
92. Linde N, Lederle W, Depner S, van Rooijen N, Gutschalk CM, Mueller MM. (2012) Vascular endothelial growth factor induced skin carcinogenesis depends on recruitment and alternative activation of macrophages. The Journal of Pathology "accepted article" DOI:10.1002/path.3989
93. Ling L, Nurcombe V and Cool SM. (2009) Wnt signalling controls the fate of mesenchymal stem cells. Gene 433; 1-7
94. Long (2008) Targeting intercellular signals for bone regeneration from bone marrow mesenchymal stem cells. Cell Cycle 7:14, 2106 – 2111
95. Loriato LB, Machado AW, Souki BQ and Pereira TJ. (2009) Late diagnosis of dentoalveolar ankylosis: Impact on effectiveness and efficiency of orthodontic treatment. American Journal of Orthodontics and Dentofacial Orthopedics 135; 799 – 808

96. Lossdörfer S, Abou Jamra B, Rath-Deschner B, Götz W, Abou Jamra R, Braumann B, Jäger A (2009) The role of periodontal ligament cells in delayed tooth eruption in patients with cleidocranial dysostosis. J Orofac Orthop. 70(6); 495 – 510

97. Mackie EJ, Ahmed YQ, Tatarczuch L, Chen K-S and Mirams M. (2008) Endochondral ossification: How cartilage is converted into bone in the developing skeleton. The International Journal of Biochemistry and Cell Biology 40; 46 - 62

98. Machado E, Fernandes MH, de Sousa Gomes P (2012) Dental stem cells for craniofacial engineering. Oral Surgery, Oral Medicine, Oral Pathology and Radiology 113 (6); 728 – 733

99. Maharaj ASR, Saint-Geniez M, Maldonado AE and D'Amore PA. (2006) Vascular Endothelial Growth Factor Localisation in the Adult. American Journal of Pathology 168 (2); 639 - 48

100. Marcellini S, Bruna A, Henriquez JP, Albistur M, Reyes AE, Barriga EH, Henriquez B and Montecino M. (2010) BMC Evolutionary Biology;10:78

101. Maeno T, Moriishi T, Yoshida CA, Komori H, Kanatani N, Izumi SI, Takaoka K, Komori T. (2011) Early onset of Runx2 expression causes craniosynostosis, ectopic bone formation and limb defects. Bone 49; 673 - 682

102. Marks SC Jr, Cahill DR. (1984) Experimental study in the dog of the non-active role of the tooth in the eruptive process. Arch Oral Biol ; 29:311–22.

103. Marks SC Jr, Cahill DR. Regional control by the dental follicle of alterations in alveolar bone metabolism during tooth eruption. J Oral Pathol 1987; 16:164–9

104. Marie PJ. (2008) Transcription factors controlling osteoblastogenesis. Archives of Biochemistry and Biophysics 473; 98 – 105

105. Martin TJ, Sims NA, Quinn JMW (2011) Chapter 8 - Interactions among osteoblasts, osteoclasts and other cells in bone in Osteoimmunology Interaction of the Immune and Skeletal Systems. Pages 227 – 267
106. Meikle MC. (2007) On the transplantation, regeneration and induction of bone: The path to bone morphogenetic proteins and other skeletal growth factors. Surgeon 5; 232 – 43
107. Miyagawa A, Chiba M, Hayashi H, Igarashi K. (2009) Compressive force induces VEGF production in Periodontal Tissues. Journal of Dental Research 88; 752 - 756
108. Milne TJ, Ichim I, Patel, B, McNaughton A, Meikle MC. (2009) Induction of osteopenia during experimental tooth movement in the rat: alveolar bone remodeling and the mechanostat theory. European Journal of Orthodontics 31; 221 - 231
109. Mine K, Kanno Z, Muramoto T, Soma K. (2005) Occlusal forces promote periodontal healing of transplanted teeth and prevent dentoalveolar ankylosis; An experimental study in rats. Angle Orthod 75; 637 - 644
110. Miyagawa A, Chiba M, Hayashi H, Igarashi K. (2009) Compressive force induces VGF production in periodontal tissues. Journal of Dental Research 88 (8); 752 - 6
111. Miyazaki T (2008) "Inhibition of the terminal differentiation of odontoblasts and their transdifferentiation into osteoblasts in Runx2 transgenic mice." Archives of Histology and Cytology 71 (2); 131 – 146
112. Moioli EK, Clark PA, Chen M, Dennis JE, Erickson HP, Gerson SL and Mao JJ. (2008) Synergistic actions of hematopoietic and mesenchymal stem/progenitor cells in vascularising bioengineered tissues. PLoS ONE; 3(12) e3922
113. Nakahama, K (2010) Cellular communications in bone homeostasis and repair. Cell. Mol Life Sci. 67; 4001 – 4009

114. Nanci A, Bosshardt DD. (2006) Structure of periodontal tissues in health and disease. Periodontology 2000 40; 11 – 28.

115. Niver EL, Leong N, Greene J, Curtis D, Ryder MI and Ho SP. (2011) Reduced functional loads alter the physical characteristics of the bone-periodontal ligament-cementum complex. Journal or Periodontal Research doi: 10.1111/j.1600-0765.2011.01396.x.

116. Pan K, Sun Q, Zhang J, Ge S, Li S, Zhao Y and Yang P (2010) Mutlilineage differentiation of dental follicle cells and the roles of Runx2 overexpression in enhancing osteoblast/cementoblast related gene expression in dental follicle cells. Cell Proliferation 43(3); 219 – 228

117. Park JY, Jeon SH and Choung PH. (2010) Efficacy of periodontal stem cell transplantation in the treatment of advanced periodontitis. Cell Transplantation; Aug 18 Epub ahead of print (Published 2011 20(2); 271 – 285).

118. Pavlidis D, Bourauel C, Rahimi A, Gotz W, Jager A. (2009) Proliferation and differentiation of periodontal ligament cells following short-term tooth movement in the rat using different regimens of loading. European Journal of Orthodontics 31; 565 - 571

119. Pham D and Kiliaridis S. (2011) Evaluation of changes in trabecular alveolar bone during growth using conventional panoramic radiographs. Acta Odontologica Scandinavica, Early Online, 1-6

120. Ponduri S, Birnie DJ and Sandy JR. (2009) Infraocclusion of secondary deciduous molars – an unusual outcome. Journal of Orthodontics 36; 186 – 9

121. Pratap J, Lian JB, Stein GS. (2011) Metastatic bone disease: Role of Transcription factors and future targets. Bone 48; 30 - 36

122. Prockop DJ. (2009) Repair of tissues by adult stem/progenitor cells (MSCs): controversies, myths, and changing paradigms. Molecular Therapy; 17(6): 939 – 46

123. Proffit WR, Frazier-Bowers SA (2009) Mechanism and control of tooth eruption: overview and clinical implications. Orthod Craniofac Res. 12(2): 59-66.

124. Raghoebar GM, Boering G, Jansen HWB, Vissink A. (1989) Secondary retention of permanent molars: a histologic study. Oral Pathology 18(8); 427 – 31

125. Raghoebar GM, Boering G and Vissink A. (1991) Clinical, radiographic and histological characteristics of secondary retention of permanent molars. Journal of Dentistry 19; 164 – 70

126. Raggatt LJ and Partridge NC. (2010) Cellular and molecular mechanisms of bone remodelling. J Biol Chem; 285(33): 25103 - 8

127. Raucci A, Bellosta P, Grassi R, Basilico C, Mansukhan A (2008) Osteoblast Proliferation or Differentiation Is Regulated by Relative Strengths of Opposing Signaling Pathways. J. Cell. Physiol. 215: 442–451

128. Ribatti D, Nico V, Crivellato E. (2011) The role of pericytes in angiogenesis. Int J Dev Biol 55; 261 - 268

129. Richman J, Handrigan GR. (2011) Reptilian tooth development. Genesis. Jan 21. doi: 10.1002/dvg.20721. [Epub ahead of print]

130. Rosner D, Becker A, Casap N, Chaeshu S. (2010) Orthosurgical treatment including anchorage from a palatal implant to correct an infraoccluded maxillary first molar in a young adult. Am J Orthod Dentofacial Orthop 138; 804 - 9

131. Rygh P, Bowling K, Hovlandsdal L, Williams S. (1986) Activation of the vascular system: A main mediator of periodontal fiber remodeling in orthodontic tooth movement. American Journal of Orthodontics 89(6); 453 – 468

132. Rygh P. (1976) Ultrastructural changes in tension zones of rat molar periodontium incident to orthodontic tooth movement. American Journal of Orthodontics 70(3); 269 - 281

133. Shalish M, Peck, S, Wasserstein A, Peck L. (2010) Increased occurrence of dental anomalies associated with infraocclusion of deciduous molars. Angle Orthod. 80; 44 – 5
134. Schinke T, Karsenty G. (2011) Transcriptional control of osteoblast differentiation and function. Chapter 5 in Principles of Bone Biology, 3rd edition pp. 301 – 319. Academic Press Inc.
135. Sedgley CM, Botero TM (2012) Dental stem cells and their sources. Dental Clinics of North America 56, 3; 549 - 561
136. San Miguel SM, Fatahi MR, Li H, Igwe JC, Aguila HL and Kalajzic I. (2010) Defining a visual marker of osteoprogenitor cells within the periodontium. Journal of Periodontal Research 45; 60-70
137. Schinke T and Karsenty G. (2008) Transcriptional control of osteoblast differentiation and function. Chapter 5 in Principles of Bone Biology. 3rd Ed. Academic Press Inc.
138. Shi S, Bartold PM, Miura M, Seo BM, Robey PG and Gronthos S. (2005) The efficacy of mesenchymal stem cells to regenerate and repair dental structures. Orthod Craniofac Res;8(3): 191 – 9
139. Shi SR, Liu C, Taylor CR. (2007) Standardization of immunohistochemistry for formalin-fixed, paraffin-embedded tissue sections based on the antigen-retrieval technique: from experiments to hypothesis. J Histochem Cytochem; 55:105-109
140. Shinmura Y, Tsuchiya S, Hata K-I, Honda MJ. (2008) Quiescent epithelial cell rests of Malassez can differentiate into ameloblast-like cells. Journal of Cellular Physiology 217(3); 728 - 38
141. Song C, Ma H, Yao C, Tao X, Gan H. (2012) Alveolar macrophage derived VEGF contributes to allergic airway inflammation in a mouse asthma model. Scandanavian Journal of Immunology. 75(6); 599 – 605 doi: 10.111/j.1365-3083.2012.02693.x

142. Steinbrech DS, Mehrara BJ, Saadeh PB, Chin G, Dudziak ME, Gerrets RP, Gittes GK, Longaker MT (1999) Hypoxia regulates VEGF expression and cellular proliferation by osteoblasts in vitro. Plast Reconstr Surg 104:738–747

143. Stellzig-Eisenhauer A, Decker E, Meyer-Marcotty P, Rau C, Fiebig BS, Kress W, Saar K, Rüschendorf F, Hubner N, Grimm T, Witt E, Weber BH. (2010) Primary failure of eruption (PFE)--clinical and molecular genetics analysis. J Orofac Orthop. 71(1); 6-16.

144. Street J, Lenehan B. (2009) Vascular endothelial growth factor regulates osteoblast survival- evidence for an autocrine feedback mechanism. Journal of Orthopaedic Surgery and Research. 4; 19 - 32

145. Stuttfeld E, Ballmer-Hofer K. (2009) Structure and Function of VEGF receptors. IUBMB Life 61(9); 915 – 922

146. Strydom H, Maltha JC, Kuijpers-Jagtman AM, Von den Hoff J. (2012) The oxytalan fibre network in the periodontium and its possible mechanical function. Archives of Oral Biology 57; 1003 – 1011

147. Sulpice E, Ding S, Muscatelli-Groux B, Bergé M, Han ZC, Plouet J, Tobelem G, Merkulova-Rainon T. (2009) Cross talk between the VEGF-A and HGF signaling pathways in endothelial cells. Biol Cell 101; 525 – 539

148. Takahasi H, Shibuya M. (2005) The vascular endothelial growth factor (VEGF)/VEGF receptor system and its role under physiological and pathological conditions. Clinical Science 109; 227 – 242

149. Tan YY, Yang Y-Q, Chai L, Wong RWK and Rabie ABM. (2011) Effects of vascular endothelial growth factor (VEGF) on MC3T3-E1. Orthodontics and Craniofacial Research 13; 223 – 228

150. Ten Cate AR. (1996) The role of epithelium in the development, structure and function of the tissues of tooth support. Oral Diseases 2; 55 - 62

151. Urbich C and Dimmeler S. (2004) Endothelial progenitor cells: Characterisation and role in vascular biology. Circulation Research; 95:343 – 53

152. Vignery A, Baron R. (1980) Dynamic histomorphometry of alveolar bone remodeling in the adult rat. Anatomical Record 196; 191 – 200

153. Wang C-Y, Su M-Z, Chang H-H, Chiang Y-C, Tao S-H, Cheng J-H, Fuh L-J, Lin C-P (2011) Tension-compression viscoelastic behaviours of the periodontal ligament. Journal of the Formosan Medical Association 111, 471 – 481

154. Wang Y, Li J, Wang Y, Lei L, Jiang C, An S, Zhan Y, Cheng Q, Zhao Z, Wang J, Jiang L (2011) Effects of hypoxia on osteoblastic differentiation of rat bone marrow mesenchymal stem cells. Mol Cell Biochem DOI 10.1007/s11010-011-1124-7

155. Watanabe T, Okafuji N, Nakano K, Shimizu T, Muraoka R, Kurihara S, Yamada K, Kawakami T. (2007) Periodontal tissue reaction to mechanical stress in mice. J Hard Tissue Biol. 16:71–74.

156. Wigen TI, Agnalt R, Jacobsen I. (2008) Intrusive luxation of permanent incisors in Norwegians aged 6 – 17 years: a retrospective study of treatment and outcome. Dental Traumatology 24; 612 – 8

157. Wilson TG and Kornman KS (eds). (1996) Fundamentals of Periodontics. Quintessence Publishing Company, Chicago.

158. Wise GE, Yao S, Henk WG (2007) Bone formation as a potential motive force of tooth eruption in the rat molar. Clin Anat. 20(6): 632-9.

159. Wise GE (2009) Cellular and molecular basis of tooth eruption. Orthodontics and Craniofacial Research 12(2); 67 – 73

160. Wise GE, He H, Gutierrez DL, Ring S and Yao S. (2011). Requirement of alveolar bone formation for eruption of rat molars. European journal of oral sciences 119; 333 - 338

161. Xiang J, Mrozik K, Gronthos S, Bartold PM. (2012) Epithelial cells rests of Malassez contain unique stem cell populations capable of undergoing epithelial-mesenchymal transition. Stem Cells and Development 21(11); 2012 – 2025

162. Yamamoto T, Li M, Liu Z, Guo Y, Hasegawa T, Masuki H, Suzuki R and Amizuka N. (2010) Histological review of the human cellular cementum with special reference to an alternating lamellar pattern. Odontology 98; 102 – 109

163. Yamawaki K, Matsuzaka K, Kokubu E and Inoue T. (2010) Effects of epidermal growth factor and/or nerve growth factor on Malassez's epithelial rest cells in vitro: expression of mRNA for osteopontin, bone morphogenetic protein 2 and vascular endothelial growth factor. Journal of Periodontal Research 45; 421 - 7

164. Yao S, Liu D, Pan F, Wise GE. (2005) Effect of vascular endothelial growth factor on RANK gene expression in osteoclast precursors and on osteoclastogenesis. Archives of Oral Biology 51; 596- 602

165. Yao S, Pan F, Wise GE (2007) Chronological gene expression of parathyroid hormone-related protein (PTHrP) in the stellate reticulum of the rat: Implications for tooth eruption. Arch Oral Biol 52; 228-232

166. Yang D-C, Yang M-H, Tsai C-C, Huang T-F, Chen Y-H, Hung S-C. (2011) Hypoxia inhibits osteogenesis in human mesenchymal stem cells through direct regulation of Runx2 by TWIST. PloS ONE 6(9); e23965

167. Zelzer E, Glotzer DJ, Hartmann C, Thomas D, Fukai N, Soker S and Olsen BR. (2001) Tissue specific regulation of VEGF expressions during bone development requires cbfa1/Runx2. Mechanisms of Development 106; 97 -106

168. Zeichner-David M. (2006) Regeneration of periodontal tissues: cementogenesis revisited. Periodontology 2000 41; 196 - 217

169. Zhang C, Tang W, Li Y, Yang F, Dowd DR, MacDonald PN. (2011) Osteoblast specific transcription factor Osterix increases Vitamin D receptor gene expression in osteoblasts. PLoS One 6(10): e26504. Epub 2011 Oct 18

170. Ziros PG, Basdra EK and Papavassiliou (2008) Runx2: of bone and stretch. The International Journal of Biochemistry and Cell Biology 40; 1659 – 1663

6. STATEMENT OF PURPOSE, AIMS and NULL HYPOTHESIS

6.1 Statement of Purpose:

Osteogenesis and angiogenesis are essential for bone remodelling and hence tooth eruption as well as orthodontic tooth movement. Runx2 is the master regulator of osteogenesis whilst VEGF controls angiogenesis. Clinically, understanding the mechanisms underpinning tooth eruption may assist in understanding why failure of eruption occurs.

6.2 Aims

6.1.1 To confirm the location of Runx2 within the rat maxillary dentoalveolar region using immunohistochemistry

6.1.2 To investigate the relationship between Runx2 expression and the different regions within the rat dentoalveolar region in an ankylosis model.

6.1.3 To confirm the location of VEGF within the rat maxillary dentoalveolar region using immunohistochemistry.

6.1.4 To investigate the relationship between VEGF expression and the different regions within the rat dentoalveolar region in an ankylosis model.

6.3 Null Hypothesis

6.2.1 There is no change over time in the expression of Runx2 in thermally induced ankylotic areas compared to non-ankylotic areas at similar locations within the dentoalveolus.

6.2.2 There is no change over time in the expression of VEGF in ankylotic areas compared to non-ankylotic areas at similar locations within the dentoalveolus.

RUNX2 EXPRESSION IN THE RAT PULP, PERIODONTAL LIGAMENT AND ALVEOLAR BONE FOLLOWING HYPOTHERMAL INSULT

ARTICLE 1

Written in the style of Archives of Oral Biology

Dr Trudy Ann STEWART (BDS Adelaide, BOccThy UQ)

Orthodontic Unit

School of Dentistry

Faculty of Health Sciences

The University of Adelaide

AUSTRALIA

March 2013

7. ARTICLES

7.1.1 Abstract:

Objective: To evaluate the expression and localisation of runt related transcription factor 2 (Runx2) in the rat dentoalveolar region post freezing injury.

Methods and Materials: The right upper first molar of 18 eight week old male Sprague-Dawley rats were subjected to a single 10 minute application of dry ice in order to produce aseptic necrosis and ankylosis within the periodontal ligament. The contralateral first molar of these rats served as an untreated control. On days 0, 4, 7, 14, and 28 post insult, the expression of Runx2 was examined via immunohistochemistry (IHC) and histomorphometry.

Results: Fibroblast-like cells in the PDL, osteoclasts in resorption lacunae along the PDL, bone lining cells, osteoblasts/osteocyte-like cells, cemental cells, odontoblastic cells, epithelial cell rests of Malassez and vascular lining cells were all found to be positive for Runx2 in both the treated and untreated groups. Statistically significant differences in the percentage of Runx2 positive cells were found in the pulp and alveolar bone but not in the PDL. Although not statistically significant, trends of changing Runx2 expression with time were noted in the pulp and alveolar bone. Runx2 expression increased at days 4, 7 and decreased at days 14 and 28 in the pulp whilst in the alveolar bone expression increased at day 4, decreased at days 7 and 14 and slightly increased at day 28.

Conclusions:

1) Runx2 is expressed by a number of cells within the rat dentoalveolus including bone cells (osteoblasts and osteocytes not differentiated between), cemental cells, ERM, bone marrow cells, fibroblast-like cells of the PDL, vascular lining cells, and odontoblasts.

2) Changes in Runx2 expression were found in the experimental pulp and alveolar bone when compared to the internal and external control groups, but not in the PDL.

3) Changes in Runx2 expression also occurred in the internal control group, suggesting that a localised insult may show a systemic impact.

4) Post-hypothermal insult, Runx2 may play an important role in the development of bony ankylosis.

Key Words: Runx2, ankylosis, rat, dentoalveolar, hypothermal insult, immunohistochemistry

7.1.2 Introduction:

Dentoalveolar ankylosis occurs when non-neoplastic bone obliterates the periodontal ligament (PDL) and fusion occurs between the alveolar bone and cementum or dentine (Raghoebar et al., 1989). Although the mechanisms leading to the development of ankylosis remain unknown, various aetiologies have been reported: local trauma causing damage to Hertwig's epithelial root sheath, disturbance to the local post emergent eruptive mechanism, local infection, genetic factors, chemical or thermal irritation, traumatic masticatory forces and pulpo-periodontal canals (Raghoebar et al., 1989; Kurol and Magnusson, 1984; Kjaer et al., 2008; Ekim and Hatibovi-Kofman, 2001). Once ankylosis occurs, a number of interarch and intraarch consequences may ensue: including, reduced eruption of the affected tooth with concurrent reduced development of adjacent alveolar bone; delayed exfoliation of the deciduous tooth; increased difficulty in performing extraction; abnormal position and development of the permanent successor; tipping of adjacent teeth; over eruption of opposing teeth; as well as dental midline shift. (Ponduri et al., 2009; Loriato et al., 2009; Rosner et al., 2010). Affected teeth are also unresponsive to conventional orthodontic treatment (Rosner et al., 2010).

Ankylosis may also be induced experimentally through mechanical, chemical and thermal means (Dreyer et al., 2000). Dreyer et al., (2000) investigated a cold thermal insult applied to the occlusal surface of a rat molar and the resultant development of aseptic resorption of the PDL and bony ankylosis. Application of a cold stimulus was noted to lead to periodontal cell necrosis, with shrinkage and lysis of odontoblasts and other pulpal cells and clastic attack of the root surface with initiation of resorption 2 to 7 days post insult (Dreyer et al., 2000).

Isolated in 1994, Runx2 (also called Cbfa-1, OSF2 and AML3) belongs to the Runx family of transcription factors (Komori, 2011). These proteins act as master regulators of cell differentiation with Runx1 being essential for haematopoietic stem cell differentiation (Komori, 2011), Runx2 for osteoblast, chondrocyte and odontoblast differentiation (Li et al., 2011) as well as vascular invasion into avascular cartilage during endochondral ossification and Runx3 for gastric epithelial cell regulation and neurogenesis (Komori, 2011; Ziros et al., 2008). Runx2 binds to the promoter regions in preosteoblasts, upregulating Osterix (Sp7) and canonical Wnt and controlling the formation of immature osteoblasts and hence bone formation (Komori, 2011). The osteogenic potential of the PDL and its possible role in the regulation of alveolar bone remodelling has been shown by prior studies investigating both the development of dentoalveolar ankylosis post hypothermal insult and orthodontic tooth movement (OTM) secondary to mechanical loading (Davidovitch, 1991; Dreyer et al., 2000; Pavlidis et al., 2009; Lossdörfer et al., 2009). Runx2 has been found during tooth development and eruption, as well as during orthodontic tooth movement and Pavlidis et al. (2009) demonstrated that Runx2 is involved in the differentiation of PDL cells into osteoblasts during tooth movement in rats using an orthodontic appliance via the ERK cascade, with a time dependent decrease in Runx2 expression following orthodontic load application (Lossdörfer et al., 2009; Lossdörfer et al., 2010; Pavlidis et al., 2009). In the dental pulp, continuous expression of Runx2 has been found to disturb odontoblast formation and lead to the formation of bone-like tissue in reparative dentine (Miyazaki et al., 2008). Runx2 expression by PDL cells, as well as alveolar bone cells, is thus potentially important for the development of bony ankylosis following hypothermal trauma.

The possible role of Runx2 in dental ankylosis has not previously been investigated using a thermally induced ankylotic model. Thus, this study aims to localise Runx2 within the rat dentoalveolus and evaluate changes in the expression of Runx2 0, 4, 7, 14 and 28 days post-hypothermal insult. The null hypothesis is that there is no difference in Runx2 expression following hypothermal insult.

7.1.3 Methods and Materials:

Animals: 18 eight week old male Sprague-Dawley rats were used in the experiment; 15 rats underwent hypothermal insult, whilst a further 3 rats acted as an external control. The University of Adelaide Animal Ethics Committee reviewed and approved this protocol for a prior study (Ethics number M-04-2004/M-023-2007).

Experimental Protocol: The rats were anaesthetized with an intramuscular injection of Hypnorm® (fentanyl citrate, 0.315 mg/ml and fluanisone 10 mg/ml; Janssen-Cilag Ltd., High Wycombe, Buckinghamshire, UK) and Hypnovel® (midazolam hydrochloride, 5 mg/ml; Roche, Berne, Switzerland) diluted 1:1 with sterile water for injection at a dosage of 2.7ml/kg of body weight. The animals were restrained in a head holding device and underwent a single 10-minute application of dry ice (compressed carbon dioxide gas at -81^{o}C, BOC Gases, Adelaide, Australia) to the right maxillary first molar crown in order to produce aseptic necrosis within the periodontal ligament and induce ankylosis. The untreated contra-lateral molars of each rat served as internal controls (Dreyer et al., 2000).

The animals were randomly divided into five groups of three, and each group of 3 animals was humanely killed by an intraperitoneal injection of Nembutal® (pentobarbitone sodium, 60 mg/ml at 20mg/ml per 100g of body weight; Boehringer Ingelheim Pty Ltd, Artarmon, Australia) on day 0, 4, 7, 14 and 28 respectively. The 3 animals in the external control group did not undergo hypothermal insult and were also humanely killed on day 0. The maxillae were then dissected out and excess soft tissues removed.

Histology: The specimens were fixed in 4% paraformaldehyde for 24 hours and stored in phosphate buffered saline (PBS) at pH 7.4 and decalcified with 4% ethylenediaminetetraacetic acid (EDTA) solution. After being dehydrated in a graded alcohol series, the specimens were embedded in paraffin, and 5μm serial sections were cut coronally through the root furcation region on a microtome (Leitz 1512 Microtome, Leica, Nussloch, Germany). These sections were mounted onto labelled aminopropyltriethoxysilane (APTS) coated glass slides. Selected sections were stained with haematoxylin and eosin (HE) for histological evaluation. Up to this stage, the materials were processed for use in a previous study (Tan, 2011).

Immunohistochemistry (IHC): 153 randomly selected sections within the furcation region of the maxillary first molars were chosen (approximately 8 sections per animal) as this region had shown the most ankylosis in previous studies performed at the University of Adelaide (Dreyer et al., 2000). Presence of ankylosis within the interradicular region was confirmed by evaluating the HE staining. Antibody optimization was performed prior to staining to determine optimal antibody dilution for minimal background staining and optimal antibody specific staining. To assess antibody specificity, both negative and positive controls were performed. For negative control sections, the anti-Runx2 antibody was omitted or an isotype-matched antibody was applied (IgG2 kappa). As a positive

control, human breast and lymph node tissue was stained with anti-Runx2 antibody as these tissues had previously been found to demonstrate Runx2 expression (see Figure 1).

IHC staining was performed with Runx2 mouse anti-rat monoclonal antibody (Abnova Corporation, Taiwan). The sections were deparaffinised and rehydrated, immersed in tris-EDTA buffer (10mM Tris Base, 1mM EDTA solution, pH 9.0) for 10 minutes in a water bath heated to 65^0C and then cooled for 20 minutes before being immersed in methanol H_2O_2 0.3%v/v for 10 minutes to block endogenous peroxidase and washed in 1xPBS three times for 5 minutes each. Then sections underwent serum blocking (provided in Vectastain Elite ABC (avidin-biotin complex) Universal Kit, Vector Laboratories, California, USA) for 60 minutes. Anti-Runx2 antibody (2.5µg/ml), diluted in PBS, was applied and the sections incubated in a wet chamber at room temperature overnight. Sections were rinsed in 1xPBS three times for 5 minutes and incubated with a secondary antibody (biotinylated horse anti-mouse IgG, Vectastain Elite ABC kit, Vector Laboratories, California, USA) according to the manufacturer instructions. This was incubated for 45 minutes at room temperature followed by the Avidin-Biotin Complex (Vectastain Elite ABC Universal Kit, Vector Laboratories, California, USA) diluted as per manufacturer instruction for a further 45 minutes. Immunoreactivity was visualised via incubation of the sections with a prediluted AEC (3-Amino-9-EthylCarbazole) solution (DAKO Australia Pty LTD., Campbellfield, Australia) in a dark room for 10 minutes. Sections were counterstained with haematoxylin for 10 seconds, rinsed in tap water and then immersed in lithium carbonate for 30 seconds before again being rinsed in tap water and mounted using aquamount (Aquatex, Merck Pty. Ltd., Victoria, Australia). Antibody optimisation was performed prior to staining. Negative controls were sections with omission of the primary antibody or sections incubated with an isotype-matched antibody (IgG2A kappa) (see Figure 1). IHC staining was performed at the same day for all samples to avoid day-to-day variability.

Figure 1: Negative and positive controls used to confirm Runx2 antibody capability and specificity.

Negative controls (x2.5 magnification ruler 0 – 2mm) A: Isotype matched control (IgG2 Kappa) applied at 2.5**µ**g/ml, B: Omission of Runx2.

Positive controls (x20 magnification ruler 0 - 200**µ**m) C: Runx2 positive cells in Breast tissue, D: Runx2 positive cells in Lymph node tissue

Note red is positive staining for Runx2, blue is haematoxylin counterstaining.

A

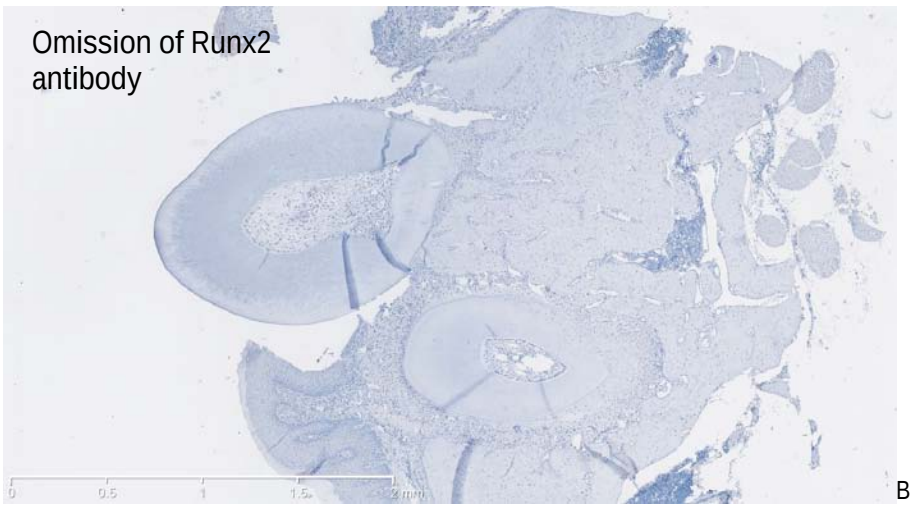

B

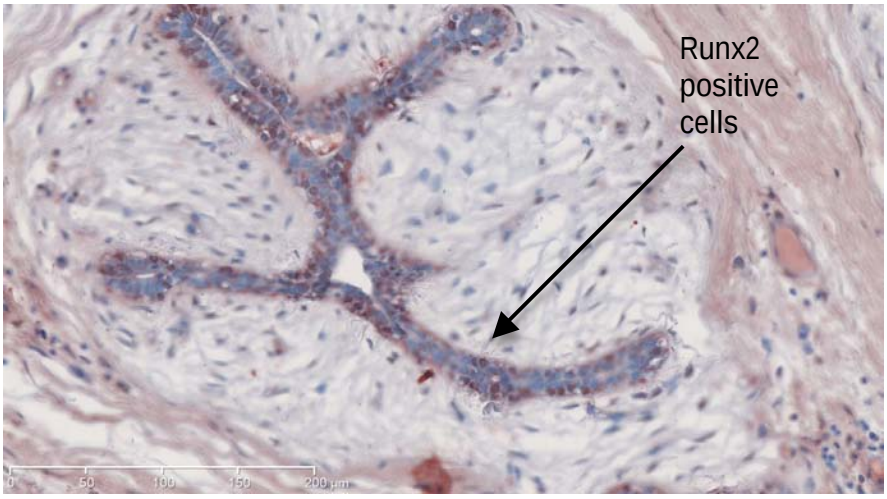

C

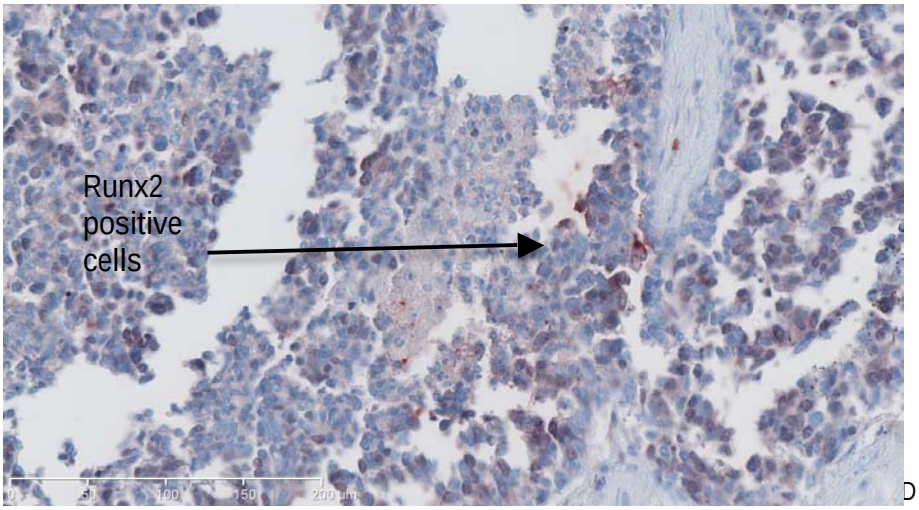

D

Histomorphometry: Sections were scanned via a Nanozoomer Slide Scanner 2.0 series (Hamamatsu Photonics K.K. 325-6 Sunayama-cho, Hamamatsu City, Shizuoka) and viewed on a personal computer (MacBook Pro with 13 inch screen) using the Nanozoomer Digital Pathology (NDP) software (Hamamatsu Photonics K.K. 325-6 Sunayama-cho, Hamamatsu City, Shizuoka)). Semi-quantitative counting, as described by Kraan et al. (2000) (score 1 to 3) of the percentage of Runx2 positive cells in the pulp, PDL and alveolar bone of each rat was performed. In every stained section, counts were performed in 3 regions of the pulp, 5 regions of the PDL and 8 regions of the alveolar bone at a magnification of x20 (see Figure 2). Counting areas were placed randomly within each of the specified tissues and were defined by a 0.02mm^2 rectangle in the pulp, 0.01mm^2

rectangle in the PDL and a 0.05mm^2 square in the alveolar bone. ImageJ software was used to define the counting areas and to count the number of positive and negative cells within the counting areas (Wayne Rasband, National Institute of Health, USA; http://rsweb.nih.gov.proxy.library.adelaide.edu.au.ij).

Figure 2: Division of section into counting areas x2.5 magnification ruler 0 – 2mm.

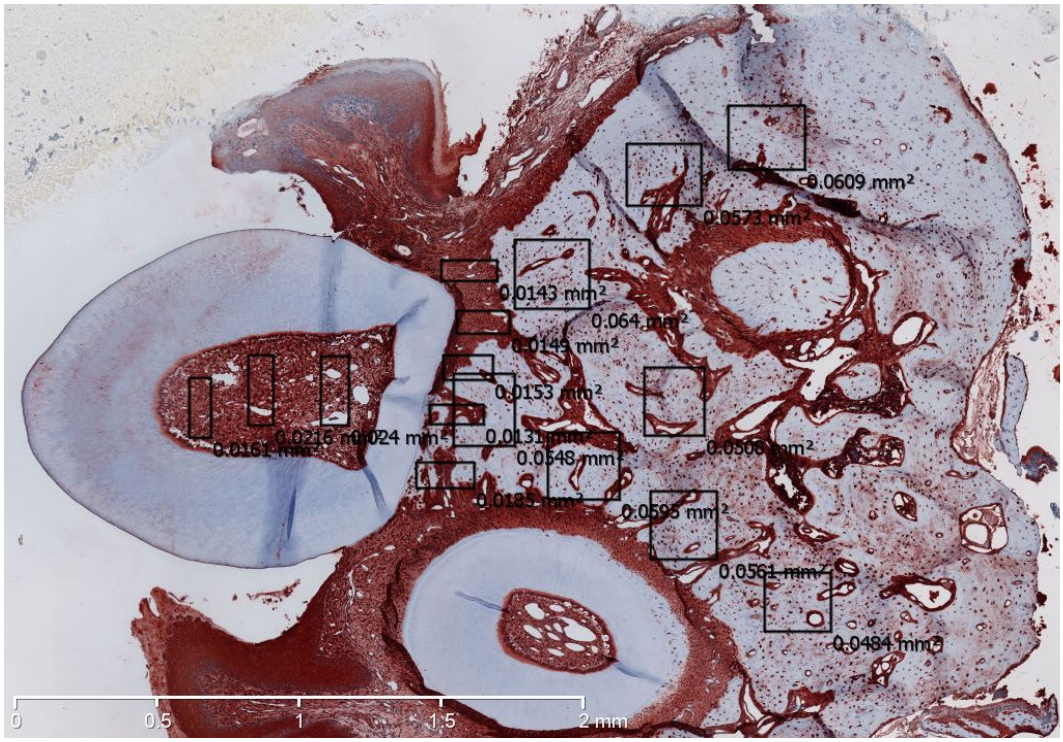

Given the difficulty counting the PDL positive fibroblasts due to the fibrous nature of the PDL, immunostaining intensity was also evaluated digitally using the ImageJ software colour deconvolution for Haematoxylin / AEC (3-Amino-9-EthylCarbazole) plugin (Wayne Rasband, National Institute of Health, USA; http://rsweb.nih.gov.proxy.library.adelaide.edu.au.ij) .

Statistical Analysis: The data were analysed using SAS 9.3 (SAS Institute Inc., Cary, NC, USA). Differences between the percentage of Runx2 positive cells between the internal control and experimental sides of the experimental rats or between the internal control (experimental rats) and external control rats were analysed using a mixed effect model. In the model, the dependent variable was the percentage of positive cells, whilst side, time and interaction between side and time were considered as fixed effects. A random effect was also included in the model to account for the dependency of measurements from the same subject. This model was chosen as the selection of rats into groups was random, so the associated effects were also thus random effects. The data from different groups of animals are independent as they were randomly selected and because observations from the same animals in the same group are often correlated (SAS institute Incs, 2011).

A negative binomial regression model was used to analyse the number of empty osteocyte lacunae, with the outcome being dead cells and the predictor being time. A Two-sample t-test was used to examine the difference in the mean Runx2 intensity between PDL closest to the cementum and the PDL closest to the alveolar bone. To determine the accuracy of counting, re-counting of 10% of rat sections was performed and analysed via Bland-Altman plots. Differences were considered significant at a p value of <0.05. For the Bland-Altman plots, it is expected that 95% of differences will lie in the limits of agreement.

7.1.4 Results:

Error Study:

Ten percent of sections were recounted (n = 191). Good intra-operator reproducibility was confirmed through the use of Bland-Altman plots, which indicated that 95% of the differences were within the limits of agreement (see Figure 3 – 6).

Figure 3: Bland-Altman plot of Initial and subsequent count of Runx2 positive cells (n=191).

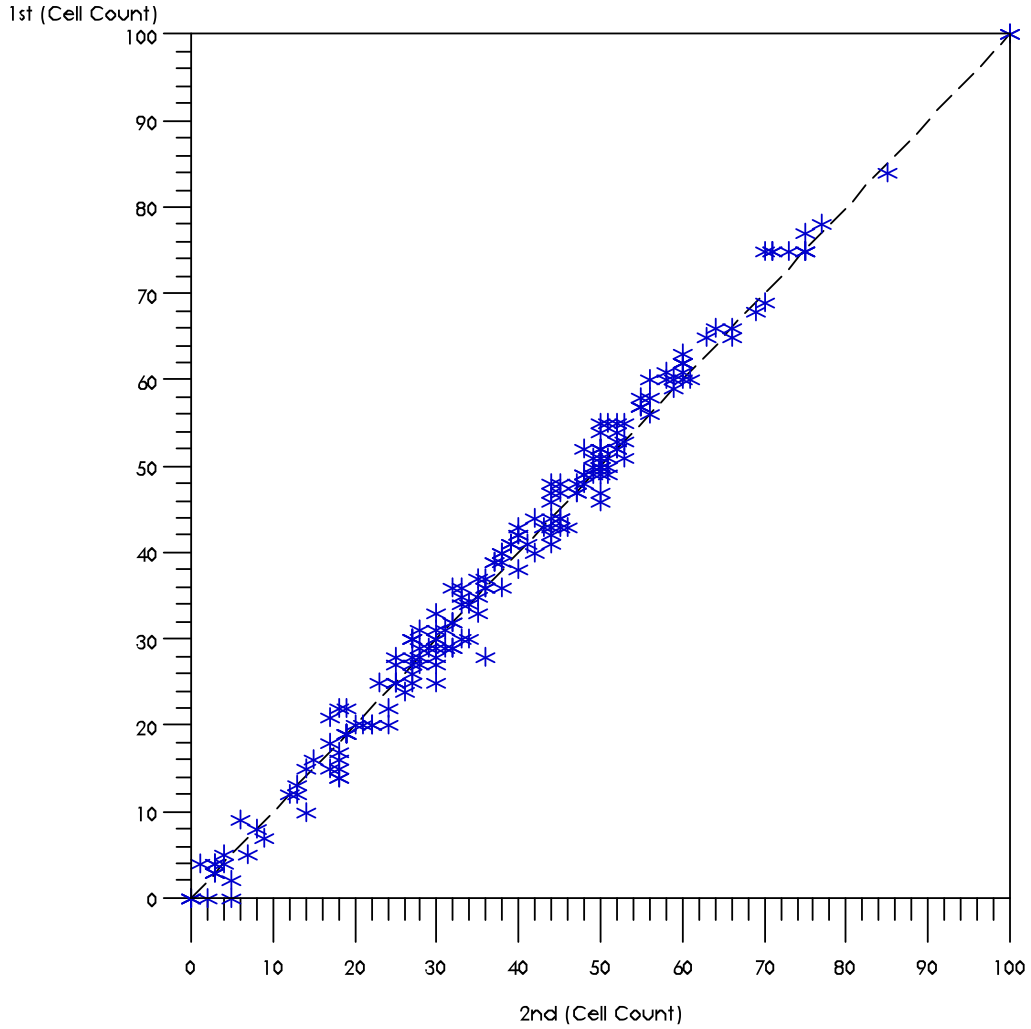

Figure 4: Bland-Altman plot indicating the difference between the initial and subsequent count of Runx2 positive cells (n=191).

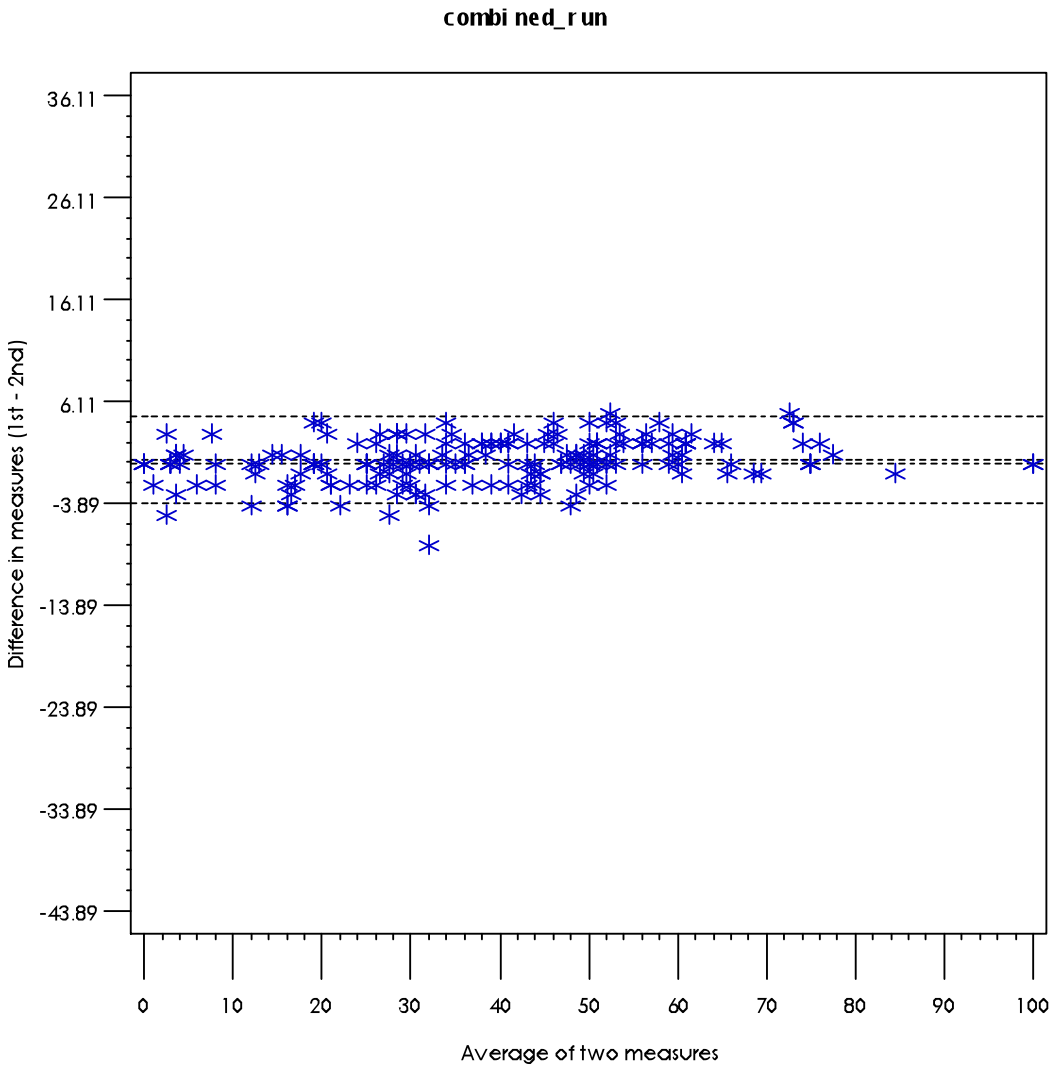

Figure 5: Bland-Altman plot of Initial and subsequent count of Runx2 negative cells (n=191).

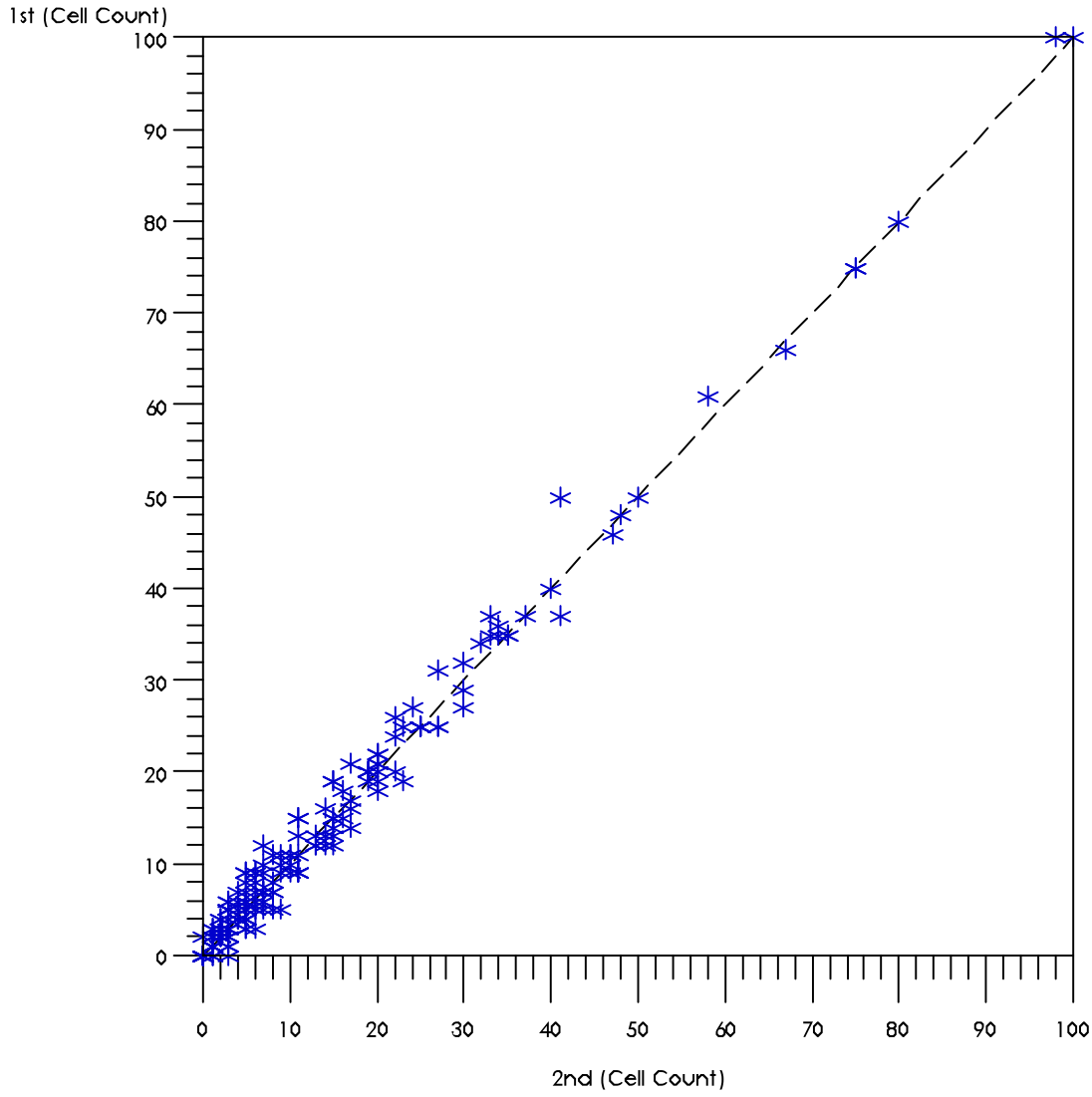

Figure 6: Bland-Altman plot indicating the difference between the initial and subsequent count of Runx2 negative cells (n=191).

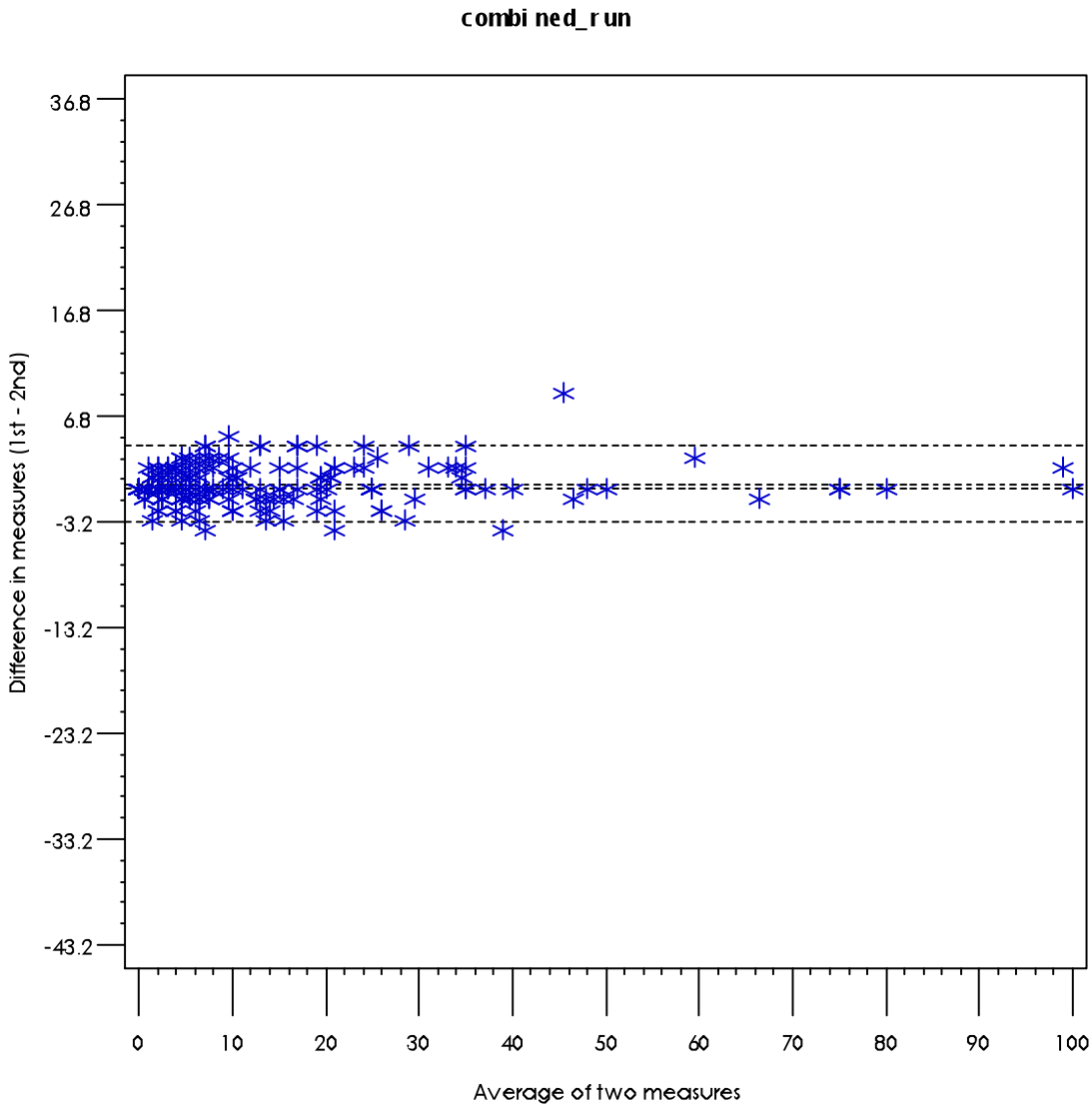

Histology:

On review of the haematoxylin and eosin stained sections very little structural difference was noted between sections at Day 0 in experimental, internal control or external control groups. Within the pulp of the experimental side, loss of integrity of the pulpal layers was visible at day 4 with disturbance to the discrete odontoblast, cell rich and core layers. Few pulpal cells remained at day 7 and 14 post insult. No disturbance to pulpal tissue was noted in the external or internal control at any time point (see Figure 7).

In regards to the periodontal ligament and alveolar bone, thinning of the PDL and fine bony trabeculae were visible in the interradicular region of all experimental animals on day 7. At day 14, widespread loss of the PDL was present, with dense bony ankylosis, but by day 28, bony replacement of the PDL was only present on one animal. No changes to PDL or alveolar bone were noted in the internal or external control groups during the above time points (see Table 1 and Figure 7).

Table1: Animals displaying ankylosis on the experimental side (RHS)

Day	0	4	7	14	28
Number of Rats	3	3	3	3	3
Number of Rats with Ankylosis	0	0	3	3	1

Figure 7: H and E Sections Day 0, 4, 7, 14 and 28 showing development of ankylosis x 10 magnification ruler 0 - 500μm (Tan, 2011).

Runx2 Immunohistochemistry:

Runx2 Positive Cells in the Dentoalveolar Region: Fibroblast-like cells in the PDL (Pavlidis et al., 2009; D'Souza et al., 1999), osteoclasts in resorption lacunae along the PDL, bone lining cells, osteoblasts/osteocyte-like cells, cemental cells, odontoblasts (Hirata et al., 2008), epithelial cell rests of Malassez (ERM) (Xiang et al., 2012), megakaryocytes and vascular endothelial cells (Amir et al., 2007) were found to stain positive for Runx2 in the experimental and control groups (see Figure 8). This is consistent with previous IHC studies.

Figure 8: Runx2 positive cells x 20 magnification ruler 0 - 200**µ**m.

A: Epithelial rest cells of Malassez, B: Bone cells, C: Osteoclasts on the outer border of the PDL, D: Odontoblastic cells, E: Fibroblast-like cells in PDL, F: Megakaryocyte-like cells in the bone marrow, G: Cemental cells in the cementum, H: Vascular endothelial cells.

Note red staining indicates Runx2 positivity, blue staining is haematoxylin counterstain.

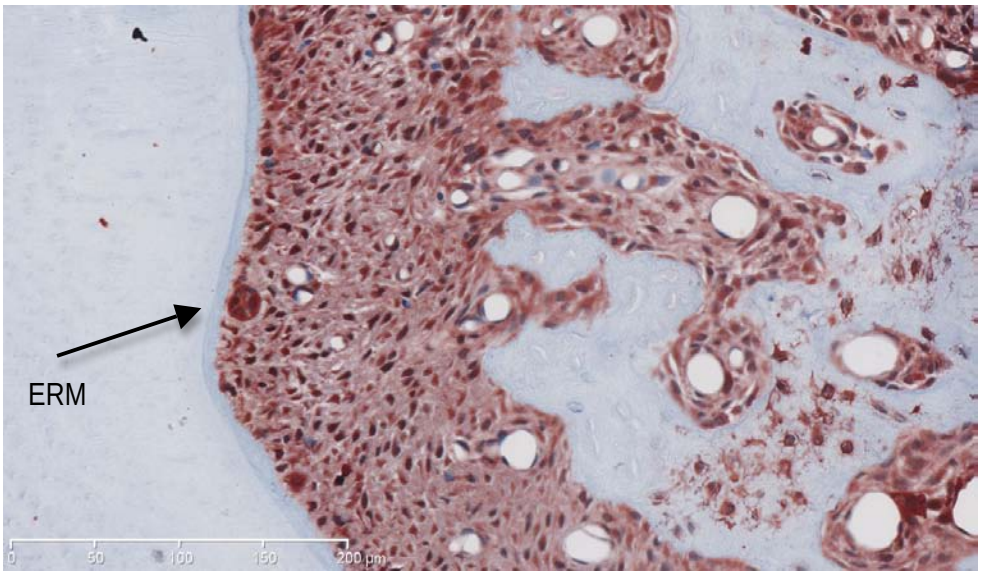

A

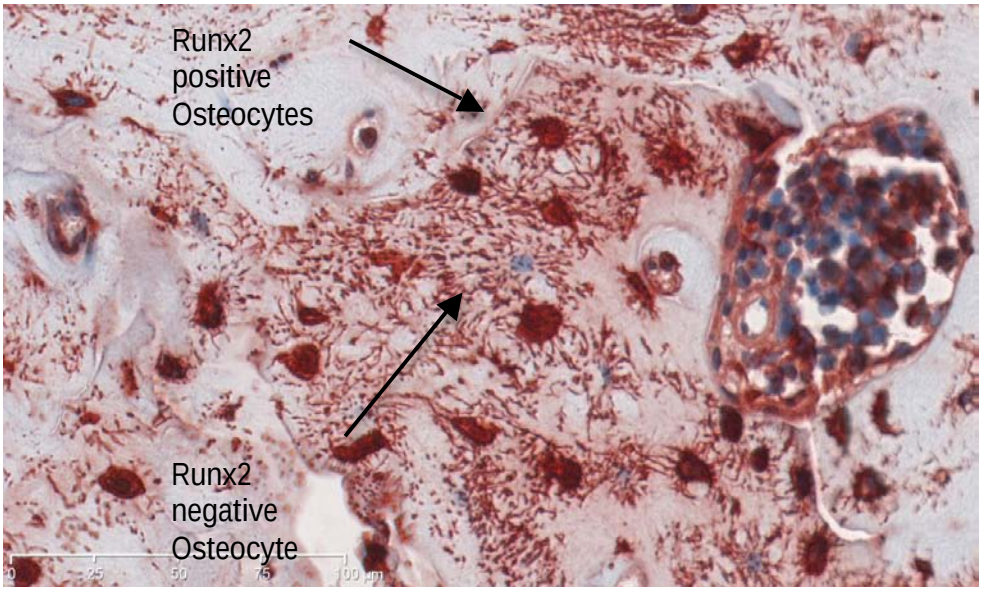
Runx2
positive
Osteocytes
Runx2
negative
Osteocyte

B

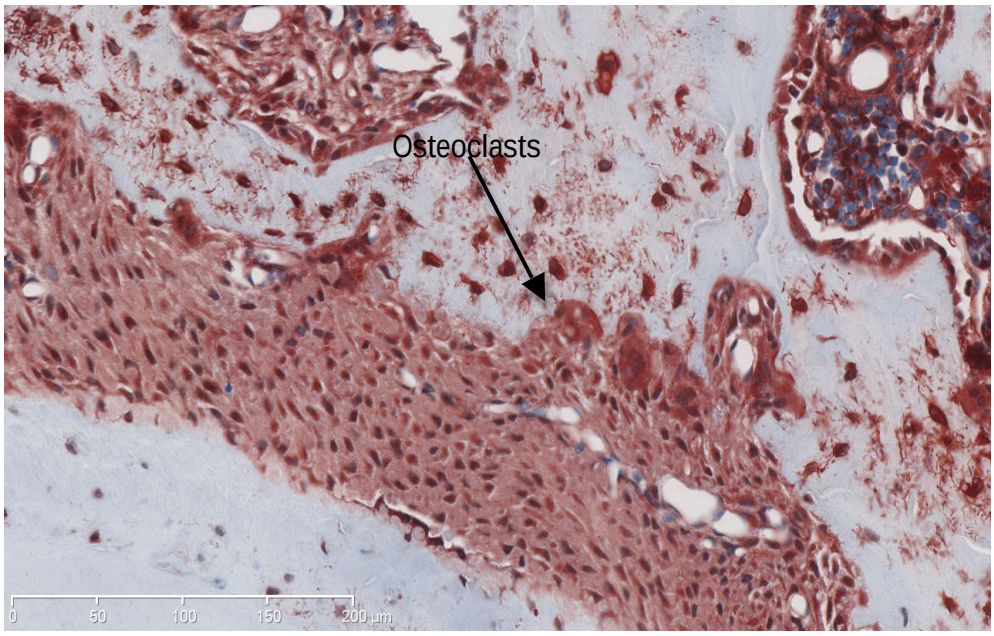
Osteoclasts

C

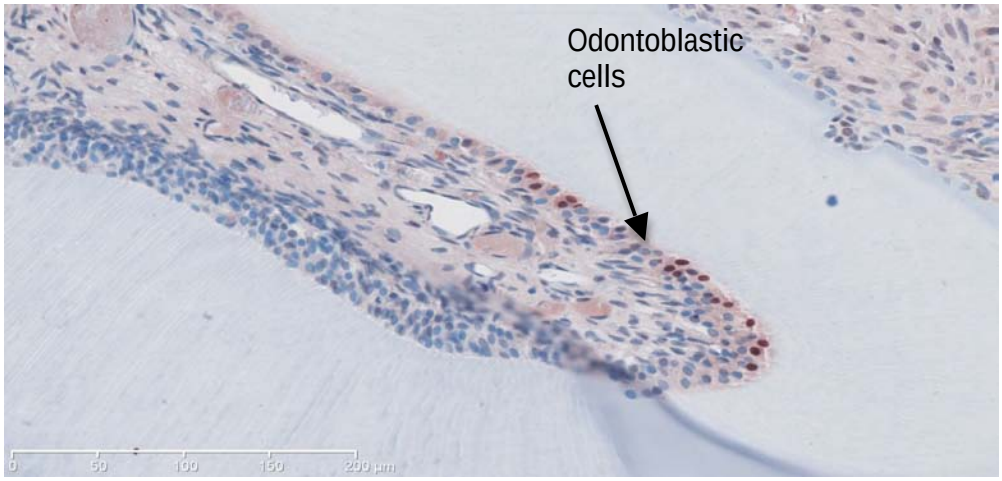
Odontoblastic
cells

D

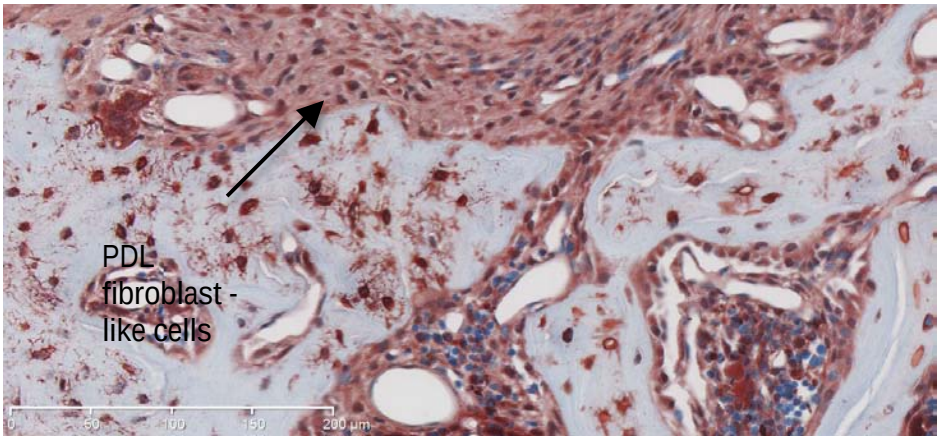
PDL
fibroblast -
like cells

E

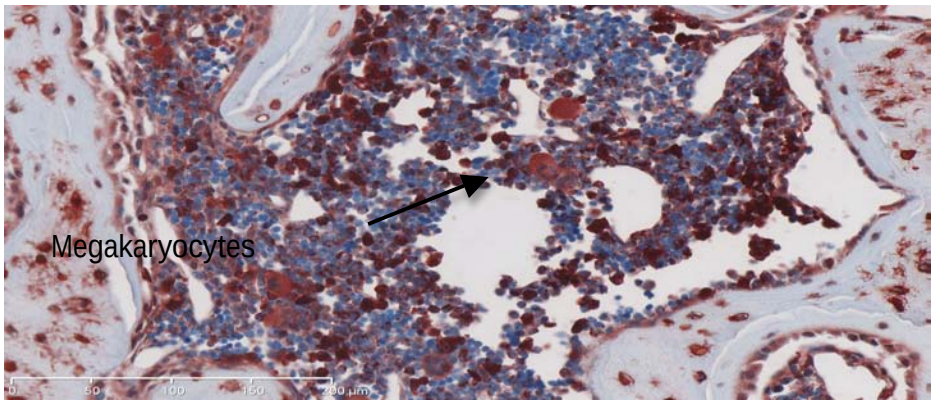
Megakaryocytes

F

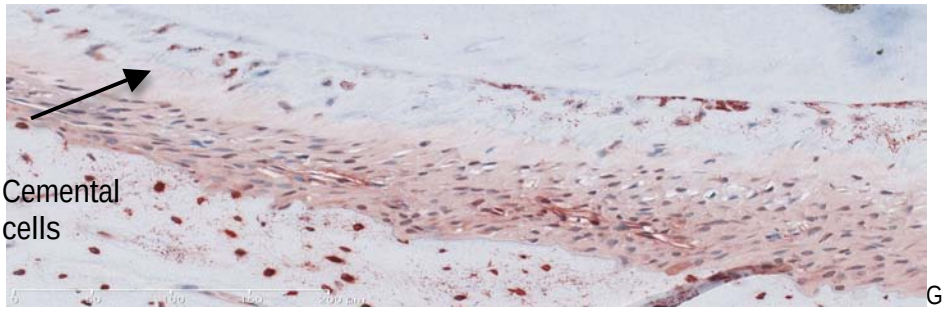
Cemental
cells

G

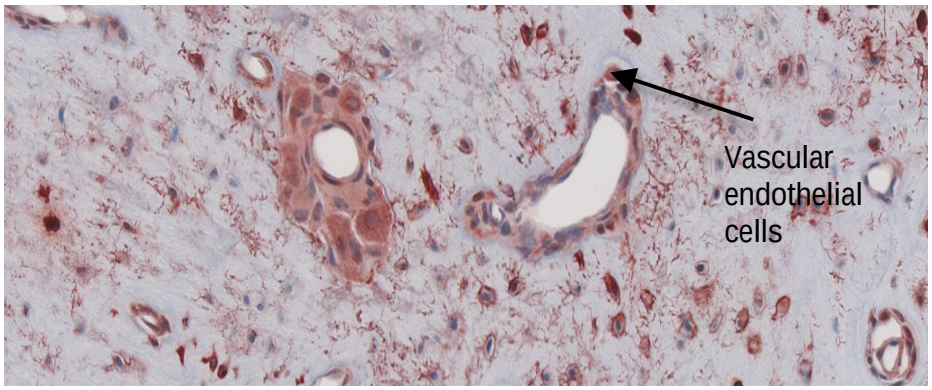
Vascular
endothelial
cells

H

Runx2 Expression in the Pulp:

Subjective evaluation showed little difference in the expression of Runx2 at day 0 in the experimental, internal control or external control pulp tissues, with few Runx2 positive cells present. At day 4, the experimental side pulp tissue demonstrated greater Runx2 staining compared to the internal or external controls. This trend continued at day 7, 14 and 28. Loss of delineated cell zones within the pulp was evident on the experimental side from day 4. However by day 28 a degree of pulpal re-organisation was present in two of the three rats. No ankylosis was present in these two animals.

Within the pulp, odontoblasts stained positively for Runx2 at day 4, 7, 14 and 28, with very few odontoblasts staining positively at day 0 in the experimental group, or in the internal or external control groups. Reparative dentine was noted from day 7. Fibroblast-like cells within the pulpal core region displayed Runx2 positivity rarely at day 0. A great increase in the number of positive cells occurred at day 4 and was maintained at days 7, 14 and 28. Few Runx2 positive fibroblast-like cells were seen in the internal or external control groups (see Figure 9).

Figure 9: Changes in Runx2 expression in pulp in the external control group and at various time points in the experimental and internal control groups

x20 magnification ruler 0 - 200**µ**m.

Note red staining indicates Runx2 positive result, blue staining indicates haematoxylin counterstain.

Day 0 External Control

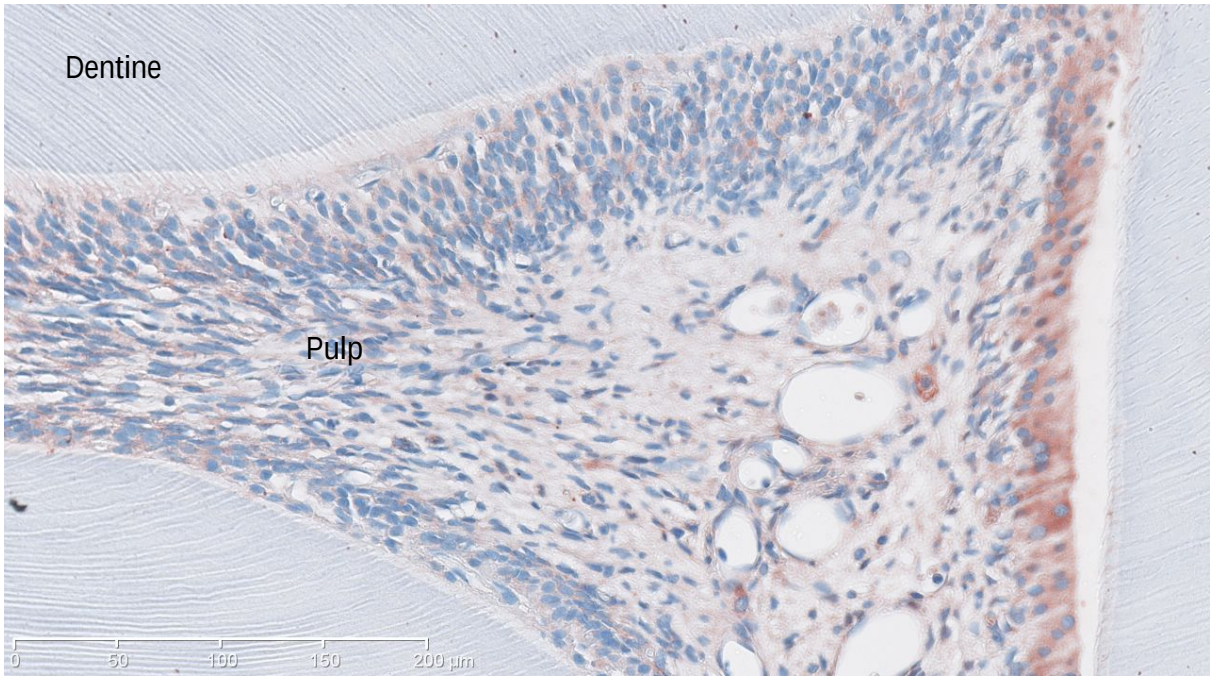

Day 0 Experimental

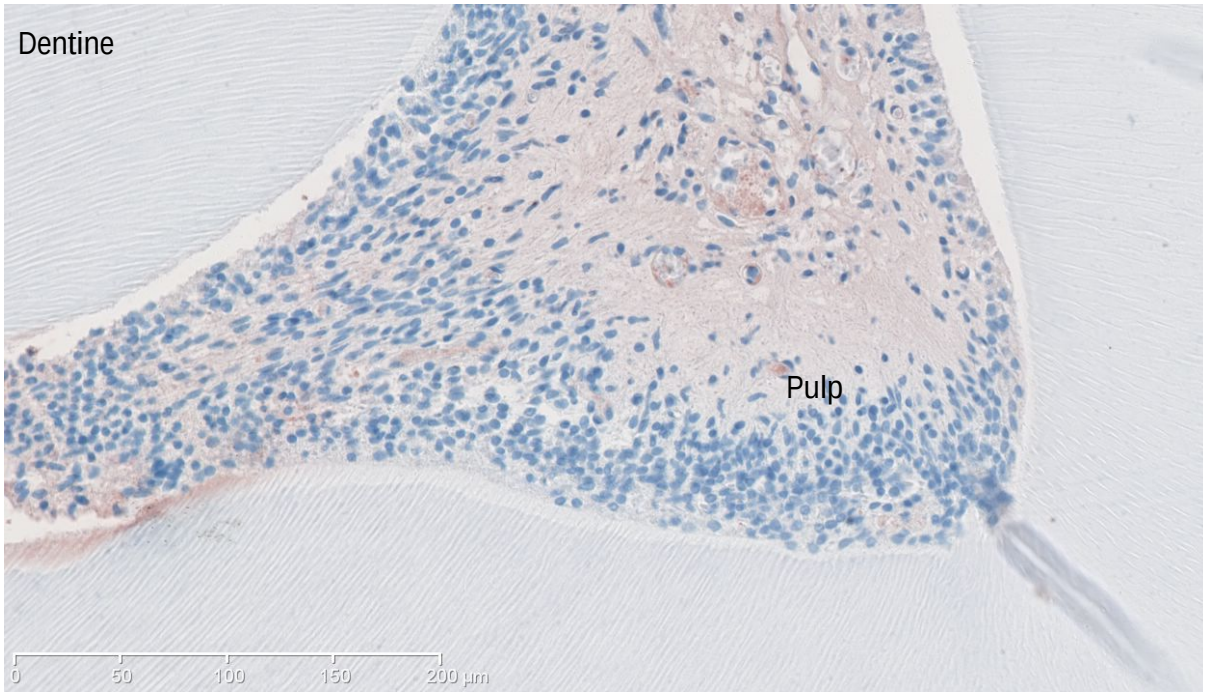

Day 0 Internal Control

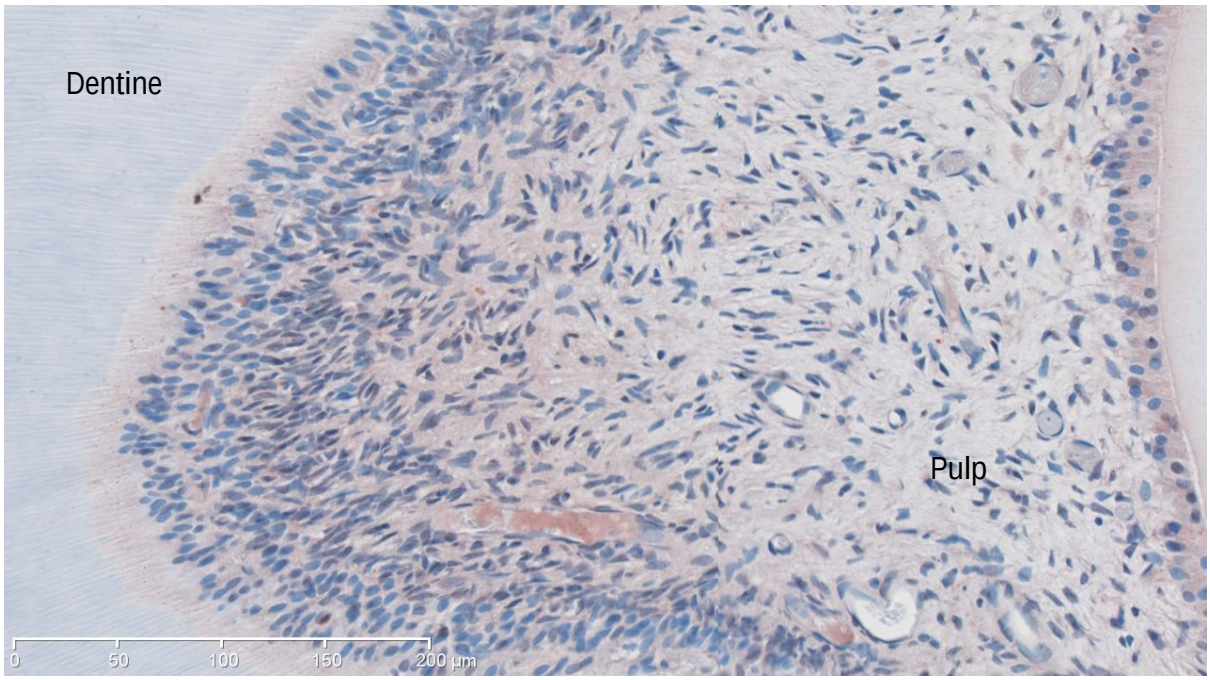

Day 4 Experimental

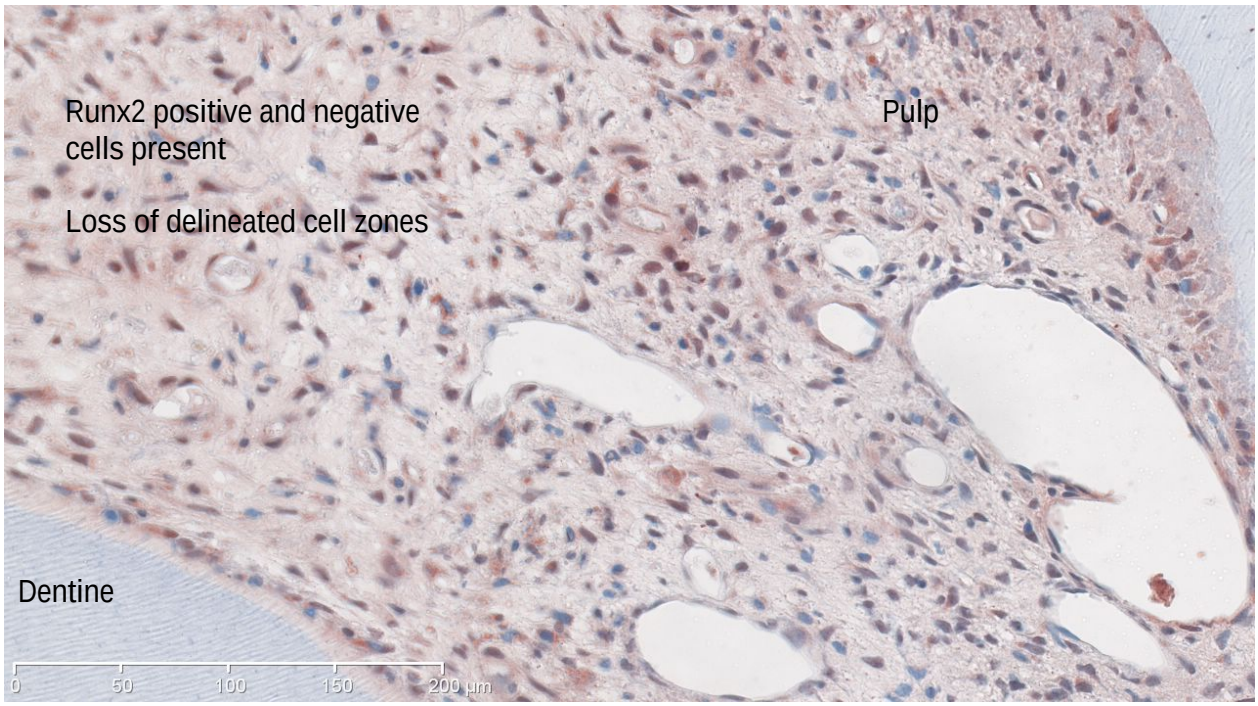

Day 4 Internal Control

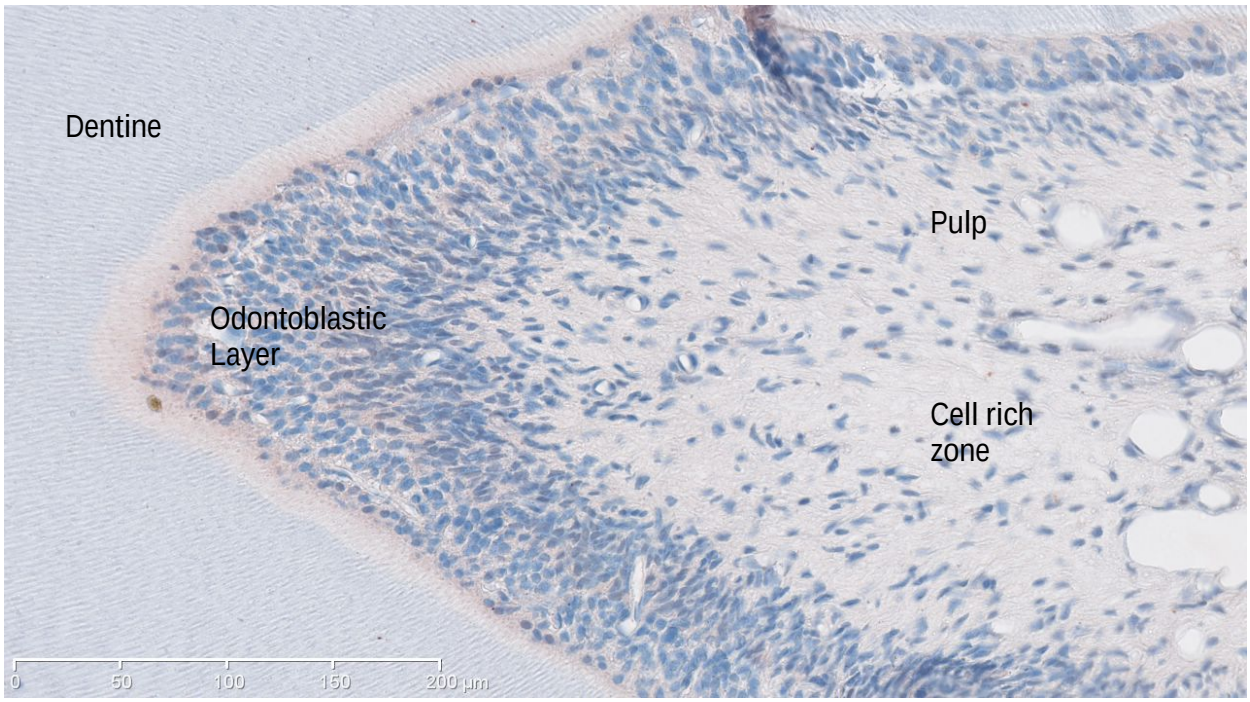

Day 7 Experimental

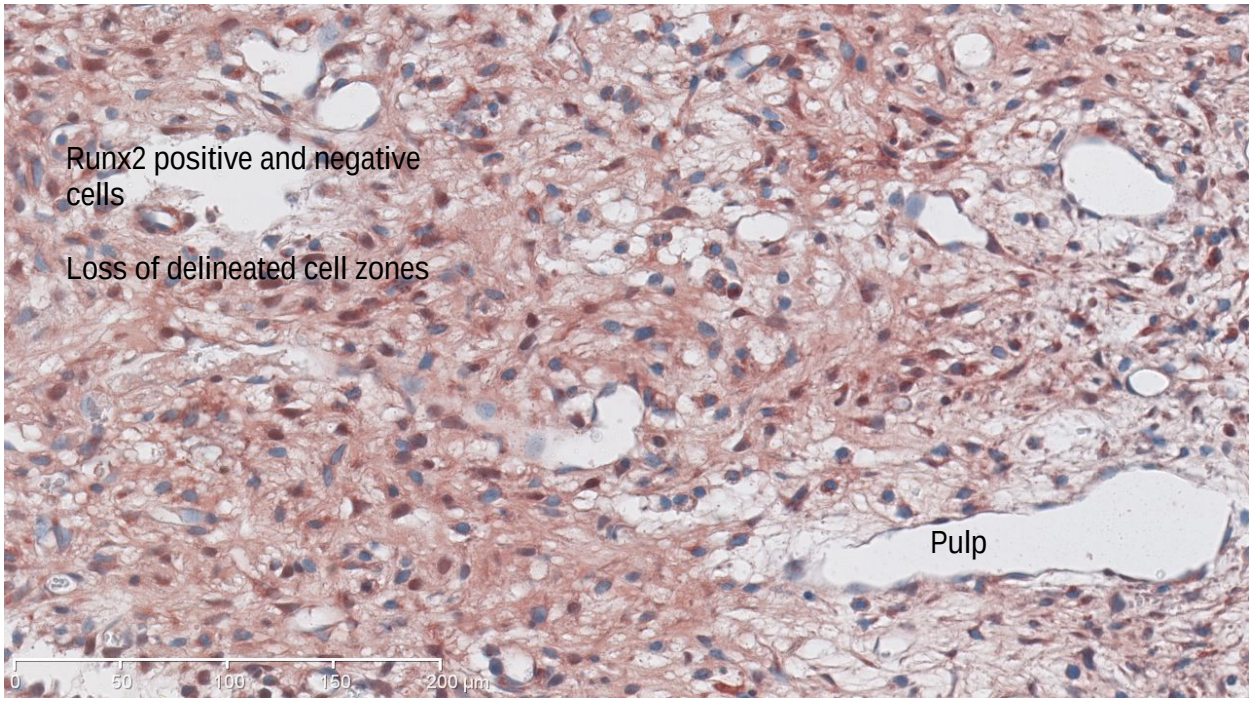

Day 7 Internal Control

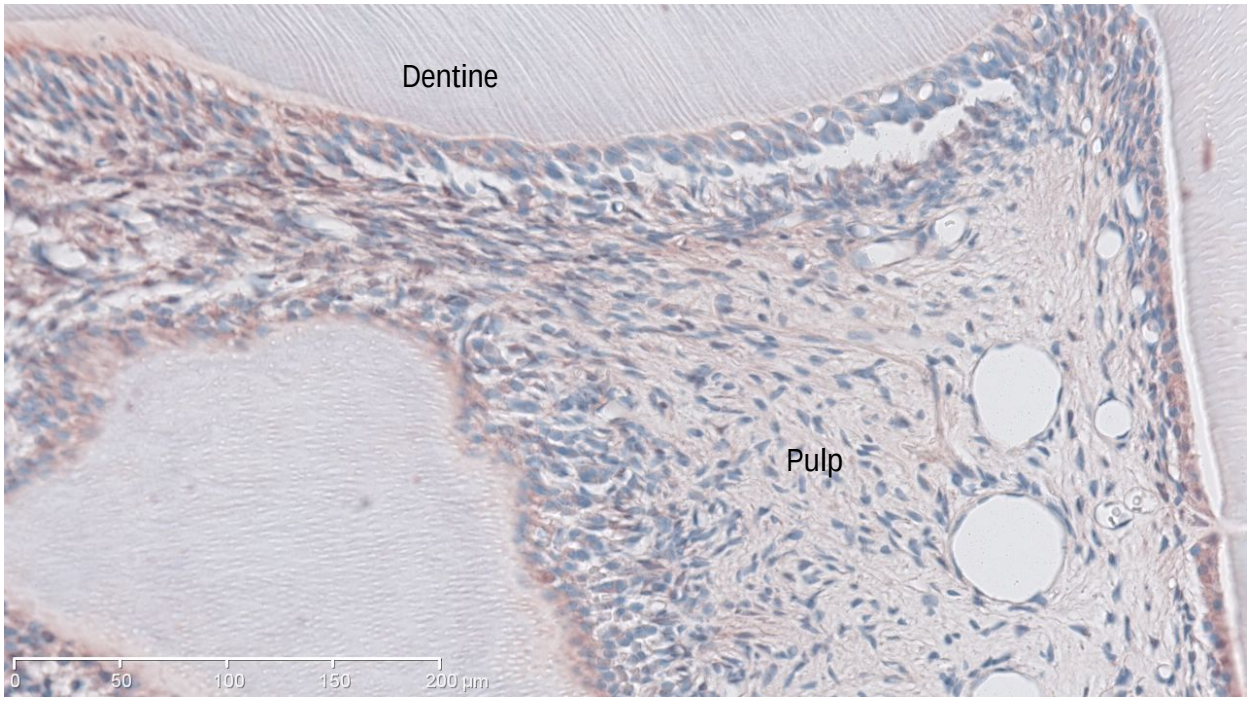

Day 14 Experimental

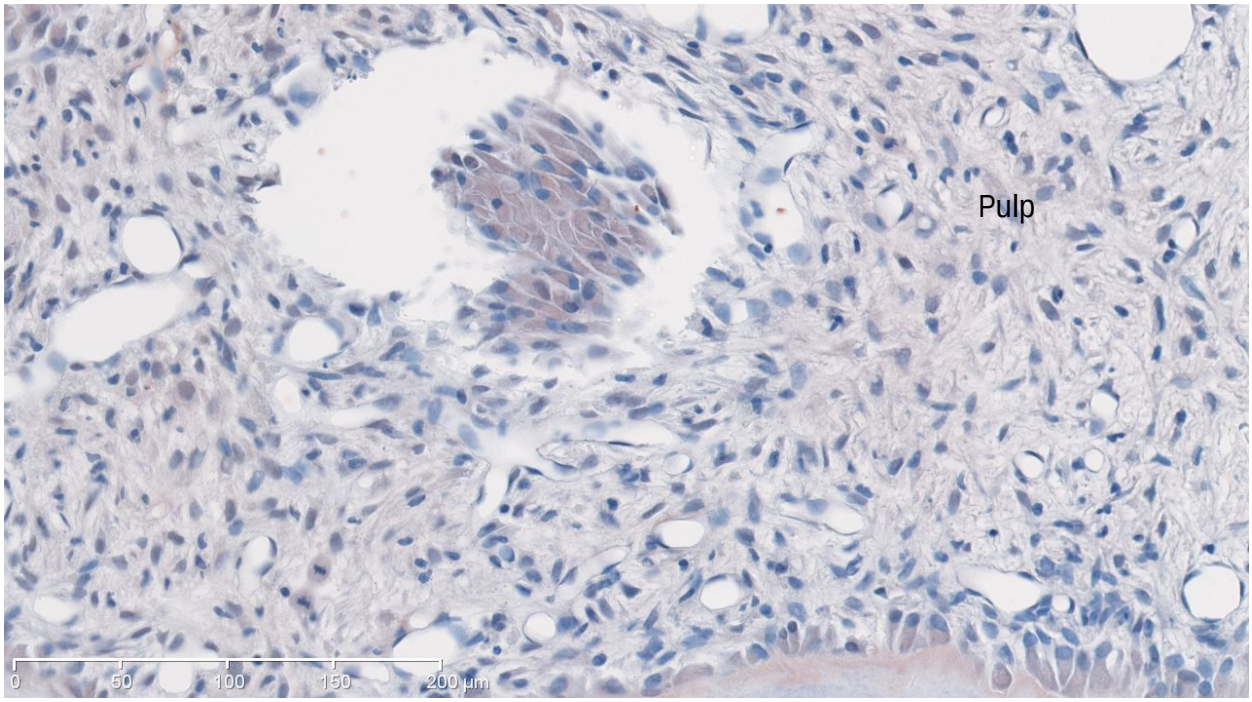

Day 14 Internal Control

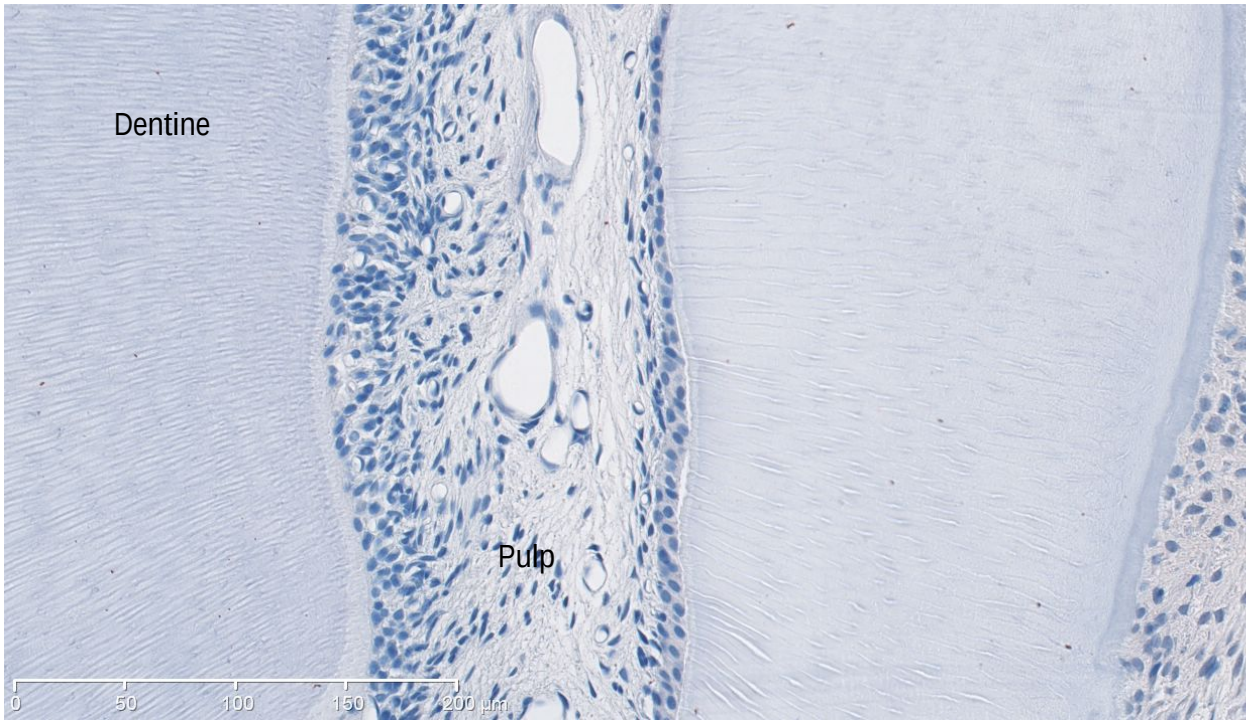

Day 28 Experimental

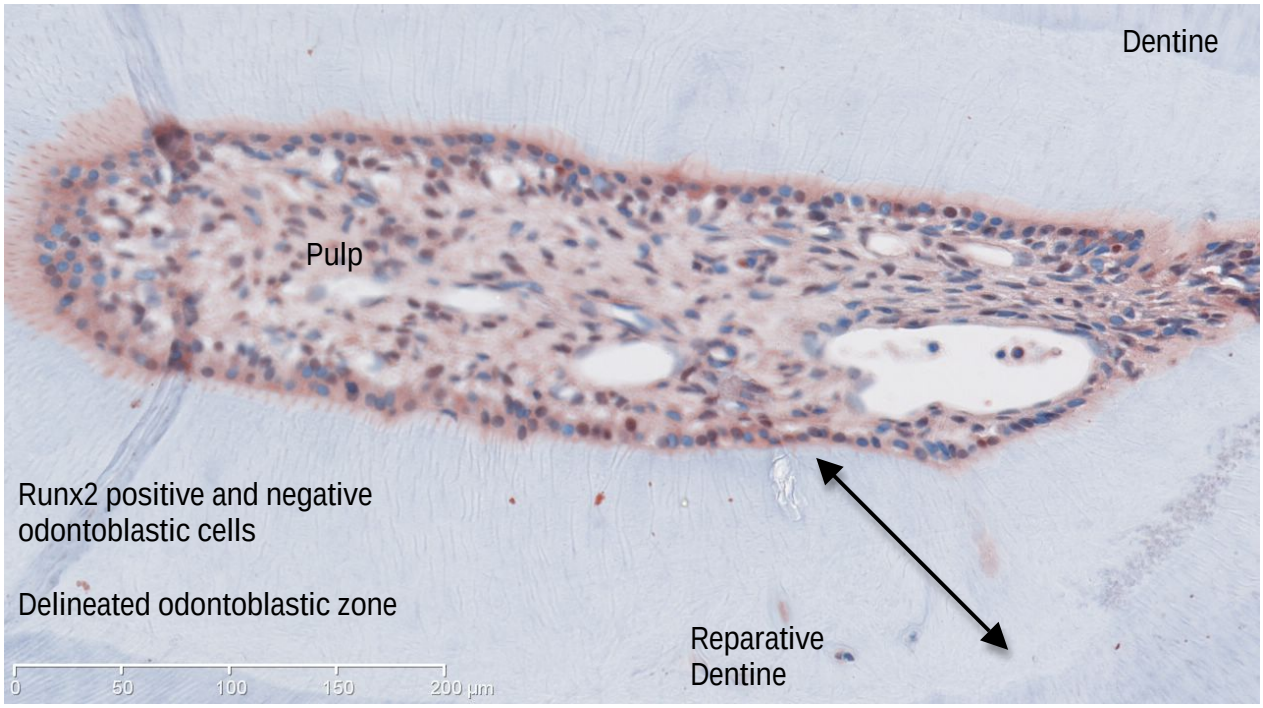

Day 28 Internal Control

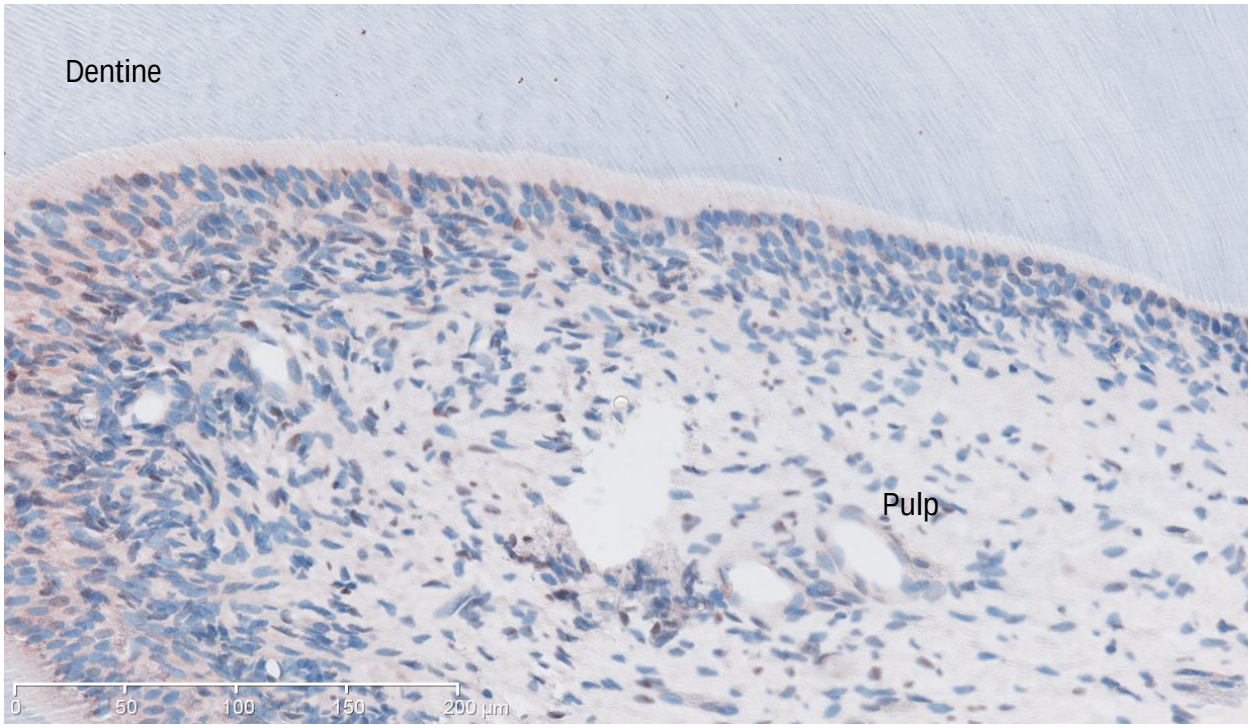

Statistically, the difference in expression of Runx2 positive cells in the experimental compared to the internal control teeth was in agreement with the subjective evaluation and overall was found to be significant ($F(1,24)=13$, $p<0.05$) with the experimental side showing on average 27.6% more positive cells than the internal control side (see Table 2).

Table 2: A comparison of the mean percentage of Runx2 positive cells in the Pulp within the experimental group at different time points and overall between the experimental and internal control groups.

R: Experimental, L: Internal Control. 0, 4, 7, 14 and 28 denote time points of the Experimental group. * $p<0.05$.

Effect		Mean	Standard Error	PValue
time	0 vs. 4	-4.3468	10.8983	0.6904
time	0 vs. 7	-6.1169	11.0046	0.5788
time	0 vs. 14	6.9390	10.8918	0.5247
time	0 vs. 28	14.4066	10.9244	0.1885
time	4 vs. 7	-1.7701	10.8742	0.8708
time	14 vs. 4	-11.2858	10.7600	0.2953
time	14 vs. 7	-13.0559	10.8676	0.2308
time	14 vs. 28	7.4676	10.7864	0.4894
time	28 vs. 4	-18.7534	10.7930	0.0836
time	28 vs. 7	-20.5235	10.9003	0.0609
side	L vs. R	-27.6033	7.6554	*0.0014

In the experimental sites, although there was a trend of increasing Runx2 positive cells in the pulp at days 4 and 7 followed by a reduction in positive cells at days 14 and 28 compared to day 0, these differences were not significant statistically (see Tables 2 and 3).

Table 3: The mean percentage of Runx2 positive cells in the Pulp within the experimental group at different time points and overall between the experimental and internal control groups.

R: Experimental, L: Internal Control. 0, 4, 7, 14 and 28 denote time points of the Experimental group.

Effect	Time	Side	Mean	Standard Error
time	0		38.6707	7.7983
time	4		43.0174	7.6131
time	7		44.7876	7.7645
time	14		31.7316	7.6038
time	28		24.2641	7.6504
side		L	22.6926	5.1523
side		R	50.2959	5.1370

A trend of changing expression of Runx2 positive cells was also noted in the internal control animals, with the number of Runx2 positive cells decreasing at days 4, 7 and 14 and increasing at day 28. See Table 4. These differences were statistically significant between days 0 and 14 and days 0 and 28 ($p<0.05$) (see Table 5).

Differences in the expression of Runx2 positive cells in the pulp of the internal control and external control rats was also calculated with a statistically significant difference noted between the external control group and internal control group at day 14 ($p<0.05$) (see Table 5).

Table 4: The mean percentage of Runx2 positive cells in the Pulp of control groups.

EC: External control. 0, 4, 7, 14, 28 denote time points of the internal control.

Effect	time	Mean	Standard Error
time	EC	33.9352	8.2041
time	0	41.2760	8.3302
time	4	28.2818	8.0235
time	7	23.2525	8.3653
time	14	7.8730	8.0085
time	28	12.5341	8.0836

Table 5: A comparison of the mean percentage of Runx2 positive cell counts in the Pulp of control groups.

EC: External control. 0, 4, 7, 14 and 28 denote time points of the Internal control group.

* $p<0.05$.

Effect		Estimate	Standard Error	PValue
time	EC vs. 0	-7.3409	11.6918	0.5311
time	EC vs. 4	5.6534	11.4753	0.6230
time	EC vs. 7	10.6827	11.7169	0.3635
time	EC vs. 14	26.0621	11.4649	*0.0245
time	EC vs. 28	21.4010	11.5175	0.0652
time	0 vs. 4	12.9942	11.5658	0.2631
time	0 vs. 7	18.0236	11.8055	0.1291
time	0 vs. 14	33.4030	11.5554	*0.0045
time	0 vs. 28	28.7419	11.6076	*0.0145
time	4 vs. 7	5.0293	11.5911	0.6650
time	14 vs. 4	-20.4088	11.3363	0.0740
time	14 vs. 7	-15.3794	11.5808	0.1863
time	14 vs. 28	-4.6611	11.3789	0.6827
time	28 vs. 4	-15.7477	11.3895	0.1690
time	28 vs. 7	-10.7183	11.6328	0.3584

Runx2 Expression in the PDL:

Subjective evaluation of the PDL showed little difference in the expression of Runx2 at day 0 in the experimental, internal control or external control PDL tissues, with an intact PDL ligament and both positive and negative fibroblast-like cells present. Positive epithelial rest cells of Malassez, blood vessel lumen and osteoclasts on the outer bony interface of the PDL were also present, as was diffuse staining of the extracellular matrix of the PDL. This diffuse staining of the extracellular matrix was present in all sections at all time points.

At day 4, sections in the experimental group presented similarly to day 0.

By day 7, changes in the PDL of experimental sites were visible with thinning of the PDL, as well as some islands of PDL cells. Positive and negative staining fibroblast-like cells were present within these islands of cells.

This trend continued at day 14, with complete loss of the PDL in the interradicular region of many sections. Few cells remained at the borders of ankylotic regions, with both positive and negative fibroblast-like cells evident.

By day 28, one animal remained very similar to those at day 14, whilst the two other animals demonstrated an intact PDL and no ankylosis (see Figure 10).

Figure 10: Changes in Runx2 expression in PDL in the external control group and at various time points in the experimental and internal control groups

x 20 magnification ruler 0 - 200**µ**m.

Note red staining indicates Runx2 positive result, blue staining indicates haematoxylin counterstain

Day 0 External Control

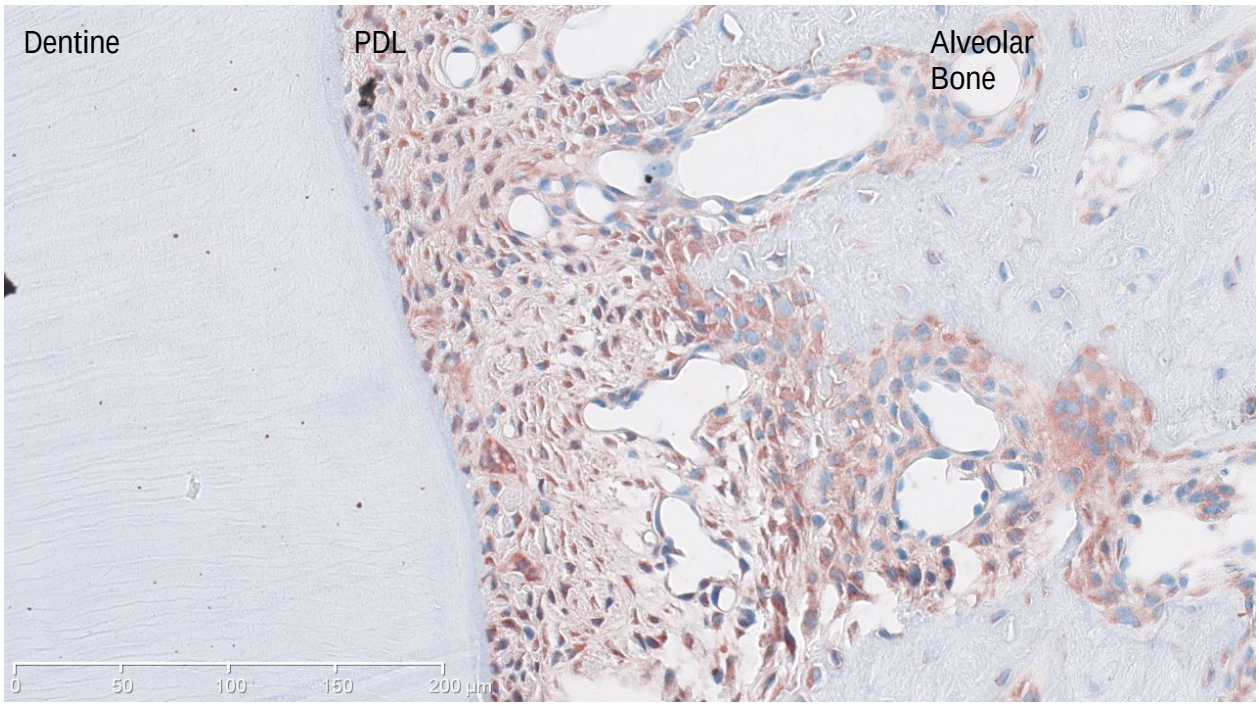

Day 0 Experimental

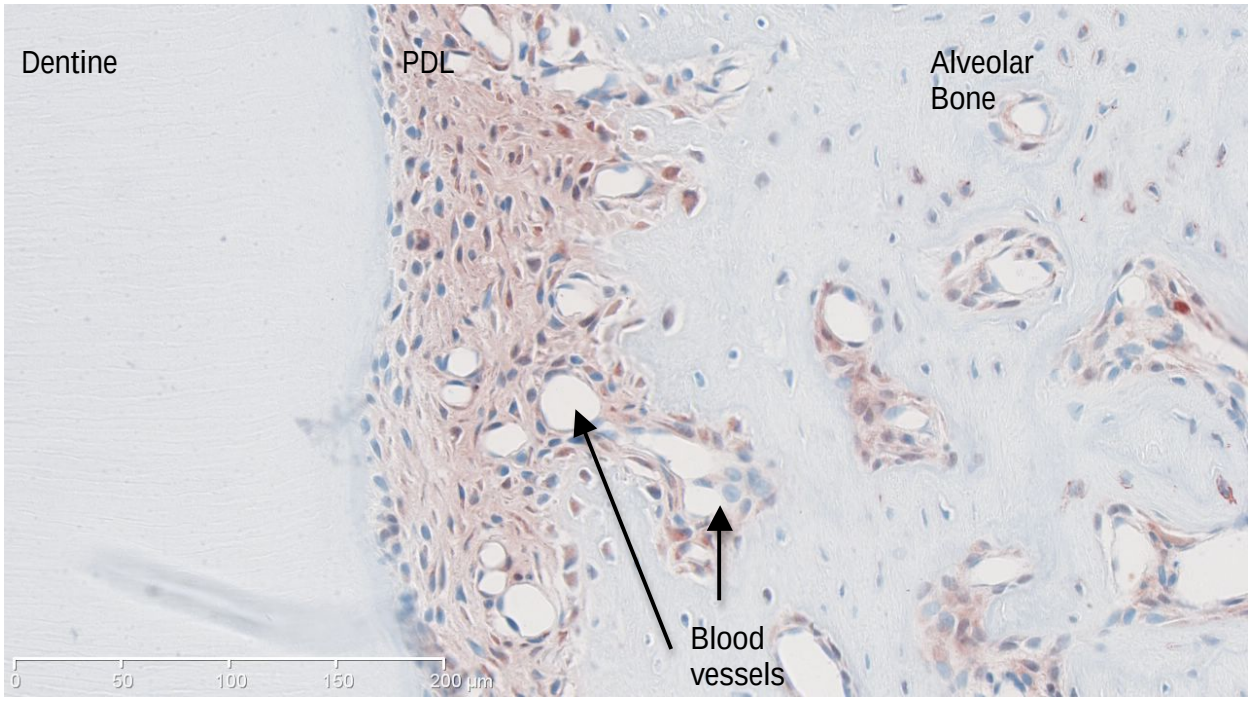

Day 0 Internal Control

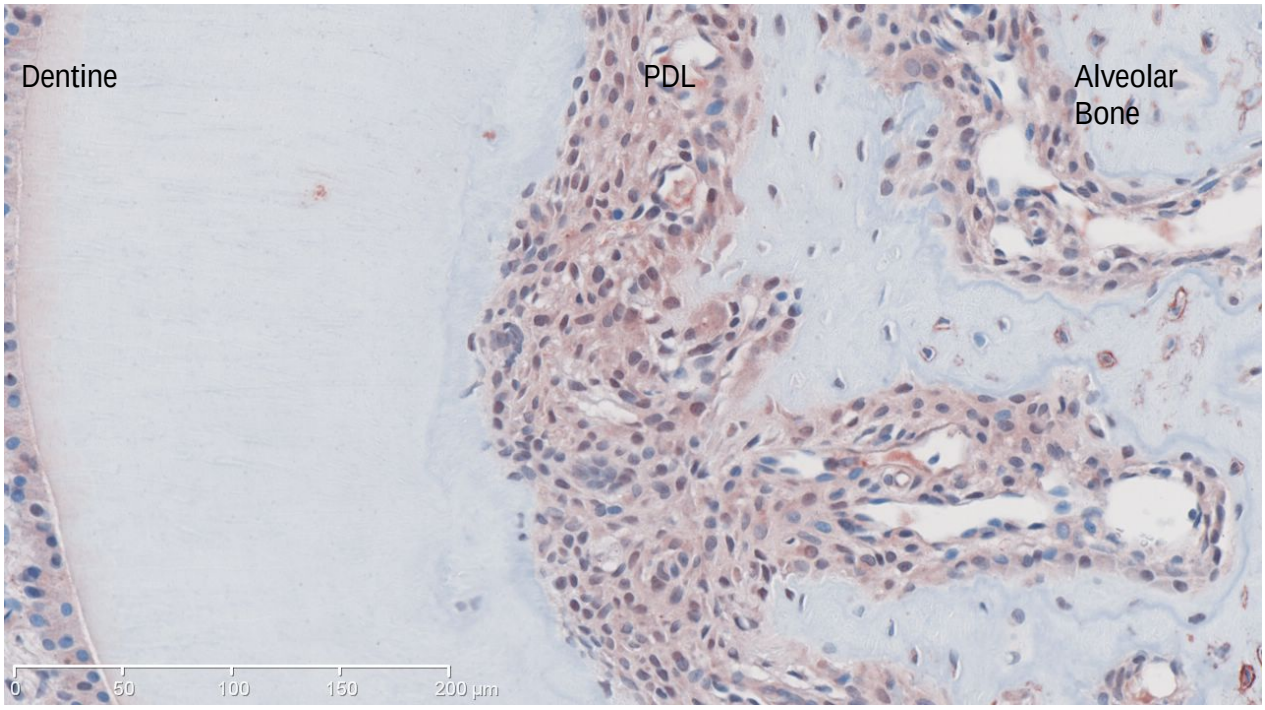

Day 4 Experimental

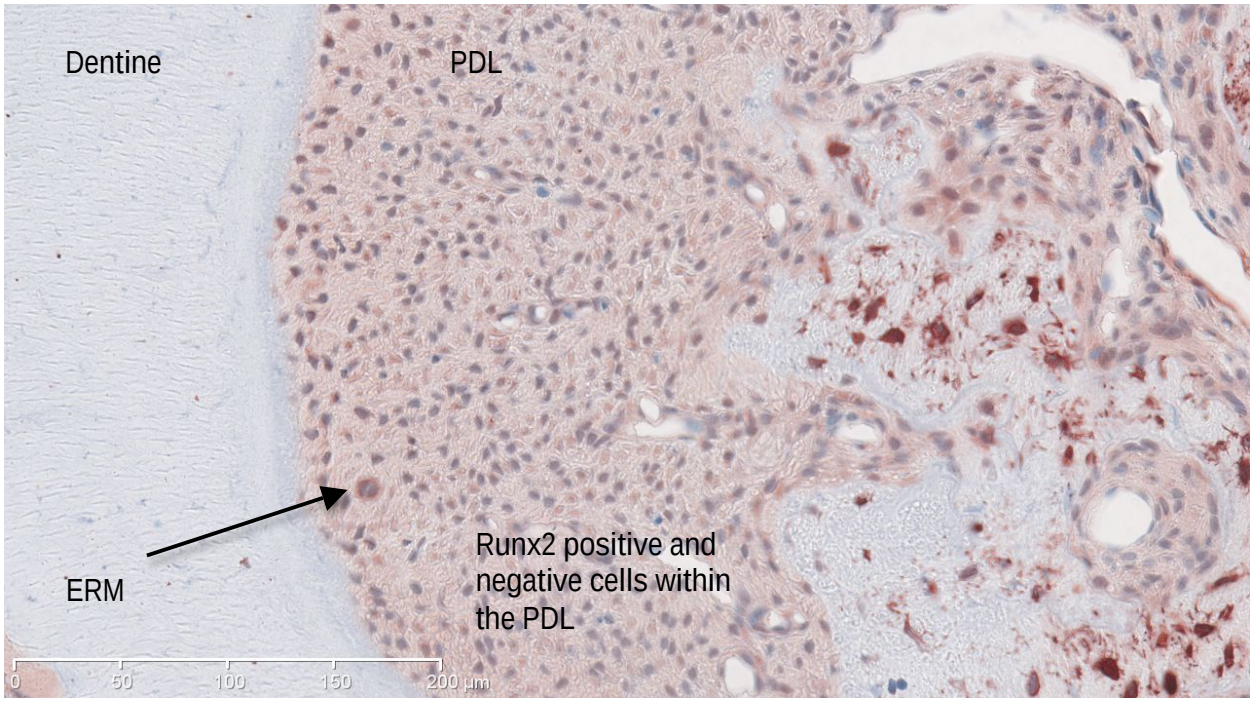

Day 4 Internal Control

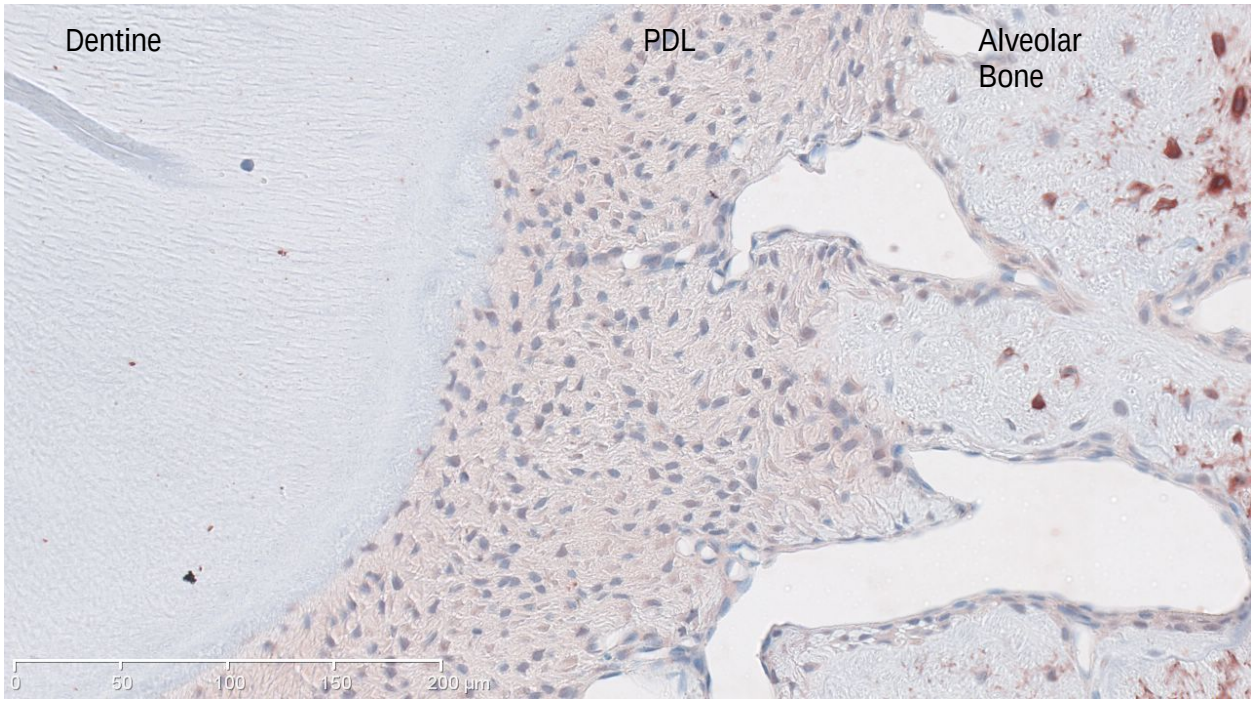

Day 7 Experimental

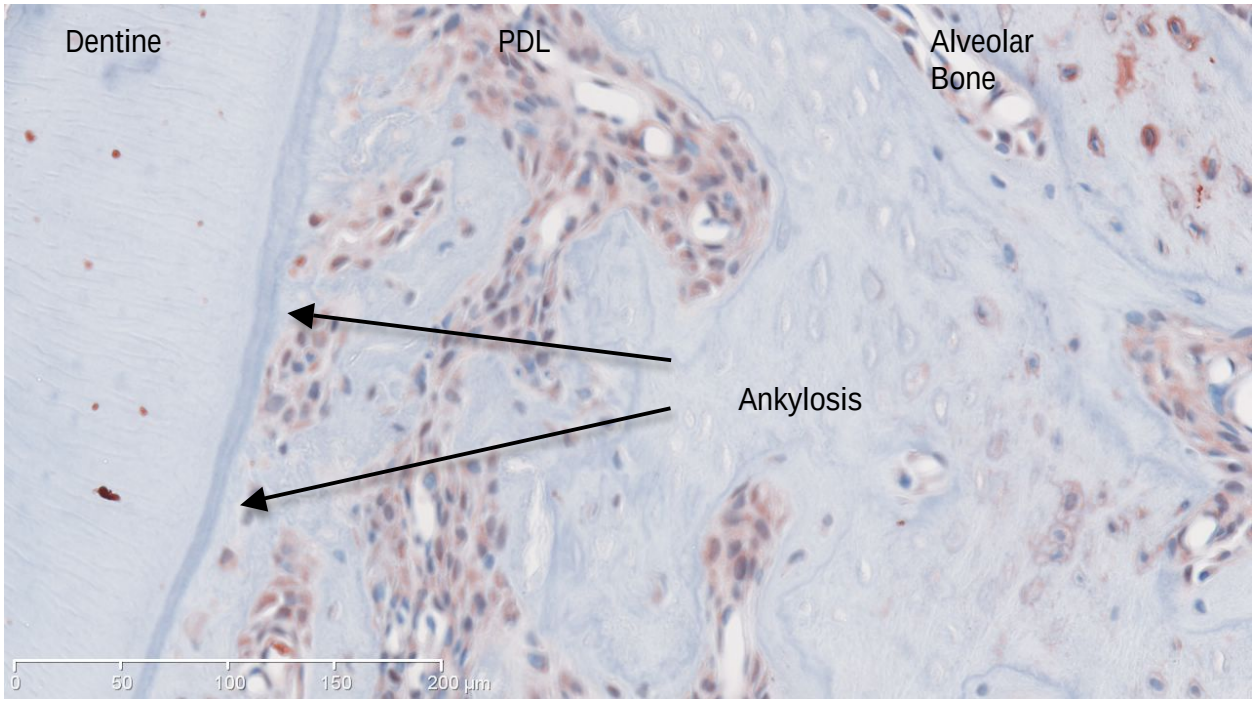

Day 7 Internal Control

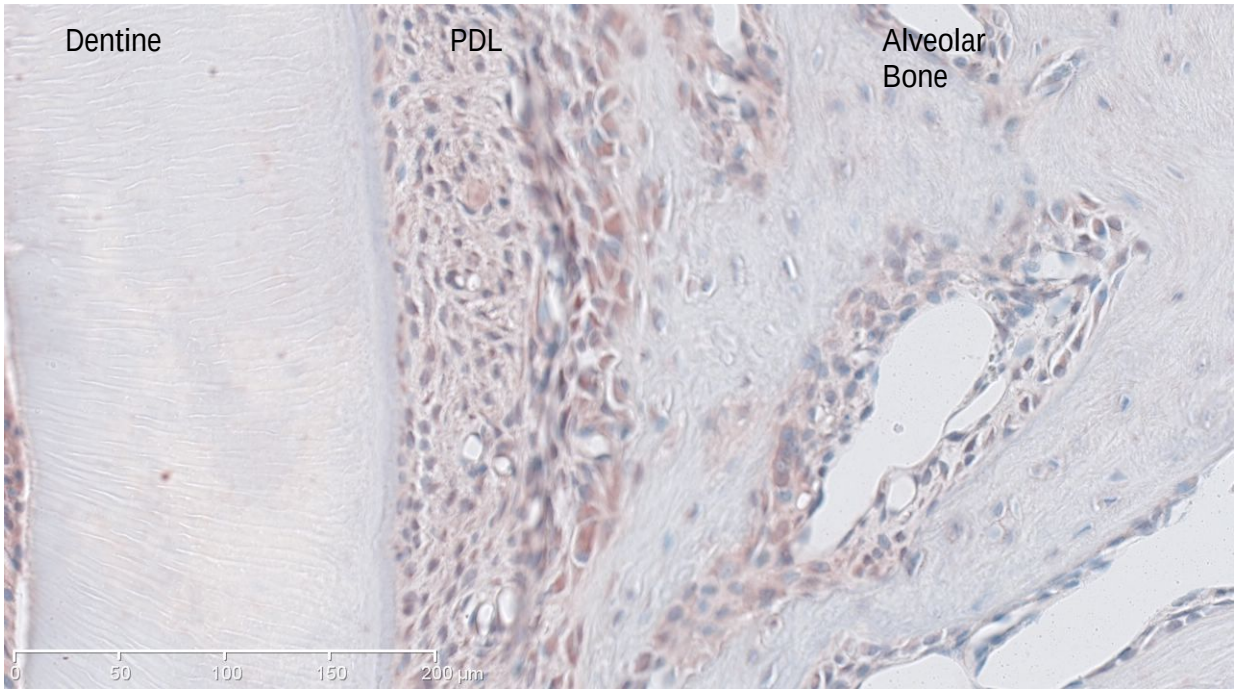

Day 14 Experimental

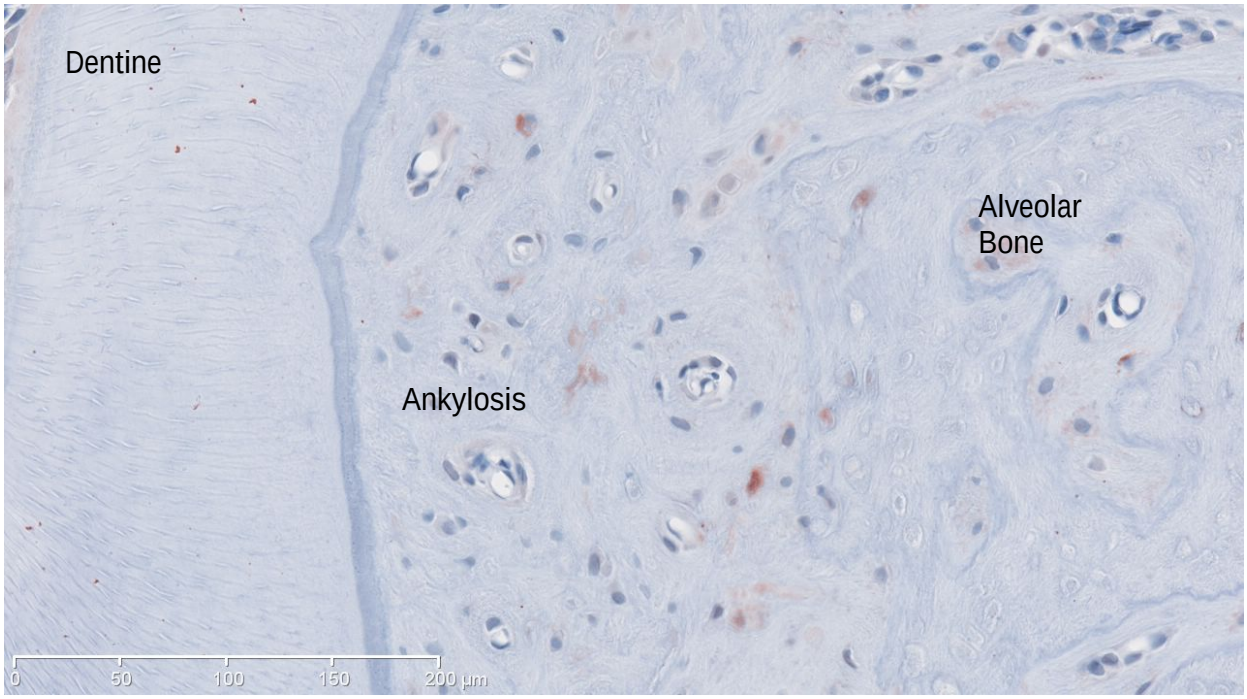

Day 14 Internal Control

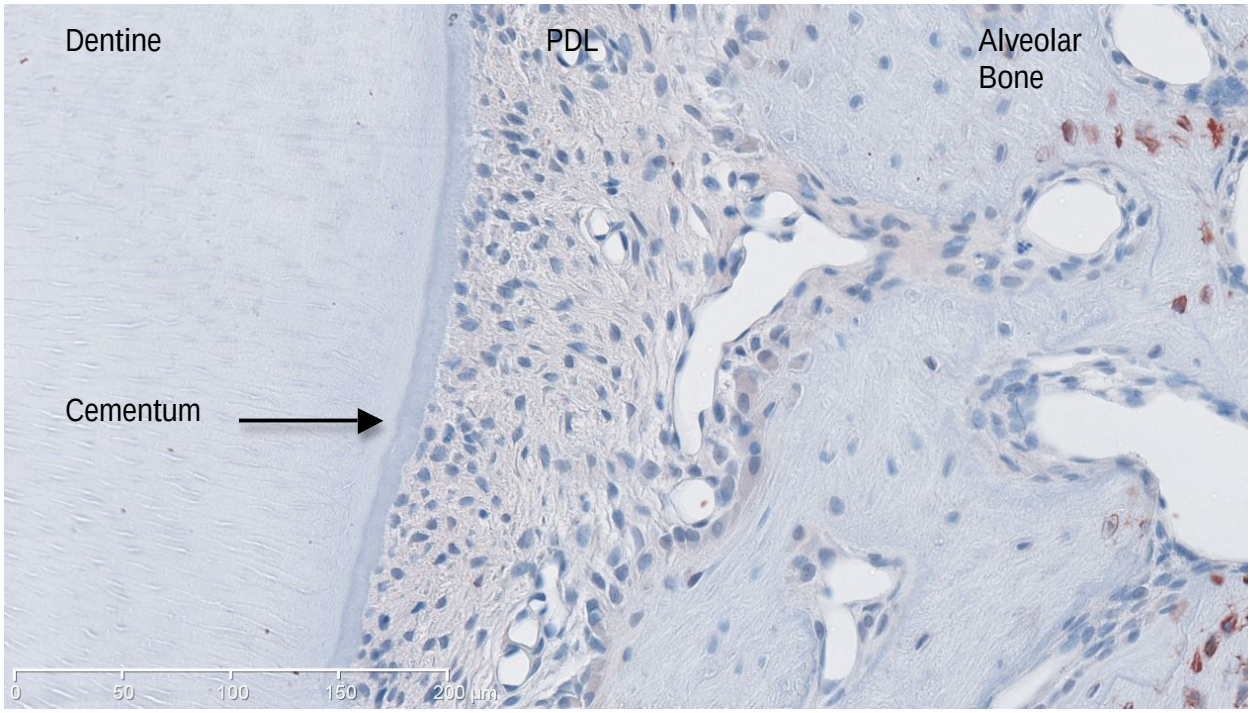

Day 28 Experimental

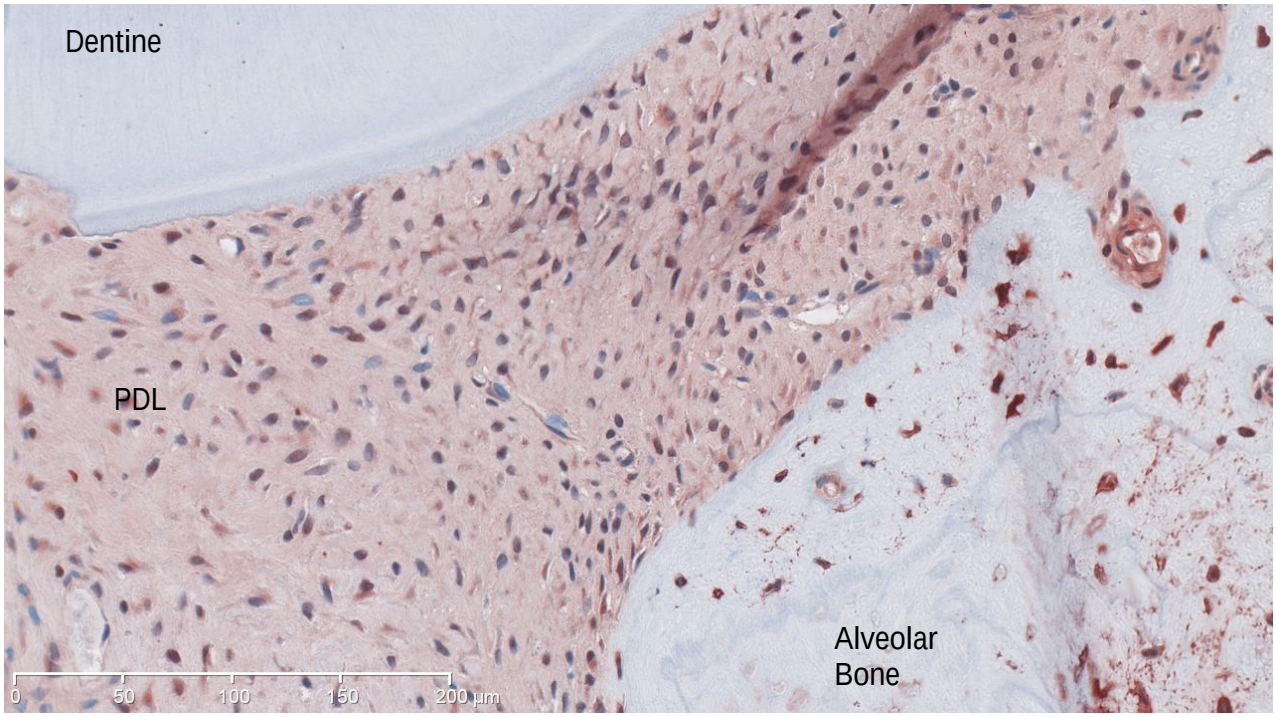

Day 28 Internal Control

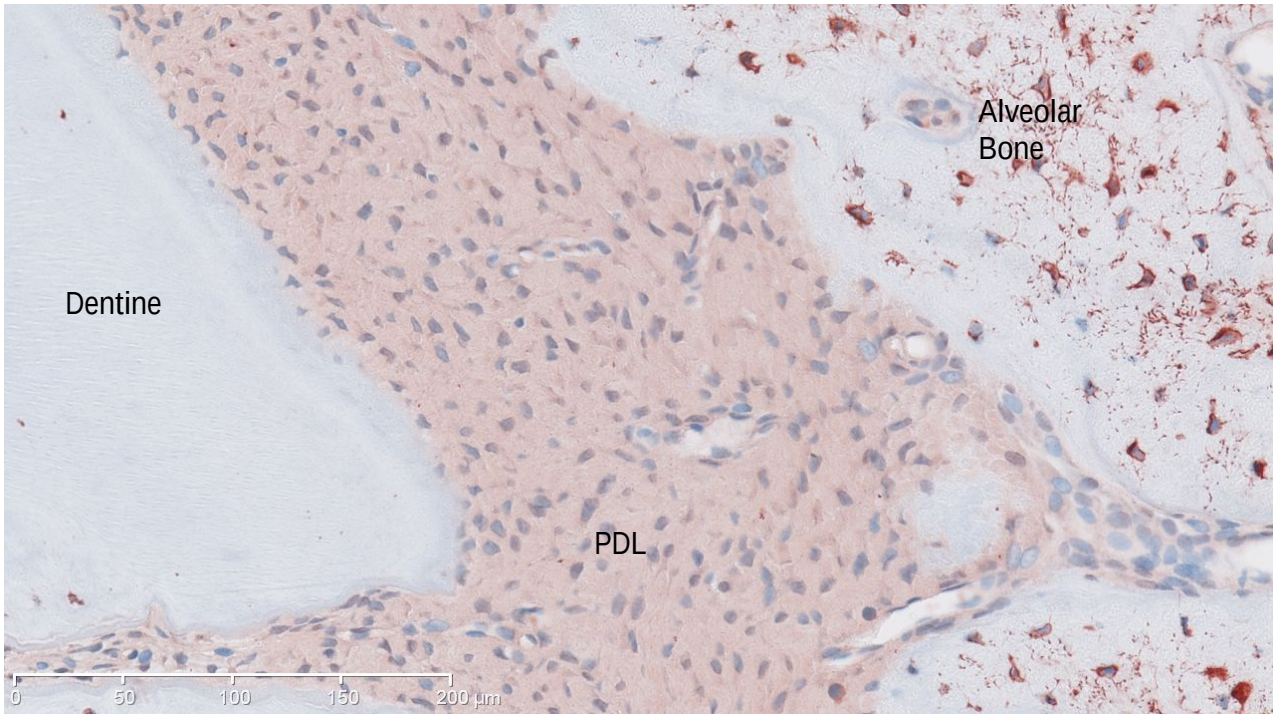

Statistically, there was agreement with the subjective evaluation in that there was no significant difference in the percentage of Runx2 positive cells between the experimental and internal control groups (p = 0.7248). There was also no significant difference between the various time points in the experimental group (p=0.5336) (see Table 6).

Table 6: The mean percentage of Runx2 positive cells in the PDL within the experimental group at different time points and overall between the experimental and internal control sides.

R: Experimental, L: Internal Control. 0, 4, 7, 14 and 28 denote time points of the experimental group.

Effect	time	side	Mean	Standard Error
time	0		88.8009	4.1171
time	4		88.1557	3.9196
time	7		85.2478	4.0208
time	14		85.9415	3.9346
time	28		79.8368	3.9708
side		R	85.1578	2.1699
side		L	86.0353	2.1688

Although there was a significant difference between the external control group and the internal control group at day 28 (p=0.0045), overall there was also no significant difference in the percentage of Runx2 positive cells between the internal and external control groups (p=0.0609). See Table 7 and 8. Within the internal control group, there was a significant difference noted between day 28 and days 4 (p=0.0168), 7 (p=0.0179) and 14 (p=0.0463) (see Table 8).

Table 7: The mean percentage of Runx2 positive cells in the PDL of control animals. EC: External control. 0, 4, 7, 14 and 28 denote time points of the Internal control.

Effect	time	Estimate	Standard Error
time	EC	91.8173	4.0503
time	0	89.9250	4.1405
time	4	88.9782	3.9246
time	7	89.0490	4.0443
time	14	86.6955	3.9144
time	28	75.4949	3.9957

Table 8: A comparison of the mean percentage of Runx2 positive cells in the PDL of control animals. EC: External control. 0, 4, 7, 14 and 28 denote time points of the Internal control. * $p<0.05$.

Effect		Estimate	Standard Error	PValue
time	ECvs. 0	1.8923	5.7921	0.7442
time	EC vs. 4	2.8391	5.6398	0.6151
time	EC vs. 7	2.7683	5.7237	0.6291
time	EC vs. 14	5.1218	5.6327	0.3641
time	EC vs. 28	16.3224	5.6895	*0.0045
time	0 vs. 4	0.9468	5.7049	0.8683
time	0 vs. 7	0.8760	5.7880	0.8798
time	0 vs. 14	3.2295	5.6979	0.5714
time	0 vs. 28	14.4301	5.7541	*0.0128
time	4 vs. 7	-0.07074	5.6355	0.9900
time	14 vs. 4	-2.2827	5.5430	0.6808
time	14 vs. 7	-2.3535	5.6284	0.6762
time	14 vs. 28	11.2006	5.5936	*0.0463
time	28 vs. 4	-13.4833	5.6007	*0.0168
time	28 vs. 7	-13.5541	5.6852	*0.0179

On inspection of the slides, increased Runx2 colour intensity was noted in PDL closest to the bone when compared to the PDL closest to the dentine. This phenomenon was confirmed via digital image analysis for staining intensity and significant differences were observed between the two regions in the majority of animals in the experimental, internal control and external control groups (see Table 9).

Table 9: Comparison of the colour intensity of the PDL on the experimental side closest to the dentine versus closest to the alveolar bone. * p<0.05.

id	Side	Variable	group1	n1	mean1	StdDev1	group2	n2	mean2	StdDev2	Mean_ difference	Lower95%CI	Upper95%CI	PValue
1	L	Count	Dentine	10918	91.212	20.6740	Bone	11130	91.667	24.0780	0.455	-0.1370	1.0470	0.1320
2	L	Count	Dentine	10815	177.224	16.4840	Bone	10815	192.448	17.8140	15.224	14.7666	15.6814	*<.0001
3	L	Count	Dentine	10914	154.057	26.9960	Bone	10500	146.553	38.0450	-7.504	-8.3907	-6.6173	*<.0001
4	L	Count	Dentine	11130	94.449	29.0200	Bone	10605	108.282	55.1880	13.833	12.6523	15.0137	*<.0001
5	L	Count	Dentine	11236	119.178	29.3310	Bone	11342	134.775	40.3980	15.597	14.6767	16.5173	*<.0001
6	L	Count	Dentine	11448	134.754	30.8100	Bone	10920	118.073	20.6020	-16.681	-17.3650	-15.9970	*<.0001
7	L	Count	Dentine	11342	205.647	23.5860	Bone	11342	208.36	21.4100	2.713	2.1267	3.2993	*<.0001
8	L	Count	Dentine	11021	125.001	35.6070	Bone	10605	108.725	31.4100	-16.276	-17.1701	-15.3819	*<.0001
9	L	Count	Dentine	8964	240.608	12.8320	Bone	9135	239.778	12.8280	-0.83	-1.2039	-0.4561	*<.0001
10	L	Count	Dentine	10700	189.588	27.7660	Bone	11128	220.355	21.6010	30.767	30.1053	31.4287	*<.0001
11	L	Count	Dentine	11433	156.385	17.9880	Bone	10608	160.275	25.1360	3.89	3.3090	4.4710	*<.0001
12	L	Count	Dentine	10400	206.88	17.1220	Bone	10712	206.513	22.4670	-0.367	-0.9049	0.1709	0.1811
13	L	Count	Dentine	11130	191.915	31.4080	Bone	11880	180.394	25.2640	-11.521	-12.2605	-10.7815	*<.0001
14	L	Count	Dentine	11660	130.253	24.8930	Bone	11448	126.751	36.6050	-3.502	-4.3106	-2.6934	*<.0001
15	L	Count	Dentine	10282	165.158	31.9970	Bone	11445	139.65	32.1370	-25.508	-26.3622	-24.6538	*<.0001
16	L	Count	Dentine	11025	220.948	18.1040	Bone	12826	215.382	21.4720	-5.566	-6.0683	-5.0637	*<.0001
17	L	Count	Dentine	10700	201.435	17.2430	Bone	10300	196.319	19.5840	-5.116	-5.6158	-4.6162	*<.0001
18	L	Count	Dentine	8712	202.293	12.7050	Bone	9792	207.333	14.1460	5.04	4.6531	5.4269	*<.0001
1	R	Count	Dentine	10918	34.728	18.5940	Bone	11550	42.461	20.2910	7.733	7.2245	8.2415	*<.0001
2	R	Count	Dentine	11660	217.612	10.1480	Bone	11025	224.187	11.5910	6.575	6.2908	6.8592	*<.0001
3	R	Count	Dentine	11024	151.807	39.7500	Bone	11024	134.595	40.6480	-17.212	-18.2734	-16.1506	*<.0001
4	R	Count	Dentine	10712	243.809	10.4780	Bone	11024	235.481	17.7350	-8.328	-8.7140	-7.9420	*<.0001
5	R	Count	Dentine	11342	90.67	34.6900	Bone	8008	123.8	30.4010	33.13	32.2075	34.0525	*<.0001
6	R	Count	Dentine	11342	128.208	36.4390	Bone	9964	154.339	45.5850	26.131	25.0125	27.2495	*<.0001
7	R	Count	Dentine	11554	224.896	19.3150	Bone	11342	226.692	19.2380	1.796	1.2966	2.2954	*<.0001
8	R	Count	Dentine	7665	61.224	30.8610	Bone	5016	71.647	48.5370	10.423	8.9123	11.9337	*<.0001
9	R	Count	Dentine	5304	212.086	19.7680	Bone	4815	217.433	14.8990	5.347	4.6686	6.0254	*<.0001
10	R	Count	Dentine	11021	103.632	27.8160	Bone	10706	166.662	24.4470	63.03	62.3342	63.7258	*<.0001
11	R	Count	Dentine	11130	183.12	12.6450	Bone	11556	194.358	11.2340	11.238	10.9263	11.5497	*<.0001
12	R	Count	Dentine	10807	162.878	28.7880	Bone	11128	167.39	26.9840	4.512	3.7731	5.2509	*<.0001
13	R	Count	Dentine	10593	129.29	32.1160	Bone	11550	111.093	32.6840	-18.197	-19.0517	-17.3423	*<.0001
14	R	Count	Dentine	11664	123.849	27.8280	Bone	10584	141.865	32.2840	18.016	17.2201	18.8119	*<.0001
15	R	Count	Dentine	10710	161.16	30.3850	Bone	10500	162.562	45.5620	1.402	0.3576	2.4464	*0.0085
16	R	Count	Dentine	7695	205.582	28.3050	Bone	9212	198.942	29.2010	-6.64	-7.5093	-5.7707	*<.0001
17	R	Count	Dentine	10712	190.163	19.7500	Bone	13320	190.745	16.6600	0.582	0.1130	1.0510	*0.0150
18	R	Count	Dentine	11016	223.509	15.4120	Bone	9135	216.643	10.4390	-6.866	-7.2247	-6.5073	*<.0001

Runx2 Expression in Alveolar Bone:

Initial observation shows that at day 0 in the experimental, internal control and external control groups, Runx2 positive and negative bone cells (osteoblasts and osteocytes not differentiated) were present with the bone lining cells staining predominately Runx2 positive. In the experimental sites more intense positive staining of bone cells was present near to areas of bone marrow. Staining appeared to be cytoplasmic in nature, with staining of the canaliculi also present particularly in areas close to the bone marrow. Blood vessel lumen endothelial cells also appeared to stain positively for Runx2.

At day 4 in the experimental group, increased positive staining of the bone cells occurred with increased canaliculi staining evident.

By day 7, a decreased number of Runx2 positive cells were present, with less canaliculi staining. This trend continued at day 14.

At day 28, an increased number of positively staining bone cells in comparison to day 0 were again seen. This trend was mirrored in the internal control.

Empty lacunae appeared in the alveolar bone directly beneath the ankylotic region at day 7. The number of empty lacunae increased at day 14 and decreased at day 28 as compared to day 0. No empty lacunae were noted in the internal or external control groups (see Figure 11).

Figure 11: Changes in Runx2 expression in alveolar bone in the external control group and at various time points in the experimental and internal control groups

x20 magnification ruler 0 - 200**µ**m.

Note red staining indicates Runx2 positive result, blue staining indicates haematoxylin counterstain

Day 0 External Control

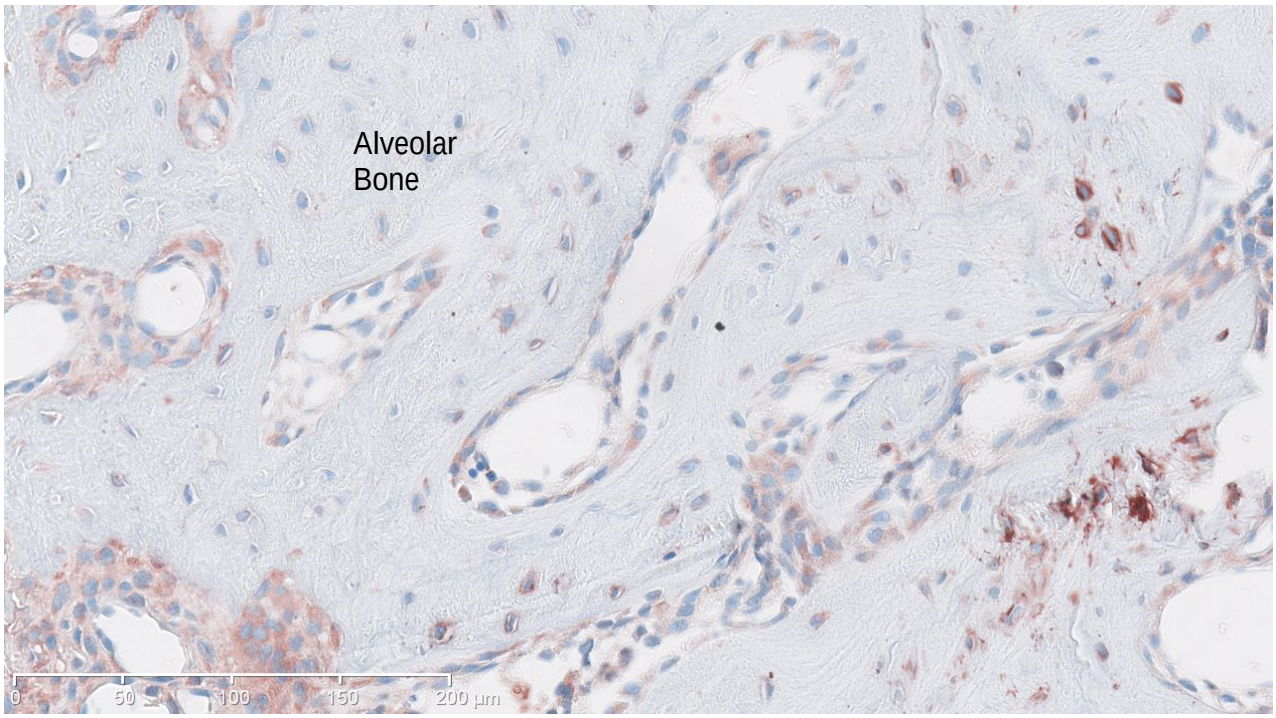

Day 0 Experimental

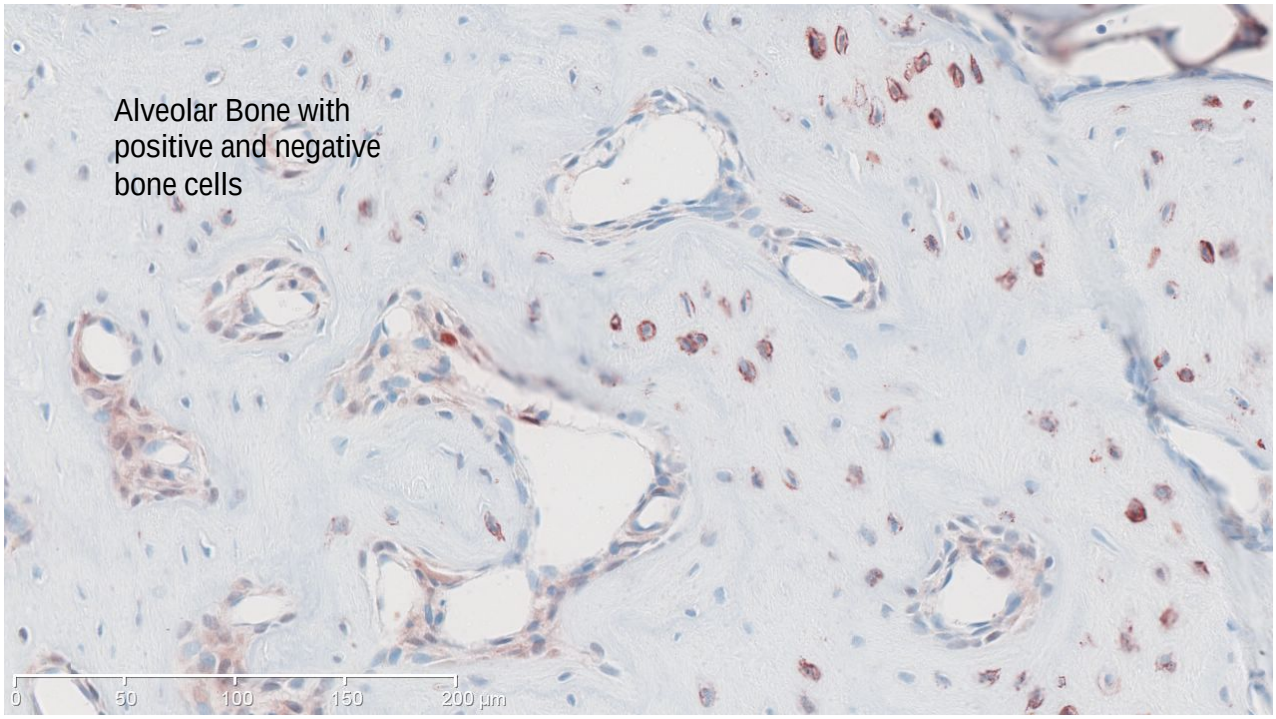

Day 0 Internal Control

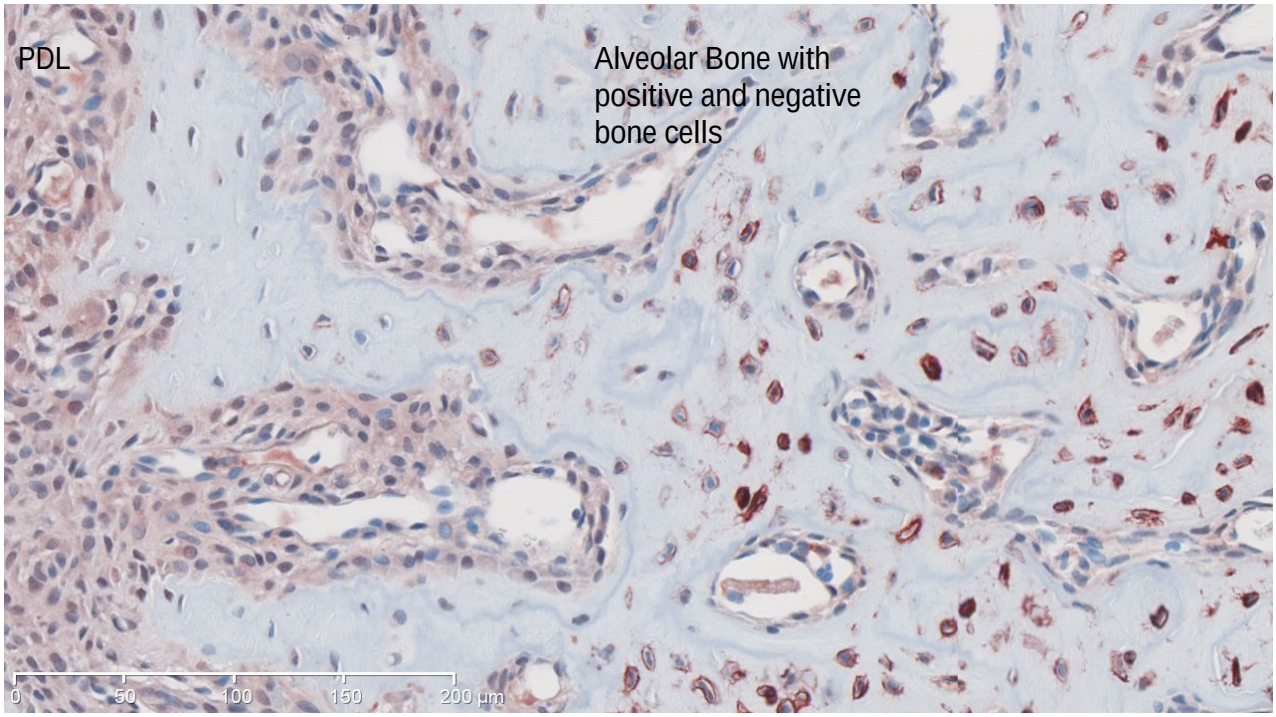

Day 4 Experimental

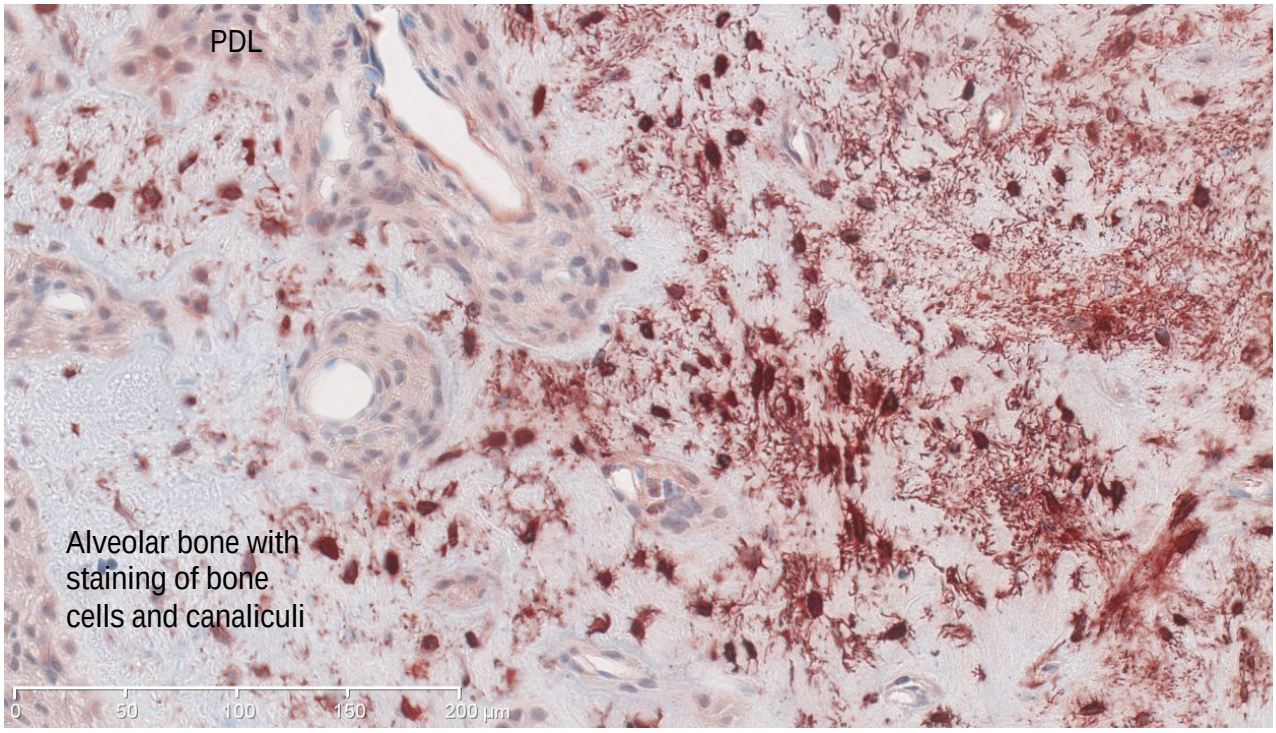

Day 4 Internal Control

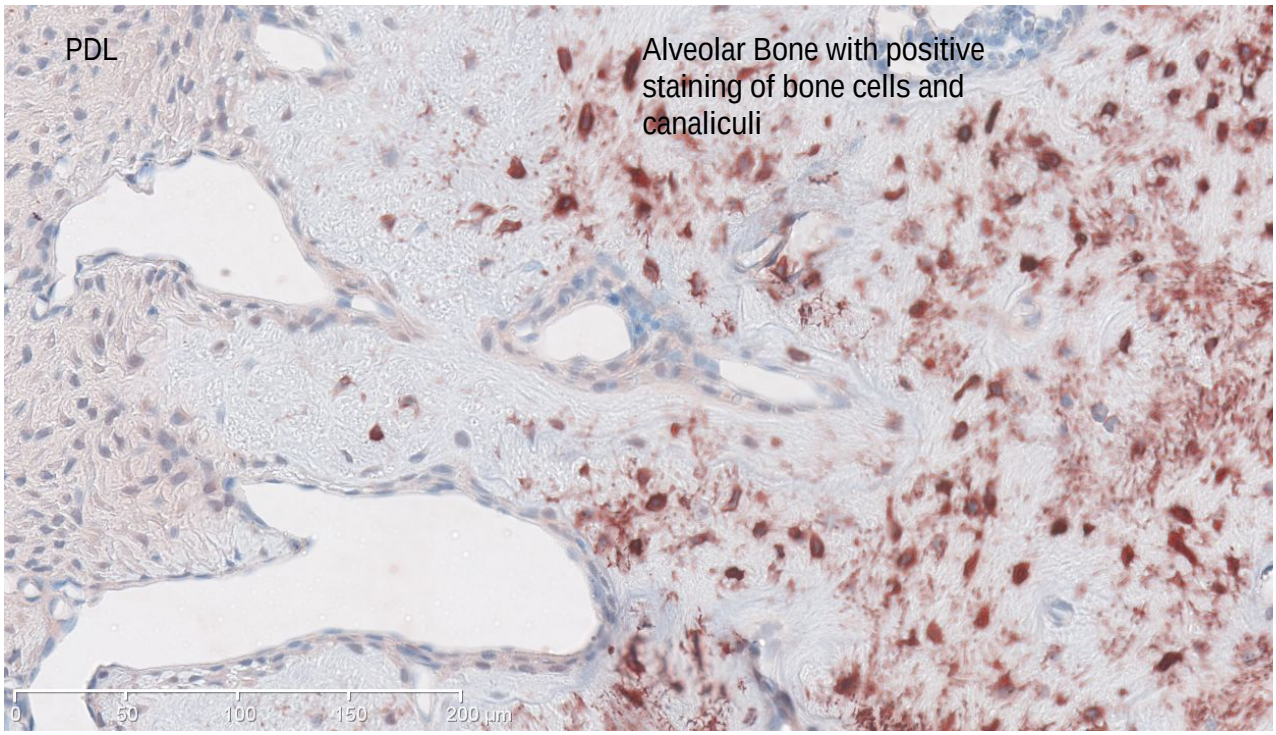

Day 7 Experimental

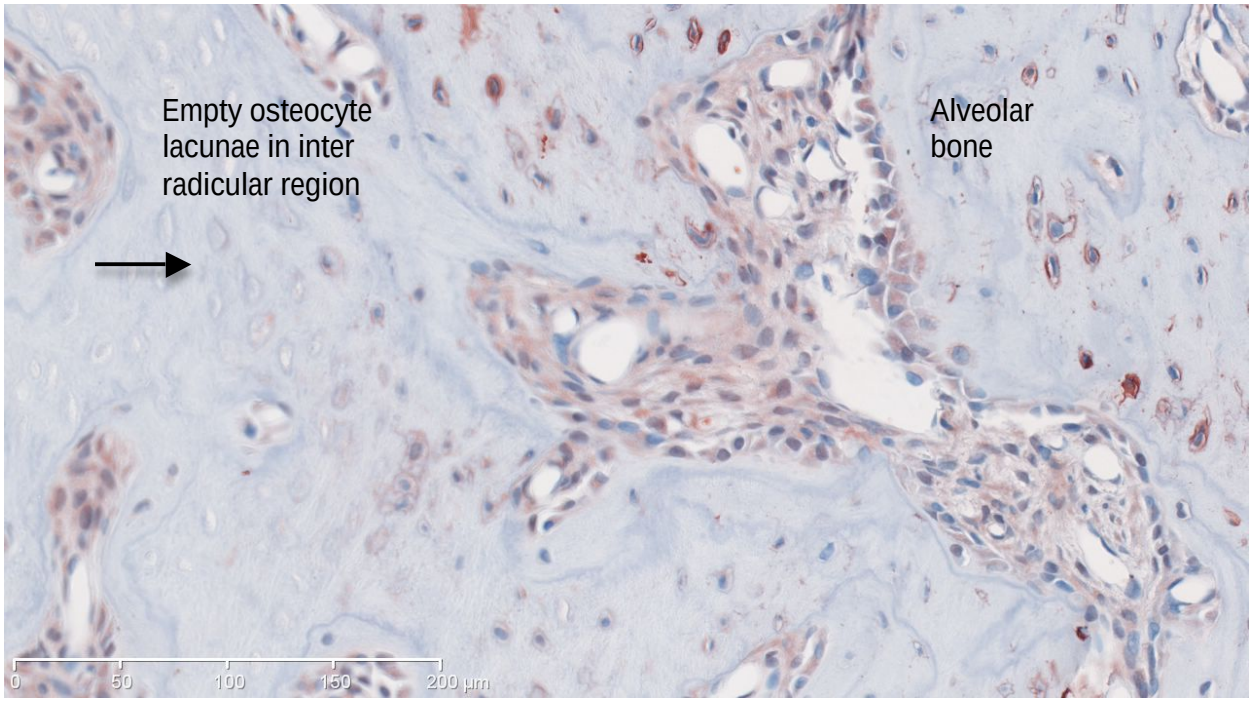

Day 7 Internal Control

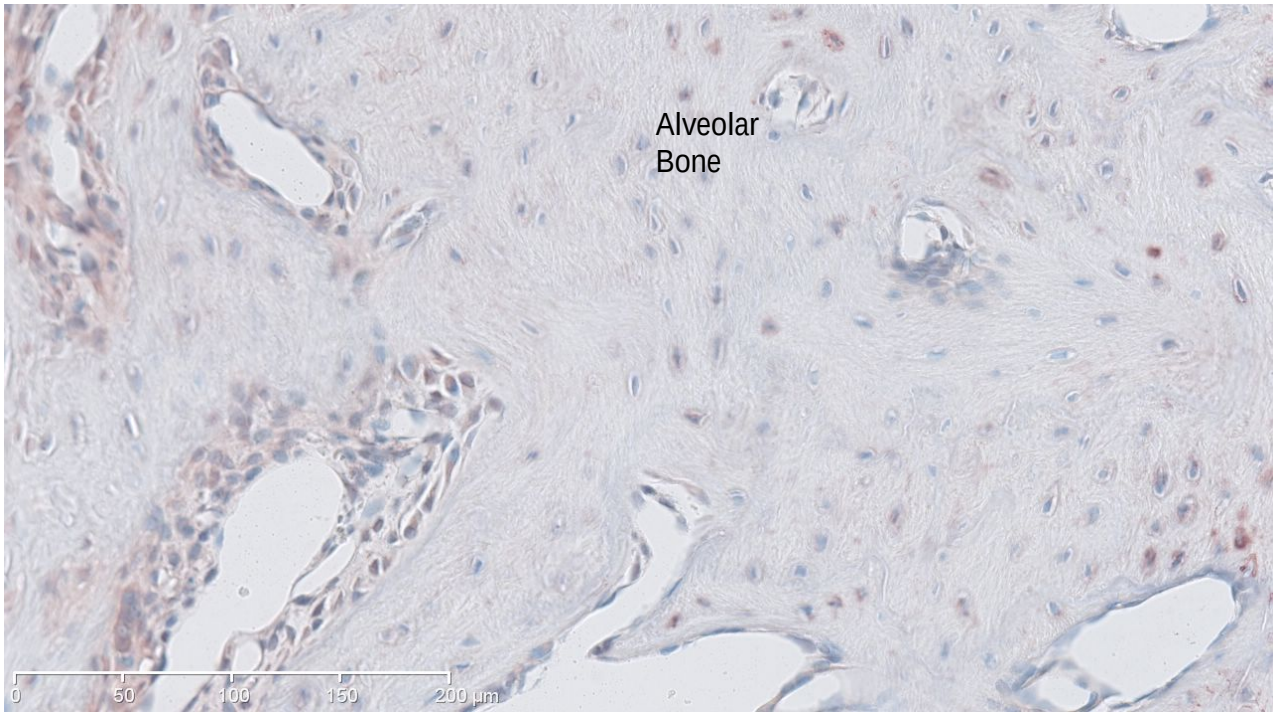

Day 14 Experimental

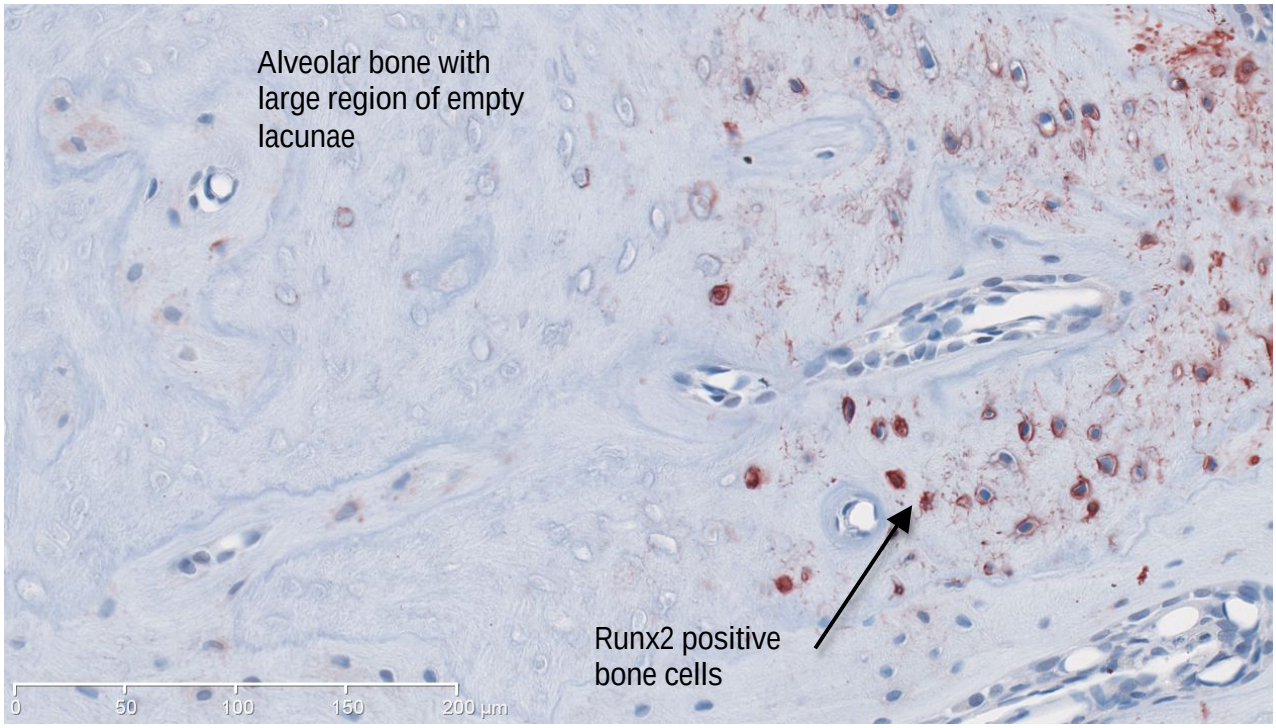

Day 14 Internal Control

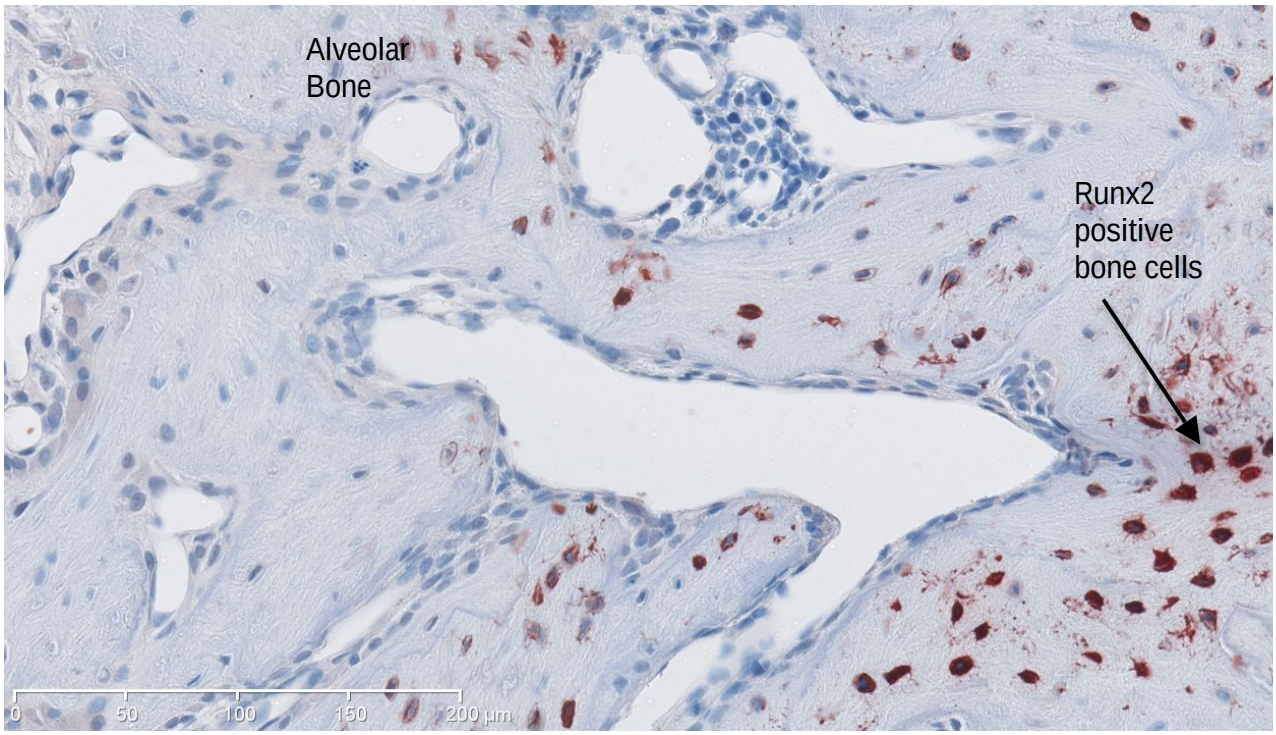

Day 28 Experimental

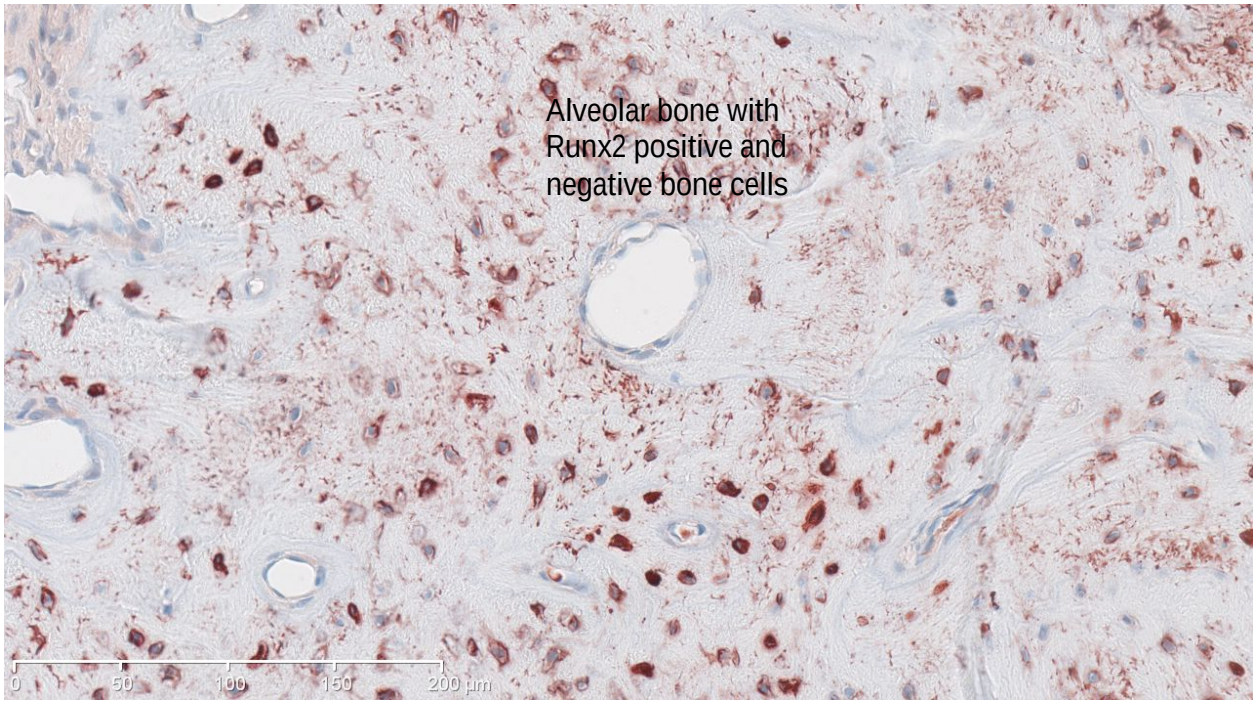

Day 28 Internal Control

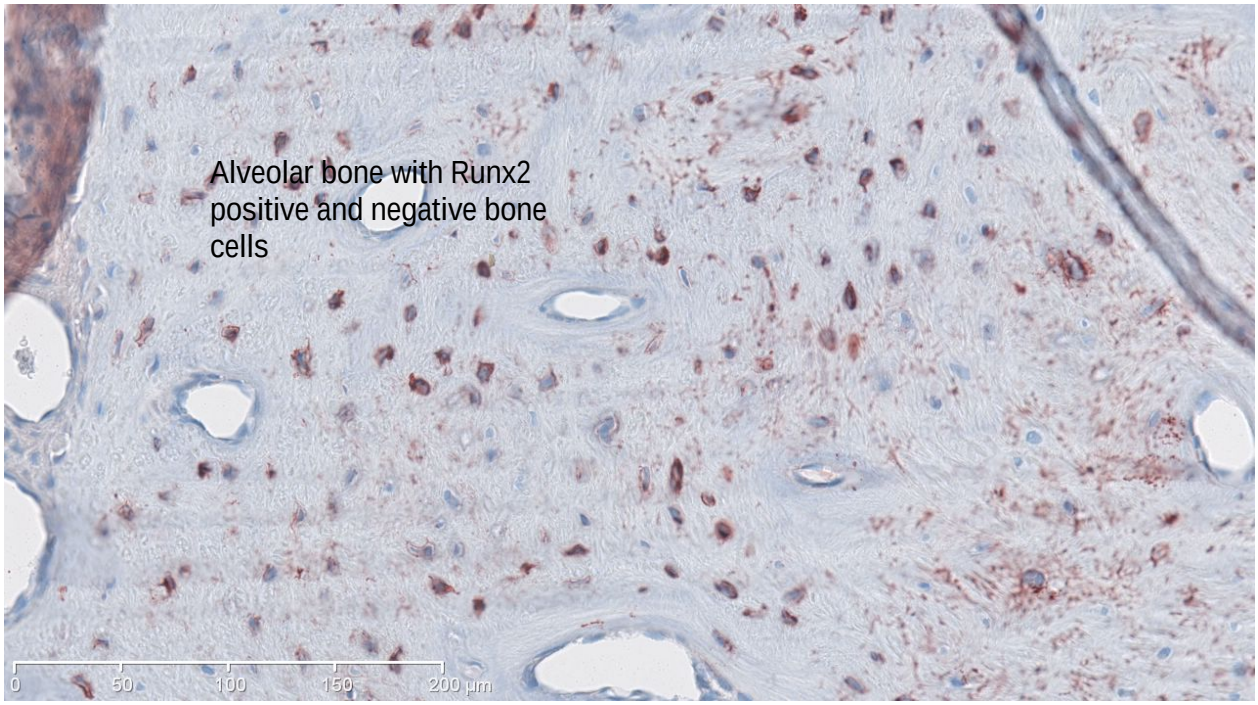

There is agreement between statistical analysis and the subjective evaluation, with a statistically significant difference observed between in the experimental and internal control sides ($p<0.05$) with the experimental side showing on average 7.19% more Runx2 positive cells than the internal control. See Table 11. Although there was not a significance difference between the percentage of Runx2 positive cells at difference time points, a trend was identifiable with the number of positive cells appearing to be increased at day 4 and decreased at days 7, 14 and slightly increased at day 28 (see Tables 10 and 11).

Table 10: The mean percentage of Runx2 positive cells in the alveolar bone at different time points in the experimental group and overall between the experimental and internal control groups.

R: Experimental group, L: Internal control group. 0, 4, 7, 14 and 28 denote time points of the experimental group.

Effect	time	side	Mean	Standard Error
time	0		81.4977	4.5082
time	4		84.0604	4.4054
time	7		72.1076	4.4727
time	14		71.8492	4.3993
time	28		74.5363	4.4407
side		L	73.2173	2.3736
side		R	80.4031	2.3718

Table 11: A comparison between the mean percentage of Runx2 positive cells at different time points in the experimental group and overall between the experimental and internal control groups in the alveolar bone.

R: Experimental group, L: Internal control group. 0, 4, 7, 14 and 28 denote time points of the experimental group. * $p<0.05$.

Effect		Mean	Standard Error	PValue
time	0 vs. 4	-2.5627	6.3033	0.6844
time	0 vs. 7	9.3901	6.3505	0.1397
time	0 vs. 14	9.6485	6.2990	0.1260
time	0 vs. 28	6.9614	6.3280	0.2717
time	4 vs. 7	11.9527	6.2780	0.0573
time	14 vs. 4	-12.2112	6.2259	0.0502
time	14 vs. 7	-0.2584	6.2737	0.9672
time	14 vs. 28	-2.6870	6.2509	0.6674
time	28 vs. 4	-9.5241	6.2552	0.1283
time	28 vs. 7	2.4286	6.3028	0.7001
side	L vs. R	-7.1858	2.5901	*0.0105

Although there was a statistically significant difference between the number of Runx2 positive cells between the external control and day 7 of the internal control ($p=0.0291$), overall there was no statistically significant difference noted between the number of Runx2 positive cells in the alveolar bone of the external and internal control groups ($p=0.0724$). As with the experimental animals, a trend for time dependent Runx2 expression was present in the internal control group with increased Runx2 positive cells at day 4, followed by decreased Runx2 positive cells at days 7 and 14 and a slight increase in positive cells at day 28. Statistical significance was noted between days 0 and 7 ($p=0.0256$) and 4 and 7 ($p=0.0132$) of the internal control group sites (see Tables 12 and 13).

Table 12: The mean percentage of Runx2 positive cells in the alveolar bone of the internal control group at difference time points and overall between internal and external control groups.

EC: External control. 0, 4, 7, 14 and 28 denote different time points of internal control.

Effect	time	Estimate	Standard Error
time	EC	80.1242	5.5182
time	0	80.5836	5.5547
time	4	82.2144	5.3769
time	7	63.0750	5.4956
time	14	68.3600	5.3649
time	28	71.6804	5.4381

Table 13: The difference in the mean percentage of Runx2 positive cell counts between two time points in the internal control group and between each time point of the internal control group and the accumulative count of the external control group.

EC: External control. 0, 4, 7, 14 and 28 denote different time points of internal control.

* $p<0.05$.

Effect		Estimate	Standard Error	PValue
time	EC vs. 0	-0.4594	7.8297	0.9532
time	EC vs. 4	-2.0902	7.7046	0.7863
time	EC vs. 7	17.0492	7.7879	*0.0291
time	EC vs. 14	11.7642	7.6962	0.1271
time	EC vs. 28	8.4438	7.7474	0.2764
time	0 vs. 4	-1.6308	7.7308	0.8330
time	0 vs. 7	17.5087	7.8138	*0.0256
time	0 vs. 14	12.2236	7.7224	0.1142
time	0 vs. 28	8.9032	7.7735	0.2527
time	4 vs. 7	19.1395	7.6885	*0.0132
time	14 vs. 4	-13.8544	7.5956	0.0689
time	14 vs. 7	5.2851	7.6800	0.4917
time	14 vs. 28	-3.3204	7.6390	0.6640
time	28 vs. 4	-10.5340	7.6475	0.1691
time	28 vs. 7	8.6055	7.7313	0.2663

A number of empty lacunae in the interradicular region beneath the ankylotic regions of the experimental animals were also noted in both the H and E and IHC stained sections. On average compared to day 0, 8.2% of empty lacunae appeared at day 7, 23.3% at day 14 and 9.4% at day 28 post-hypothermal insult. No empty lacunae were noted in the internal or external control groups (see Table 14 and Figure 12).

Table 14: Percentage of empty lacunae for each time point in the experimental group.

*p<0.05

Effect	time	Mean	StdErr	P-Value	% of dead cells
time	0 - 7	-2.4957	0.4948	*<.0001	0.08244
time	0 - 14	-1.4564	0.3779	*0.0001	0.2331
time	0 - 28	-2.3569	0.7809	*0.0025	0.09471

Figure 12: Empty lacunae noted in the interradicular region beneath the ankylotic areas in the experimental animals x 10 magnification ruler 0 - 500**µ**m.

Note red staining indicates Runx2 positive result, blue staining indicates haematoxylin counterstain.

Day 0 Experimental

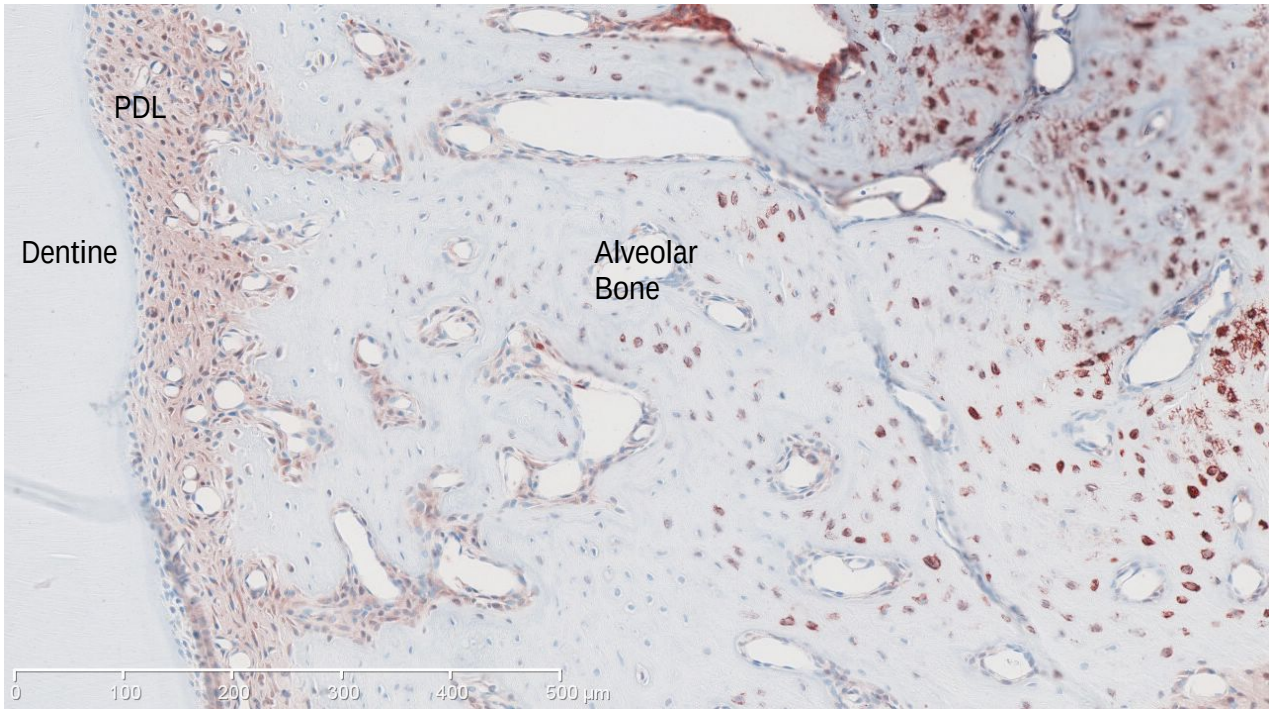

Day 4 Experimental

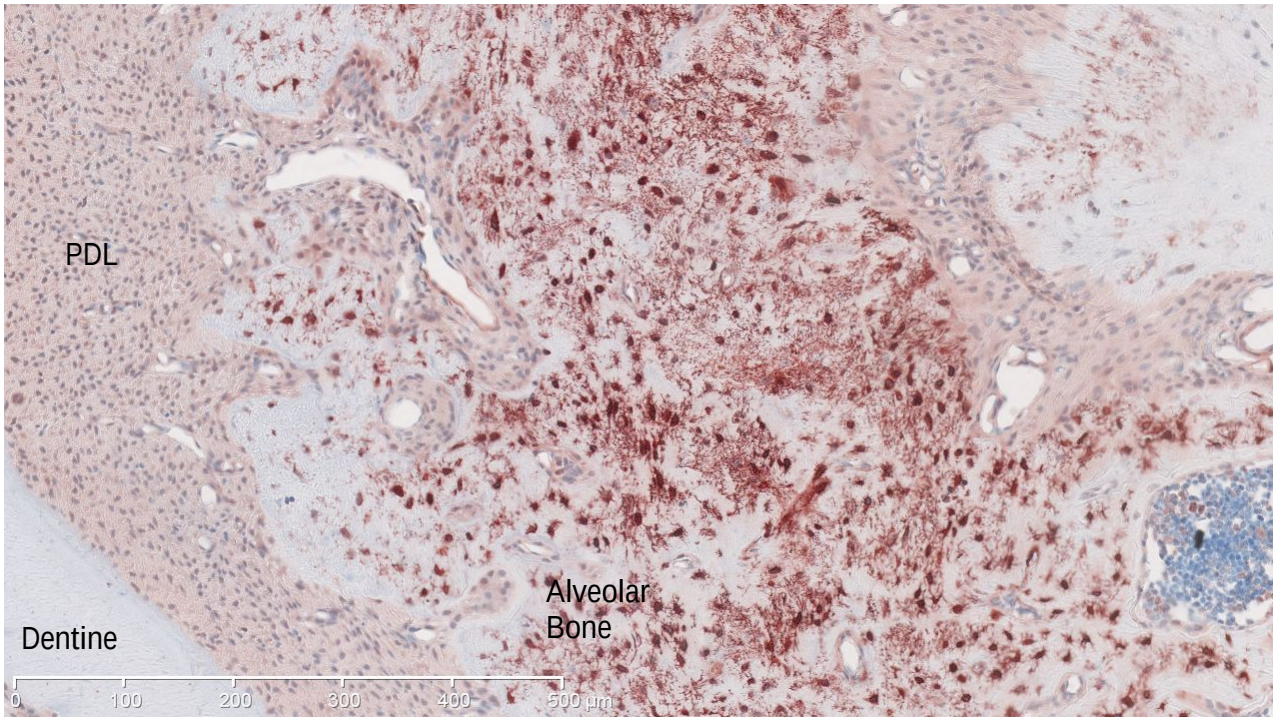

Day 7 Experimental

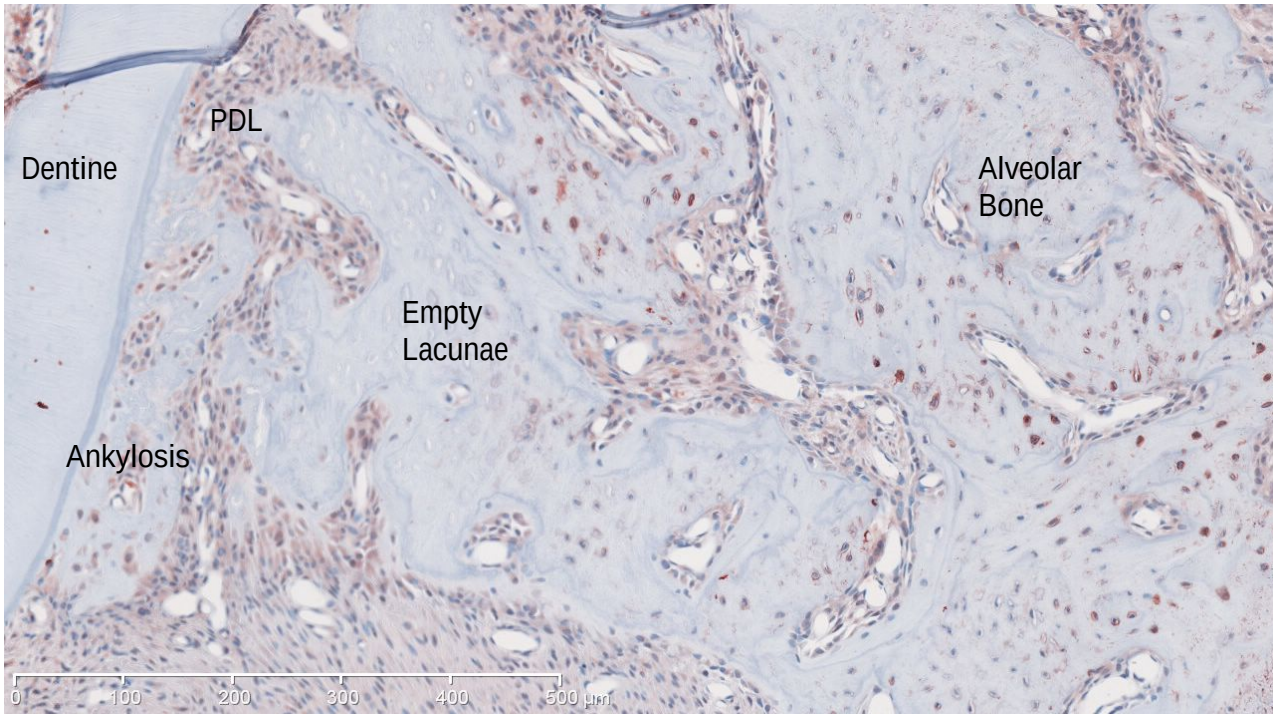

Day 14 Experimental

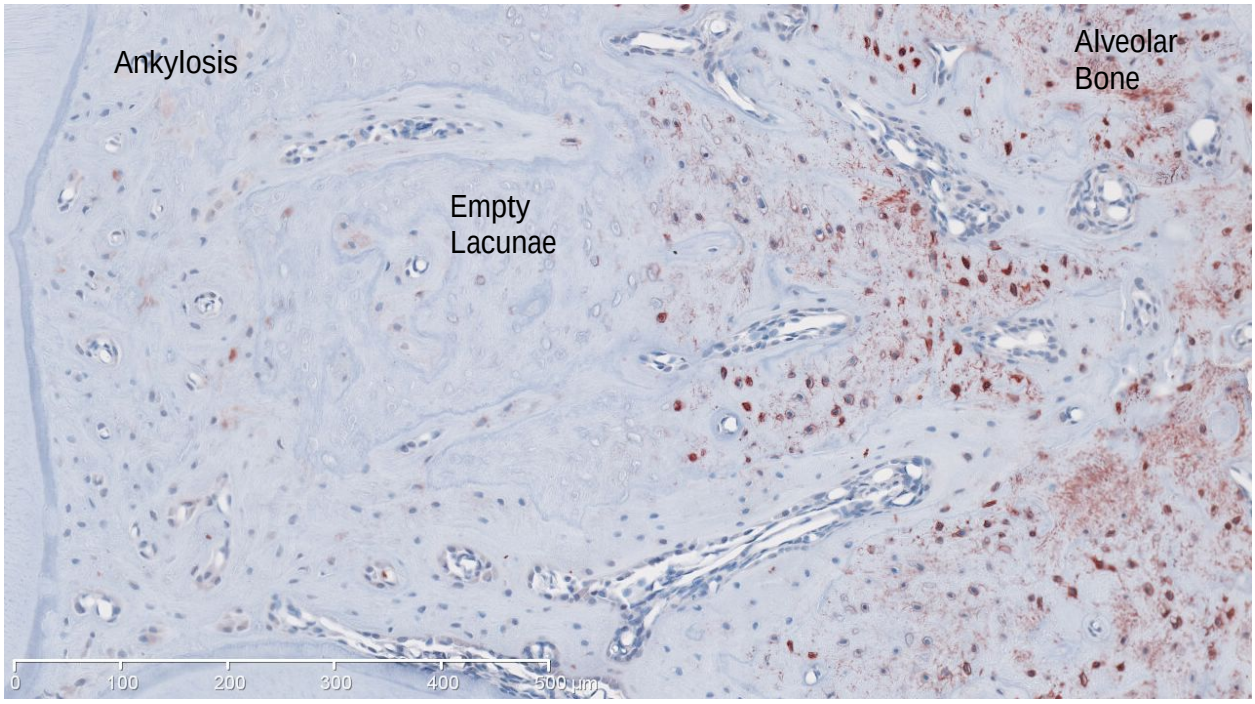

Day 28 Experimental

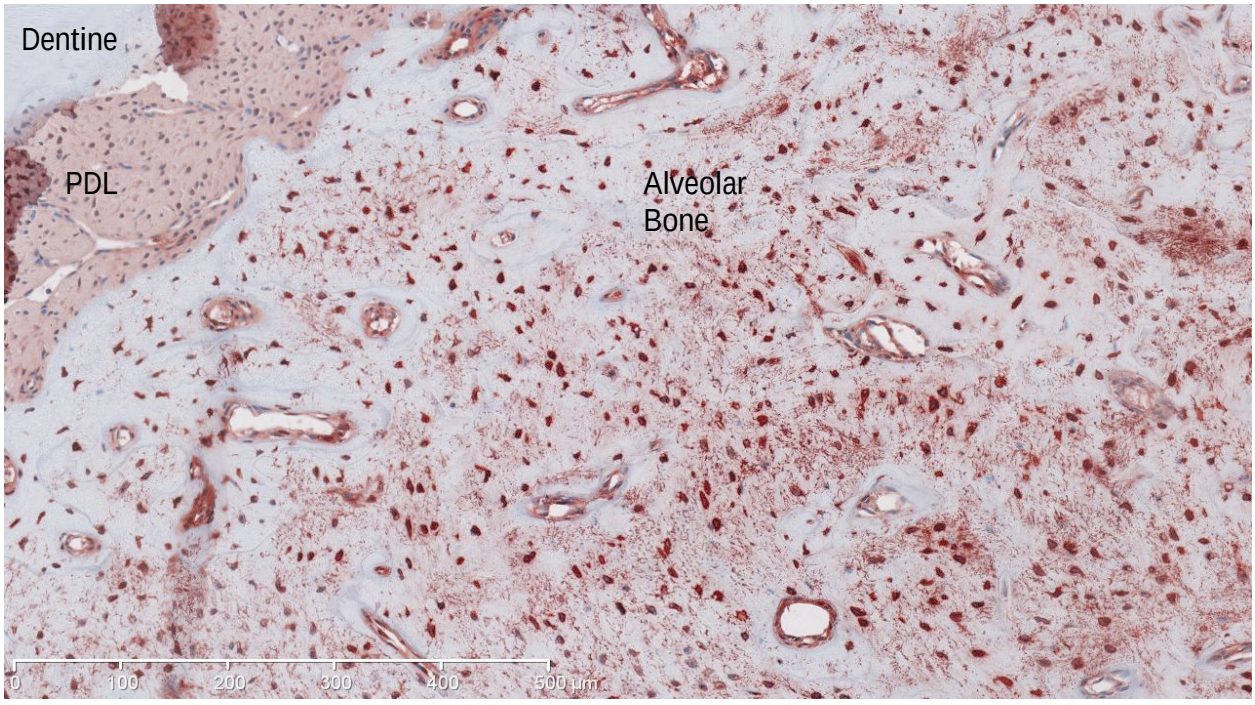

7.1.5 Discussion:

Like previous studies, Runx2 positivity was identified in a number of cells types, including bone-lining cells, osteoclasts in resorption lacunae along the PDL, megakaryocytes in the bone marrow, bone cells, cemental cells and endothelial cells. However, although the Runx2 protein is present, this does not indicate that the Runx2 gene is present, as the protein may have been transported from another region. Xiang et al. (2012) found Runx2 mRNA in ERM using RT-PCR, indicating the expression of Runx2 at the gene level in these cells and hence the capability of protein production. The current study demonstrates the Runx2 protein in ERM and confirms Runx2 production.

Miyazaki et al. (2008) examined Runx2 expression in the dental development in 0, 3, 7, 14, 21 and 28 day old mice using immunohistochemistry. Continuous expression of Runx2 in odontoblasts was found to disturb odontoblast differentiation, inducing odontoblasts to differentiate to osteoblasts and leading to the formation of bone-like structure (Miyazaki et al., 2008). Increased numbers of Runx2 positive pulpal cells were noted statistically, with a subjective increase in Runx2 positive odontoblasts noted. In the current study, reparative dentine was present from day 7 (see Figure 13). Aguiar and Arana-Chavez (2007) found reparative dentine devoid of dentinal tubules and resembling bone with odontoblast-like cells resembling osteoblasts rather than odontoblasts in 28 male Wistar rats 10 days post extrusive injury, with increasing depth of reparative dentine up to 60 days post injury. Given the increased expression in Runx2, perhaps pre-odontoblasts have differentiated into osteoblasts following hypothermal injury leading to the formation of reparative dentine. Further markers to differentiate between odontoblasts and osteoblasts would be required to substantiate this.

Figure 13: Reparative dentine in the experimental group at Day 14

A: x 5 magnification ruler 0 – 1mm, B: x 10 magnification ruler 0 - 500μm, C: x 40 magnification ruler 0 - 100μm.

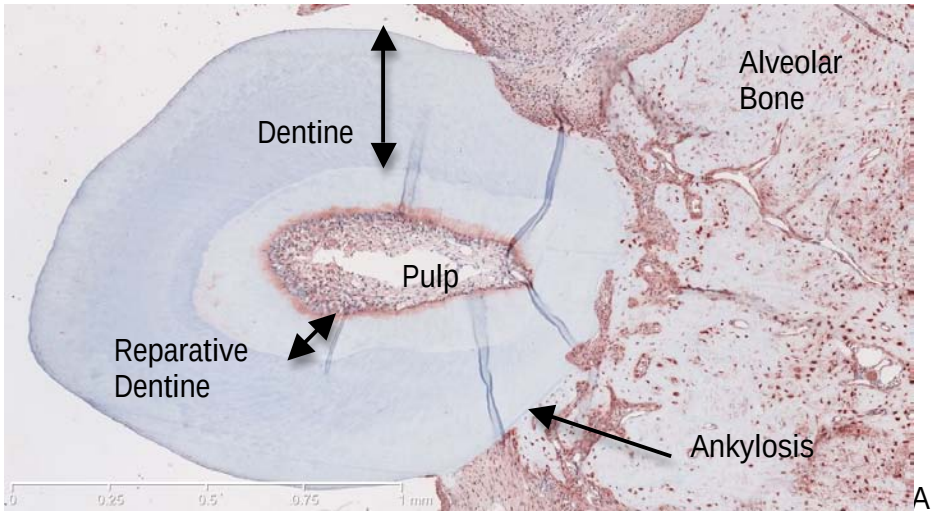

A

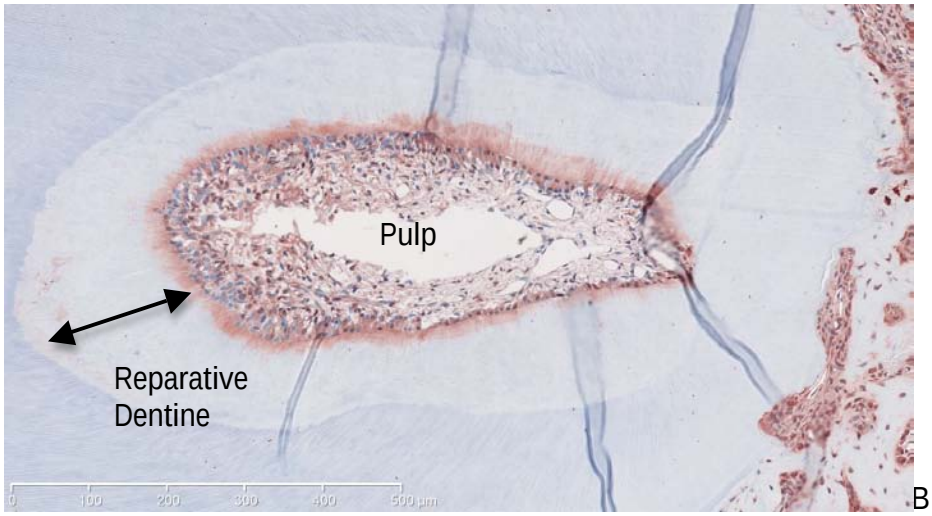

B

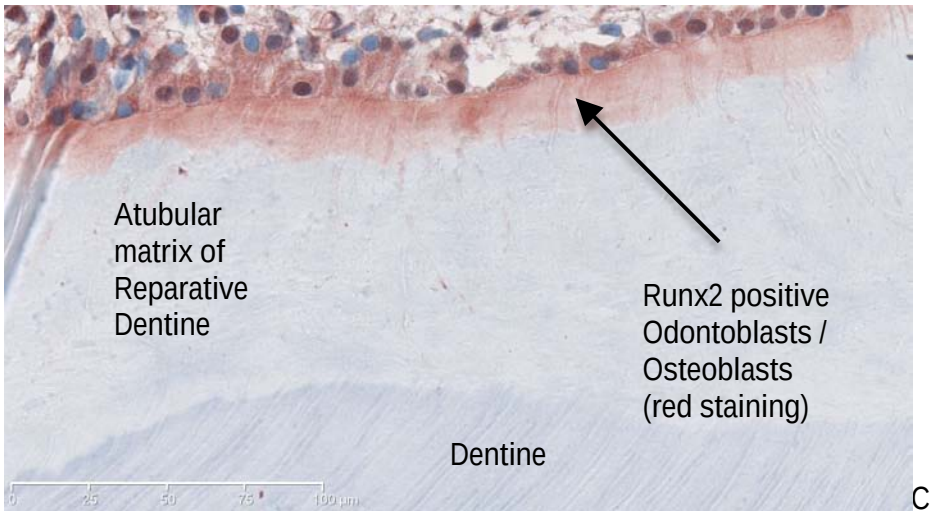

C

Although no prior studies have reviewed Runx2 in an ankylotic model, Runx2 expression has been reviewed using a mechanical model of orthodontic tooth movement. Brooks et al. (2009) reviewed Runx2 expression during tooth movement in 22 male Sprague Dawley rats 3 hours and 24 hours post placement of a 10 grams orthodontic force using a split mouth design. A time dependent increase in Runx2 expression was identified in the tension region of the PDL 24 hours post force application. This finding was not present in all animals and the author felt that this inconsistency was due to the difference in force application between the animals.

Pavlidis et al. (2009) reviewed Runx2 expression in 25 twelve-week-old male Wistar rats using a T loop (0.016x0.022 inch stainless steel orthodontic appliance) placed between the maxillary molars and a high resolution three-dimensional force/torque transducer to apply constant and intermittent forces of varying magnitude (see Figure 14). In two group of 5 rats, constant forces for 4 hours of 0.25 or 0.5N were applied, whilst in the third group of rats, constant forces for 2 hours of 0.1N were applied. A further group of 5 rats underwent an intermittent forces of 0.1N applied over 4 hours. The remaining five animals served as a control. The animals were killed after either 1 or 2 days. As with the current study, Runx2 expression was demonstrated in the PDL with no significant difference in the expression of Runx2 between the mesio-coronal and disto-coronal PDL. As with Brooks et al. (2009), Pavlidis et al. (2009) identified a time dependent change in Runx2 expression, although Pavlidis et al. identified a statistically significant ($p<0.05$) decrease in Runx2 expression only in the animals that underwent constant force application (Pavlidis et al., 2009).

Figure 14: Diagrammatic representation of the experimental procedure for orthodontic force application. Runx2 positive cell numbers were counted a) mesio-coronal and b) disto-coronal PDL. (Diagram from Pavlidis et al., 2009.)

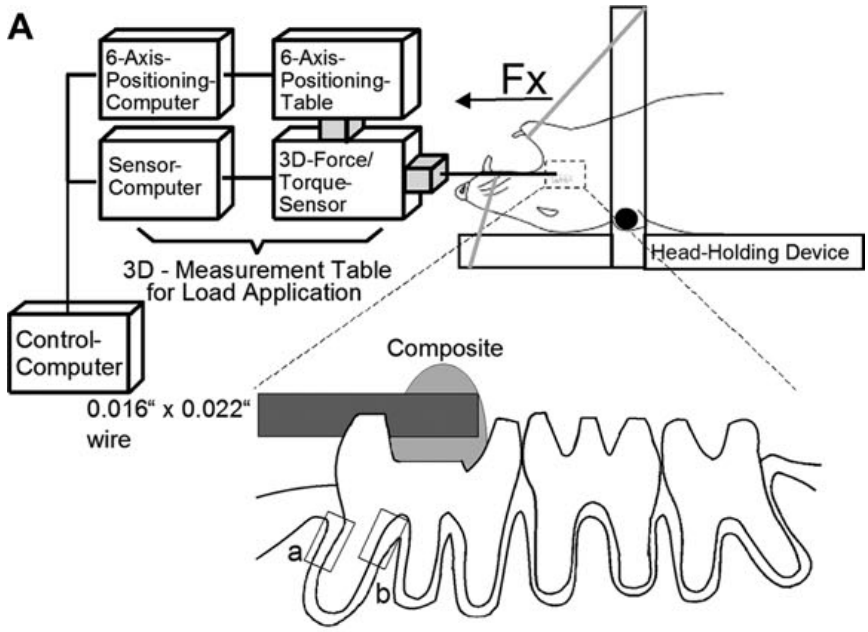

Within the PDL, no time dependent change in Runx2 expression was found in the current study. This may be due to the type of cell damage which occurred due to a mechanical deformation of PDL cells compared to a hypothermal insult and differences in the degree of PDL cell survival and blood flow to the region post insult. Also, the initial changes in Runx2 expression may not be demonstrated by the current study due to the timing of the second measurement, day 4 post-hypothermal insult. Within the alveolar bone in the current study, a number of empty lacunae appeared in the alveolar bone beneath the ankylotic region. This phenomenon may indicate an extensive depth of damage to the area and destroy cells that would otherwise contribute to Runx2 expression in the PDL post insult.

In the current study, Runx2 expression was found to vary significantly within the alveolar bone in the experimental compared to the control animals. Although not statistically significant, the number of Runx2 positive cells appeared to increase at day 4, decrease at days 7 and 14 and again slightly increase at day 28. Signs of ankylosis were noted at day 7. Given that no changes in Runx2 levels were noted in the PDL, perhaps changing Runx2 expression within the adjacent alveolar bone drives the development of ankylosis. Runx2 expression from the pulp may also be important with changes in expression and the development of reparative dentine noted in this region. Further study is required with smaller time point increments and using markers to differentiate between mesenchymal stem cells, odontoblasts and osteoblasts.

7.1.6 Conclusion:

1) Runx2 is expressed by a number of cells within the rat dentoalveolus including bone cells (osteoblasts and osteocytes not differentiated between), cemental cells, ERM, bone marrow cells, fibroblast-like cells of the PDL, vascular lining cells, and odontoblasts.

2) Changes in Runx2 expression were found in the experimental pulp and alveolar bone when compared to the internal and external control groups, but not in the PDL.

3) Changes in Runx2 expression also occurred in the internal control compared to the external control group, suggesting that a localised insult may show a systemic impact.

4) Post hypothermal insult Runx2 may play an important role in the development of bony ankylosis.

7.1.7 References

1. Aguiar MC, Arana-Chavez VE. (2007) Ultrastructural and immunocytochemical analysis of osteopontin in reactionary and reparative dentine formation after extrusion of upper rat incisors. J Anat 210 (4); 418- 427
2. Amir LR, Jovanonvic A, Perdijk FB, Toyosawa S, Everts V, Bronkers A (2007) Immunolocalization of sibling and RUNX2 proteins during vertical distraction osteogenesis in the human mandible. J Histochem Cytochem 55 (11); 1095 – 1104 Epub July 11
3. Brooks PJ, Nilforoushan D, Manolson MF, Simmons CA, Gong S-G (2009) Molecular markers of early orthodontic tooth movement. Angle Orthodontist 79; 1108 – 1113
4. D'Souza RN, Aberg T, Gaikwad J, Cavender A, Owen M, Karsenty G, Thesleff I (1999) Cbfa1 is required for epithelial-mesenchymal interactions regulating tooth development in mice. Development 126:2911–2920
5. Davidovitch Z. (1991) Tooth movement. Crit Rev Oral Biol Med 2(4); 411 - 450
6. Dreyer CW, Pierce AM and Lindskog S. (2000) Hypothermic insult to the periodontium: a model for the study of aseptic tooth resorption. Endodontics and Dental Traumatology 16; 9 – 15
7. Ducy P, Zhang R, Geoffroy V, Ridall AL, Karsenty G. (1997) Osf2/Cbfa1: a transcriptional activator of osteoblast differentiation. Cell. 1997 89(5); 747 - 754
8. Ekim SL and Hatibovic-Kofman S. (2001) A treatment decision-making model for infraoccluded primary molars. International Journal of Paediatric Dentistry 11; 340 – 6
9. Hirata A, Sugahara T, Nakamura H. (2009) Localization of Runx2, Osterix and Osteopontin in Tooth Root Formation in Rat Molars. J Histochem Cytochem 57(4); 397 - 403
10. Harada H, Tagashira S, Fujiwara T, Yamaguchi A, Komori T, Nakasuka M. (1999) Cbfa1 isoforms exert functional differences in osteoblast differentiation. J Biol Chem 274(11); 6972 - 6978
11. Kjaer I, Fink-Jensen M and Andreasen JO. (2008) Classification and sequelae of arrested eruption of primary molars. International Journal of Paediatric Dentistry 18; 11 - 7
12. Komori T (2011) Signalling Networks in Runx2-Dependent Bone Development. Journal of Cellular Biochemistry 112: 750 – 755
13. Kraan MC, Haringman JJ, Ahern MJ, Breedveld FC, Smith MD, Tak PP (2000) Quantification of the cell infiltrate in synovial tissue by digital image analysis. Rheumatology 39; 43 – 49

14. Kurol J and Magnusson BC. (1984) Infraocclusion of primary molars: a histologic study. European Journal of Oral Sciences 92; 564 – 76
15. Li S, Kong H, Yao N, Yu Q, Wang P, Lin Y Kuang R, Zhao X, Xu J, Zhu Q, Ni L. (2011) The role of runt related transcription factor 2 (Runx2) in the late stage of odontoblast differentiation and dentin formation. Biochemical and Biophysical Research Communications 410; 698 – 704
16. Loriato LB, Machado AW, Souki BQ and Pereira TJ. (2009) Late diagnosis of dentoalveolar ankylosis: Impact on effectiveness and efficiency of orthodontic treatment. American Journal of Orthodontics and Dentofacial Orthopedics 135; 799 – 808
17. Lossdörfer S, Abou Jamra B, Rath-Deschner B, Götz W, Abou Jamra R, Braumann B, Jäger A (2009) The role of periodontal ligament cells in delayed tooth eruption in patients with cleidocranial dysostosis. J Orofac Orthop. 70(6); 495 – 510
18. Miyazaki T (2008) "Inhibition of the terminal differentiation of odontoblasts and their transdifferentiation into osteoblasts in Runx2 transgenic mice." Archives of Histology and Cytology 71 (2); 131 – 146
19. Pavlidis D, Bourauel C, Rahimi A, Gotz W, Jager A. (2009) Proliferation and differentiation of periodontal ligament cells following short-term tooth movement in the rat using different regimens of loading. European Journal of Orthodontics 31; 565 – 571
20. Ponduri S, Birnie DJ and Sandy JR. (2009) Infraocclusion of secondary deciduous molars – an unusual outcome. Journal of Orthodontics 36; 186 – 9
21. Raghoebar GM, Boering G, Jansen HWB, Vissink A. (1989) Secondary retention of permanent molars: a histologic study. Oral Pathology 18(8); 427 – 31
22. Rosner D, Becker A, Casap N, Chaeshu S. (2010) Orthosurgical treatment including anchorage from a palatal implant to correct an infraoccluded maxillary first molar in a young adult. Am J Orthod Dentofacial Orthop 138; 804 - 9
23. SAS institute Inc. (2011) SAS/STAT 9.3 User's Guide. Cary, NC.
24. Tan CW (2011) A Qualitative Investigation of RANKL, RANK and OPG in a Rat Model of Transient Ankylosis. Honours Project, The University of Adelaide, Adelaide, Australia.
25. Xiang J, Mrozik K, Gronthos S, Bartold PM. (2012) Epithelial cells rests of Malassez contain unique stem cells populations capable of undergoing epithelial-mesenchymal transition. Stem cells and Development 21(11); 2012 – 2025
26. Ziros PG, Basdra EK and Papavassiliou (2008) Runx2: of bone and stretch. The International Journal of Biochemistry and Cell Biology 40; 1659 – 1663

VEGF EXPRESSION IN THE RAT PULP, PERIODONTAL LIGAMENT AND ALVEOLAR BONE FOLLOWING HYPOTHERMAL INSULT

ARTICLE 2

Written in the style of Archives of Oral Biology

Dr Trudy Ann STEWART (BDS Adelaide, BOccThy UQ)

Orthodontic Unit

School of Dentistry

Faculty of Health Sciences

The University of Adelaide

AUSTRALIA

March 2013

7.2.1 Abstract:

Objective: To evaluate the expression of vascular endothelial factor (VEGF) in the rat dentoalveolar region following a hypothermal insult.

Methods and Materials: The right upper first molars of 18 eight week old male Sprague-Dawley rats were subjected to a single 10 minute application of dry ice in order to produce aseptic necrosis and ankylosis within the periodontal ligament. The contralateral first molar of these rats served as an untreated control. On days 0, 4, 7, 14 and 28 after the insult, the expression of VEGF was examined via immunohistochemistry (IHC) and histomorphometry and statistically evaluated.

Results: Statistically significant differences were found in the levels of VEGF positive cells in the pulp, periodontal ligament (PDL) and alveolar bone. In the pulp, a statistically significant difference was found between VEGF positive cells on the experimental side compared to the control, with increased numbers of VEGF positive cells on the experimental side up to day 7 and decreased numbers at day 14 and 28. In the alveolar bone and PDL, although a statistically significant difference was found between the experimental and control sides, there was no significant interaction with time. However, VEGF positive cell numbers appeared to decrease in the PDL at days 4, 7 and 14 and increase at day 28. In the alveolar bone, VEGF positive cell numbers were greater at day 4 than at days 7, 14 and 28.

Conclusion:

1) VEGF is expressed by a number of cells within the rat dentoalveolus including bone cells (osteoblasts and osteocytes not differentiated between), osteoclasts, fibroblast-like cells of the PDL, vascular lining cells, and odontoblasts.

2) Changes in VEGF expression were found in the experimental pulp, PDL and alveolar bone when compared to the internal and external control groups.

3) Changes in VEGF expression with time were noted in the pulp, PDL and alveolar bone. A statistically significant interaction was found between time and VEGF expression in the pulp only.

4) Changes in VEGF expression also occurred in the internal control group, suggesting that a localised hypothermic insult may lead to a systemic impact.

5) Post hypothermal insult VEGF may play a role in the development of bony ankylosis.

Key Words: VEGF, ankylosis, rat, dentoalveolar, immunohistochemistry.

7.2.2 Introduction:

Bony remodelling is essential for healing in the periodontium, as well as permitting orthodontic tooth movement. Trauma to the periodontal ligament (PDL) and its supporting alveolar bone, whether by orthodontic appliances or other means, leads to regions of hypoxia as the vascular supply is interrupted followed by zones of hyalinisation and subsequent bony resorption (Wang et al., 2011). Subsequent healing of the periodontium occurs through differentiation of mesenchymal stem cells (MSCs) to various cells types including osteoblasts and fibroblasts, as well as the growth of new blood vessels (Wang et al., 2011).

VEGF (vascular endothelial growth factor) belongs to the superfamily of Platelet Derived Growth Factors (PDGF) and has been classified into a number of subgroups (Takahashi and Shibuya, 2005; Bates, 2010). VEGF (also known as VEGF-A) is a major regulator of physiologic and pathologic angiogenesis and is secreted by both normal and pathologic cells, as well as in tissues undergoing growth or remodelling (Klagsbrun and D'Amore, 1996; Canavese et al; 2010). A number of factors act to regulate VEGF expression including hypoxia, growth factors, p53 mutation, oestrogen, thyroid stimulating hormone, tumour promoters and nitric oxide (Takahasi and Shibuya, 2005).

VEGF is also involved in bone ossification, modelling and remodelling, with VEGF directly affecting osteoblastic cells through it's regulation of ALP (alkaline phosphatase), OCN (osteocalcin) and OPG (osteoprotegerin) expression via the VEGFR2 signalling pathway (Street and Lenehan, 2009; Tan et al., 2011). Conversely, osteoblasts are able to produce VEGF in normal and pathological conditions in order to stimulate new vessel growth during osteogenesis (Kim et al., 2002; Corrado et al., 2011). This expression of VEGF is upregulated by a number of cytokines and growth factors including prostaglandin E_1 and E_2, transforming growth factor ß1, insulin-like growth factor I and 1,25 dihydroxyvitamin D_3 (Kim et al., 2002; Corrado et al., 2011). Osteoblasts are also able to influence

the production of VEGF through their modulation of hypoxia-inducible factor 1α (HIF-1α) (Kim et al., 2002). Lowered tissue oxygenation, for example in wound healing, stabilizes HIF-1α, upregulating genes involved in angiogenesis, cell survival, the glycolytic pathway and apoptosis (Lee et al., 2012; Koch et al., 2011). Runx2, the master transcriptional activator of bone formation, is also able to both bind and stabilize HIF-1α, inducing and maintaining microvessels during bone formation (Lee et al., 2012). Indeed, Runx2 knockout mice have been found to show no VEGF expression at all (Zhang et al., 2011).

Dentoalveolar ankylosis occurs when non-neoplastic bone obliterates the periodontal ligament and fusion occurs between the alveolar bone and cementum or dentine (Raghoebar et al., 1989; Kurol and Magnusson, 1984; Lee et al., 2009; Loriato et al., 2009; Arakeri et al., 2010; Andersson et al., 1984). Dentoalveolar ankylosis has been recorded in two dental conditions: infraocclusion and external root replacement resorption.

Infraocclusion (also called secondary retention, submergence, reimpaction or ankylosis) is the cessation of post-emergent tooth eruption when no evidence of a physical barrier or abnormal tooth position is present (Raghoebar et al., 1989; Kurol and Magnusson, 1984; Kurol and Olson, 1991; Ekim and Hatibovi-Kofman, 2001; Ponduri et al., 2009). The prevalence of infraocclusion in the community has been reported to range between 1.3% and 8.9%, with siblings displaying a significantly higher incidence (Ekim and Hatibovi-Kofman, 2001; Kjaer et al., 2008). No difference in occurrence has been identified between males and females (Kjaer et al., 2008). Kurol and Magnusson (1984) reported that the frequency of infraocclusion decreased with age, and that teeth with permanent successors present may erupt normally as local factors involved in deciduous tooth exfoliation may overcome the ankylosis. Generally, deciduous mandibular molars are most frequently affected, followed by the permanent mandibular second molars and permanent maxillary

second molars (Ekim and Hatibovi-Kofman, 2001; Kjaer et al., 2008; Loriato et al., 2009; Shalish et al., 2010).

Once ankylosis occurs, a number of interarch and intraarch consequences may ensue: including, reduced eruption of the affected tooth with concurrent reduced development of adjacent alveolar bone; delayed exfoliation of the deciduous tooth; increased difficulty in performing extraction; abnormal position and development of the permanent successor; tipping of adjacent teeth; over eruption of opposing teeth; as well as dental midline shift. (Ponduri et al., 2009; Loriato et al., 2009; Rosner et al., 2010). Affected teeth are also unresponsive to conventional orthodontic treatment (Rosner et al., 2010). Infraocclusion has been linked with various other dental abnormalities: tooth agenesis; microdont maxillary incisor teeth; delayed tooth development; palatally displaced canine teeth and mandibular second premolar distal angulation (Shalish et al., 2010). It is due to this linkage that a genetic predisposition to infraocclusion has been proposed (Shalish et al 2010).

The development of ankylosis and external root replacement resorption may also occur secondary to trauma to the periodontal ligament (Andersson et al., 1984). The majority of dental injuries involve the anterior teeth, and in addition to damage to the dental hard tissues and gingivae, the periodontal ligament and alveolar bone may be impacted upon (Hevoca et al., 2010). Healing depends upon a range of factors: stage of root development, type and extent of injury and root anatomy as well as the presence of bacterial contamination and repeated injury (Hecova et al., 2010; Andreason et al., 2006). Complications may occur weeks, months or even years post trauma (Hecova et al., 2010). External root resorption is a serious complication post -trauma which may be divided into surface resorption, replacement resorption / ankylosis and inflammatory resorption. A higher incidence of inflammatory and replacement resorption have been reported in dental intrusive luxation and avulsion injuries (Hecova et al., 2010). Root resorption is predominately found on the apical part of

the root (58%) although the coronal (23%) and central (19%) root surfaces may also be affected (Crona Larsson et al., 1991). There is no effective treatment for replacement resorption, with root resorption leading to eventual tooth loss (Wigen et al., 2008). Infraocclusion of the affected tooth, impaction and altered mesial drift of adjacent teeth, reduced development of the alveolar process and altered dental midline may occur (Andreason et al., 2006).

Within the research arena, ankylosis may also be induced experimentally through mechanical, chemical and thermal means. Dreyer et al., (2000) investigated a cold thermal insult applied to the occlusal surface of a rat molar and the resultant development of aseptic resorption. Application of a cold stimulus was noted to lead to periodontal cell death, with shrinkage and lysis of odontoblasts and other pulpal cells and clastic attack of the root surface with initiation of resorption 2 to 7 days post insult (Dreyer et al., 2000).

VEGF has been located in the PDL during orthodontic tooth movement and local administration of recombinant VEGF has been shown to enhance tooth movement (Chae et al., 2011; Miyagawa et al., 2009). No studies, however, have investigated the role of VEGF in ankylosis. This study aims to review the changes in expression of VEGF via immunohisotochemistry 0, 4, 7, 14 and 28 days post hypothermal insult. The null hypothesis is that there is no difference in VEGF expression following hypothermal insult.

7.2.3 Methods and Materials:

Animals: Eighteen eight-week-old male Sprague-Dawley rats were used in the experiment; fifteen rats were subjected to a hypothermal insult, whilst three rats served as an untreated external control. The University of Adelaide Animal Ethics Committee reviewed and approved this protocol for a prior study (Ethics number M-04-2004/M-023-2007).

Experimental Protocol: The animals were randomly divided into six groups of three. One group served as a control, while each rat in the experimental groups was anaesthetized with an intramuscular injection of Hypnorm® (fentanyl citrate, 0.315 mg/ml and fluanisone 10 mg/ml; Janssen-Cilag Ltd., High Wycombe, Buckinghamshire, UK) and Hypnovel® (midazolam hydrochloride, 5 mg/ml; Roche, Berne, Switzerland) diluted 1:1 with sterile water for injection at a dosage of 2.7ml/kg of body weight. The animals were restrained in a head holding device and underwent a single 10-minute application of dry ice (compressed carbon dioxide gas at -81^{o}C, BOC Gases, Adelaide, Australia) to the right maxillary first molar crown in order to produce aseptic necrosis within the periodontal ligament and induce ankylosis. The untreated contra-lateral molars of each rat served as internal controls.

The animals were sacrificed by an intraperitoneal injection of Nembutal® (pentobarbitone sodium, 60 mg/ml at 20mg/ml per 100g of body weight; Boehringer Ingelheim Pty Ltd, Artarmon, Australia) on day 0, 4, 7, 14 and 28 respectively. The 3 animals in the control group did not undergo hypothermal insult and were also killed on day 0. The maxillae were then dissected out and excess soft tissues removed.

Histology: The specimens were fixed in 4% paraformaldehyde for 24 hours and stored in phosphate buffered saline (PBS) at pH 7.4 and decalcified with 4% ethylenediaminetetraacetic acid (EDTA)

solution. After dehydration in a graded alcohol series, the specimens were embedded in paraffin, and 5µm serial sections were cut coronally through the root furcation region on a microtome (Leitz 1512 Microtome, Leica, Nussloch, Germany). These sections were then mounted onto labelled aminopropyltriethoxysilane (APTS) coated glass slides. Randomly selected sections were stained with haematoxylin and eosin to identify if and where areas of ankylosis had occurred. Please note the experimental protocol and H and E staining were performed as part of a prior study by Tan, 2011. Slides were stored at room temperature until immunohistochemical staining was performed.

Antibodies:

Antibody optimisation was performed prior to staining to determine optimal antibody dilution for minimal background staining and optimal antibody specific staining. To assess antibody specificity, negative and positive controls were performed. For negative control sections, the anti-VEGF antibody was omitted or isotype-matched antibodies were applied (IgG1kappa). For a positive control, human lung tissue was stained with anti-VEGF antibody (see Figure 1.) 213 randomly selected serial sections were then stained with anti-VEGF monoclonal antibody (mAbs)(Novus Biologicals, Littleton, USA).

Figure 1: Positive and negative controls demonstrating capability and specificity of VEGF antibody. Note a positive VEGF response stains red. Blue indicates haematoxylin counterstain.

Human lung tissue displaying VEGF positivity x 20 magnification ruler 0 - 200**µ**m.

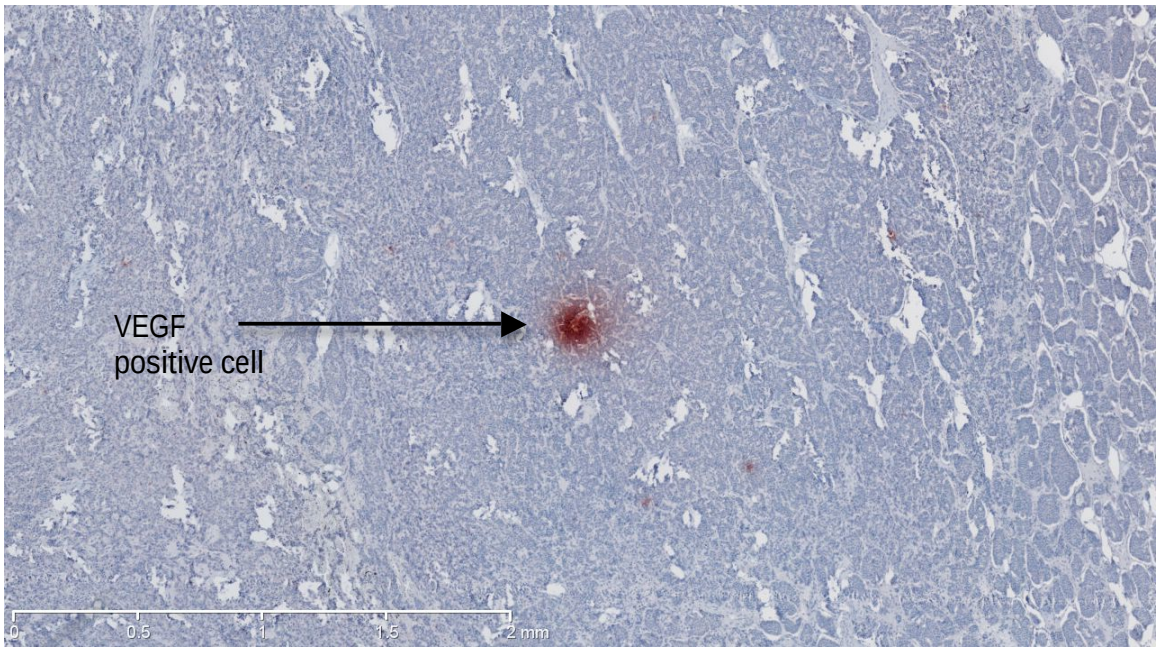

Omission of Anti - VEGF monoclonal antibody x2.5 magnification ruler 0 – 2mm.

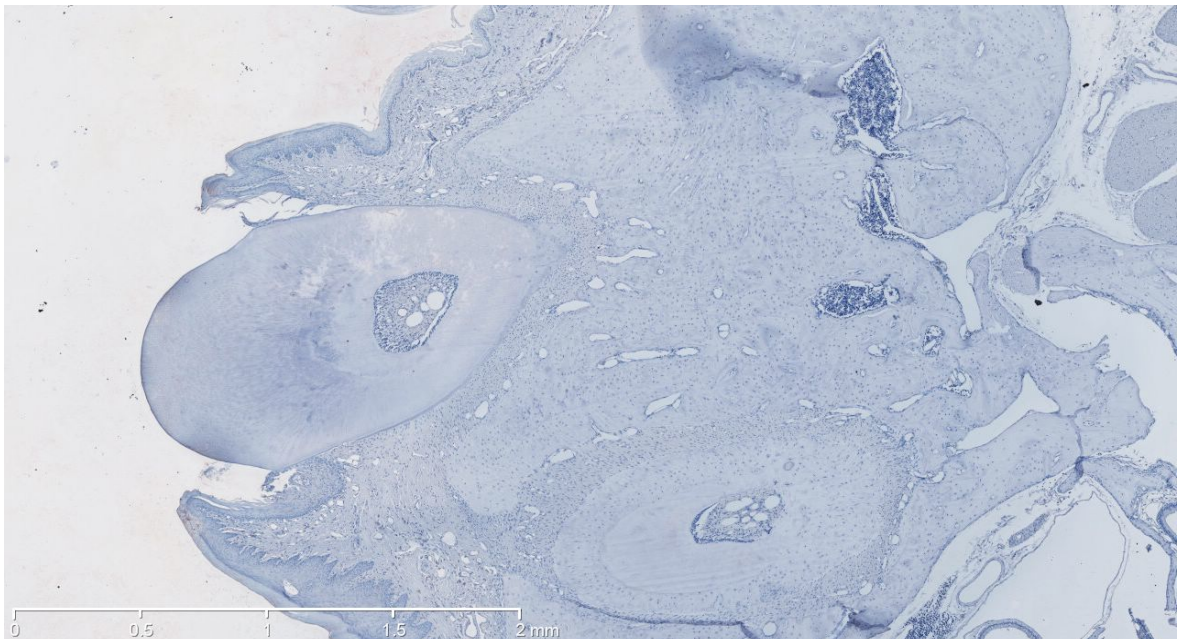

Isotype matched control antibody applied (IgG1 Kappa) x2.5 magnification ruler 0 – 2mm

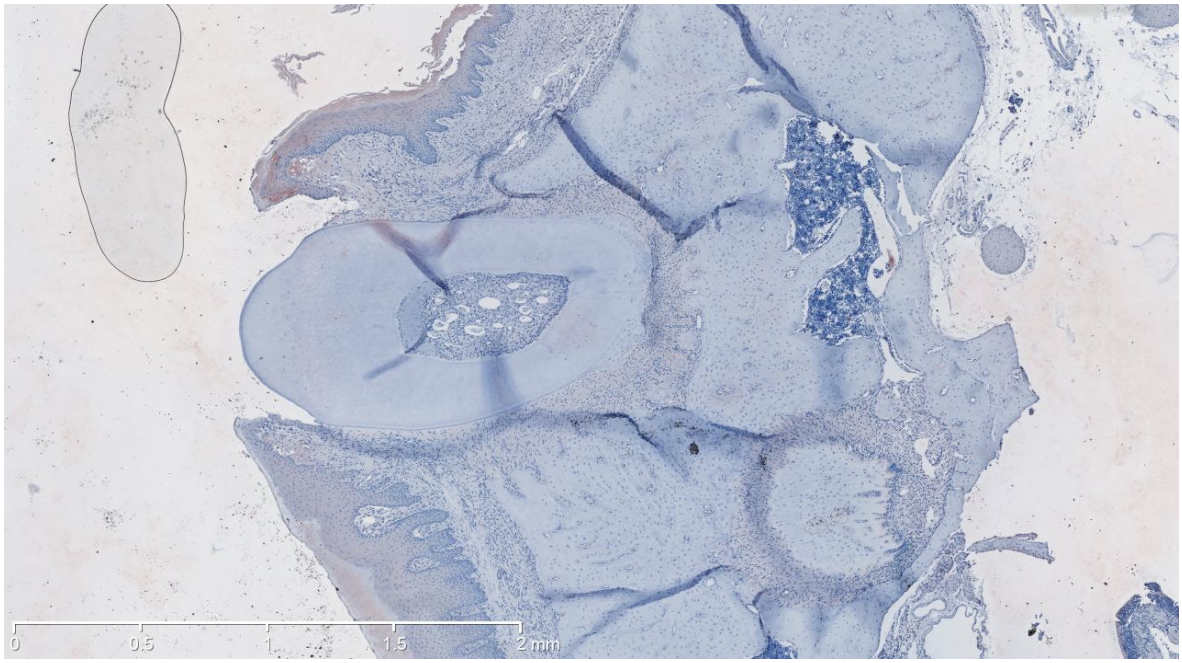

Immunohistochemical Staining:

After dewaxing and rehydration, the sections were immersed in tris-EDTA (pH 9.0) for 10 minutes in a water bath heated to 65^0C, soaked for 10 minutes in methanol H_2O_2 0.3%v/v to block endogenous peroxidase and washed in 1xPBS three times for 5 minutes each. The sections underwent serum blocking (provided in Vectastain Elite Avidin-Biotin Complex (ABC) Universal Kit, Vector Laboratories, California, USA) for 60 minutes according to manufacturer instructions. Anti-VEGF mAbs (1:100 concentration of 1mg/ml), diluted in PBS, was applied and the sections incubated in a wet chamber at room temperature overnight. Sections were rinsed in 1xPBS three times for 5 minutes and incubated with a secondary antibody (biotinylated horse anti mouse/rabbit IgG provided in the Vectastain Elite ABC Universal Kit, Vector Laboratories, California, USA) as per manufacturer instructions for 45 minutes at room temperature followed by the Avidin-Biotin Complex (Vectastain Elite ABC Kit Vector Laboratories, California, USA) for a further 45 minutes. Immunoreactivity was visualised via incubation of the sections with a solution of prediluted 3-Amino-9-EthylCarbazole

(AEC) (DAKO Australia Pty LTD., Campbellfield, Australia) in a dark room for 10 minutes. Sections were counterstained with haematoxylin for 10 seconds, rinsed in tap water and soaked in lithium carbonate for 30 seconds before rinsing in tap water and mounted using Aquamount (Aquatex, Merck Pty. Ltd., Victoria, Australia).

Morphometry: Stained sections of the maxillary first molars were scanned via a Nanozoomer Slide Scanner 2.0 series (Hamamatsu Photonics K.K. 325-6 Sunayama-cho, Hamamatsu City, Shizuoka) and viewed on a personal computer (MacBook Pro with 13 inch screen) using the Nanozoomer Digital Pathology (NDP) software (Hamamatsu Photonics K.K. 325-6 Sunayama-cho, Hamamatsu City, Shizuoka)). Semiquantitative counts, as described by Kraan et al. (2000), of the VEGF IHC positive cells were performed in 3 regions of the pulp, 5 regions of the PDL and 8 regions of the alveolar bone in each section (see Figure 2). Counting areas were placed randomly within each of the specified tissues and were defined by a 0.02mm^2 rectangle in the pulp, 0.01mm^2 rectangle in the PDL and a 0.05mm^2 square in the alveolar bone. ImageJ software was used to define the counting areas and to count the number of positive and negative cells within the counting areas (Wayne Rasband, National Institute of Health, USA; http://rsweb.nih.gov.proxy.library.adelaide.edu.au.ij).

Figure 2: A: Division of the section for counting x 2.5 magnification.

B: 0.02mm^2 rectangle in the pulp

C: 0.01mm^2 rectangle in the PDL

D: 0.05mm^2 square in the alveolar bone x 40 magnification ruler 0 - 500**µ**m.

Note red staining indicates VEGF positivity, blue staining indicates haematoxylin counterstain.

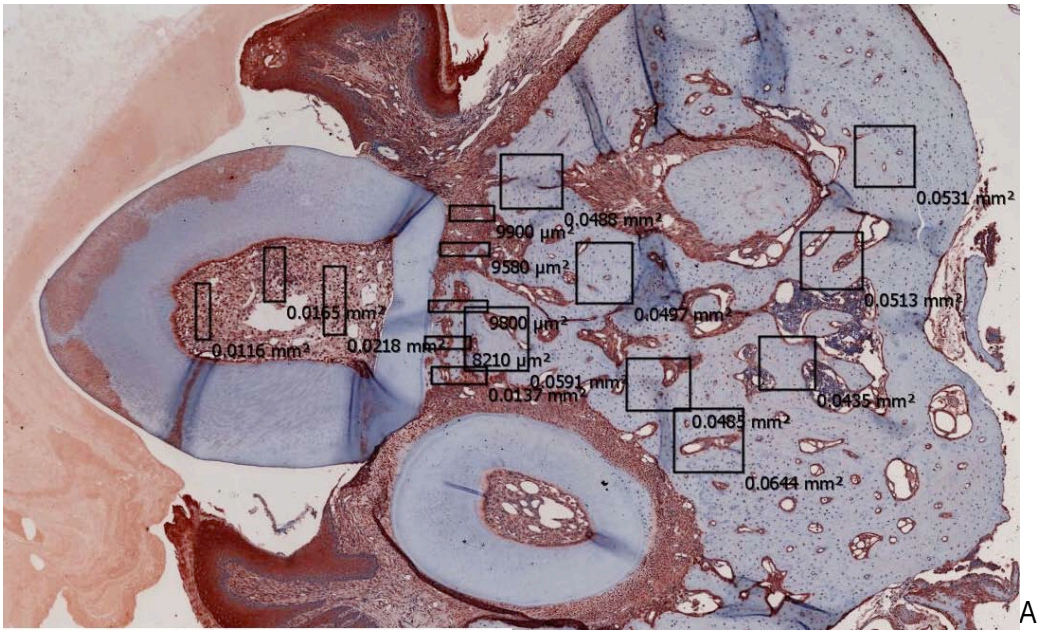

A

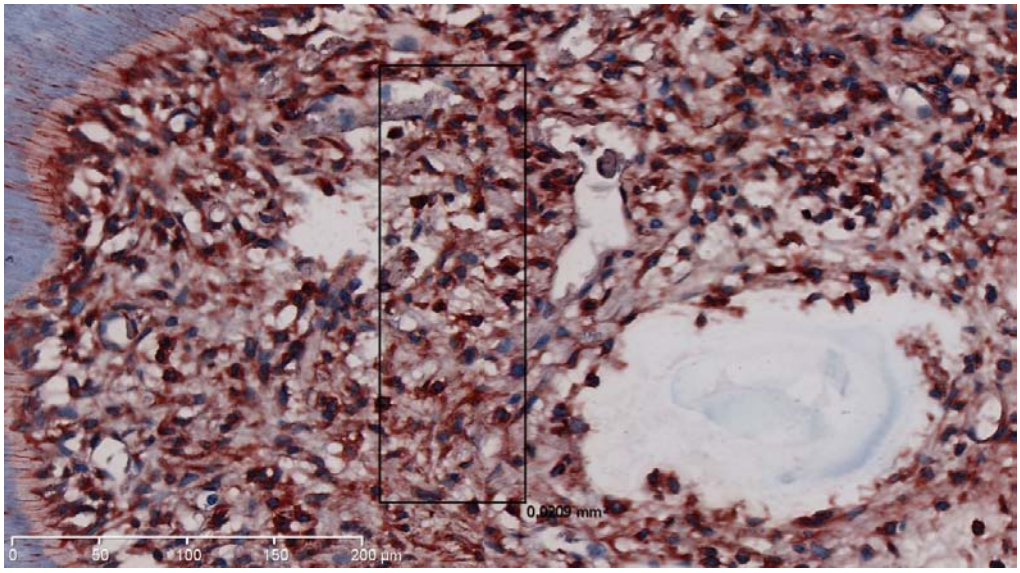

B

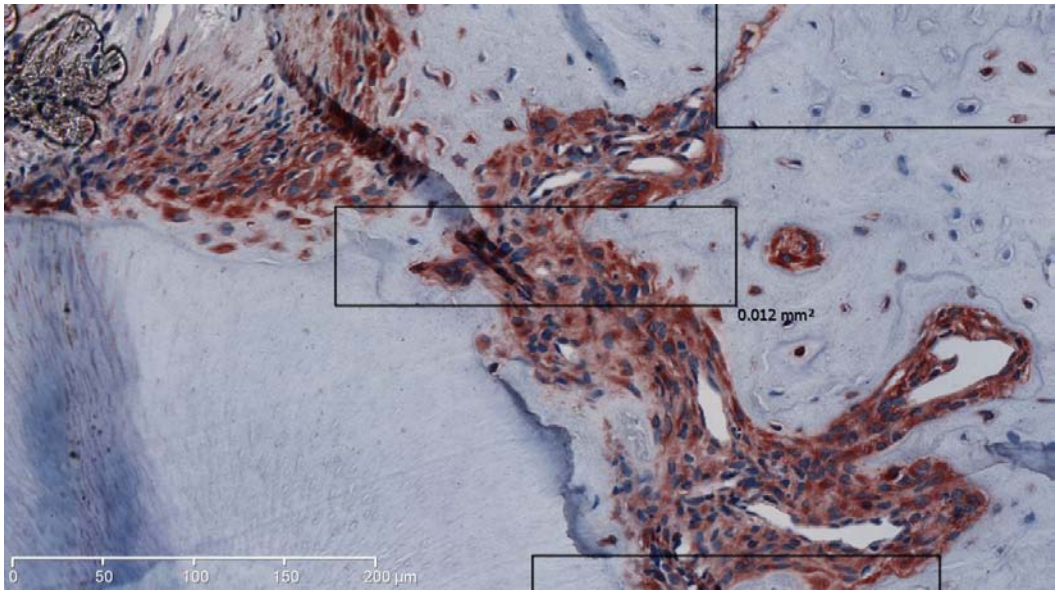

C

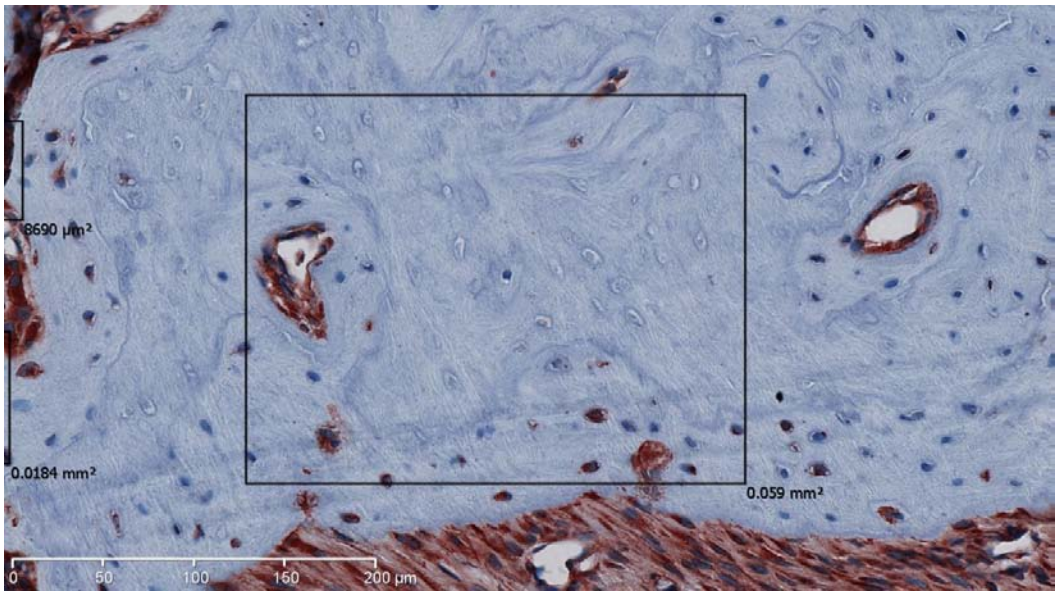

D

Statistical Analysis:

The data were analysed using SAS 9.3 (SAS Institute Inc., Cary, NC, USA). Differences between the percentage of VEGF positive cells in the internal control and experimental sides of the experimental rats or between the internal control (experimental rats) and external control rats were analysed by mixed effect models. In the model, the dependent variable was percentage of positive cells, whilst side, time and interaction between side and time were considered as fixed. A random effect was also included in the model to account for the dependency of measurements from the

same subject. This model was chosen as the selection of rats into groups was random, so the associated effects were also thus random effects, the data from different groups of animals are independent as they were randomly selected and because observations from the same animals in the same group are often correlated (SAS institute Incs, 2011). To determine error, re-counting of 10% of rat sections was performed and analysed via Bland-Altman plots, also using SAS 9.3. The level of significance was set at $p<0.05$.

7.2.4 Results:

Error Study:

Ten percent of sections were recounted (n = 192). Good intra-operator reproducibility was confirmed through the use of Bland-Altman plots, which indicated that 95% of the differences were within the limits of agreement (see Figure 3 – 6).

Figure 3: Bland-Altman plot of initial and repeated counts of VEGF positive cells n=192.

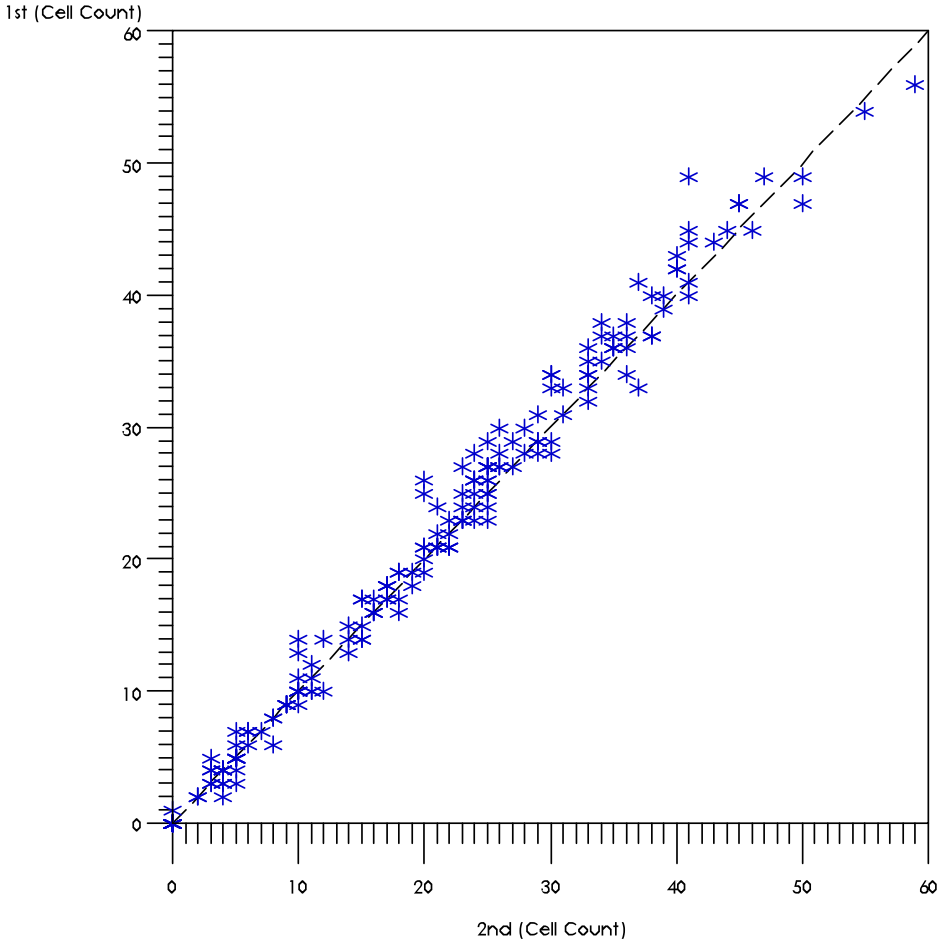

Figure 4: Bland-Altman plot demonstrating the difference between the initial and subsequent count of VEGF positive cells.

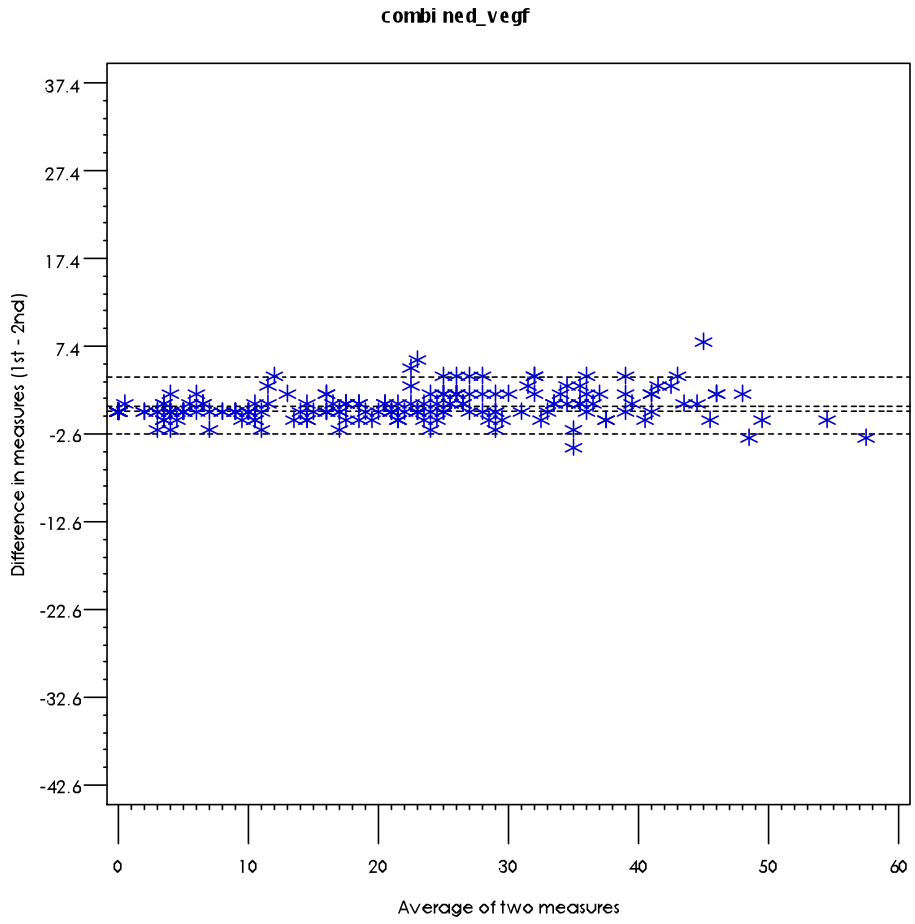

Figure 5: Bland-Altman plot of initial and repeated counts of VEGF negative cells n=192.

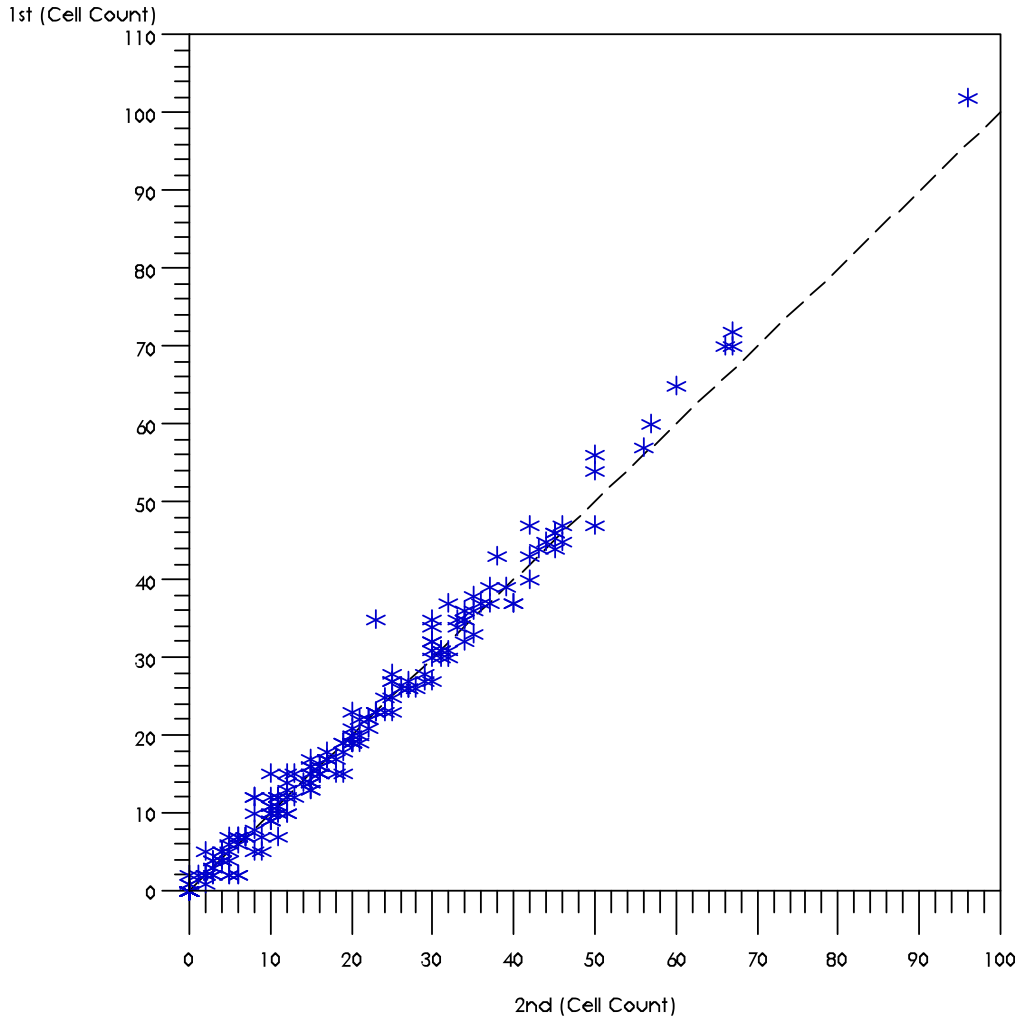

Figure 6: Bland-Altman plot demonstrating the difference between the initial and subsequent measurement of VEGF negative cells.

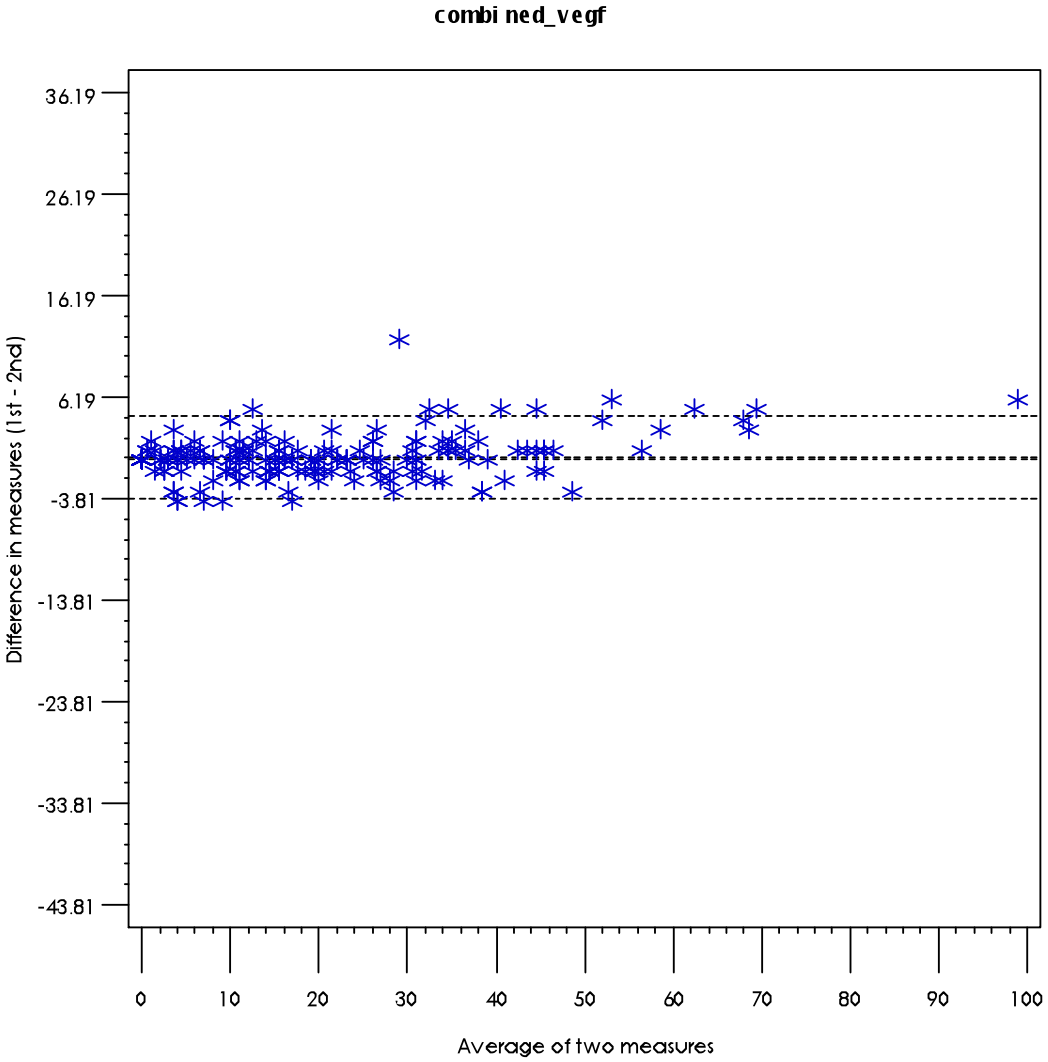

Histology:

On review of the haematoxylin and eosin stained sections very little difference was noted between sections at Day 0 in experimental, internal control or external control groups. Within the pulp of the experimental group, loss of integrity of the pulpal layers was visible at day 4 with disturbance to the discrete odontoblast, cell rich and core layers. Few pulpal cells remained at day 7 and 14 post insult. No disturbance to pulpal tissue was noted in the external control or in the internal control animals at any time point.

In regards to the periodontal ligament and alveolar bone, thinning of the PDL and fine bony trabeculae were visible in the interradicular region on all experimental animals on day 7. At day 14, widespread loss of the PDL was present, with dense bony ankylosis, but by day 28, bony replacement of the PDL was only present on one animal. No changes to PDL or alveolar bone were noted in the external control or the internal control groups at any of the above time points (see Table 1 and Figure 7).

Table1: Animals displaying ankylosis on the experimental side (RHS)

Day	0	4	7	14	28
Number of Rats	3	3	3	3	3
Number of Rats with Ankylosis	0	0	3	3	1

Figure 7: H and E Experimental group sections Day 0, 4, 7, 14 and 28 showing the development of ankylosis (Tan, 2011) x 10 magnification ruler 0 - 500**µ**m.

VEGF Immunohistochemical Staining:

VEGF Positive Cells in the Dentoalveolar Region: A number of cells were positive for VEGF. These included vascular endothelial cells, bone cells (osteoblasts / osteocytes / bone lining cells), osteoclast-like cells, periodontal ligament cells (fibroblasts, epithelial cell rests of Malassez (ERM)) and bone marrow cells in both experimental and control animals. Increased staining intensity for VEGF was noted particularly in association with blood vessels (see Figure 8).

Figure 8: Cells staining positive for VEGF including ERM (A) megakaryocytes (B) bone cells (C), osteoclasts (D) and vascular endothelial cells (E) x 20 magnification ruler 0 – 200**µ**m. Sections from both experimental and control animals. Note red staining indicates VEGF positivity. Blue indicates haematoxylin counterstain.

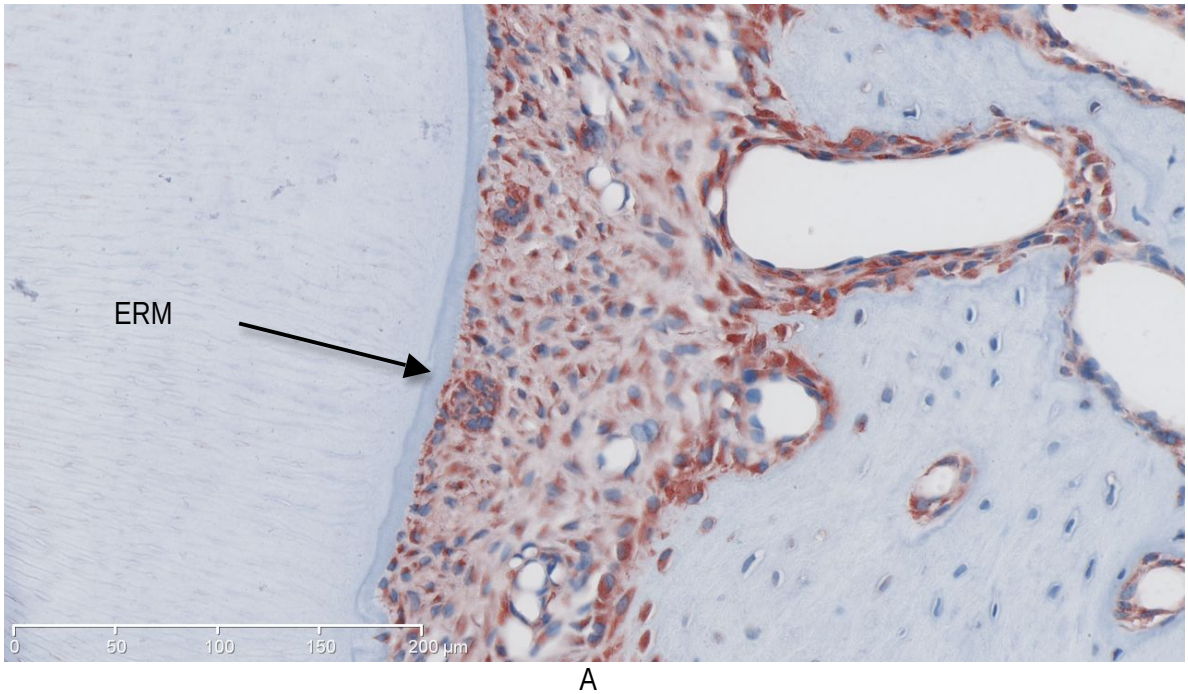

A

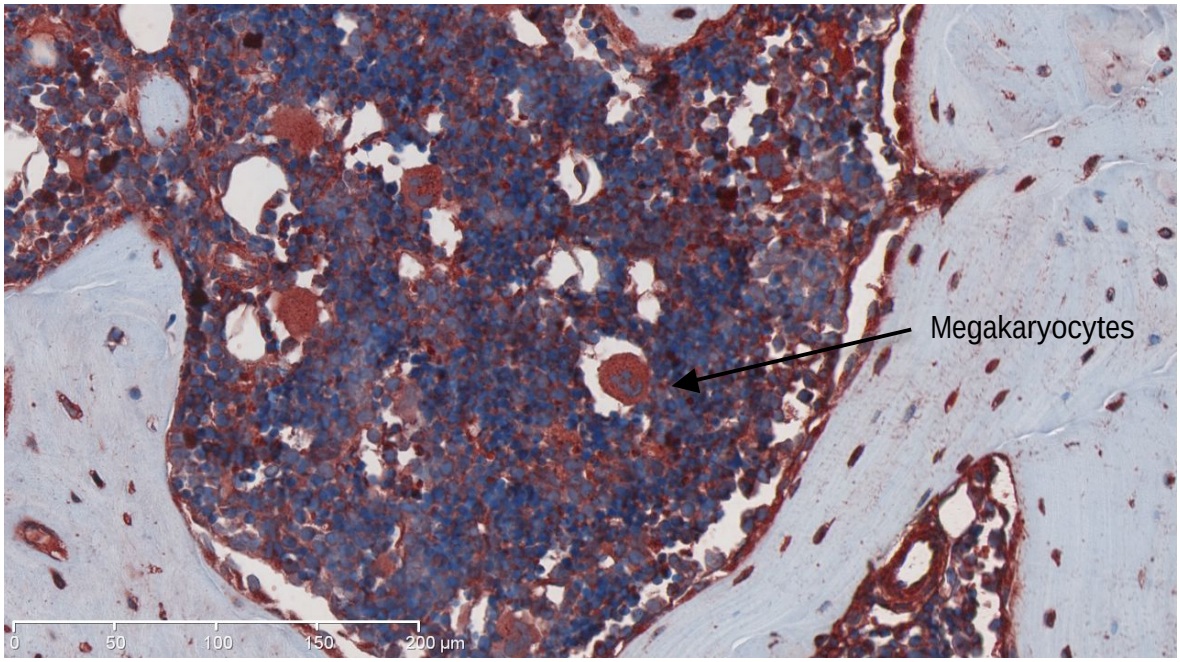
Megakaryocytes
0
50
100
150
200 µm

B

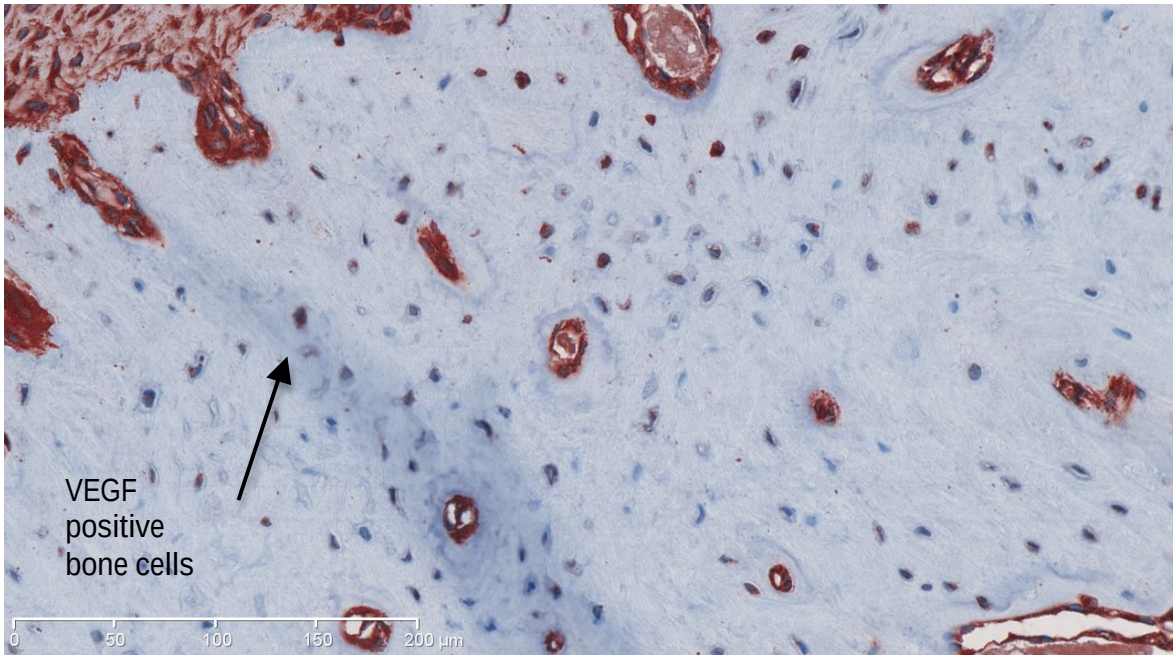
VEGF
positive
bone cells
0
50
100
150
200 µm

C

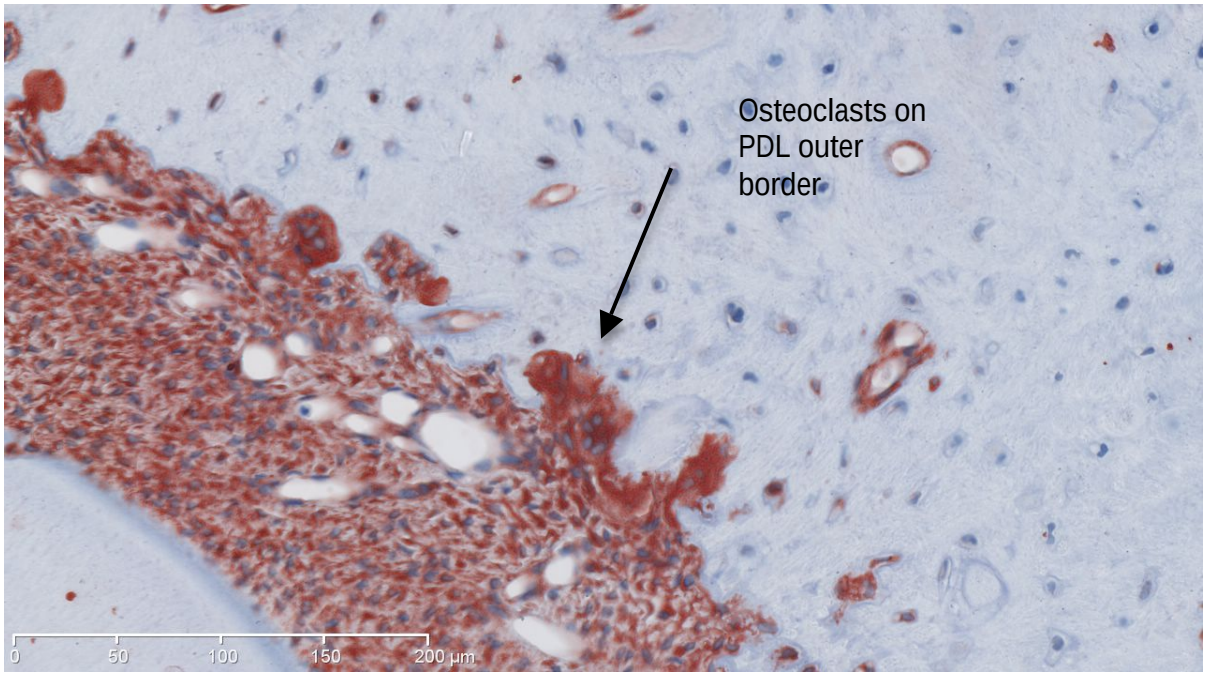
Osteoclasts on
PDL outer
border
0
50
100
150
200 µm

D

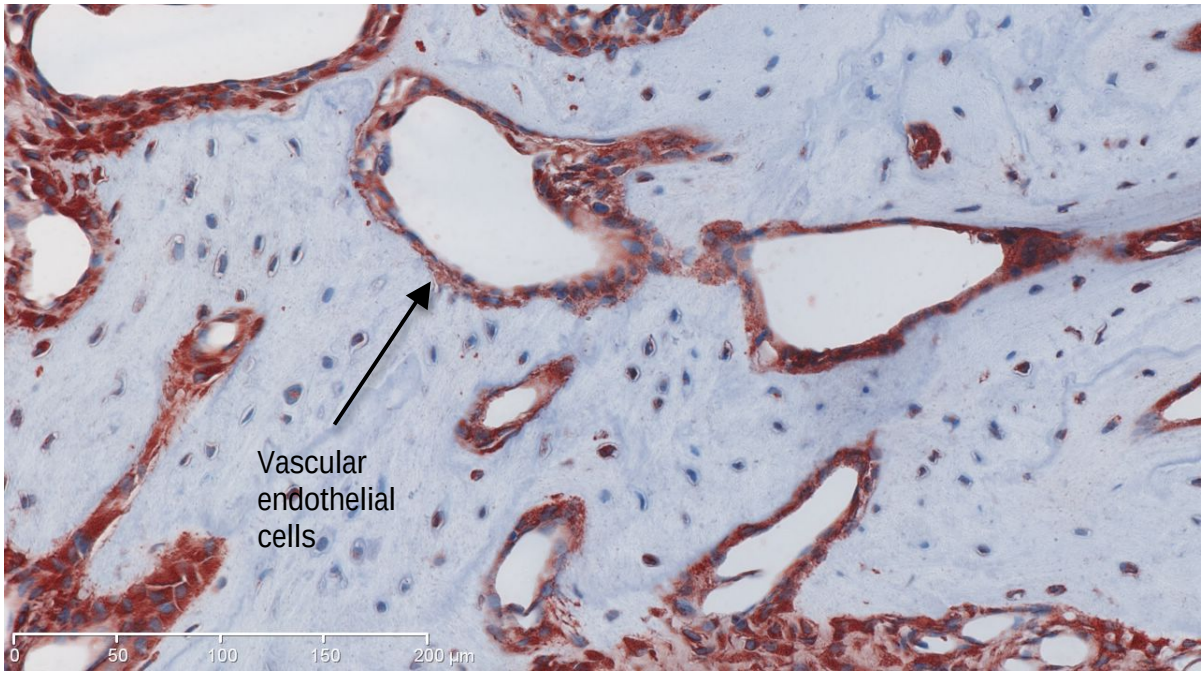
Vascular
endothelial
cells
0
50
100
150
200 µm

E

VEGF Expression in the Pulp:

Subjective evaluation showed little difference in the expression of VEGF at day 0 in the experimental, internal control or external control pulp tissues, with the majority of pulpal cells staining negative for VEGF. Of the VEGF positive cells, the majority were present in the core region of the pulp and appeared to be endothelial cells surrounding blood vessels or fibroblast-like cells. Generalised positive staining was also present in the extracellular pulpal tissues.

At day 4, the experimental side pulp tissue demonstrated disruption to the distinct pulpal layers, with a greater number of fibroblast-like cells staining positive for VEGF compared to the internal controls. Within the disrupted odontoblast layer, VEGF positive and negative odontoblast cells were present with an increased staining intensity compared to other regions of the pulp and the control pulps. These trends continued at day 7 and 14. By day 28 distinct pulpal organisation was present in two of the three rats. Both of these rats also demonstrated an intact PDL and no ankylosis. In the third rat, pulpal disruption as well as loss of the PDL and ankylosis was present.

Within the pulp, odontoblasts stained positively for VEGF at day 4, 7, 14 and 28, with very few odontoblasts staining positively at day 0 in the experimental group, or in the internal or external control groups. Fibroblast-like cells within the pulpal core region also demonstrated increased positivity at days 4, 7, 14 and 28 compared to the pulps of the control animals (see Figure 9).

Figure 9: VEGF expression in the pulp in the external control and over time in the experimental and internal control animals x20 magnification ruler 0 - 200µm. Red indicates Runx2 positive staining whilst blue indicated haematoxylin counterstaining.

Day 0 External Control

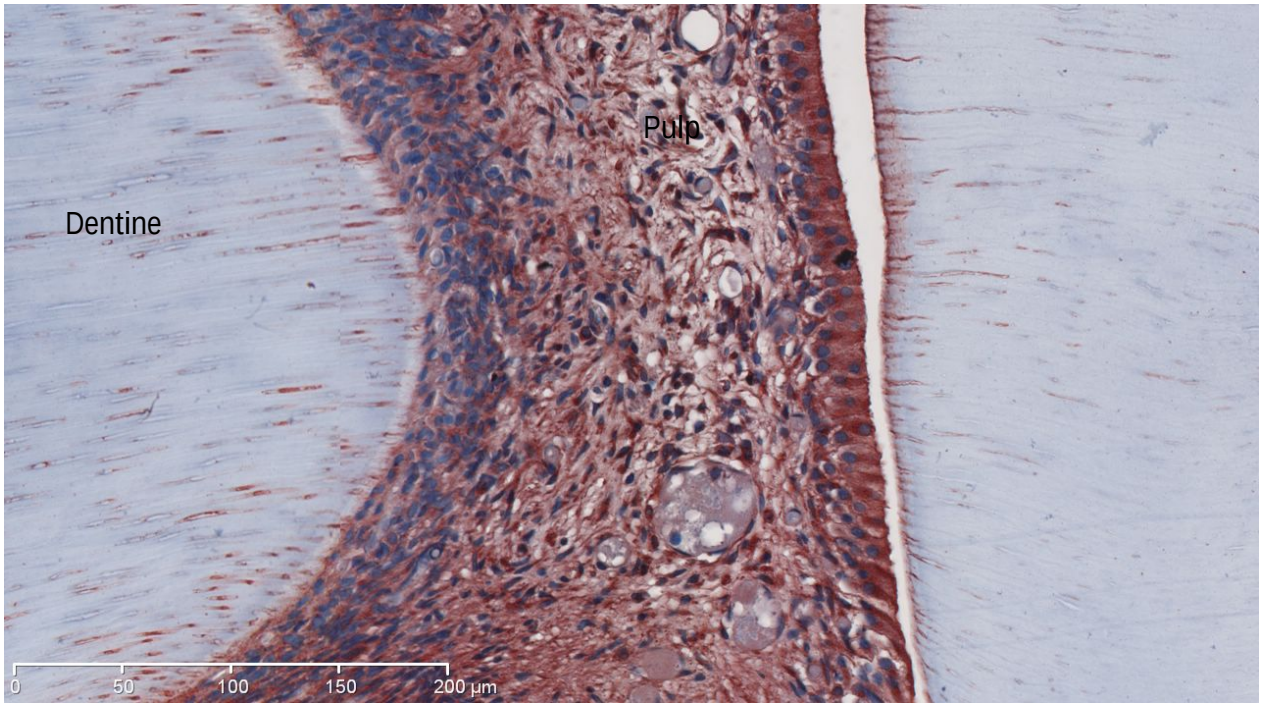

Day 0 Experimental

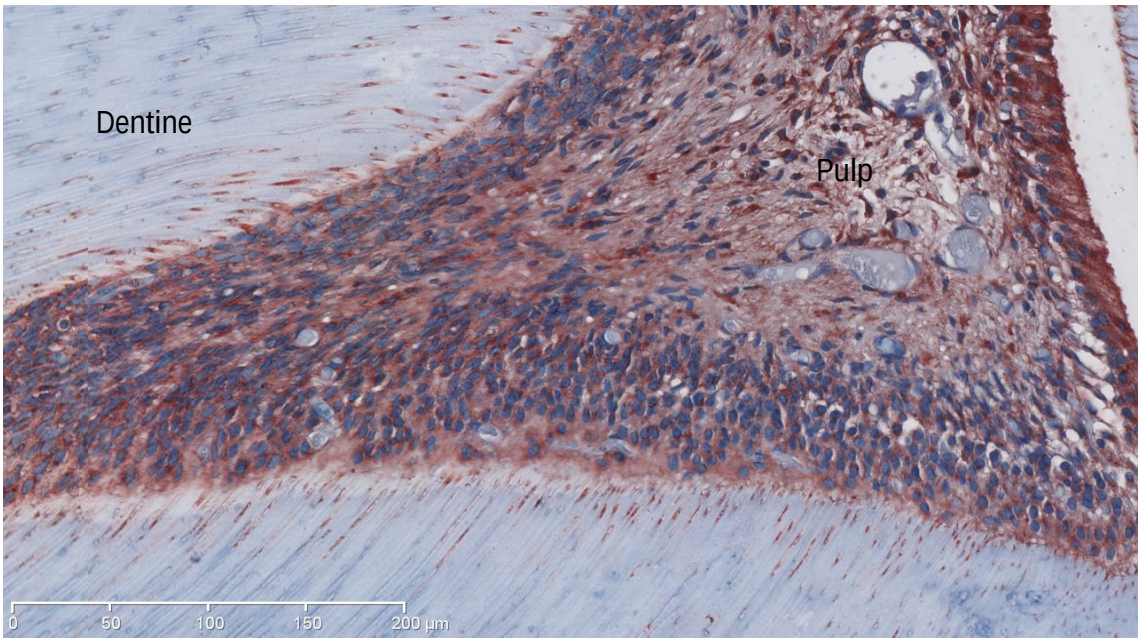

Day 0 Internal Control

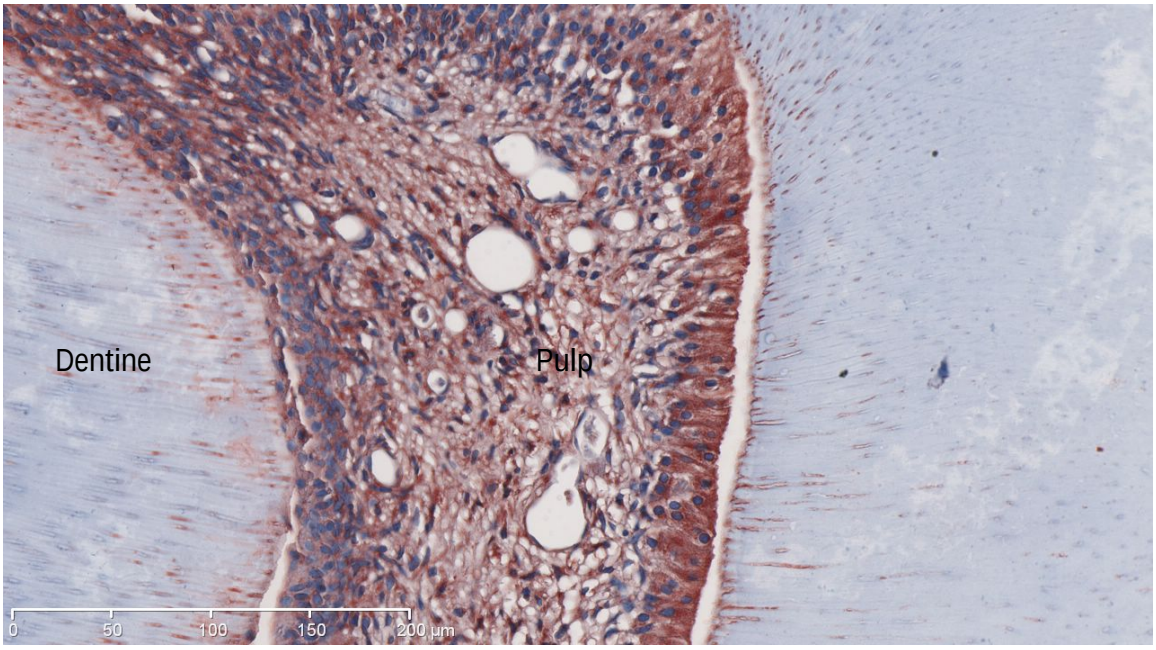

Day 4 Experimental

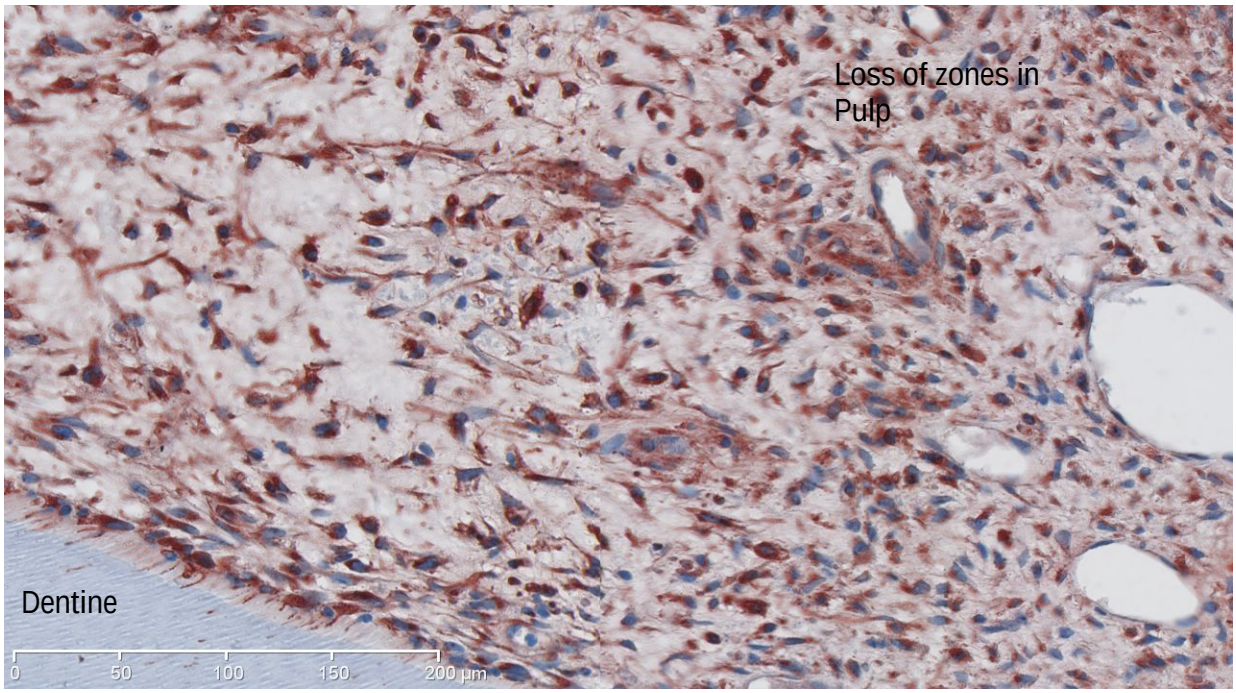

Day 4 Internal Control

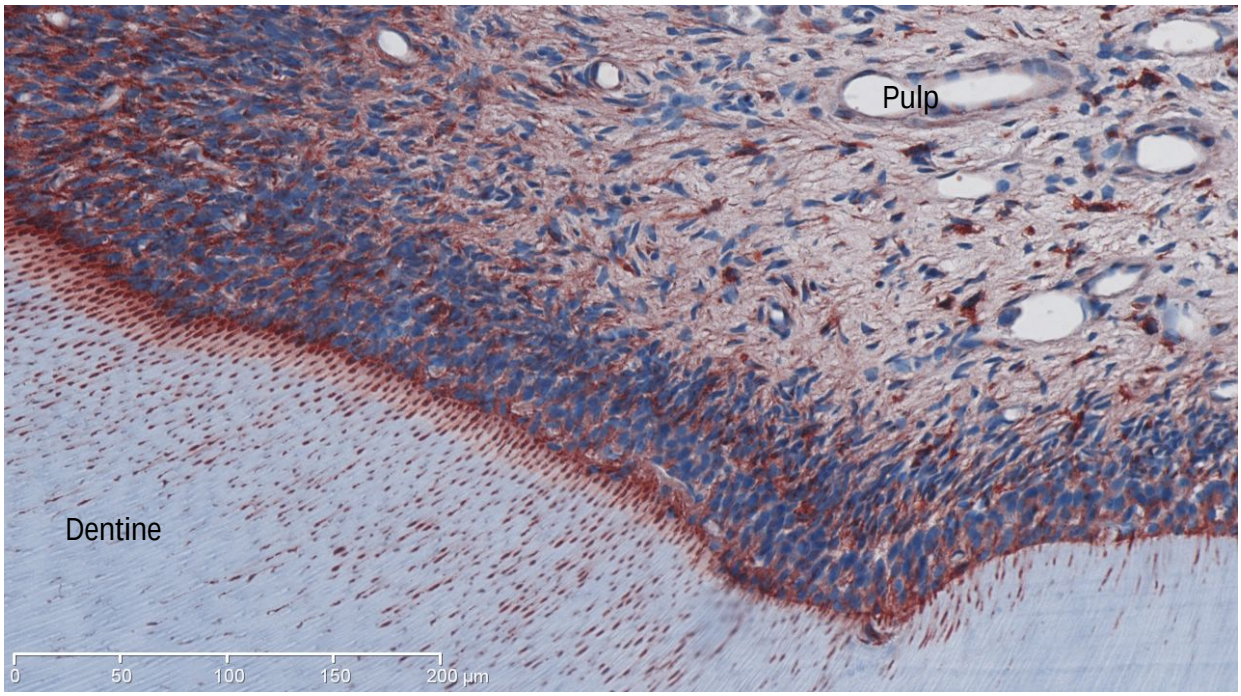

Day 7 Experimental

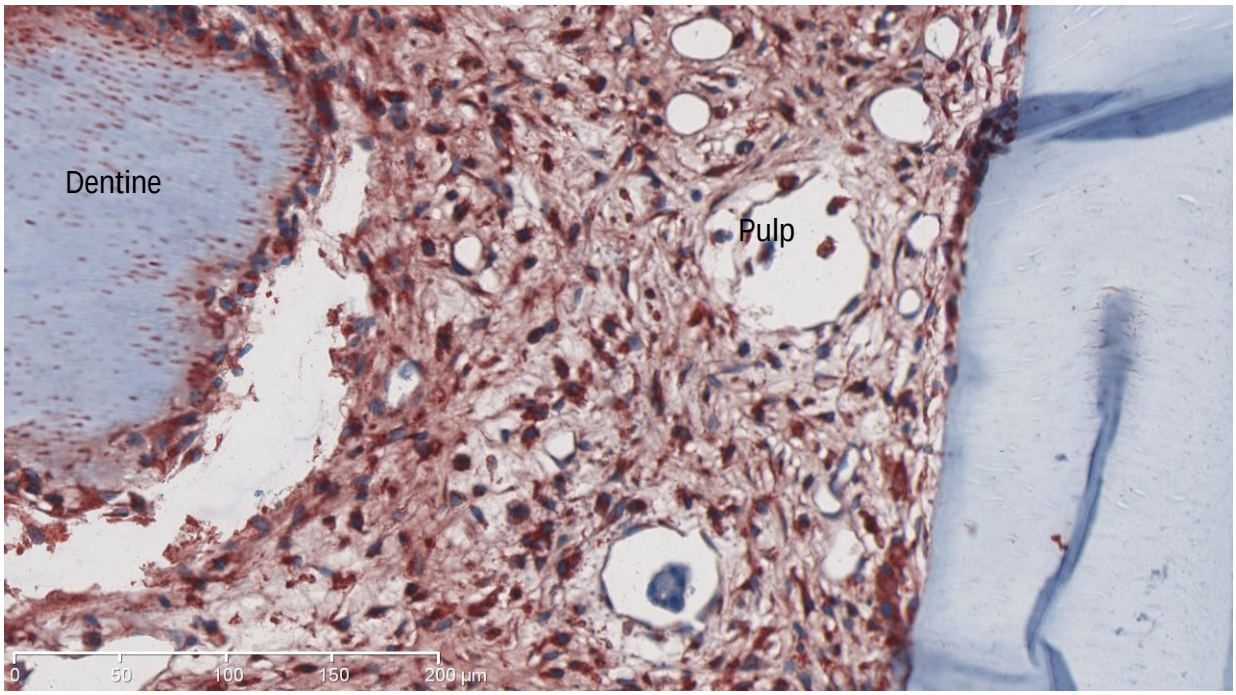

Day 7 Internal Control

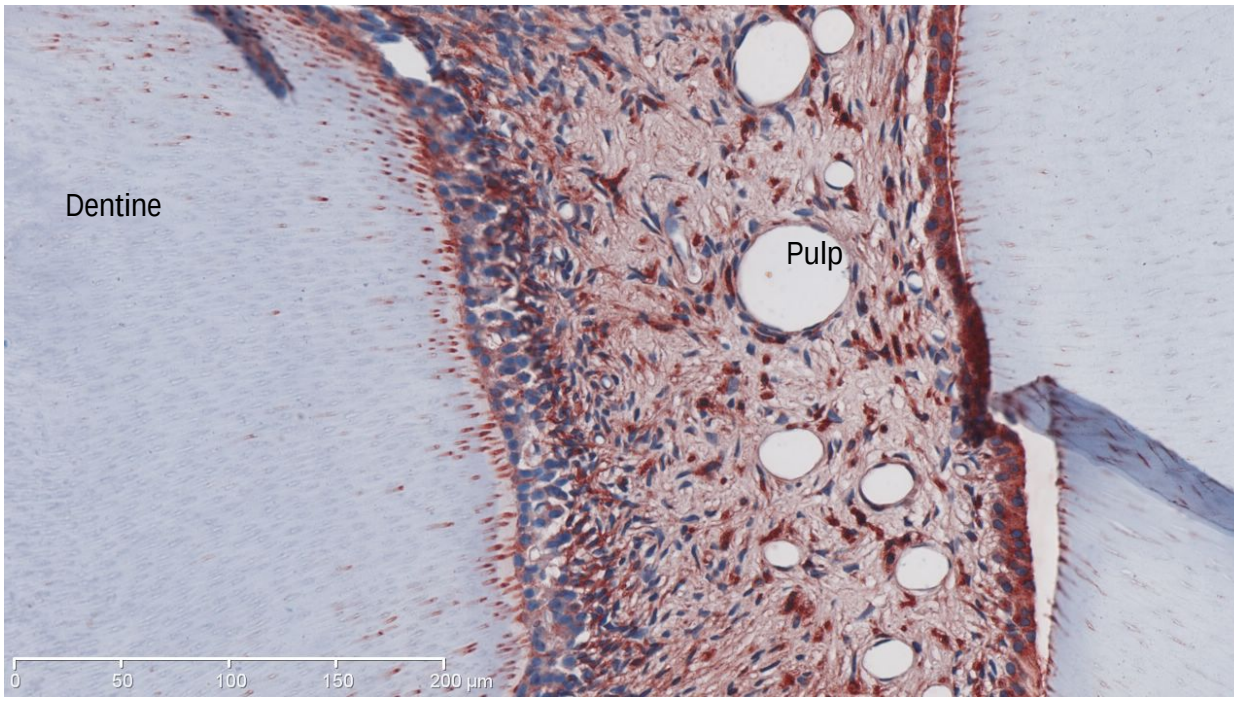

Day 14 Experimental

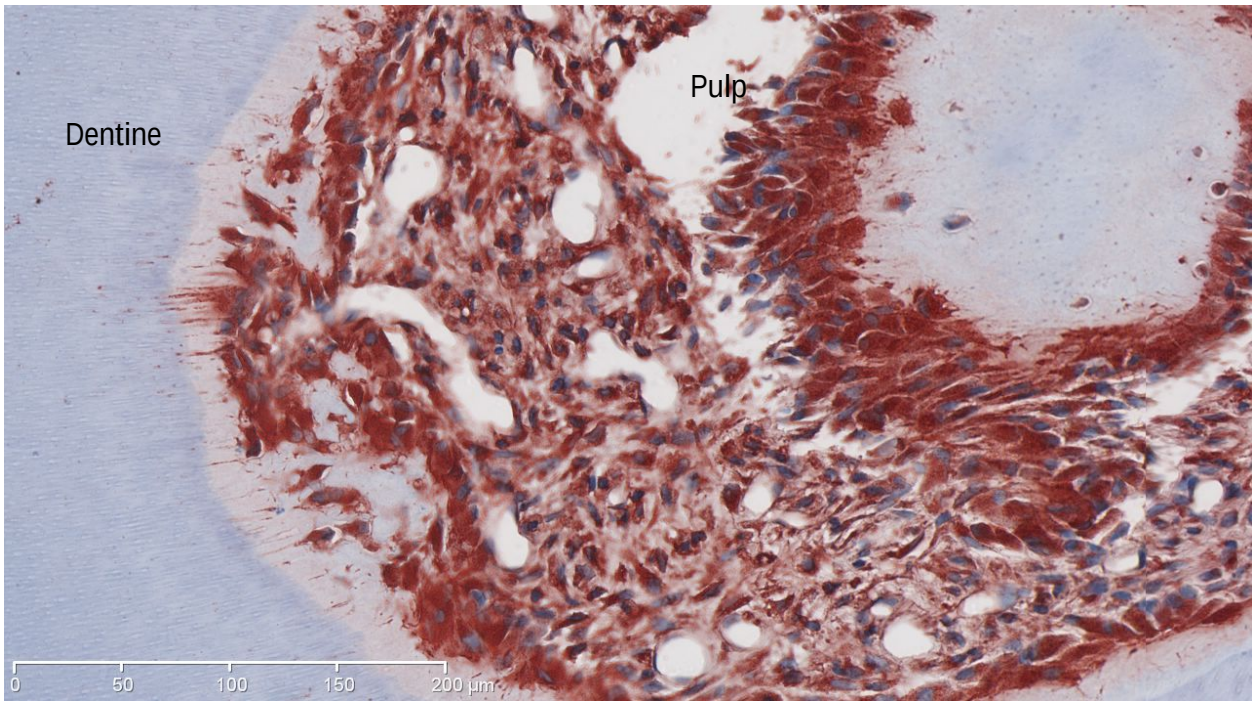

Day 14 Internal Control

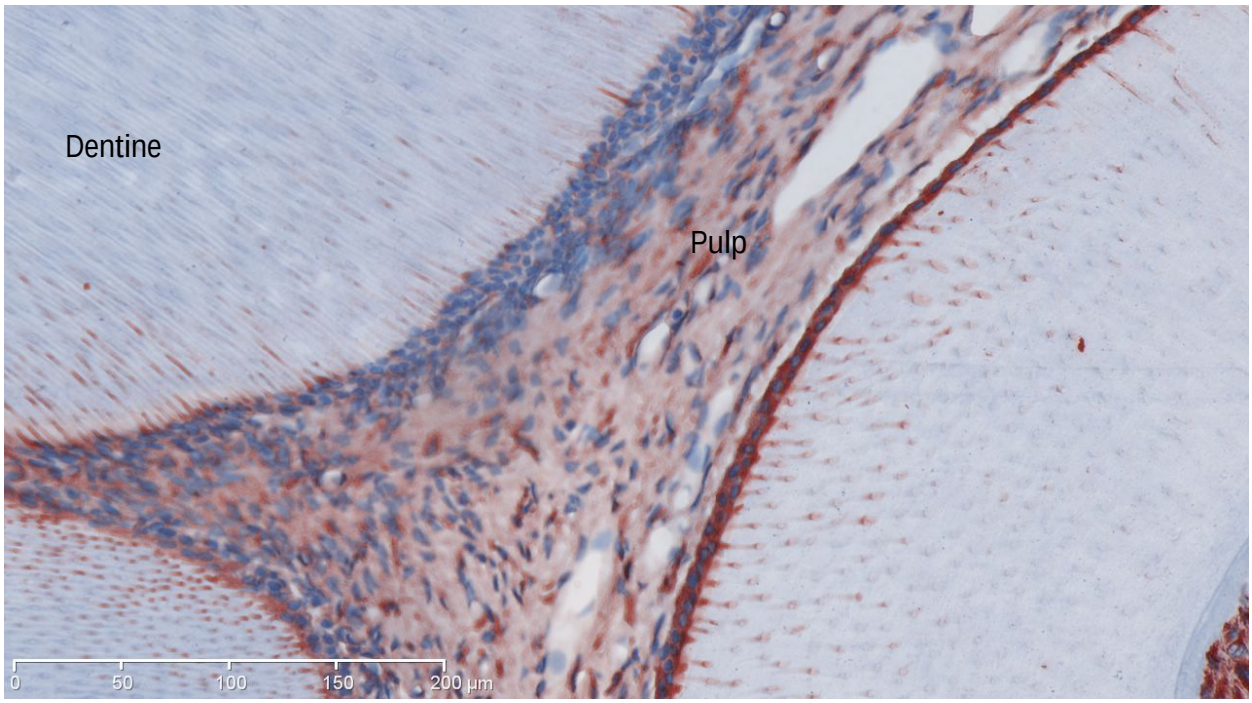

Day 28 Experimental

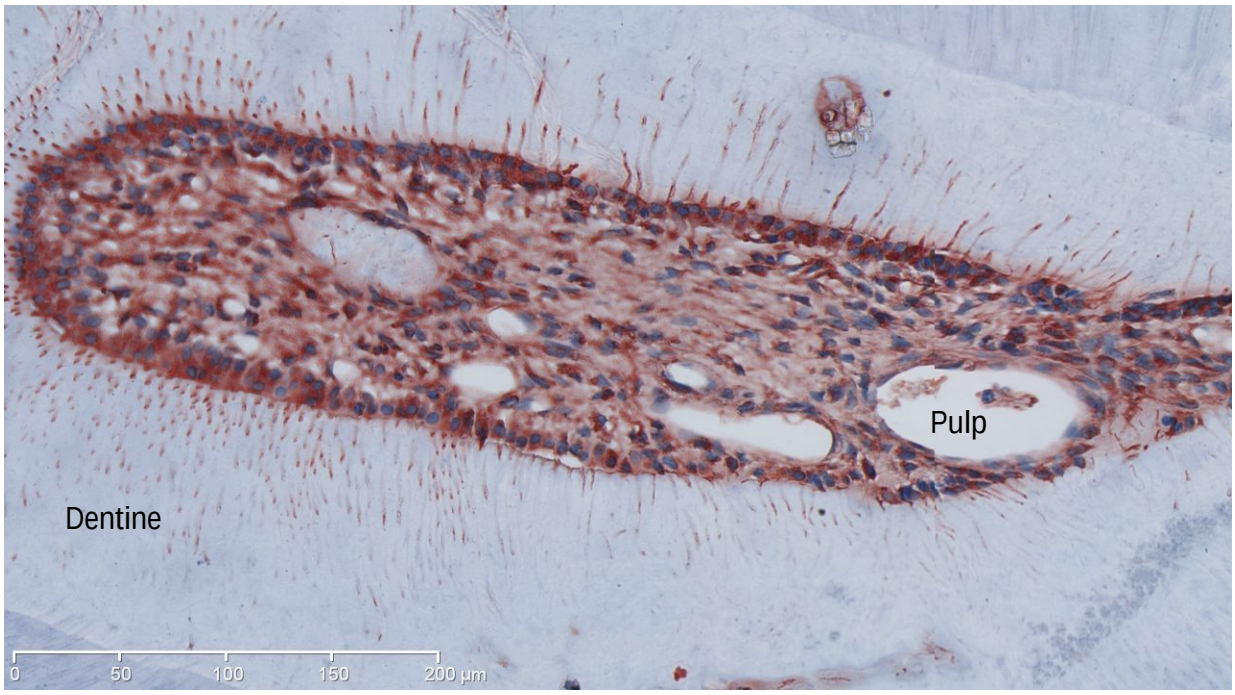

Day 28 Internal Control

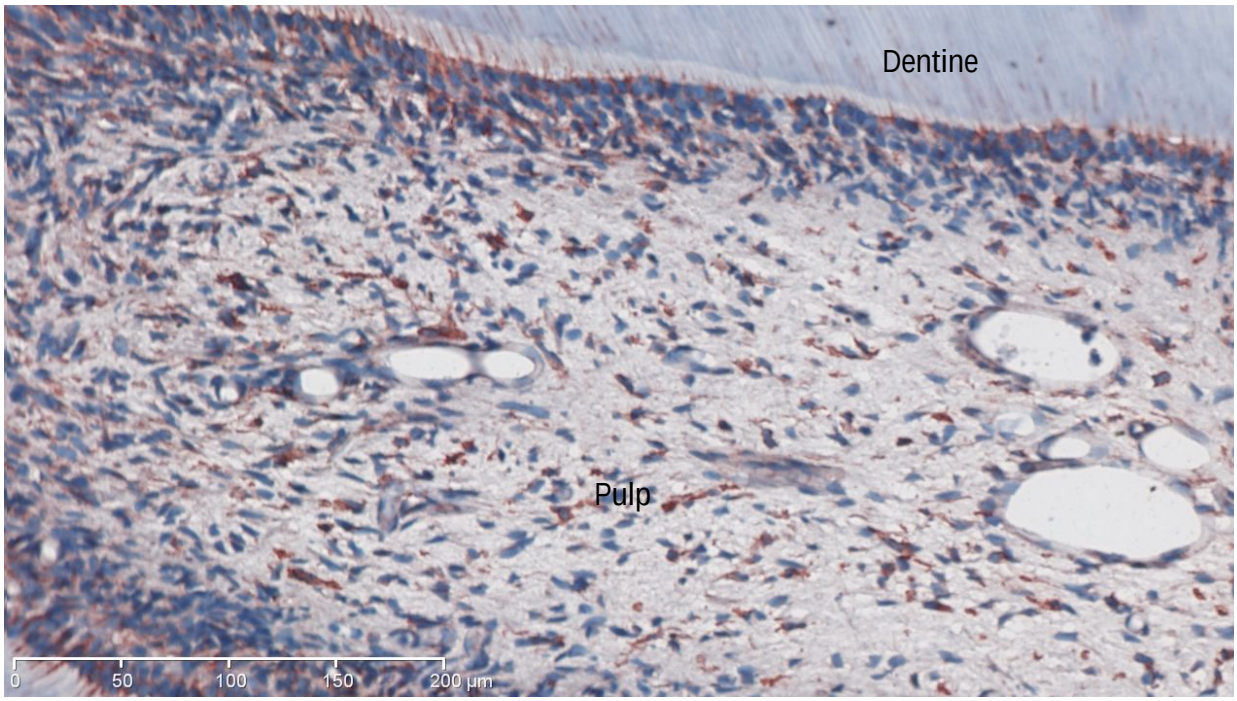

The differences noted between the pulpal tissues of the experimental and control animals were also noted statistically (see Tables 2 and 3). There was a statistically significant difference in the percentage of VEGF positive cells on the experimental compared to the internal control side ($p<0.001$). A statistically significant difference was also found between the percentage of VEGF positive cells on the experimental side at the various time points ($p<0.001$) with VEGF positive cells being more numerous at days 4 and 7, than at days 14 and 28. This trend was also noted in the internal control animals, although the changes were not as great (see Table 2). On average, at day 4 the percentage of positive cell counts on the experimental side was higher than that on the internal control by 36% whilst by day 14 the percentage of positive cell counts on the experimental side was on average higher than that on the internal control by 24%. A significant interaction between side and time was found with the experimental side showing an increased number of positive cells compared to the internal control ($p=0.043$) (see Table 3).

Table 2: The mean percentage of VEGF positive cells in the pulp of experimental and internal control animals.

R: Experimental group, L: Internal Control group

Effect	time	side	Mean	Standard Error
time*side	0	L	7.8987	3.1909
time*side	4	L	6.2922	3.3445
time*side	7	L	26.1818	4.1065
time*side	14	L	12.4395	3.2065
time*side	28	L	19.8756	3.5021
time*side	0	R	8.1301	10.8212
time*side	4	R	42.6890	10.8888
time*side	7	R	87.7800	10.7858
time*side	14	R	36.4314	10.8528
time*side	28	R	43.1145	10.9252

Table 3: A comparison of the mean percentage of VEGF positive cells in the pulp between 2 time points within the experimental group and between the experimental and internal control sites at different time points.

R: Experimental group, L: Internal control group. 0, 4, 7, 14 and 28 denote time points of the experimental group and internal control groups.

*p<0.05 ** p<0.001

Effect	Time side vs. _time _side				Estimate	Standard Error	PValue
time*side	0	L	0	R	-0.2314	11.1791	0.9835
time*side	0	L	4	L	1.6065	4.6226	0.7285
time*side	0	L	7	L	-18.2831	5.2005	**0.0005
time*side	0	L	14	L	-4.5408	4.5237	0.3165
time*side	0	L	28	L	-11.9769	4.7378	*0.0121
time*side	0	R	4	R	-34.5589	15.3514	*0.0253
time*side	0	R	7	R	-79.6499	15.2785	**<.0001
time*side	0	R	14	R	-28.3013	15.3259	0.0660
time*side	0	R	28	R	-34.9844	15.3772	*0.0238
time*side	4	L	4	R	-36.3968	11.2887	**0.0014
time*side	4	L	7	L	-19.8896	5.2961	**0.0002
time*side	4	R	7	R	-45.0910	15.3265	*0.0036
time*side	7	L	7	R	-61.5982	11.4402	**<.0001
time*side	14	L	4	L	6.1474	4.6333	0.1858
time*side	14	L	7	L	-13.7422	5.2101	*0.0089
time*side	14	L	14	R	-23.9918	11.2136	*0.0334
time*side	14	L	28	L	-7.4361	4.7483	0.1186
time*side	14	R	4	R	-6.2576	15.3737	0.6843
time*side	14	R	7	R	-51.3486	15.3009	**0.0009
time*side	14	R	28	R	-6.6832	15.3995	0.6647
time*side	28	L	4	L	13.5835	4.8426	*0.0054
time*side	28	L	7	L	-6.3061	5.3970	0.2438
time*side	28	L	28	R	-23.2389	11.3716	*0.0421
time*side	28	R	4	R	0.4255	15.4249	0.9780
time*side	28	R	7	R	-44.6654	15.3523	*0.0040

A statistically significant difference ($p<0.05$) between the VEGF positive cells in control animals was also noted (see Tables 4 and 5). On average, the percentage of VEGF positive cells was higher in the external control group with the number of VEGF positive cells being less at day 0 and 4 in the internal control group, then greater with a spike of VEGF expression at day 7, followed again by a decrease at day 14. There was little difference between the internal and external control groups at day 28.

Table 4: The mean of percentage of VEGF positive cells in the pulp in the internal and external control groups.

EC: External control. 0, 4, 7, 14 and 28 denote time points of the Internal control group.

Effect	time	Estimate	Standard Error
time	EC	17.1400	3.8967
time	0	8.1072	3.4048
time	4	6.2635	3.5021
time	7	25.5721	4.3097
time	14	12.6624	3.4358
time	28	19.5633	3.5723

Table 5: A comparison of the mean percentage of VEGF positive cells in the pulp between 2 time points of the internal control and between different time points of the internal control and the external control group.

EC: External control. 0, 4, 7, 14 and 28 denote time points of the Internal control group.

* p<0.05, **p<0.001.

Effect		Estimate	Standard Error	PValue
Time	EC vs. 0	9.0329	5.1746	0.0832
Time	EC vs. 4	10.8765	5.2392	*0.0399
Time	EC vs. 7	-8.4321	5.8101	0.1491
Time	EC vs. 14	4.4777	5.1951	0.3903
Time	EC vs. 28	-2.4232	5.2864	0.6474
Time	0 vs. 4	1.8436	4.8844	0.7065
Time	0 vs. 7	-17.4650	5.4924	**0.0018
Time	0 vs. 14	-4.5552	4.8371	0.3481
Time	0 vs. 28	-11.4561	4.9350	*0.0218
Time	4 vs. 7	-19.3086	5.5532	**0.0007
Time	14 vs. 4	6.3988	4.9061	0.1944
Time	14 vs. 7	-12.9098	5.5117	*0.0207
Time	14 vs. 28	-6.9009	4.9565	0.1662
Time	28 vs. 4	13.2997	5.0026	**0.0088
Time	28 vs. 7	-6.0088	5.5978	0.2851

VEGF Expression in the PDL:

A subjective evaluation of the PDL showed little difference in the expression of VEGF at day 0 in the experimental, internal control or external control PDL tissues, with an intact PDL ligament and both positive and negative fibroblast-like cells present. Positive blood vessel lumen and osteoclasts on the outer bony interface of the PDL were also present, as was diffuse staining of the extracellular matrix of the PDL. This diffuse staining was present in all samples.

At day 4, sections presented similarly to day 0, although there was increased staining intensity along the PDL bone interface and around blood vessels in both the experimental and internal control animals.

At day 7 in the experimental group, changes in the PDL were visible with thinning of the PDL, as well as some islands of PDL cells. VEGF positive and negative staining cells were present within these islands of cells and there was increased intensity of VEGF staining.

At day 14, there was complete loss of the PDL in the interradicular region of many sections in the experimental animals. Few cells remained in ankylotic regions, with the majority being positive for VEGF.

By day 28, one animal remained very similar to those in the experimental group at day 14, whilst the two other animals demonstrated an intact PDL and no ankylosis. In these two animals, staining of the PDL was similar to that described at day 0 (see Figure 10).

Figure 10: VEGF expression in the PDL in the external control and over time in the experimental and internal control animals x20 magnification ruler 0 - 200**µ**m.

Red indicates Runx2 positive staining whilst blue indicated haematoxylin counterstaining.

Day 0 External Control

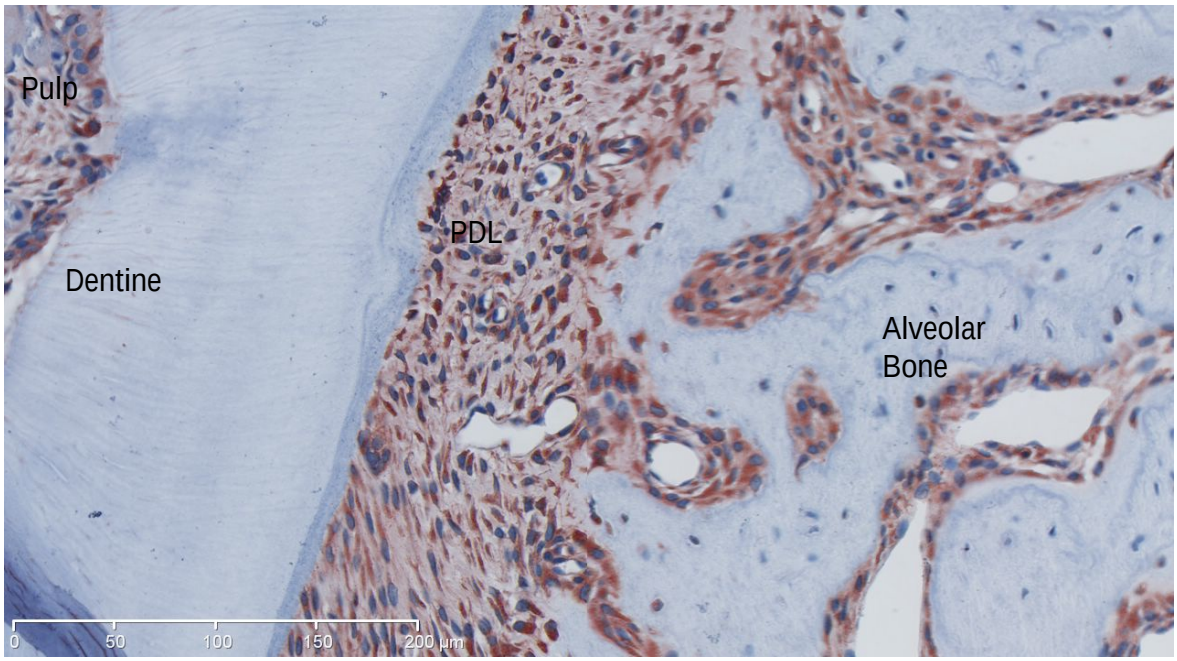

Day 0 Experimental

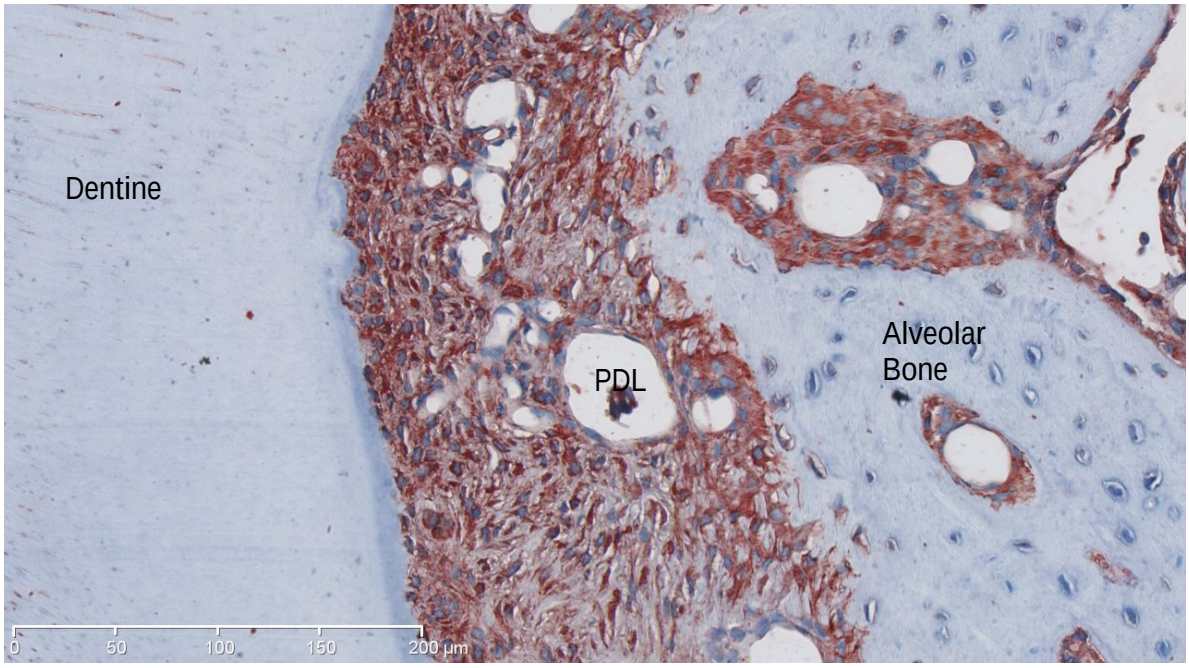

Day 0 Internal Control

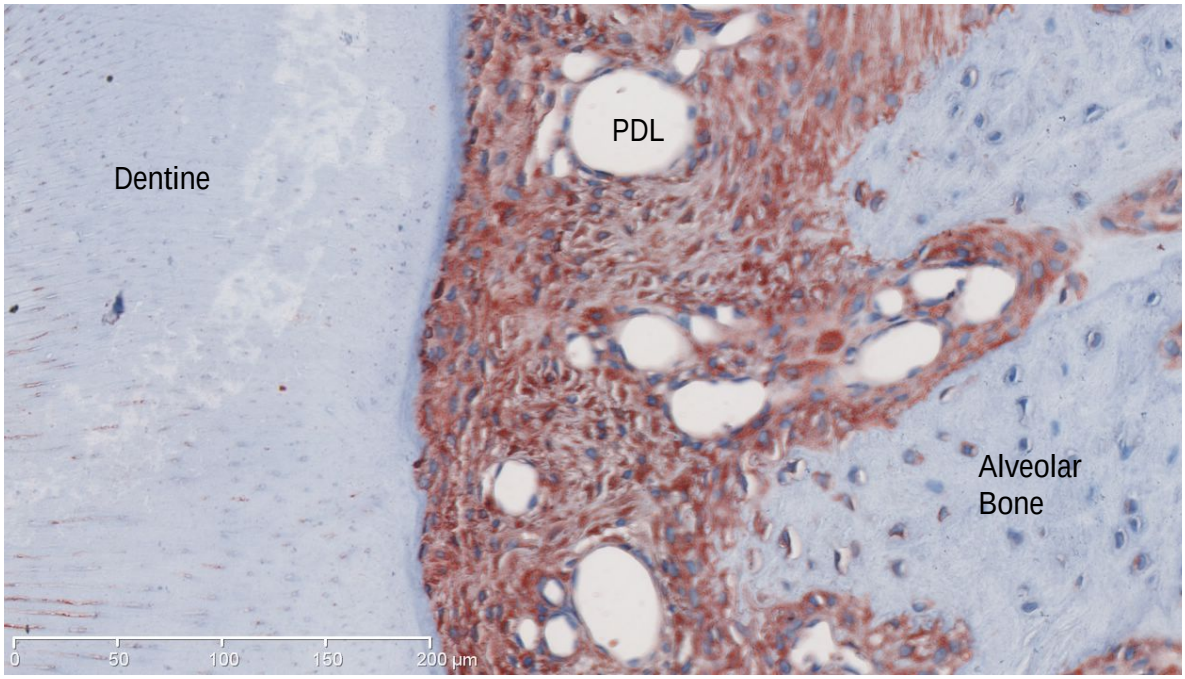

Day 4 Experimental

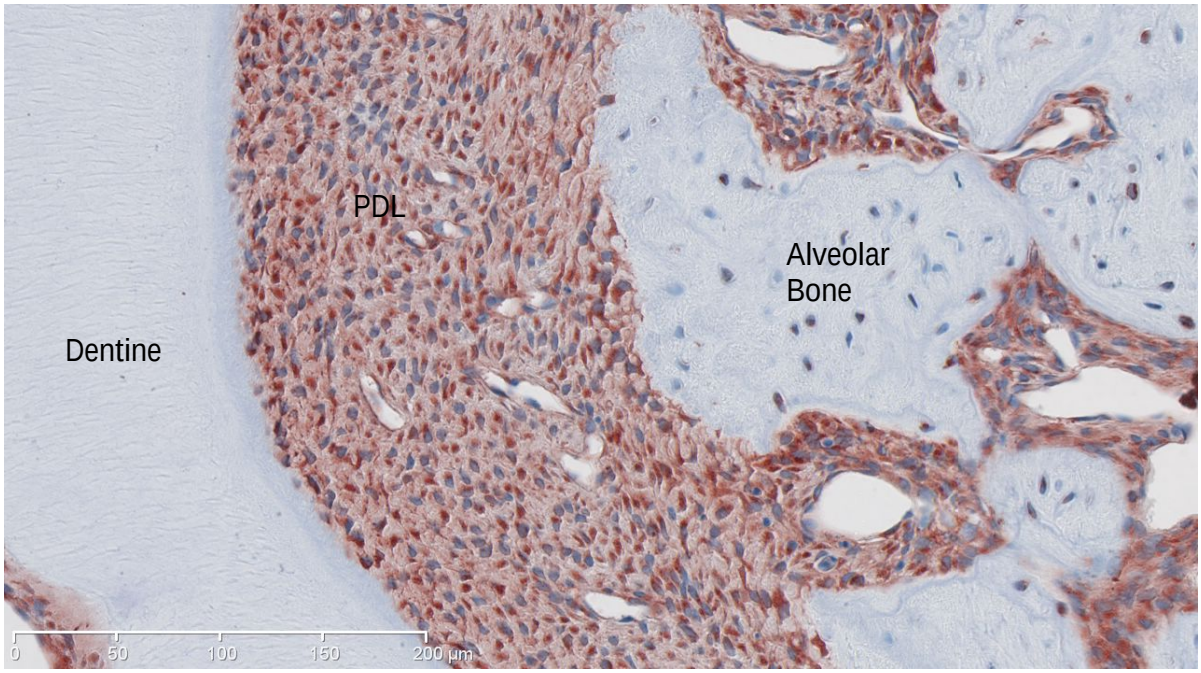

Day 4 Internal Control

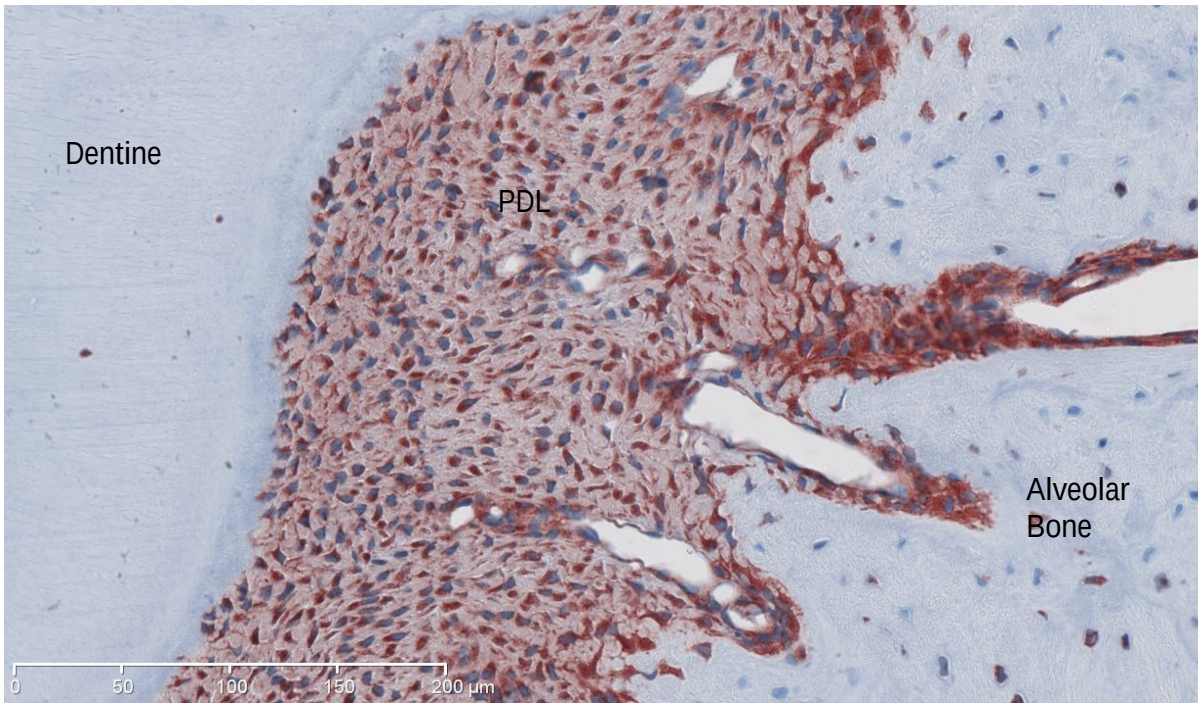

Day 7 Experimental

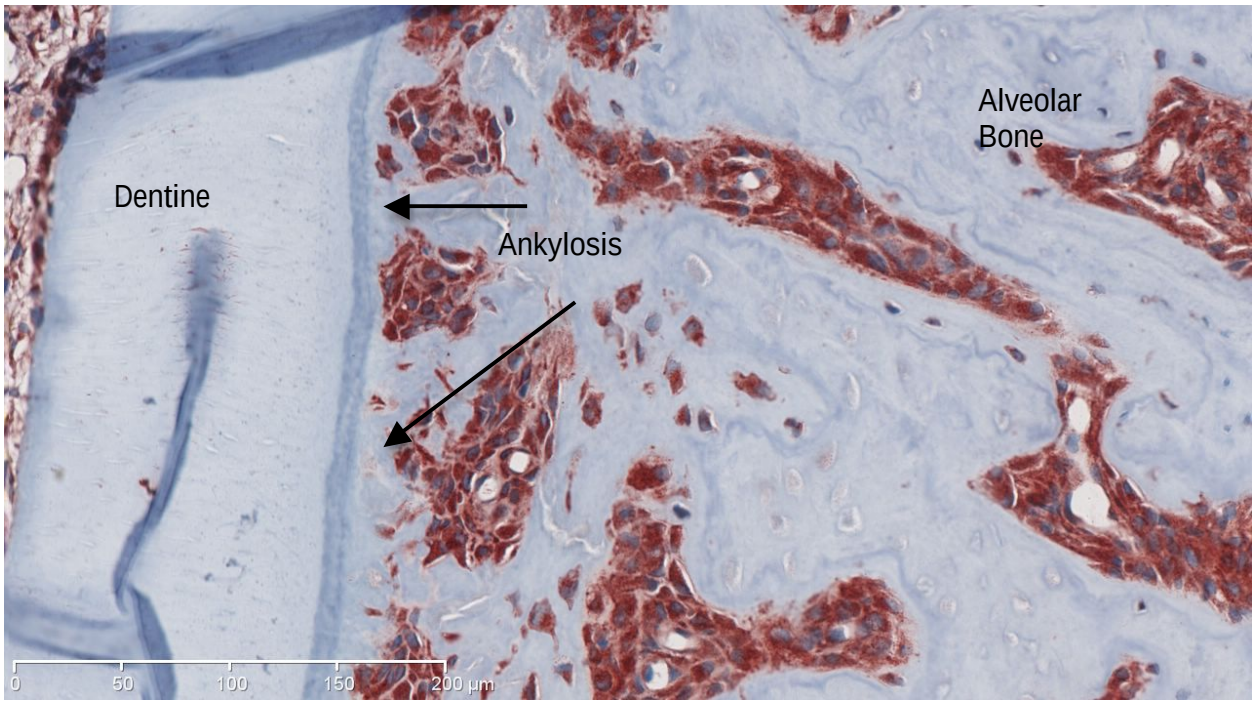

Day 7 Internal Control

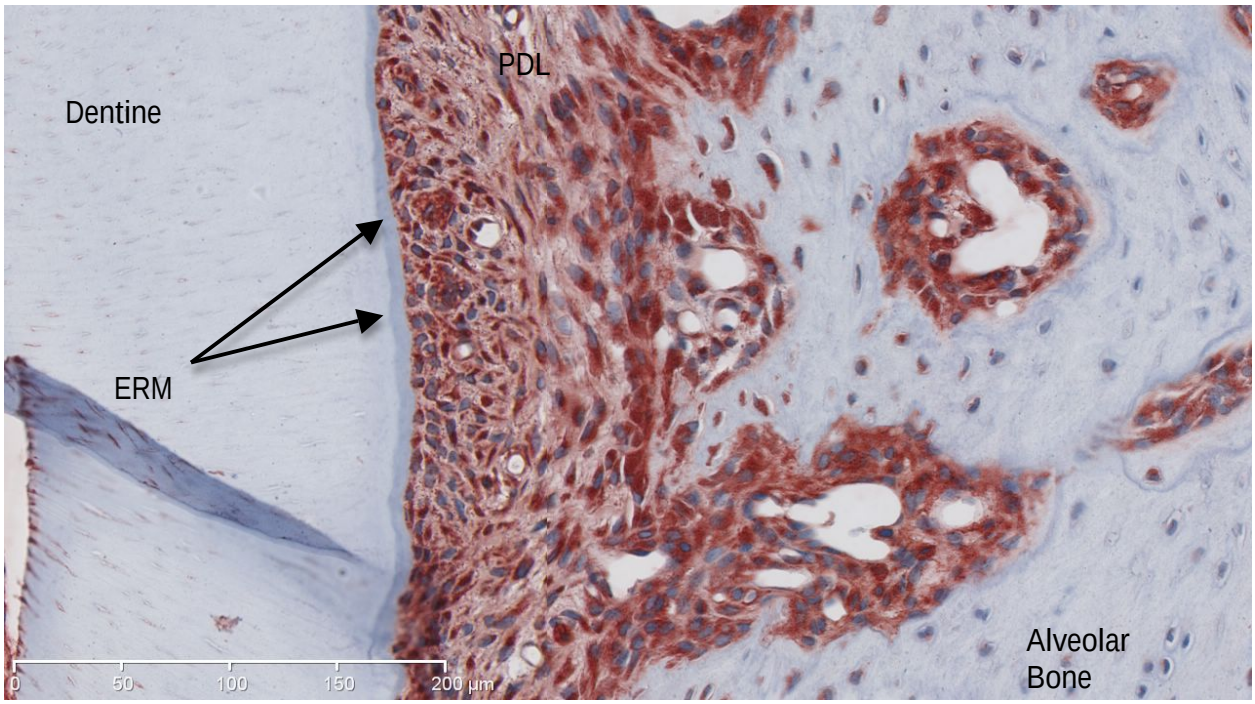

Day 14 Experimental

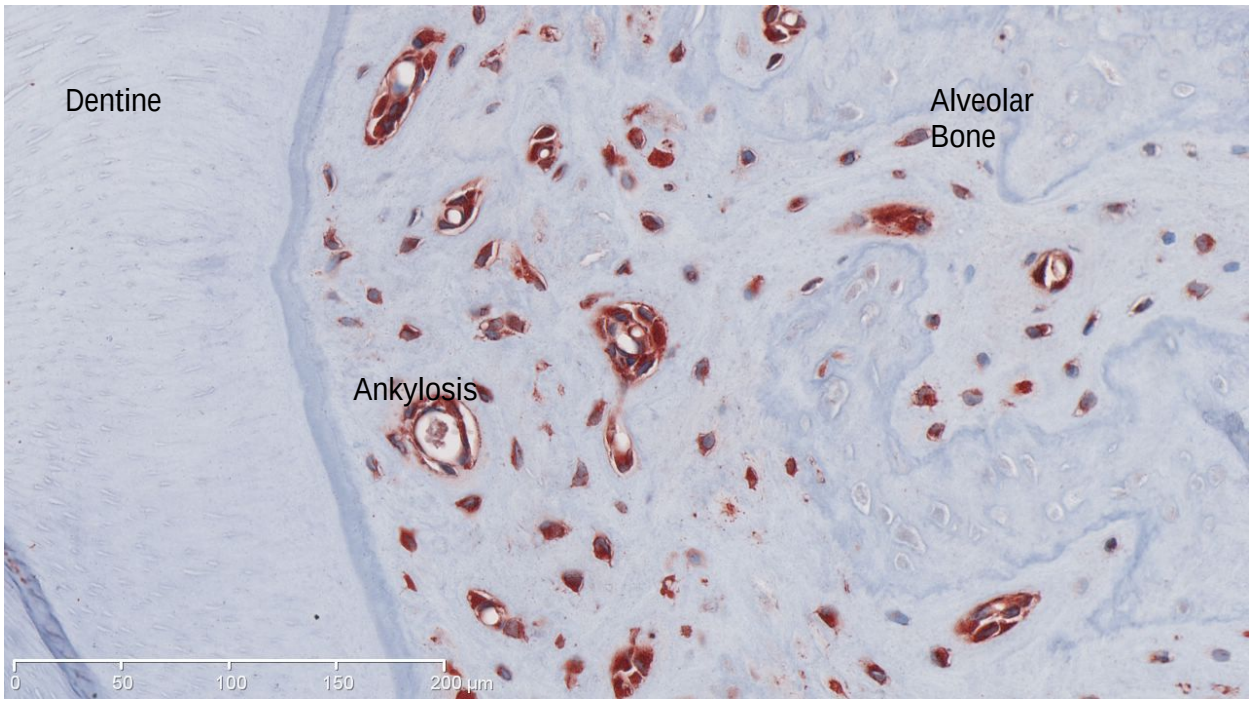

Day 14 Internal Control

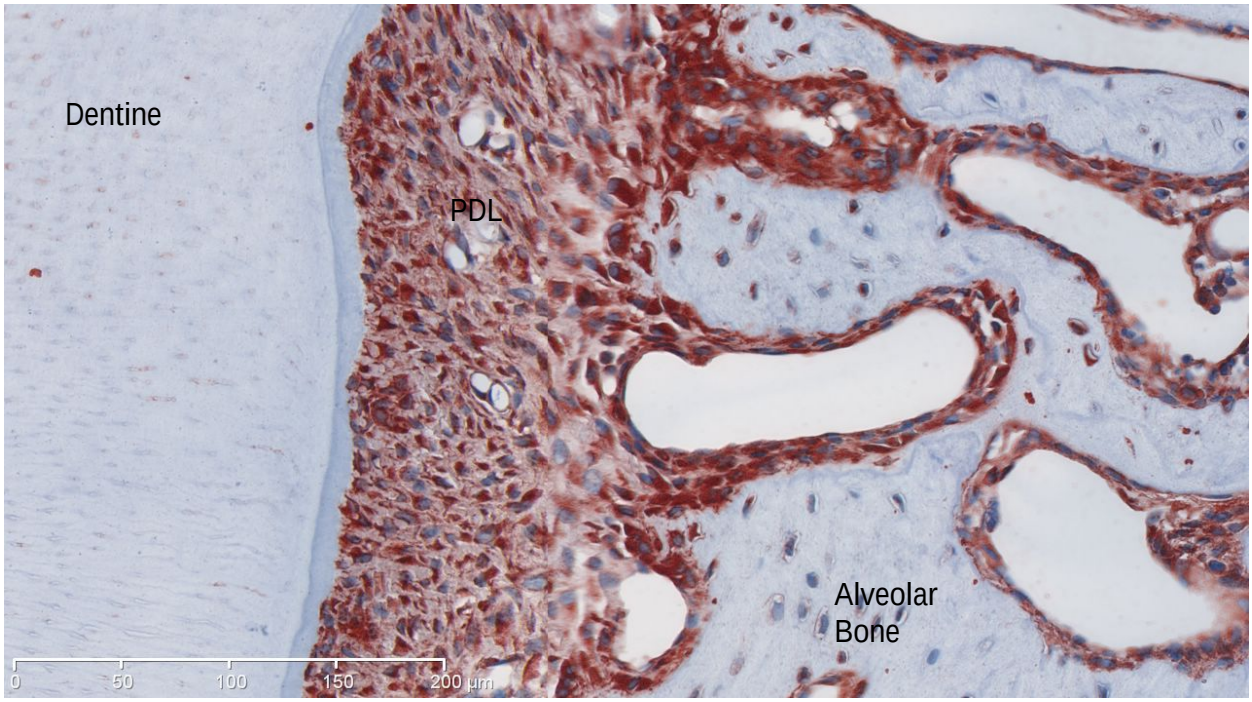

Day 28 Experimental

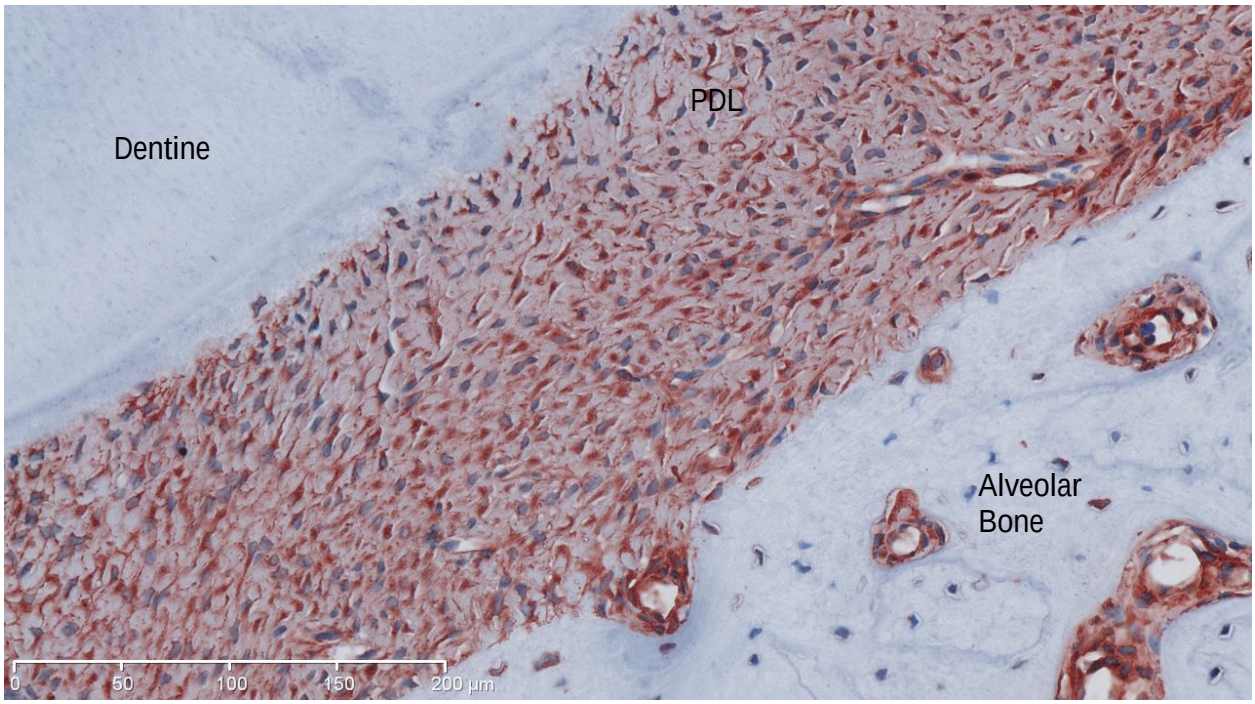

Day 28 Internal Control

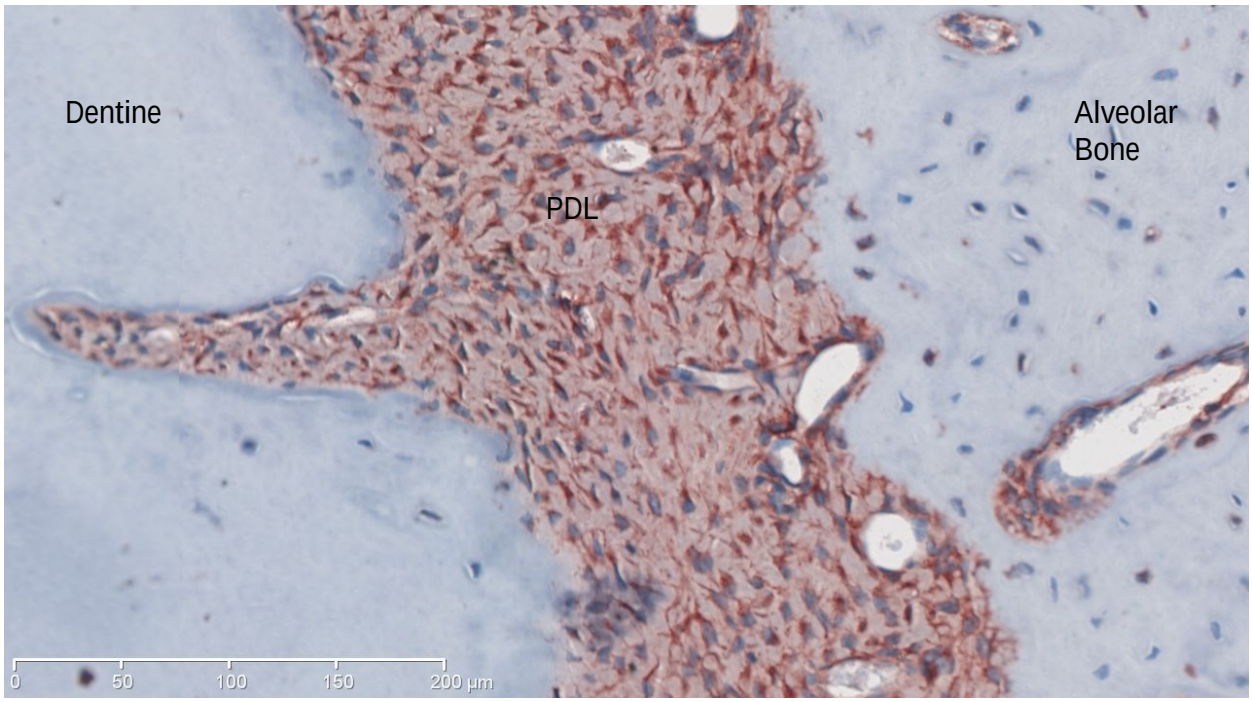

The statistics positively supported the descriptive analysis with a statistically significant difference between the percentages of VEGF positive cells in the PDL on the experimental side compared to the internal control side ($p = 0.0059$) (see Tables 6 and 7). Although not significant, the number of VEGF positive cells decreased from days 0 to 14 post insult, then increased day 28. The percentage of VEGF positive cells was higher on the control side by, on average, 20.2%, when compared to the experimental side at any given time point.

Table 6: The mean percentage of VEGF positive cells in the PDL of experimental animals at different time points and an accumulative percentage of the VEGF positive cells in the experimental and internal control animals.

R: Experimental Group, L; Internal Control group.

0, 4, 7, 14, 28 denote time points of the experimental group.

Effect	time	side	Mean	Standard Error
time	0		80.4982	5.4284
time	4		78.2239	5.6754
time	7		76.1531	5.5132
time	14		69.8193	5.4548
time	28		85.2520	5.5799
side		L	88.0925	2.1033
side		R	67.8861	6.6831

Table 7: The difference of mean percentage of VEGF positive cells in the PDL between the experimental animals at different time points and overall between the accumulated mean percentage of the experimental and internal control sites.

R: Experimental group, L: Internal control group.

0, 4, 7, 14, 28 denote time points of the experimental group. * p<0.05.

Effect	Time side vs. _time _side				Estimate	Standard Error	PValue
time	0		4		2.2742	6.6077	0.7309
time	0		7		4.3451	6.4440	0.5005
time	0		14		10.6788	6.3810	0.0950
time	0		28		-4.7538	6.5123	0.4658
time	4		7		2.0708	6.6937	0.7572
time	14		4		-8.4046	6.6335	0.2059
time	14		7		-6.3338	6.4705	0.3282
time	14		28		-15.4326	6.5385	0.0187
time	28		4		7.0280	6.7592	0.2990
time	28		7		9.0989	6.5996	0.1687
side		L		R	20.2064	6.6904	0.0059

Overall, there were no significant differences (p = 0.2344) between the external and internal control groups at all time points (see Tables 8 and 9). Within the internal control group, however, there was a statistically significant difference in the number of VEGF positive cells between days 14 and 28 (see Table 9).

Table 8: The mean percentage of VEGF positive cells in the PDL of control animals.

EC: External Control. Internal control divided by time points day 0, 4, 7, 14 and 28.

Effect	time	Estimate	Standard Error
time	EC	86.2294	4.4928
time	0	89.6806	4.2361
time	4	87.6164	4.4057
time	7	86.8693	4.2853
time	14	80.2945	4.2576
time	28	95.7537	4.3134

Table 9: A comparison of the differences of mean percentage of VEGF positive cells in the PDL of control animals between 2 time points of the internal control and between the internal and external control groups.

EC: External control. 0, 4, 7, 14 and 28 denote time points of the Internal control group.

* $p<0.05$.

Effect		Estimate	Standard Error	PValue
time	EC vs. 0	-3.4512	6.1750	0.5768
time	EC vs. 4	-1.3870	6.2925	0.8257
time	EC vs. 7	-0.6399	6.2088	0.9180
time	EC vs. 14	5.9349	6.1897	0.3386
time	EC vs. 28	-9.5243	6.2282	0.1275
time	0 vs. 4	2.0643	6.1119	0.7359
time	0vs. 7	2.8113	6.0256	0.6412
time	0 vs. 14	9.3861	6.0060	0.1194
time	0 vs. 28	-6.0730	6.0457	0.3162
time	4 vs. 7	0.7470	6.1460	0.9034
time	14 vs. 4	-7.3219	6.1268	0.2333
time	14 vs. 7	-6.5748	6.0408	0.2775
time	14 vs. 28	-15.4592	6.0608	*0.0114
time	28 vs. 4	8.1373	6.1657	0.1882
time	28 vs. 7	8.8843	6.0802	0.1453

VEGF Expression in the Alveolar Bone:

At day 0 in the experimental, internal control and external control groups, VEGF positive and negative bone cells (osteoblasts and osteocytes not differentiated) were present within the alveolar bone. No VEGF positive staining of canaliculi was present. Blood vessel lumen endothelial cell staining appeared particularly intense.

At day 4, an increased number of bone cells staining positive for VEGF in both the experimental and internal control groups were seen. This trend continued at days 7 and 14, with increased intensity of the blood vessel lumen staining also noted. Positive bone cells appeared more frequently closer to the PDL.

At day 28, VEGF positive and negative bone cells were present in both the experimental and internal control animals. Empty lacunae were also visible beneath the ankylotic region at day 7. The empty lacunae were increased in number at day 14 and decreased at day 28. Empty lacunae were not noted in the internal or external control groups and appeared to be insult related (see Figure 11).

Figure 11: VEGF expression in the alveolar bone in the external control and over time in the experimental and internal control animals x20 magnification ruler 0 - 200**µ**m.

Red indicates Runx2 positive staining whilst blue indicated haematoxylin counterstaining.

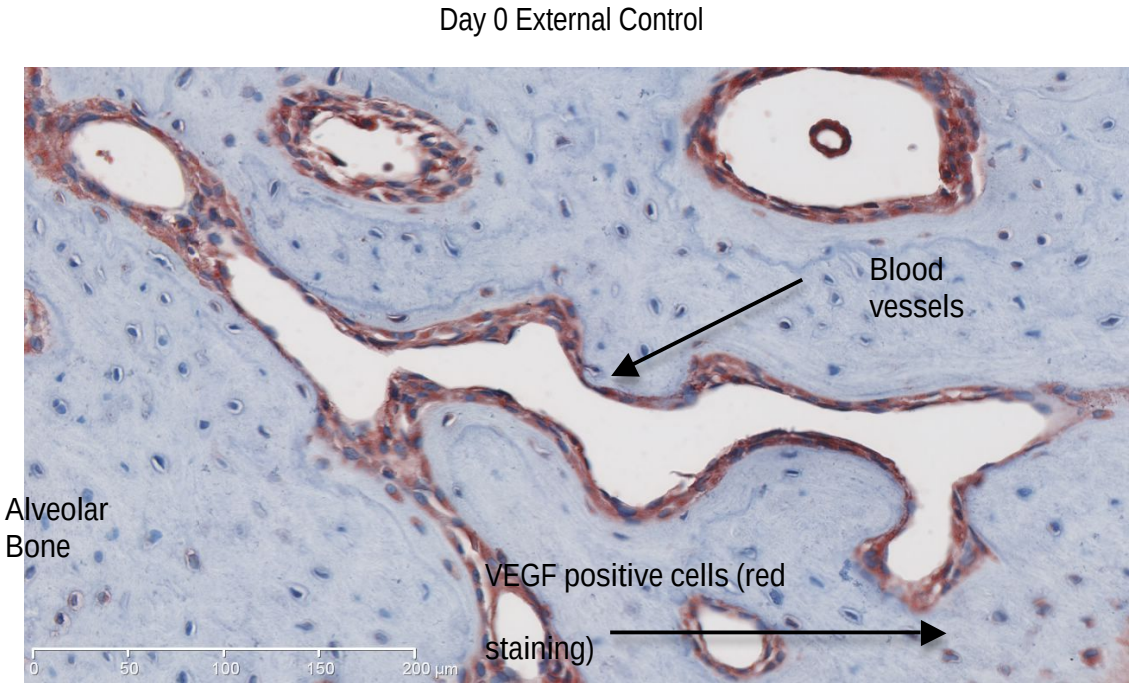

Day 0 Experimental

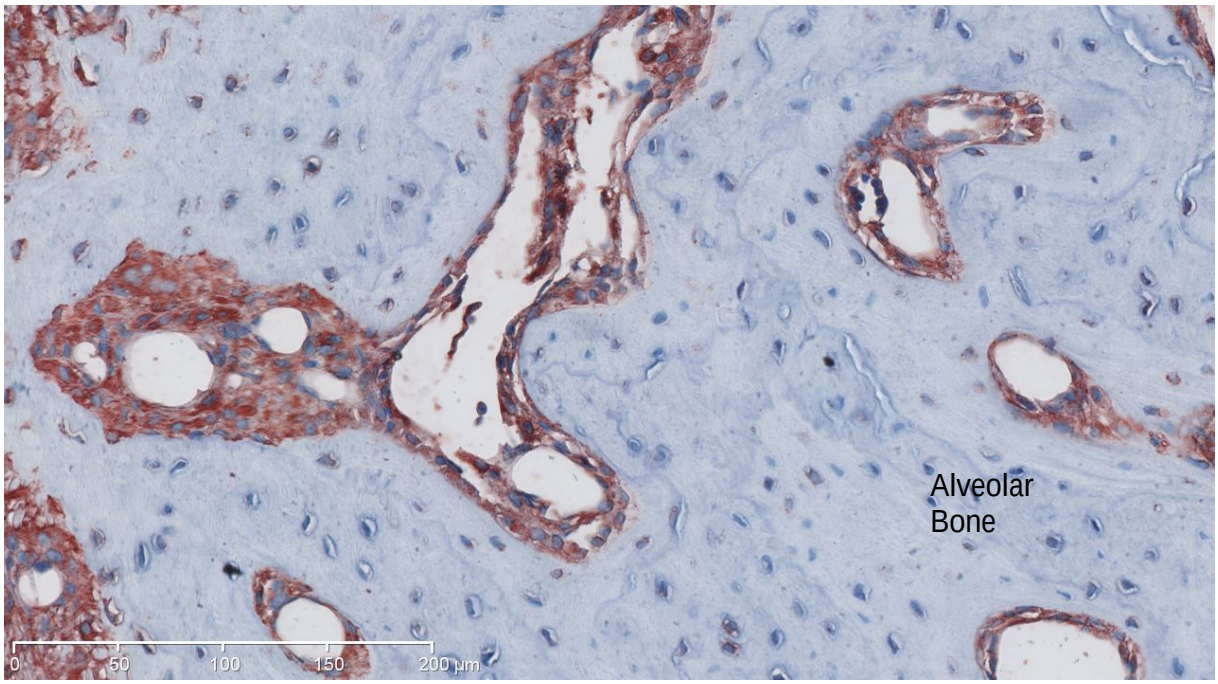

Day 0 Internal Control

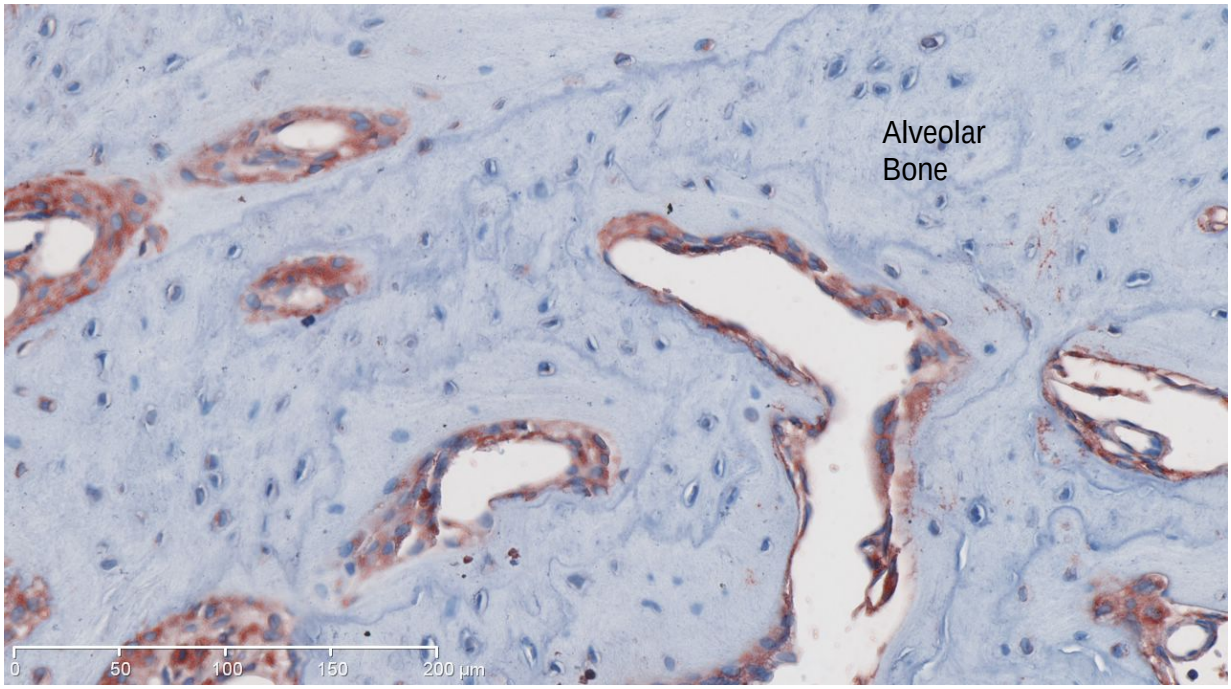

Day 4 Experimental

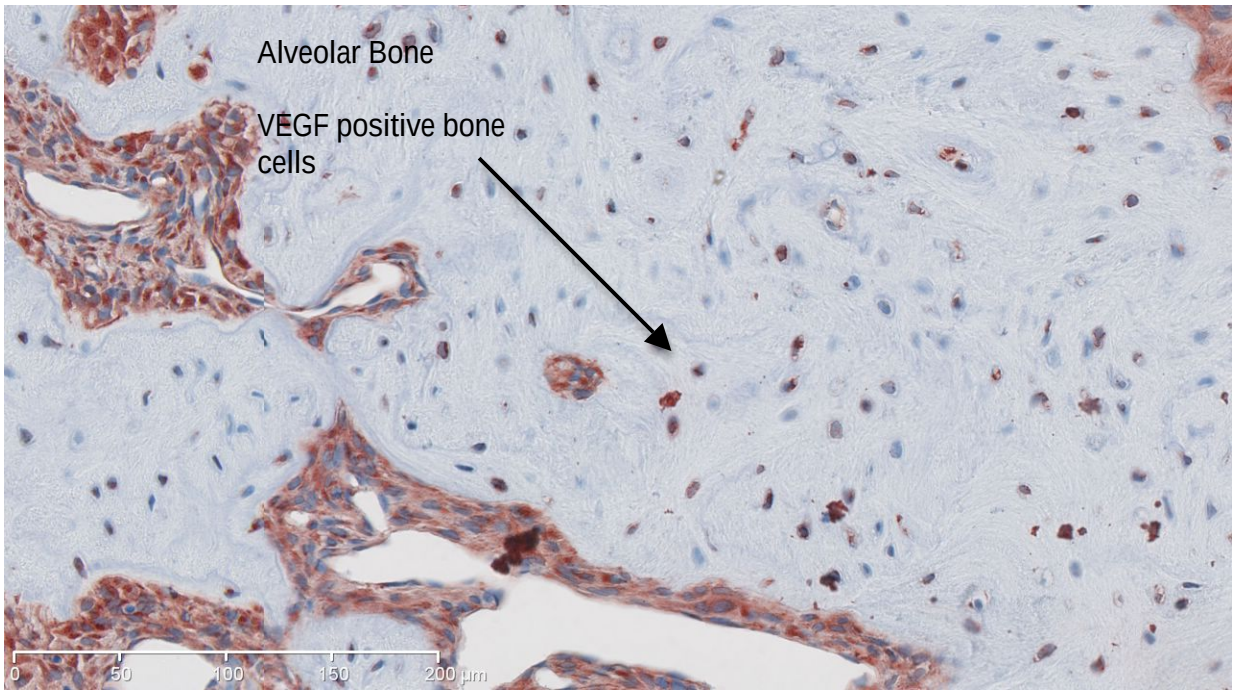

Day 4 Internal Control

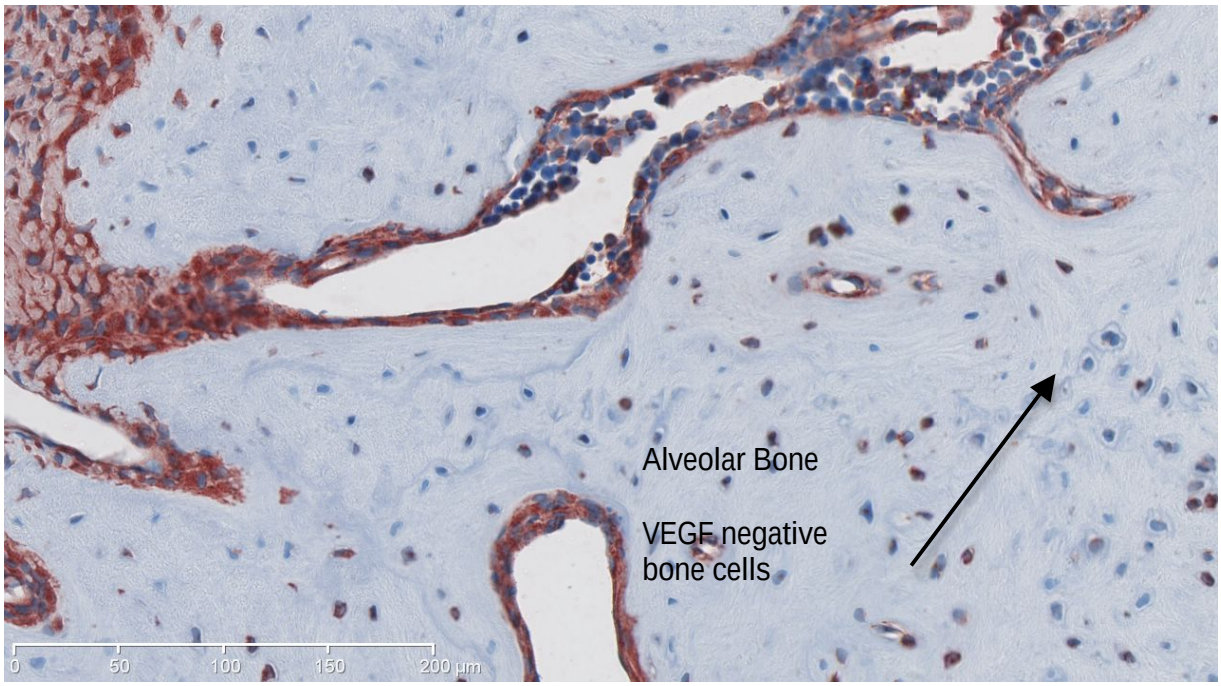

Day 7 Experimental

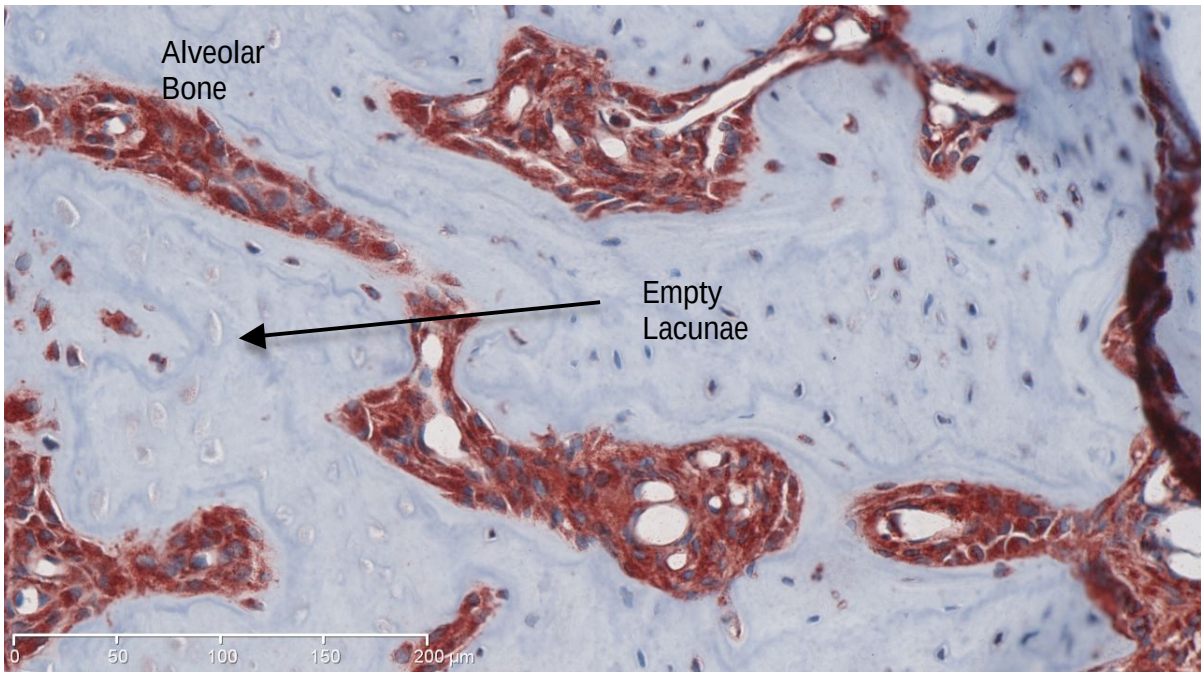

Day 7 Internal Control

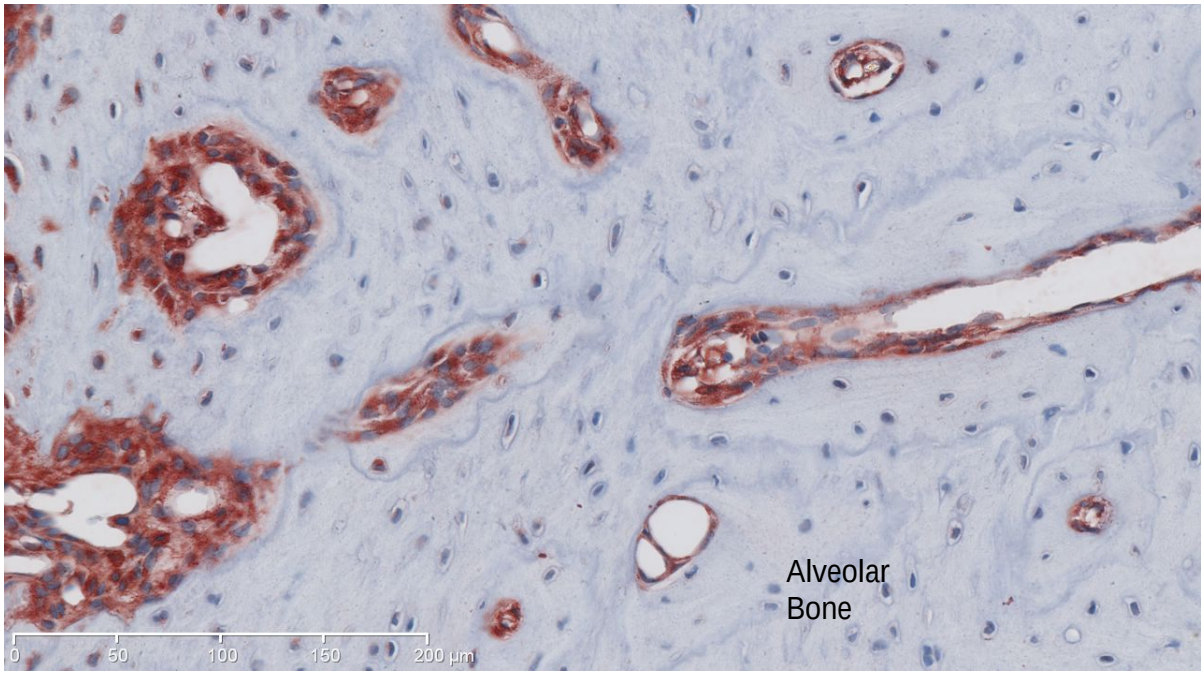

Day 14 Experimental

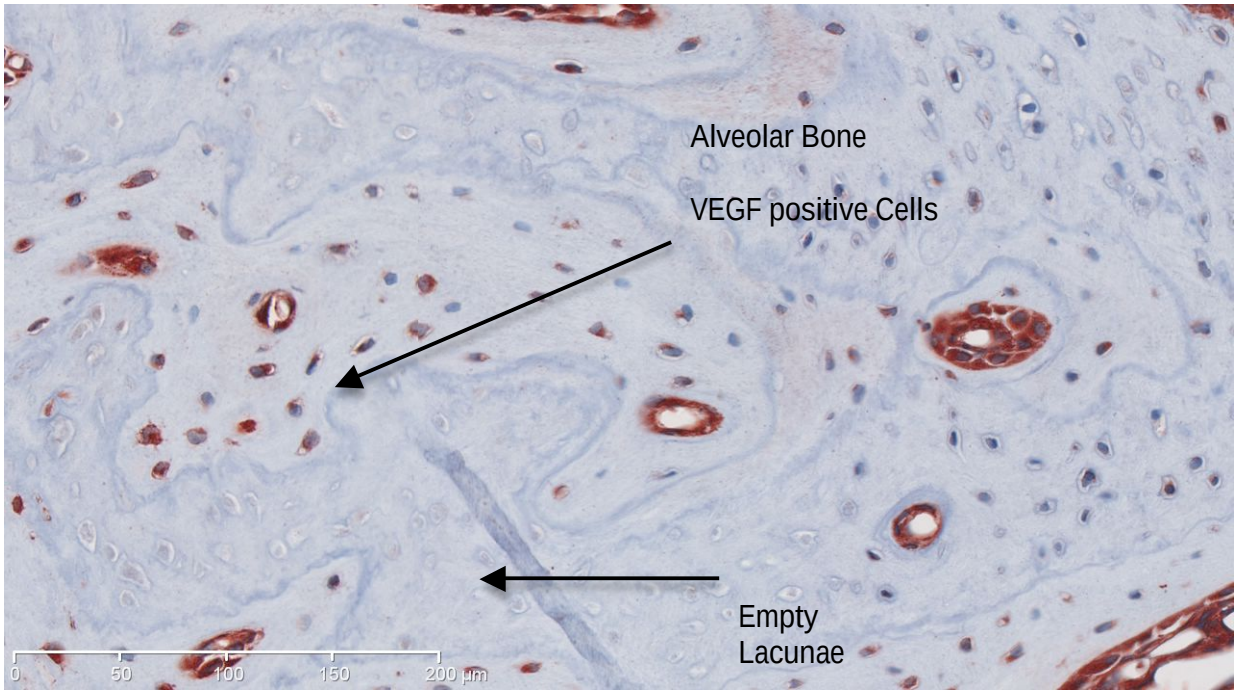

Day 14 Internal Control

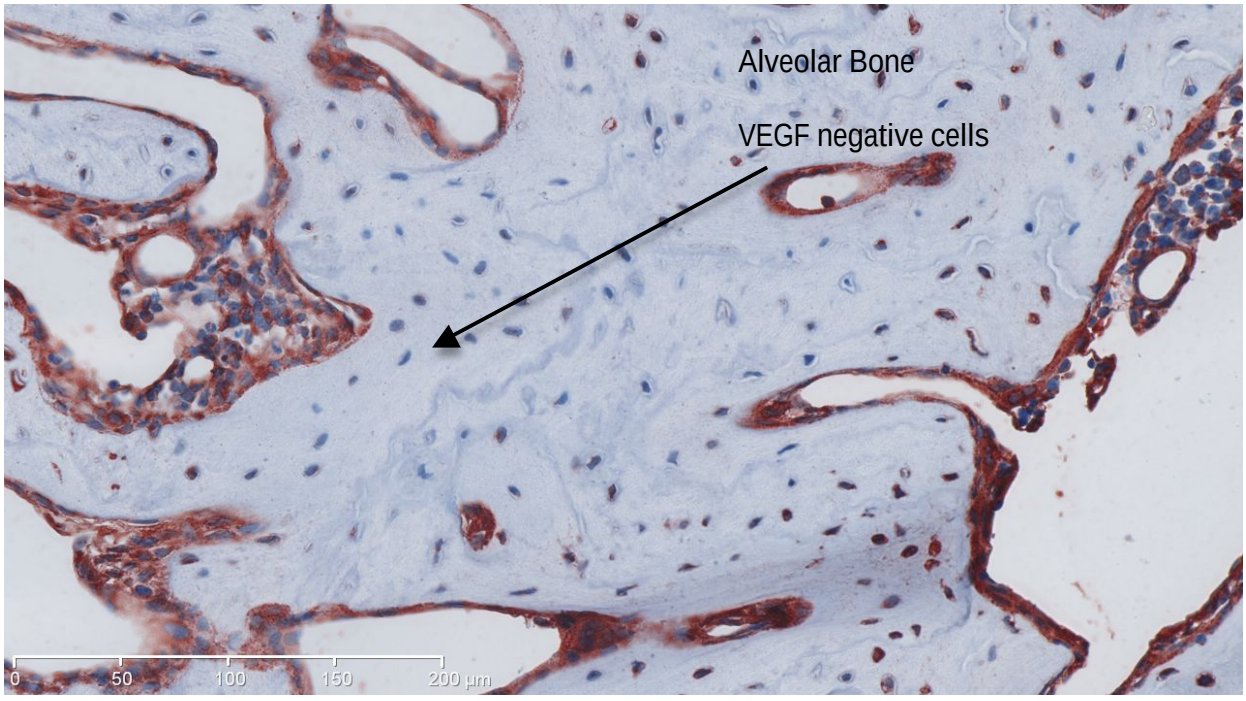

Day 28 Experimental

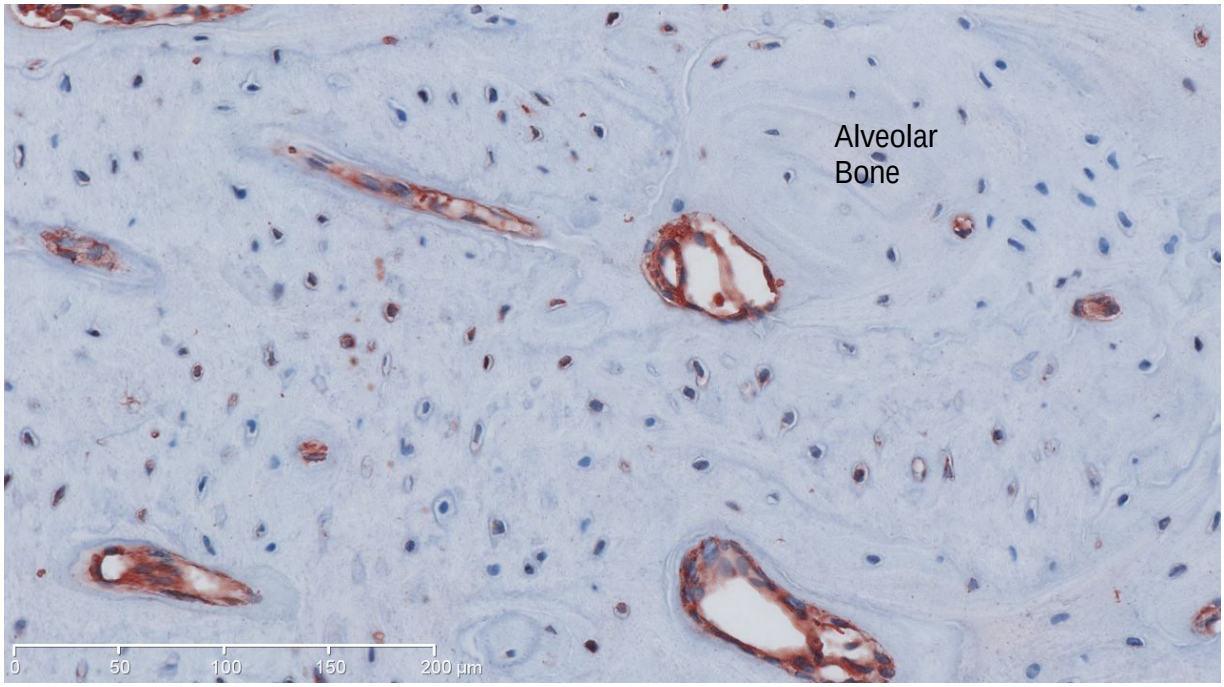

Day 28 Internal Control

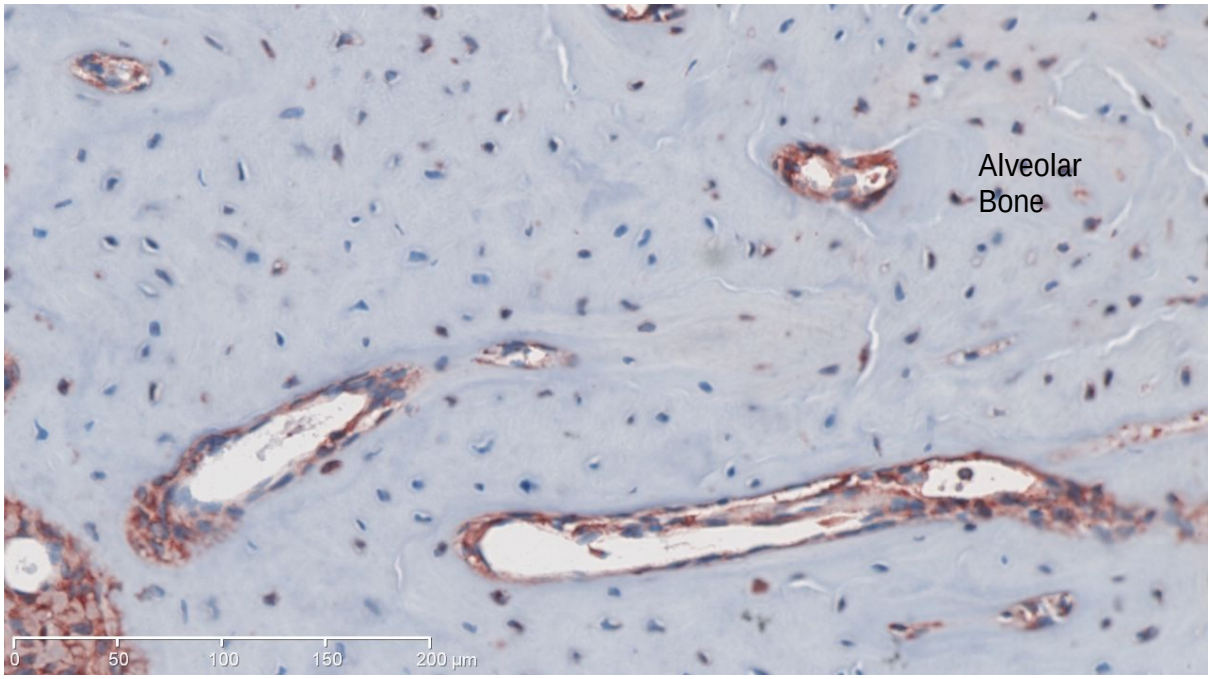

Statistically, there was a significant difference in the percentage of VEGF positive cells on the experimental compared to the internal control side ($p<0.05$) with the experimental side showing on average 8.28% more positive cells than the control side. Although there was not a statistically significant difference found between the percentage of VEGF positive cells and time ($p=0.3311$), a trend of increasing percentage of VEGF positive cells was seen at day 4 with minimal change day 7 before gradually decreasing days 14 and 28 (see Tables 10 and 11).

Table 10: The mean percentage of VEGF positive cell counts in the experimental group at different time points and the accumulative percentage of the experimental and internal control groups.

R: Experimental group, L: Internal Control group. 0, 4, 7, 14 and 28 denote time points of the experimental group.

Effect	time	side	Estimate	Standard Error
time	0		58.5276	5.7773
time	4		65.0006	5.8016
time	7		62.4506	5.7919
time	14		52.4957	5.7791
time	28		50.5150	5.8289
side		L	53.6556	2.7780
side		R	61.9402	2.7732

Table 11: Comparison of the mean percentage of VEGF positive cells in the alveolar bone of between 2 time points of the experimental group and overall between the accumulated experimental and internal control groups.

R: Experimental group, L: Internal Control group. 0, 4, 7, 14 and 28 denote time points of the experimental group. * p<0.05.

Effect	Time side vs. _time _side				Estimate	Standard Error	PValue
time	0		4		-6.4730	8.1875	0.4294
time	0		7		-3.9230	8.1806	0.6317
time	0		14		6.0319	8.1716	0.4606
time	0		28		8.0126	8.2069	0.3292
time	4		7		2.5500	8.1979	0.7558
time	14		4		-12.5049	8.1888	0.1271
time	14		7		-9.9549	8.1820	0.2241
time	14		28		1.9808	8.2082	0.8094
time	28		4		-14.4856	8.2240	0.0786
time	28		7		-11.9356	8.2172	0.1468
side		L		R	-8.2846	1.9858	0.0003

Between the internal and external control groups, a significant difference (p<0.05) was noted in the percentage of VEGF positive cells counts at difference time points (see Tables 12 and 13). On average the internal control group had 11.6% more VEGF positive cells than the external control group.

Table 12: The mean percentage of VEGF positive cells in the alveolar bone of control animals.

EC: External control. 0, 4, 7, 14 and 28 denotes time points of internal control group.

Effect	time	Estimate	Standard Error
time	EC	49.9374	4.0047
time	0.	53.2178	3.1605
time	4	61.5466	3.2265
time	7	56.5826	3.3517
time	14	47.1772	3.2339
time	28	49.3447	3.6589

Table 13: A comparison of the difference of mean percentage of VEGF positive cells in the alveolar bone between 2 time points of the internal control group and between the external and internal control group at different time points.

EC: External control. 0, 4, 7, 14 and 28 denotes time points of internal control group.

*p<0.05.

Effect		Estimate	Standard Error	PValue
Time	EC vs. 0	-3.2804	5.2216	0.5302
Time	EC vs. 4	-11.6092	5.1310	*0.0242
Time	EC vs. 7	-6.6452	5.2218	0.2039
Time	EC vs. 14	2.7602	5.1523	0.5924
Time	EC vs. 28	0.5927	5.4787	0.9139
Time	0 vs. 4	-8.3288	4.6087	0.0714
Time	0 vs. 7	-3.3648	4.6068	0.4655
Time	0 vs. 14	6.0406	4.5217	0.1823
Time	0 vs. 28	3.8731	4.8143	0.4216
Time	4 vs. 7	4.9640	4.6529	0.2866
Time	14 vs. 4	-14.3694	4.5609	*0.0017
Time	14 vs. 7	-9.4054	4.7887	0.0502
Time	14 vs. 28	-2.1675	5.0030	0.6651
Time	28 vs. 4	-12.2019	5.0320	0.0157
Time	28 vs. 7	-7.2379	4.9519	0.1446

7.2.5 Discussion:

As with previous authors, a number of cells in the dentoalveolar region including vascular endothelial cells, bone cells (osteoblasts / osteocytes / bone lining cells), osteoclasts in resorption lacunae along the PDL (Bletsa et al., 2012) and periodontal ligament cells (fibroblast like cells, epithelial cell rests of Malassez (ERM)), were found to be positive for VEGF in both experimental and control animals (Yamawaki et al., 2010; Miyagawa et al., 2009; Suthin et al., 2003).

Although VEGF expression has not been reviewed previously using an ankylotic model, Miyagawa et al. (2009) used IHC and Real-time Reverse-transcriptase-polymerase chain-reaction (RT-PCR) to examine VEGF mRNA expression in fifteen male, six week old Wistar rats following the application of a 150mN mechanical force between the upper right and left first molars. PDL cells adjacent to hyalinised tissues and alveolar bone on the compression side were noted to be strongly positive for VEGF 7 days post force application. VEGF expression was noted in monocytes and osteoclasts on the compression side. On the tension side, moderate VEGF expression was also noted in osteoblasts and PDL cells. Miyagawa et al. theorized that intermittent forces such as with chewing, may lead to VEGF expression in PDL cells regardless of tooth movement. Whilst the current study also identified VEGF expression in the experimental and internal control groups, it differs from Miyagawa et al. in that a significant difference was found between the two groups with a significantly higher expression of VEGF positive cells in the internal control group by on average 20%. Also, a decreasing trend (non significant) in VEGF levels on the experimental side was identified between days 0 to 14 post insult, with VEGF levels increasing to near internal control levels at day 28. These differences may be due to the type and degree of insult to the PDL region, with orthodontic tooth movement temporarily occluding blood vessels compared to extensive cell death and damage to

blood vessels by hypothermal insult. This more extensive insult possibly decreases the numbers of cells in the region, therefore delaying the VEGF response.

Yamawaki et al. (2010) reviewed the expression of VEGF in epithelial cell rests of Malassez within the PDL in vitro using porcine PDL cells and RT-PCR. Yamawaki et al. found that expression of VEGF mRNA was lower in ERM when treated with nerve growth factor and upregulated in cells treated with epithelial growth factor. Following hypothermal insult, the PDL and its resident cells are damaged, with thinning and loss of the PDL at day 7 and 14 shown with H and E staining. Therefore, as above, the number of cells available to release VEGF are decreased perhaps leading to a decreased VEGF expression as seen in this current study.

However, bone turnover is occurring and a blood supply, and hence VEGF expression, is required. In the alveolar bone, a significant difference was also noted in the VEGF expression between the experimental and control groups with the experimental group significantly greater than that of the control. Conversely to the PDL, the alveolar bone displayed a trend of increased VEGF expression compared to the internal control group up to day 7, with levels close to that of the internal control group at days 14 and 28. This trend is in agreement with the timeline for raised VEGF expression as found by Miyagawa et al. (2009).

Within the pulp in the current study, VEGF expression significantly increased up to day 7 before decreasing day 14 and 28. Bletsa et al. (2012), however, found that VEGF gene expression (RT-PCR) in the pulp significantly increased after 10 days, remaining increased at 21 days and that VEGF protein expression (IHC) was increased at both 10 days and 21 days. Again, this difference may be due to the type of insult, with Bletsa et al. causing a pulp exposure with a carbide bur on the right maxillary and mandibular molar teeth of 26 female Wistar rats. The insult in this instance was

ongoing with bacterial infection of the pulp exposure leading to an acute inflammatory response with bone destruction after 7 to 20 days. In comparison, the hypothermal insult was of 10 minutes duration but lead to rapid cell death. The rats in Bletsa et al.'s study were divided into two groups and killed at day 10 and 21 days. Changes in VEGF expression may have been noted at an earlier time frame had these time points also been included.

7.2.6 Conclusions:

1) VEGF is expressed by a number of cells within the rat dentoalveolus including bone cells (osteoblasts and osteocytes not differentiated between), osteoclasts, fibroblast-like cells of the PDL, vascular lining cells, and odontoblasts.

2) Changes in VEGF expression were found in the experimental pulp, PDL and alveolar bone when compared to the internal and external control groups.

3) Changes in VEGF expression with time were noted in the pulp, PDL and alveolar bone. A statistically significant interaction was found between time and VEGF expression in the pulp only.

4) Changes in VEGF expression also occurred in the internal control group, suggesting that a localised hypothermic insult may lead to a systemic impact.

5) Post-hypothermal insult, VEGF may play a role in the development of bony ankylosis.

7.2.7 References:

1. Andersson L, Blomlöf L, Lindskog S, Feiglin B, Hammarström L. (1984) Tooth ankylosis. Clinical, radiographic and histological assessments. Int. J. Oral Surg. 13; 423 - 31
2. Bates DO (2010) Vascular endothelial growth factors and vascular permeability. Cardiovascular Research Advance Access published April 16, 2010.
3. Bletsa A, Virtej A, Berggreen E. (2012) Vascular Endothelial Growth Factors and Receptors are Upregulated during Development of Apical Periodontitis. Journal of Endodontics 38(5); 628 - 635
4. Canavese M, Altruda F, Ruzicka T, Schauber J. (2010) Vascular endothelial growth factor (VEGF) in the pathogenesis of psoriasis – A possible target for novel therapies. Journal of Dermatological Science, Doi 10.1016/j.jdermsci2010.03.023
5. Chae HS, Park H-J, Hwang HR, Kwon A, Lim W-H, Yi WJ, Han D-H, Kim YH, Baek J-H. (2011) The effects of antioxidants on the production of pro-inflammatory cytokines and orthodontic tooth movement. Mol Cells 32; 189 – 196
6. Corrado A, Neve A, Cantatore FP. (2011) Expression of vascular endothelial growth factor in normal, osteoarthritic and osteoporotic osteoblasts. Clin Exp Med Nov 29. Epub ahead of print (Published 2013 13(1); 81 – 4).
7. Crona-Larsson G, Bjarnason S, Norén JG (1991) Effect of luxation injuries on permanent teeth. Endod Dent Traumatol 7; 199 - 206
8. Dreyer CW, Pierce AM and Lindskog S. (2000) Hypothermic insult to the periodontium: a model for the study of aseptic tooth resorption. Endodontics and Dental Traumatology 16; 9 – 15
9. Ekim SL and Hatibovic-Kofman S. (2001) A treatment decision-making model for infraoccluded primary molars. International Journal of Paediatric Dentistry 11; 340 – 6
10. Hecova H, Tzigkounakis V, Merglova V, Netolicky J. (2010) A retrospective study of 889 injured permanent teeth. Dental Traumatology 26; 466 – 75
11. Kim HH (2002) Stabilization of hypoxia inducible factor 1 alpha in the hypoxic stimuli induced expression of vascular endothelial growth factor in osteoblastic cells. Cytokine 17(1); 14 – 27
12. Kjaer I, Fink-Jensen M and Andreasen JO. (2008) Classification and sequelae of arrested eruption of primary molars. International Journal of Paediatric Dentistry 18; 11 - 7

13. Klagsbrun M, D'Amore PA. (1996) Vascular endothelial growth factor and its receptors. Cytokine and Growth Factor Reviews 7(3) 259 – 270
14. Koch S, Tugues S, Li X, Gualandi L, Claesson-Welsh, L (2011) Signal transduction by vascular endothelial growth factor receptors Biochem J, 437 (2011), pp. 169–183
15. Kurol J and Magnusson BC. (1984) Infraocclusion of primary molars: a histologic study. European Journal of Oral Sciences 92; 564 – 76
16. Kurol J and Olson L. (1991) Ankylosis of primary molars – a future periodontal threat to the first permanent molars? European Journal of Orthodontics 13; 404 - 9
17. Lee SH, Che X, Jeong JH, Choi JY, Lee YJ, Lee YH, Bae SC, Lee YM (2012) Runx2 stabilizes hypoxia-inducible factor-1α through competition with pVHL and stimulates angiogenesis in growth plate hypertrophic chondrocytes. J Biol Chem. Feb 20. Epub ahead of print (Published 2012 287 (18); 14760 – 14771 doi: 10.1074/jbc.M112.340232
18. Loriato LB, Machado AW, Souki BQ and Pereira TJ. (2009) Late diagnosis of dentoalveolar ankylosis: Impact on effectiveness and efficiency of orthodontic treatment. American Journal of Orthodontics and Dentofacial Orthopedics 135; 799 – 808
19. Miyagawa A, Chiba M, Hayashi H, Igarashi K. (2009) Compressive force induces VGF production in periodontal tissues. Journal of Dental Research 88 (8); 752 - 6
20. Ponduri S, Birnie DJ and Sandy JR. (2009) Infraocclusion of secondary deciduous molars – an unusual outcome. Journal of Orthodontics 36; 186 – 9
21. Raghoebar GM, Boering G, Jansen HWB, Vissink A. (1989) Secondary retention of permanent molars: a histologic study. Oral Pathology 18(8); 427 – 31
22. Rosner D, Becker A, Casap N, Chaeshu S. (2010) Orthosurgical treatment including anchorage from a palatal implant to correct an infraoccluded maxillary first molar in a young adult. Am J Orthod Dentofacial Orthop 138; 804 - 9
23. Shalish M, Peck, S, Wasserstein A, Peck L. (2010) Increased occurrence of dental anomalies associated with infraocclusion of deciduous molars. Angle Orthod. 80; 44 – 5
24. Street J, Lenehan B. (2009) Vascular endothelial growth factor regulates osteoblast survival- evidence for an autocrine feedback mechanism. Journal of Orthopaedic Surgery and Research. 4; 19 - 32
25. Takahasi H, Shibuya M. (2005) The vascular endothelial growth factor (VEGF)/VEGF receptor system and its role under physiological and pathological conditions. Clinical Science 109; 227 – 242
26. Tan CW (2011) A Qualitative investigation of RANKL, RANK and OPG in a Rat Model of Transient Ankylosis. Honours Project, The University of Adelaide, Adelaide, Australia.

27. Tan YY, Yang Y-Q, Chai L, Wong RWK and Rabie ABM. (2011) Effects of vascular endothelial growth factor (VEGF) on MC3T3-E1. Orthodontics and Craniofacial Research 13; 223 – 228
28. Wang Y, Li J, Wang Y, Lei L, Jiang C, An S, Zhan Y, Cheng Q, Zhao Z, Wang J, Jiang L (2011) Effects of hypoxia on osteoblastic differentiation of rate bone marrow mesenchymal stem cells. Mol Cell Biochem DOI 10.1007/s11010-011-1124-7
29. Wigen TI, Agnalt R, Jacobsen I. (2008) Intrusive luxation of permanent incisors in Norwegians aged 6 – 17 years: a retrospective study of treatment and outcome. Dental Traumatology 24; 612 – 8
30. Zhang C, Tang W, Li Y, Yang F, Dowd DR, MacDonald PN. (2011) Osteoblast specific transcription factor Osterix increases Vitamin D receptor gene expression in osteoblasts. PLoS One 6(10): e26504. Epub 2011 Oct 18

8. CONCLUDING REMARKS

8.1 Conclusions:

8.1.1 A reliable ankylotic reaction is not produced by a single 10 minute application of dry ice due to animal biologic variation as well as operator technique variation.

8.1.2 Anti Runx2 monoclonal antibody (Abnova Corporation, Taiwan) is a reliable and robust marker for bone cells, epithelial rest cells of Malassez, cemental cells and odontoblasts when using the ABC based retrieval system. Within the PDL, fibroblast-like cells as well as the surrounding ground substance stained positively for Runx2 making counting of positive Runx2 cells difficult.

8.1.3 Anti-VEGF monoclonal antibody (Novus Biologicals, Littleton, USA) is a reliable marker for bone cells, epithelial cell rests of Malassez, endothelial cells and fibroblast-like cells in the pulp and PDL using an ABC based retrieval system.

8.1.4 The use of the contralateral side as a control is unreliable due to the probable change in masticatory pattern secondary to the inflammation and possibly pain induced by the thermal trauma. A fluctuation in VEGF and Runx2 levels may also occur due to systematic alteration of these factors.

8.1.5 Immunohistochemistry can be extremely technique sensitive requiring strict attention and adherence to protocol for every aspect of the tissue preparation and processing including environmental fluctuations.

8.1.6 A significant difference between the experimental and control groups was found for both VEGF and Runx2 and, although an interaction between time and expression was not significant for all but the VEGF expression in the pulp, trends in the expression of VEGF and Runx2 were noted. The null

hypothesis that the expression of Runx2 and VEGF does not differ post-hypothermal insult is, therefore, rejected.

8.2 Strengths and Weaknesses:

The rats were used from a previous study, which although following the University of Adelaide Animal Ethics Committee principles of replacement, reduction and refinement, limited the power of this study as only 15 experimental rats were available. Given that the rats had already been processed, the duration between the hypothermal insult and sacrifice of the animal were also predetermined.

8.3 Suggestions for Future Work:

Future work could review the expression levels of other cytokines that influence both osteogenesis and haematopoiesis and may also be involved in ankylosis development. For example IL-3 has been found to enhance human osteoblast differentiation from MSC and increase osteogenesis via its action on bone morphogenetic protein 2. However, it also is an important regulator of haematopoiesis and a potent inhibitor of osteoclastogenesis and bone resorption.

In regards to VEGF and Runx2, co-localisation of these factors via double immunohistochemical staining and immunofluorescence would be useful to further our knowledge on how these factors interact. Protocols were designed for both of these techniques (see Figures 1 and 2 and 9.1.4.3).

Figure 1: Co-localisation of VEGF and Runx2 Day 7 using immunofluorescence.

A: DAPI to strongly stain cell DNA B: VEGF (CY3 stain), C: Runx2 (FITC stain) and D: Runx2 and VEGF (CY3 and FITC). Areas of co-localisation seen on the outskirts of the ankylotic region in the PDL were in close proximity to blood vessels.

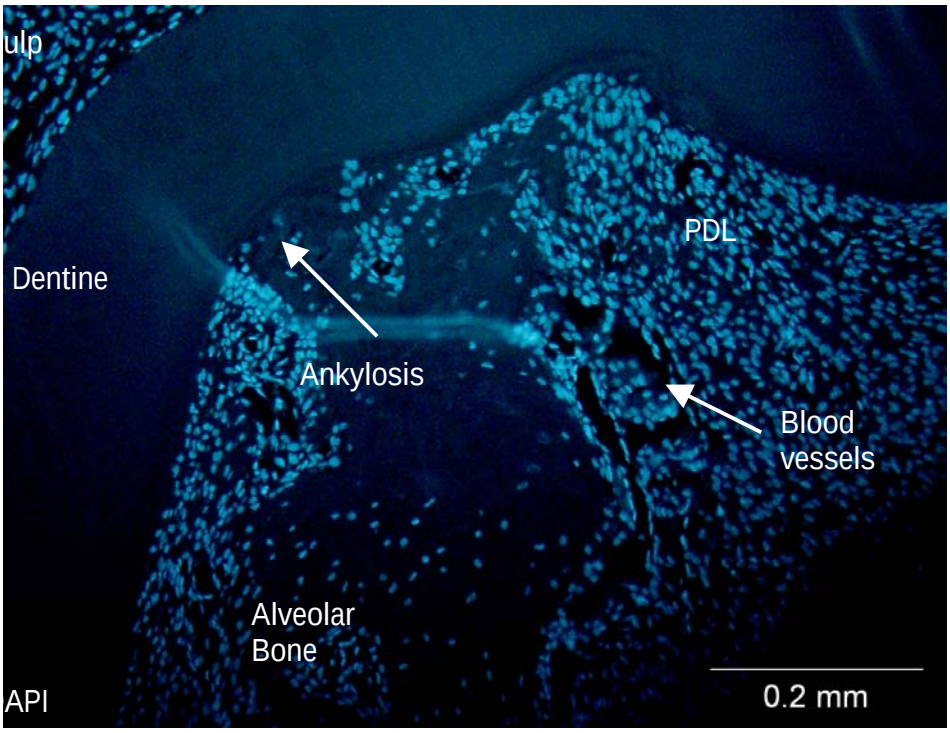

A

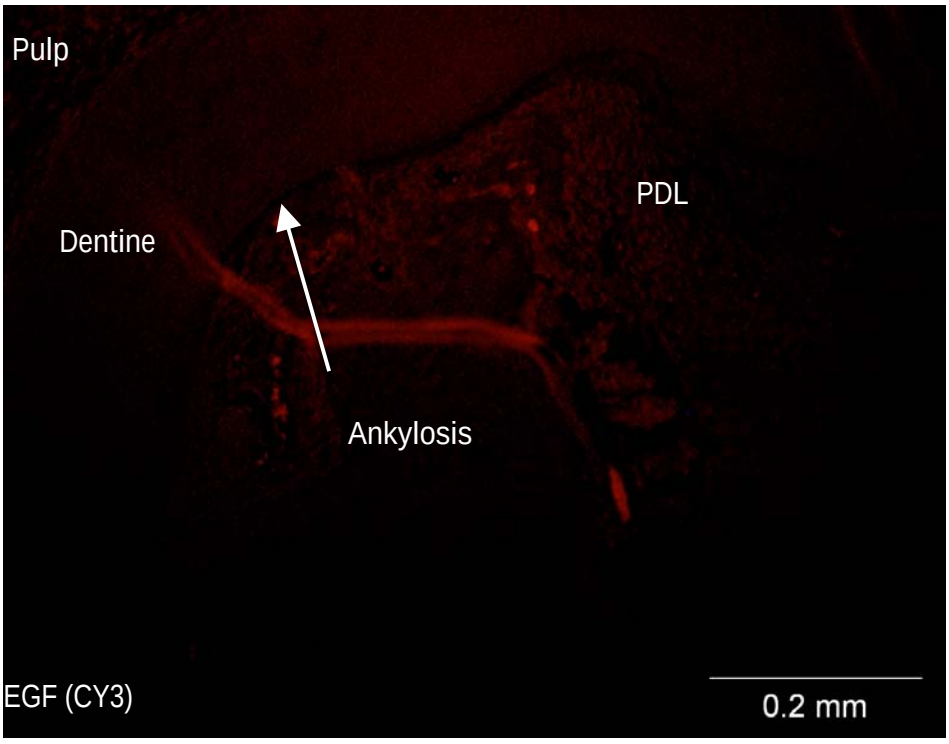

B

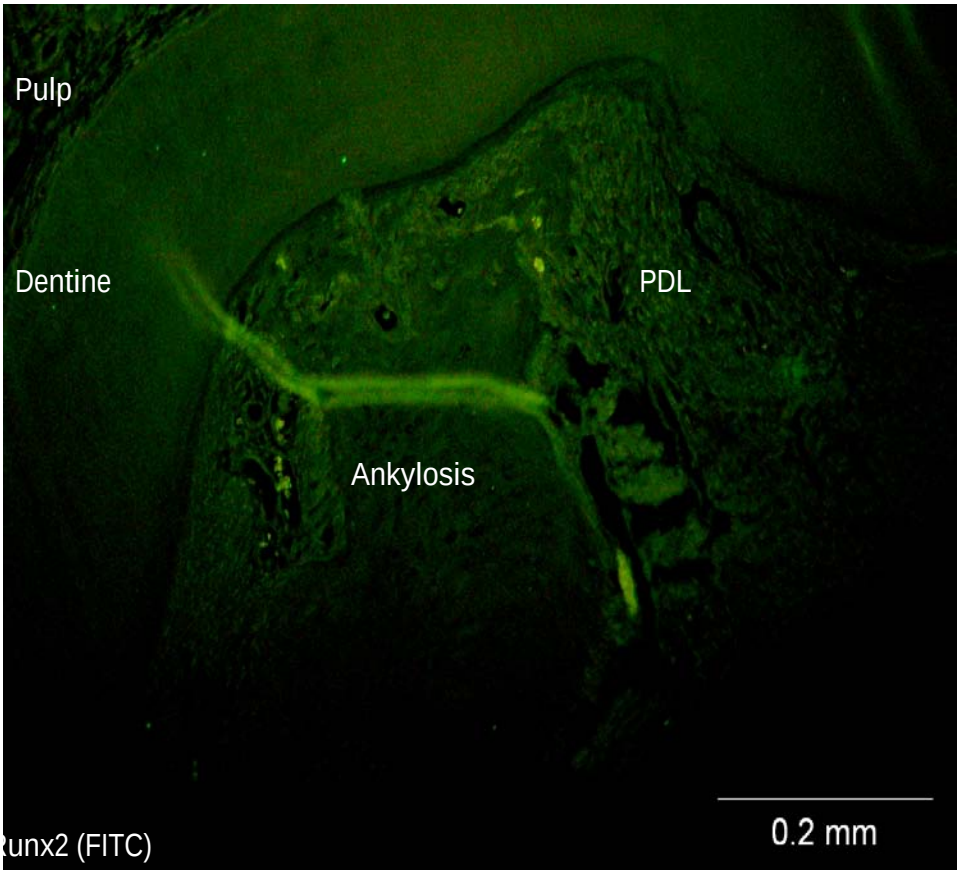
Pulp
Dentine
PDL
Ankylosis
0.2 mm
unx2 (FITC)
C

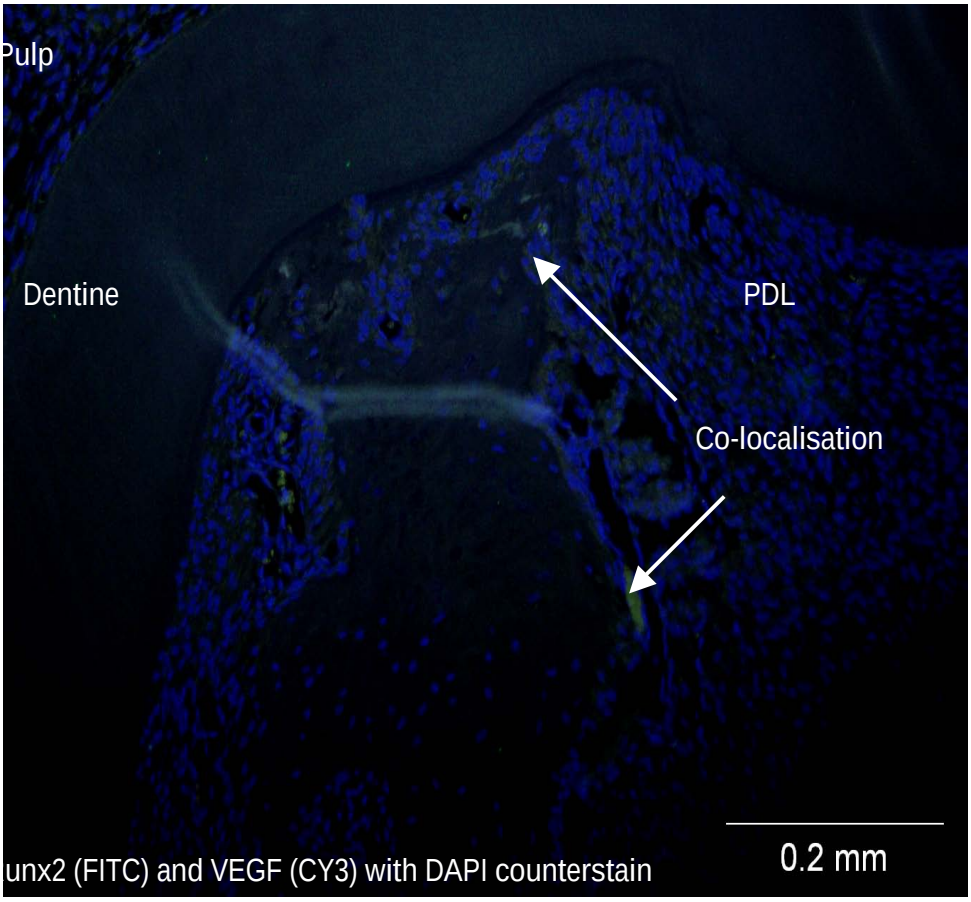
ulp
Dentine
PDL
Co-localisation
0.2 mm
unx2 (FITC) and VEGF (CY3) with DAPI counterstain
D

Figure 2: Co-localisation of Runx2 and VEGF Day 7 using double immunohistochemical staining of serial sections. Co-localisation noted in bone cells.

A: Runx2 only, B: VEGF only, C: Runx2 and VEGF x2.5 magnification ruler 0 – 2mm.

D: Runx2 and VEGF positive bone cells x 40 magnification ruler 0 - 100**µ**m.

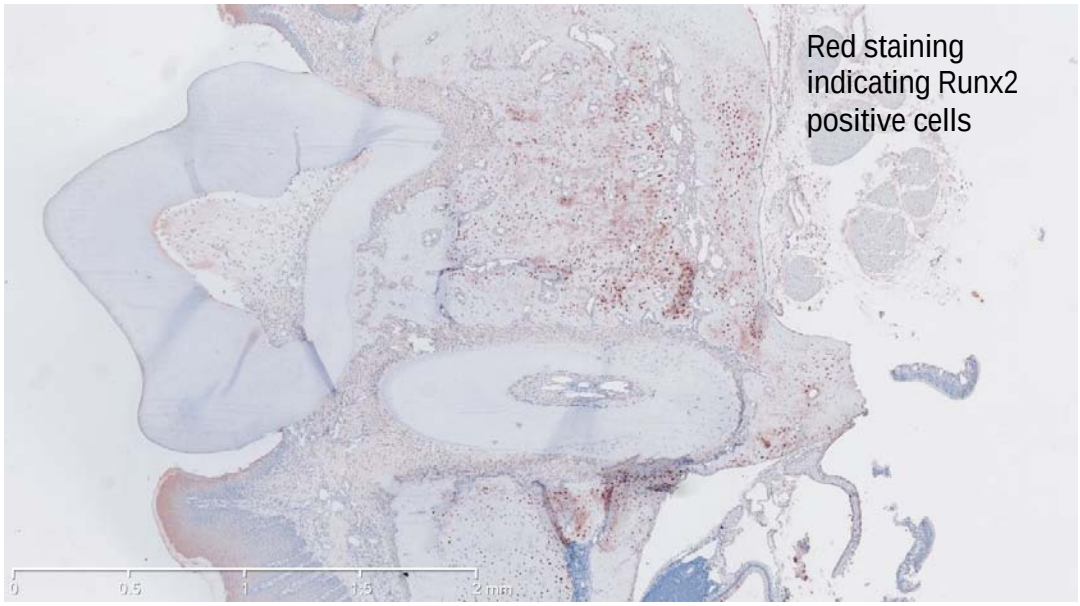

A

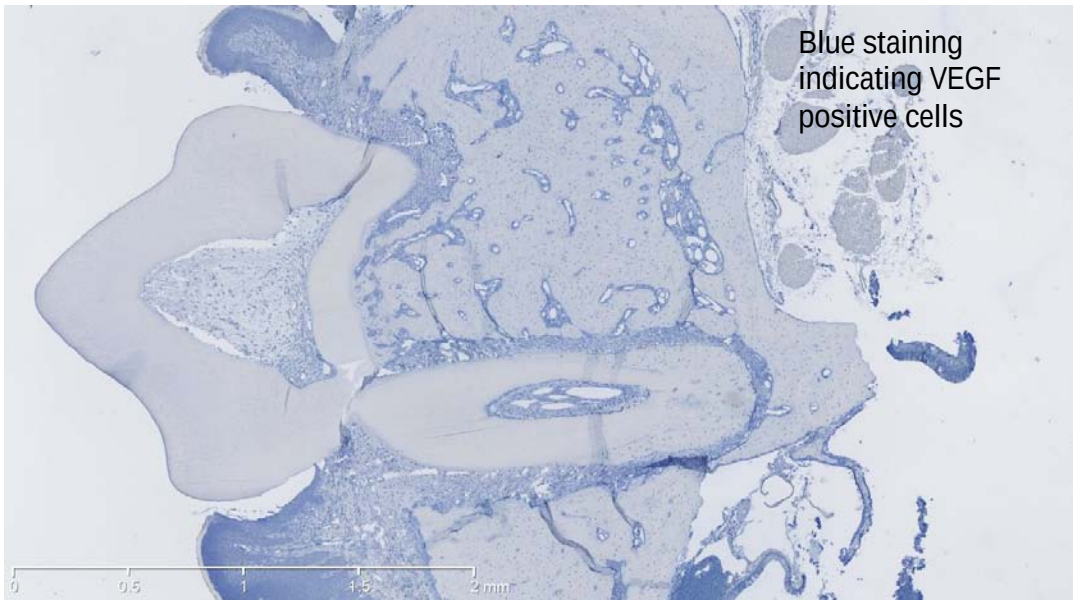

B

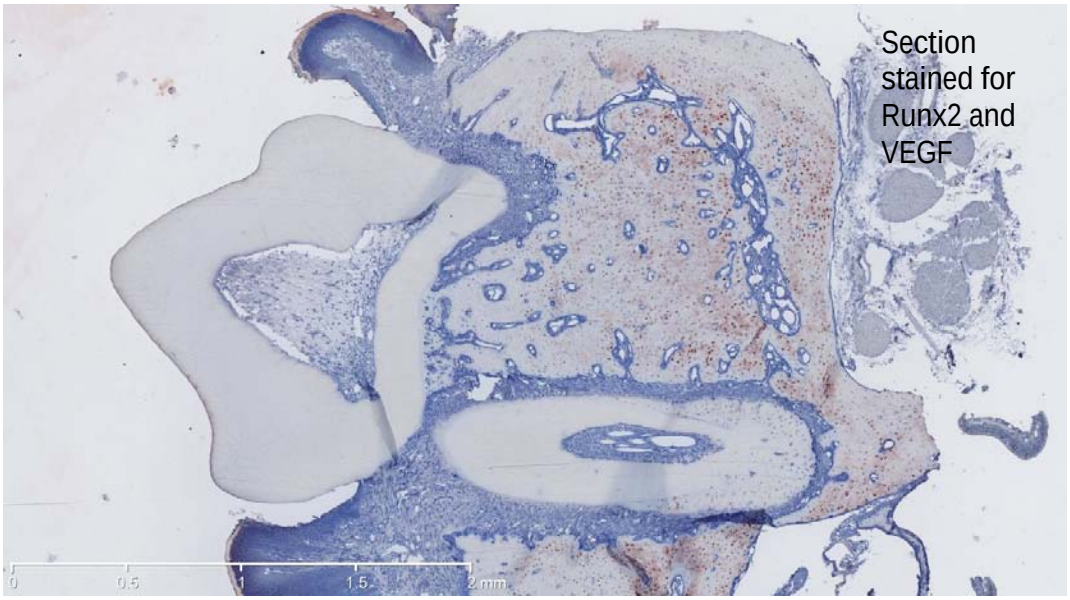
Section stained for Runx2 and VEGF
0
0.5
1
1.5
2 mm

C

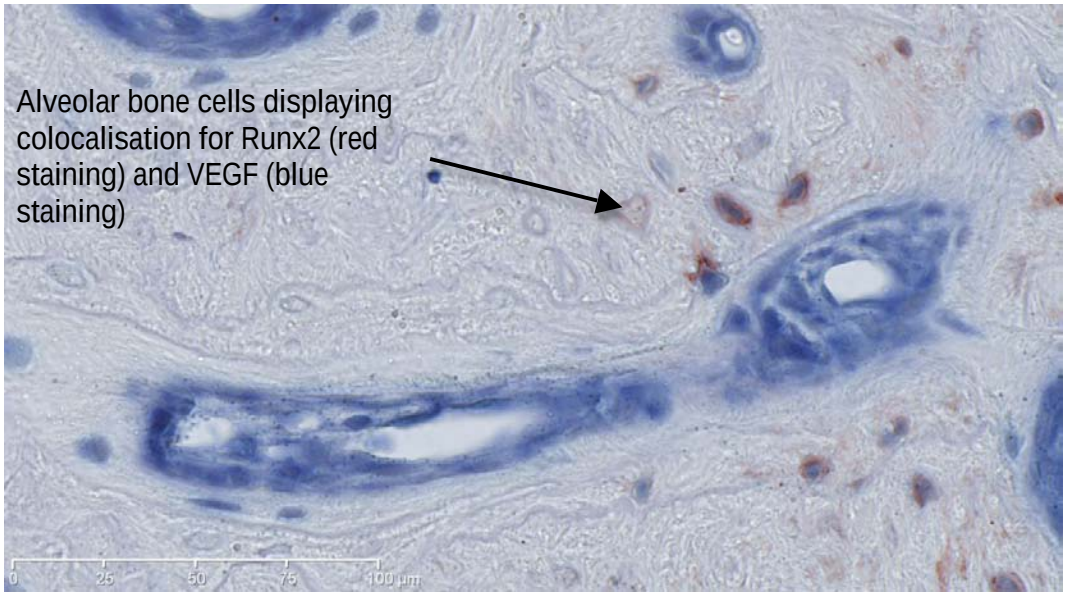
Alveolar bone cells displaying colocalisation for Runx2 (red staining) and VEGF (blue staining)
0
25
50
75
100 µm

D

9. APPENDICES

9.1.Material Utilized and Staining Method:

9.1.1 Materials Utilized:

Tris-EDTA Buffer (10mM Tris Base, 1mM EDTA solution, pH 9.0)

Tris base	1.21g
EDTA	0.37g
MilliQ water	1L

5 x Phosphate Buffered Saline (pH 7.2 – 7.4)

Sodium di-hydrogen orthophosphate	3.93gm
Di-sodium hydrogen orthophosphate	15.2gm
Sodium chloride	45.0gm
MilliQ water	1L

5 x Tris-Phosphate Buffered Saline (pH 7.2-7.4)

Tris base	30.275gm
Sodium di-hydrogen orthophosphate	3.93gm
Di-sodium hydrogen orthophosphate	15.2gm
Sodium chloride	45.0gm
MilliQ water	1L

Endogenous Peroxidise Block

NaN3 (sodium azide) Labchem, Auburn, Australia	0.1%
H2O2	1% (added before use)
In Tris-PBS	

Normal Donkey Serum in Tris PBS

Jackson ImmunoResearch Laboratories Inc, PA

Store at -20 degrees Celsius

Linking Antibody:

Donkey anti-mouse IgG (Biotin-SP conjugated Affin Pure anti-mouse)

Jackson ImmunoResearch Laboratories Inc, PA.

Use 1/200 dilution in Tris-PBS + 1% BSA

APAAP complex (Mouse monoclonal)

DAKO, Denmark

Use 1/50 dilution in Tris-PBS +1% BSA

Tris [hydroxymethyl] methylamine (Tris HCL) (0.2mM, pH 8.2)

Tris base	2.42gm
MilliQ water	100mL

Tris-Glycine (0.1mM, pH 7.2)

Tris Base	1.2114gm
Glycine	1.5014gm
MilliQ water	100mL

Autoclave and store at 4 degrees Celsius

Goat anti-mouse IgG-fluorescein isothiocyanate (FITC)

Southern Biotech, 160A Oxmoor Blvd, Birmingham, AL 35209

Use dilution of 1/50 in 1% BSA

Cyanine 3 (CY3) conjugated affinity pure Fab Fragment Donkey anti rabbit IgG

Jackson Immunoresearch Laboratories

Use dilution of 1/50 in 1% BSA

Slowfade Gold Antifade Reagent

Invitrogen Molecular Probes, Eugene, Oregan.

1% BSA

1gm Albumin from Bovine Serum (electrophoresis grade) Sigma Aldrich Pty Ltd, Sydney, Australia.

100mL PBSx1

Vectastain Elite ABC Kit;

Vector Laboratories Inc., Burlingame, CA, USA

1. Blocking Serum (normal serum): add 3 drops (150ul) of stock (yellow label) to 10mL of buffer.

2. Biotinylated Antibody: add 3 drops (150ul) of normal blocking serum (yellow label) to 10mL of buffer and then add 1 drop (50ul) of biotinylated antibody stock (blue label)

3. Reagent: Add 2 drops of reagent A (gray label) to 5mL of buffer, followed by 2 drops of reagent B. Mix and allow stand for 30 minutes.

VEGF (A) Antibody (VG1):

Product Code and Company: VEGF antibody (NB100-664), Novus Biologicals, Littleton, CO, USA

Package: Each vial contains 0.1mg of 1.0mg/mL concentration buffered with Tris-Glycine (150mM NaCl pH 7.5) and preserved in 0.05% sodium azide

Source: Mouse monoclonal

Istoype: IgG1 Kappa

Application: Recommended for detection of VEGF of human, rat, mouse or canine origin via Western Blotting, Immunofluorescence, Immunohistochemistry (including frozen and paraffin embedded sections). High temperature treatment of formalin fixed tissue sections using 1mM EDTA, pH 8.0 must be performed prior to immunostaining.

Dilution suggested 1:20 to 1:50 using ABC method.

Storage: 4 degrees Celsius in short term. -20 degrees Celsius in long term, guaranteed for 6 months from date of receipt

Runx2 Antibody (MO4):

Product Code and Company: Runx2 monoclonal antibody, clone 4D5, purified mouse immunoglobulin (H00000860-MO4), Abnova Corp., Taipei, Taiwan.

Package: Each vial contains 0.1mg of 0.5mg/mL concentration of Runx2 buffered with phosphate buffered saline (pH7.2)

Source: Mouse monoclonal

Istoype: IgG2

Application: Recommended for detection of Runx2 of human or rat, origin via Western Blotting (cell lysate and recombinant protein techniques), Immunofluorescence, Immunohistochemistry (paraffin embedded sections), Elisa (sandwich and recombinant protein techniques).
High temperature treatment of formalin fixed tissue sections using 1mM EDTA, pH 8.0 must be performed prior to immunostaining.
Dilution suggested 3ug/ml (using human placental tissue).

Storage: 2-8 degrees Celsius in short term. -20 degrees Celsius in long term, guaranteed for 3 months from date of receipt

9.1.2 Paraffin Removal Protocol:

1. Histolene 1 for 10 minutes

2. Histolene 2 for 10 minutes

3. 100% ethanol for 5 minutes

4. 95% ethanol for 5 minutes

9.1.3 Antigen Retrieval Protocol:

1. Tris-EDTA, pH 9.0 heated to 75^{o}C in water bath

2. Slides immersed in tris-EDTA for 10 minutes

3. Slides immersed in tris-EDTA left to cool to room temperature for 20 minutes

4. Wash in MilliQ water 3 times for 5 minutes

9.1.4 Immunohistochemical Staining Protocol:

9.1.4.1 Runx2:

Incubation with Blocking Serum:

1. PAP (hydrophobic) pen around each section

2. Endogenous Peroxidase block (H_2O_2 0.3% in methanol) for 10 minutes room temperature

3. Wash in PBSx1 3 times for 5 minutes

4. Prepare diluted normal horse blocking serum (Vectastain Elite ABC Kit) 50µl of yellow label (horse serum) in 5mL of PBSx1 and place on all sections

5. Incubate for 20mins and remove excess, do not wash

Application of Primary Antibody:

1. Prepare Runx2 monoclonal antibody (M04), clone 4D5 (Abnova Corporation, Taipei, Taiwan) 1:200 dilution of 0.5mg/mL diluted in PBSx1.

2. Apply to all slides with exception of negative controls

3. Place in wet chamber overnight at room temperature

Day 2:

Application of Secondary Antibody:

1. Wash PBSx1 3 times 5 minutes

2. Secondary antibody (Vectastain Elite ABC Kit) 2 drops of yellow label (horse serum), 5mL PBSx1 and 2 drops of blue label (biotynylated horse anti-goat antibody IgG stock) pipette onto sections and rest for 45 minutes at room temperature

3. Immediately make Vectastain Elite ABC reagent (2 drops reagent A, 2 drops reagent B, 5mL PBSx1) and leave for 30 minutes at room temperature

Application of ABC Reagent:

1. Wash slides PBSx1 3 times 5 minutes

2. Place previously made ABC reagent 45 minutes at room temperature

3. Wash slides PBSx1 3 times 5 minutes

Application of AEC (3-Amino-9-ethylcarbazole) substrate chromagen:

1. AEC (premixed drop ready to use) 10 minutes, room temperature, covered in dark cupboard

2. Wash MilliQ water 2 times 5 minutes

Counterstain:

1. Counterstain with Haematoxylin 10 seconds

2. Wash in tap water until water runs clear

3. Lithium carbonate 30 seconds

4. Rinse in tap water

Mounting:

1. Mount cover slips to slides using 1 drop of aqueous mounting medium (Aquamount) whilst slides still damp.

9.1.4.2 VEGF:

Incubation with Blocking Serum:

1. PAP (hydrophobic) pen around each section

2. EP block for 10 minutes room temperature

3. Wash in PBSx1 3 times for 5 minutes

4. Blocking serum (Vectastain ABC Kit) 50µl of yellow label in 5mL of PBSx1

Application of Primary Antibody:

1. VEGF monoclonal antibody (VG1) (Novus Biologicals, Littleton, USA) 1:100 dilution of 1.0mg/mL diluted in PBSx1

2. Apply to all sections with exception of negative controls

3. Place in wet chamber overnight, room temperature

Day 2:

Application of Secondary Antibody:

1. Wash PBSx1 3 times 5 minutes

2. Secondary antibody (Vectastain Elite ABC Kit) 2 drops of yellow label (horse serum), 5mL PBSx1 and 2 drops of blue label (biotynylated horse anti-goat antibody IgG stock) pipette onto sections for 45 minutes at room temperature

3. Immediately make Vectastain Elite ABC reagent (2 drops reagent A, 2 drops reagent B, 5mL PBSx1) leave for 30 minutes, room temperature

Application of ABC Reagent:

10. Wash slides PBSx1 3 times 5 minutes

11. Place previously made Vectastain Elite ABC reagent on all sections for 45 minutes at room temperature

12. Wash slides PBSx1 3 times 5 minutes

Application of AEC (3-Amino-9-ethylcarbazole) substrate chromagen:

13. Place AEC (premixed drop ready to use) on all slides for 10 minutes at room temperature, covered in a dark cupboard

14. Wash MilliQ water 2 times 5 minutes

Counterstain:

15. Counterstain with Haematoxylin 10 seconds

16. Wash in tap water until water runs clear

17. Lithium carbonate 30 seconds

18. Rinse in tap water

Mounting:

19. Mount cover slips to slides using 1 drop of aqueous mounting solution (Aquamount)

9.1.4.3 Dual Staining to Co localise Runx2 and VEGF (via Alkaline Phosphatase Anti-Alkaline Phosphatase (APAAP) Method):

Incubation with Blocking Serum:

1. PAP (hydrophobic) pen around each section

2. EP block for 10 minutes room temperature

3. Wash in PBSx1 3 times for 5 minutes

4. Blocking serum (Vectastain Elite ABC Kit) 50µl of yellow label in 5mL of PBSx1

Application of Primary Antibody:

1. Runx2 monoclonal antibody (M04), clone 4D5 (Abnova Corporation, Taipei, Taiwan) 1:400 dilution of 0.5mg/mL diluted in PBSx1

2. Place in wet chamber overnight

Day 2:

Application of Secondary Antibody:

1. Wash PBSx1 3 times 5 minutes

2. Secondary antibody (Vectastain ABC Kit) 2 drops of yellow label (horse serum), 5mL PBSx1 and 2 drops of blue label (biotynylated horse anti-goat antibody stock) pipette onto sections for 45 minutes at room temperature

3. Immediately make ABC reagent (2 drops reagent A, 2 drops reagent B, 5mL PBSx1) leave for 30 minutes, room temperature

Application of ABC Reagent:

1. Wash slides PBSx1 3 times 5 minutes

2. Place previously made ABC reagent 45 minutes, room temperature

3. Wash slides PBSx1 3 times 5 minutes

Application of AEC (3-Amino-9-ethylcarbazole) substrate chromagen:

1. AEC (premixed drop ready to use) 10 minutes, room temperature, covered in dark cupboard

Incubation with Blocking Serum:

1. Wash TrisPBSx1 3 times 2 minutes

2. Incubate in 0.1M Tris Glysine pH7.2 at room temperature for 60 minutes

3. Block with 20% Normal Donkey Serum (diluted in TrisPBSx1) for 40 minutes at room temperature

Application of Primary Antibody:

1. VEGF monoclonal antibody (VG1) (Novus Biologicals, Littleton, USA) 1:50 dilution of 1.0mg/mL diluted in TrisPBSx1 and 1% BSA (Sigma Albumin from Bovine Serum)

2. Place in wet chamber overnight

Day 3:

Application of Secondary Antibody:

1. Wash slides TrisPBSx1 3 times 2 minutes

2. Add secondary antibody Donkey anti-mouse IgG1 1:200 diluted in TrisPBSx1 and 1% BSA

Application of APAAP:

1. Wash in TrisPBSx1 3 times 2 minutes

2. APAAP 1:50 diluted in Tris PBS and 1% BSA room temperature for 45 minutes

3. Wash in TrisPBSx1 3 times for 2 minutes

Application of Vector Blue chromagen:

1. Vector Blue (5mL 100mM Tris-HCL pH8.2 add 2 drops reagent 1 and mix 2 drops of reagent 2 and mix and 2 drops of reagent 3 and mix). Develop in dark for 30 minutes.

2. Rinse with tap water

Counterstain:

1. Counterstain with Haematoxylin 10 seconds

2. Wash in tap water until water runs clear

3. Lithium carbonate 30 seconds

4. Rinse in tap water

Mounting:

1. Mount cover slips to slides using aqueous mounting solution (Aquamount) whilst slides still damp

9.1.5 Immunofluorescence staining protocol to co-localise VEGF and Runx2

Day 1:

Incubation with Blocking Serum and Application of Antibody:

1. PAP (hydrophobic) pen around each section
2. 1% BSA diluted in PBS x1 30 – 60 minutes
3. No wash, prepare Runx2 monoclonal antibody 1:400 dilution of 0.5mg/mL diluted in PBS x1

4. Apply to all slides
5. Place in wet chamber overnight at room temperature

Day 2:

Application of Immunofluorescent Chromagen and second primary antibody:

1. Wash PBSx1 3 times 5 minutes
2. Prepare FITC 1:50 diluted in 1%BSA
3. Incubate for 60 minutes in the dark at room temperature
4. Wash PBSx1 3 times for 5 minutes in dark
5. Prepare and apply VEGF 1:50 of 1mg/mL diluted in 1% BSA
6. Incubate in wet chamber in dark overnight at room temperature

Day 3:

Application of second Immunofluorescent Chromagen:

1. Wash PBSx1 3 times 5 minutes in dark
2. Prepare and apply CY3 1:50 diluted in 1% BSA
3. Incubate for 60 minutes in dark at room temperature
4. Wash PBSx1 3 times 5 minutes in dark

Counterstain:

1. Prepare DAPI counterstain 1:1000in PBSx1
2. Apply DAPI for 10 minutes in dark at room temperature
3. Wash PBSx1 3 times 5 minutes

Mounting:

1. Mount cover slips to slides using 1 drop of slowfade gold antifade reagent (Invitrogen molecular probes)